


Fall 12-15-2017

Evaluating Potential for Water Quality Decline in Maine Lakes

Kaci N. Fitzgibbon

University of Maine, kaci.fitzgibbon@maine.edu

Follow this and additional works at: <https://digitalcommons.library.umaine.edu/etd>

 Part of the [Biogeochemistry Commons](#), [Environmental Monitoring Commons](#), [Fresh Water Studies Commons](#), [Sustainability Commons](#), and the [Water Resource Management Commons](#)

Recommended Citation

Fitzgibbon, Kaci N., "Evaluating Potential for Water Quality Decline in Maine Lakes" (2017). *Electronic Theses and Dissertations*. 2780.
<https://digitalcommons.library.umaine.edu/etd/2780>

This Open-Access Thesis is brought to you for free and open access by DigitalCommons@UMaine. It has been accepted for inclusion in Electronic Theses and Dissertations by an authorized administrator of DigitalCommons@UMaine. For more information, please contact um.library.technical.services@maine.edu.

**EVALUATING POTENTIAL FOR WATER QUALITY DECLINE IN
MAINE LAKES**

By

Kaci Fitzgibbon

B.S. Kent State University, 2015

A THESIS

Submitted in Partial Fulfillment of the

Requirements for the Degree of

Master of Science

(in Earth and Climate Sciences)

The Graduate School

The University of Maine

December 2017

Advisory Committee:

Aria Amirbahman, Professor of Civil and Environmental Engineering, Co-
Advisor

Stephen Norton, Professor Emeritus of Earth and Climate Sciences, Co-Advisor

Sean Smith, Associate Professor of Earth and Climate Sciences

EVALUATING POTENTIAL FOR WATER QUALITY DECLINE IN MAINE LAKES

By Kaci Fitzgibbon

Thesis Co-Advisors: Dr. Aria Amirbahman and Dr. Stephen Norton

An Abstract of the Thesis Presented
in Partial Fulfillment of the Requirements for the
Degree of Master of Science
(in Earth and Climate Sciences)
December 2017

Understanding lake vulnerability with respect to eutrophication and loss of water quality is important for sustainability of aquatic ecosystems. This project aims at identifying and quantifying the effects of relevant physiochemical, climate, and watershed characteristics on lake vulnerability in order to develop management decision tools for the Maine Department of Environmental Protection (MEDEP). In a changing chemical and physical environment, using independent variables from each of these categories and then relating them to the summer lake epilimnetic phosphorus (P) concentrations allows for development of models to inform stakeholders of lake vulnerability to eutrophication problems.

We studied 24 lakes covering a range of trophic states (oligotrophic to mesotrophic) in Maine, USA. The lakes are classified as either dimictic or polymictic and may develop anoxic hypolimnia during stratification. Lake water samples were collected twice in June and August 2015, and analyzed for a variety of elements, with a primary focus on P. August epilimnetic P ranged from 1.9 to 21.0 $\mu\text{g/L}$ (henceforth ppb). Sediment samples from the deepest point were collected in June 2015, and were sequentially extracted and analyzed for P, aluminum (Al), and iron (Fe). The results show

that lakes with sediment having a NaOH-extractable Al to dithionite-reducible Fe ratio ($Al_{NaOH}:Fe_{BD}$) > 3 and a NaOH-extractable Al to dithionite-reducible P ratio ($Al_{NaOH}:P_{BD}$) > 25 are less susceptible to internal P release, and have lower epilimnetic P concentrations. Ratios can thereby be used as sediment indicators for hypolimnetic P release under anoxic conditions.

Three types of regression models (regression tree analysis, multiple linear regression (MLR), and quantile regression (QR)) were developed in order to broaden understanding of different aspects impacting lake eutrophication using data from the 24 study lakes that represented relevant lake physiochemical, climate, and watershed characteristics. A larger database of lakes from the Maine Department of Environmental Protection (96), and the Lake Environment Association (23) were then used to validate the models by analyzing the goodness of fit. The regression tree analysis was performed to detect dominant drivers in relation to the August epilimnetic P concentrations, revealing that to best predict the lake epilimnetic P, parameters representing physiochemical, climate and watershed characteristics are necessary independent variables. Of the approaches tested for MLR, the best fits to the observed data were obtained by one or more physiochemical variables and one watershed variable ($R^2 > 0.78$). Regression quantiles were used to estimate changes in epilimnetic P as a function of the agriculture area: watershed area (Ag:WA) ratio ranked by sediment $Al_{NaOH}:P_{BD}$ and area depth (Z_{avg}), all parameters that were shown to be important predictors in the MLR models. The structure of QR is robust for developing nutrient reduction targets for lake management. Using this approach, we determined that the reduction in Ag:WA to meet a specific epilimnetic P target (15 ppb) should be the first priority to mitigate

eutrophication in Maine lakes. Using multiple regression models to identify and quantify factors that influence lake eutrophication allows us to classify susceptible lakes and inform stakeholders about appropriate practices for lake stewardship.

ACKNOWLEDGEMENTS

This research was funded by grants from the Senator George J. Mitchell Center for Sustainability Solutions, the Maine Outdoor Heritage Fund, and the Maine Department of Environmental Protection (DEP). I thank the DEP for providing field equipment and sampling assistance throughout my research, with a special thanks to Linda Bacon, Jeff Dennis, Jeremy Deeds, and Douglas Sutor for their criticism and support along the way. I thank all of the people who helped me in the field aspects; Josh Noll, Mark Dennis, Douglas Sutor, Denise Blanchette, volunteers in the Maine Volunteer Lake Monitoring Program (VLMP), and Scott Williams (Executive Director of the Maine VLMP). Additionally, I thank Colin Holme (Assistant Director of Lakes Environmental Association, LEA) for providing a dataset of additional lakes.

I thank the Sawyer Environmental Chemistry Laboratory at the University of Maine for providing use of the laboratory. I thank Benjamin Burpee and Heather Doolittle, for their time explaining laboratory procedures for the study, and also Mike Handley for making sure I received the required laboratory space and equipment.

I thank my advisory committee: Drs. Aria Amirbahman, Steve Norton, and Sean Smith, for their endless supply of hypotheses and for helping me to see my research from another perspective. I give special thanks to my co-advisor, Dr. Aria Amirbahman for constantly challenging me to be a better researcher and for his guidance. I thank Professor Bill Halteman for his insight into the statistical realm. I thank my fellow officemates for their support and willingness to read multiple sections of my thesis. Finally, I am thankful to my family and friends who have supported and encouraged me throughout.

TABLE OF CONTENTS

ACKNOWLEDGEMENTS.....	ii
LIST OF TABLES.....	vi
LIST OF FIGURES.....	vii
CHAPTER 1: INTRODUCTION.....	1
1.1 External Loading.....	1
1.2 Internal Phosphorus Loading to Lakes.....	2
1.2.1 Chemical Mechanisms.....	3
1.2.1.1 The Role of Iron.....	3
1.2.1.2 The Role of Aluminum.....	4
1.2.2 Biological Mechanisms.....	6
1.2.3 Physical Mechanisms.....	6
1.3 Internal Mixing.....	7
CHAPTER 2: METHODS AND MATERIALS.....	10
2.1 Field Sites.....	10
2.2 Aqueous Collection and Analysis.....	12
2.3 Sediment Collection and Analysis.....	12
2.4 Pre-existing Data Compilation.....	14
2.5 Model Development.....	16
2.5.1 Regression Tree Analysis.....	17
2.5.2 Linear Regression Analysis.....	19
2.5.3 Percentile Selection Quantile Regression Analysis.....	22

CHAPTER 3: RESULTS.....	24
3.1 Physiochemical Characteristics.....	24
3.1.1 Morphometric Characteristics.....	24
3.1.2 Surficial Sediment Fractionation.....	26
3.1.3 Sediment Phosphorus.....	27
3.1.4 Sediment Iron.....	27
3.1.5 Sediment Aluminum.....	27
3.1.6 The $Al_{NaOH}:Fe_{BD}$ and $Al_{NaOH}:P_{BD}$ Ratios.....	28
3.1.7 Water Chemistry.....	32
3.2 Climate Factors.....	34
3.3 Watershed Characteristics.....	37
3.4 Statistical Modeling Results.....	38
3.4.1 Regression Tree.....	38
3.4.2 Multiple Linear Regression.....	41
3.4.3 Quantile Regression.....	47
CHAPTER 4: DISCUSSION.....	53
4.1 Regression Tree Model.....	53
4.2 Multiple Linear Regression Models.....	55
4.3 Percentile Selection-Quantile Regression.....	58
4.4 Modeling Limitations.....	61
CHAPTER 5: CONCLUSIONS.....	64
REFERENCES.....	66
APPENDIX A: MIDAS IDENTIFICATION.....	72

APPENDIX B: SEDIMENT AND WATER CHEMISTRY DATA.....	75
APPENDIX C: MODEL PARAMETERS.....	112
APPENDIX D: LAND COVER DATA.....	126
APPENDIX E: PRECIPITATION DATA.....	146
APPENDIX F: FIELD MAPS AND LOCATION.....	150
BIOGRAPHY OF THE AUTHOR.....	178

LIST OF TABLES

Table 2.1: Selected Properties of the 2015 Lakes.....	11
Table 2.2: Data from the Study (2015) and other organizations (DEP + LEA).....	21
Table 3.1: Multiple Linear Regression Equation Results from the 2015 Study Lakes.....	43
Table 3.2: Multiple Linear Regression Equation Coefficients.....	44
Table A1: Midas Identification.....	72
Table B1: Sediment Chemistry from the Surface (0-2 cm).....	75
Table B2: Sediment Chemistry from the Bottom (8-10 cm).....	83
Table B3: Sediment Calcium Fractionation (0-2; 8-10 cm).....	90
Table B4: Cations and Secchi Transparency.....	98
Table B5: Anions and pH.....	105
Table C1.1: Significant Parameters: Watershed and Chemistry.....	112
Table C1.2: Significant Parameters: Physiochemical and Climate.....	119
Table C2: Model Parameters: Coefficient of Determination, R^2	124
Table D1: Land cover Identification Key.....	127
Table D2.1: Land cover Area (ha.) from type 2 to 12.....	128
Table D2.2: Land cover Area (ha.) from type 13 to 27.....	132
Table D3.1: Adjacent Land cover Area (ha.) from type 2 to 12.....	136
Table D3.2: Adjacent Land cover Area (ha.) from type 13 to 26.....	140
Table D4: Road, Direct Watershed, and Lake Areas (ha.).....	144
Table E1: Precipitation (precip) data.....	146
Table F1: Latitude and Longitude of Sample Sites.....	151

LIST OF FIGURES

Figure 3.1: The Osgood Index (Eq. 1) versus the August epilimnetic P.....	25
Figure 3.2: The area-averaged depth (Eq. 2) versus the August epilimnetic P.....	25
Figure 3.3: Sediment $Al_{NaOH}:Fe_{BD}$ versus Epilimnetic P.....	30
Figure 3.4: Sediment $Al_{NaOH}:P_{BD}$ versus Epilimnetic P.....	30
Figure 3.5: Sediment $Al_{NaOH}:Fe_{BD}$ versus Hypolimnetic P.....	31
Figure 3.6: Sediment $Al_{NaOH}:P_{BD}$ versus Hypolimnetic P.....	31
Figure 3.7: DOC versus Epilimnetic P.....	32
Figure 3.8: Epilimnetic pH versus Epilimnetic P.....	33
Figure 3.9: Hypolimnetic Temperature versus Epilimnetic P.....	34
Figure 3.10: Schmidt Stability versus Epilimnetic P.....	36
Figure 3.11: Ag:WA Ratio versus Epilimnetic P.....	38
Figure 3.12: Regression Tree Analysis for Epilimnetic P.....	40
Figure 3.13: The Multiple Linear Regression Model Determined by AIC.....	45
Figure 3.14: The Multiple Linear Regression Model Determined by RSS.....	46
Figure 3.15: Ag:WA, lower 75 th percentile $Al_{NaOH}:P_{BD}$ versus log epilimnetic P.....	49
Figure 3.16: Ag:WA, lower 50 th percentile $Al_{NaOH}:P_{BD}$ versus log epilimnetic P.....	50
Figure 3.17: Ag:WA, lower 75 th percentile Z_{avg} versus log epilimnetic P.....	51
Figure 3.18: Ag:WA, lower 50 th percentile Z_{avg} versus log epilimnetic P.....	52
Figure B1: Sequential Extraction (P, Fe, Al) of Sediment Cores.....	92
Figure D1: Land cover Map 2004 (MEGIS).....	126
Figure F1: Map of All Study Sites (2015 + DEP + LEA).....	150
Figure F2: The Land Cover Type for the 2015 Study Sites.....	154

CHAPTER 1: INTRODUCTION

Phosphorus (P) is a limiting nutrient in many freshwater ecosystems. Small amounts of P are beneficial to freshwater ecosystems; however, excessive amounts are the leading cause of eutrophication, resulting from water pollution (Wetzel, 2001). Eutrophication occurs when a plethora of nutrients results in the explosive growth of aquatic plants and algae. Lakes offer multiple ecosystem services such as drinking water supplies, aquatic habitats, and recreational uses. A new field of sustainability science has emerged, which has a goal of understanding the fundamental interactions between nature and society. Sustainability research focuses on promoting the education of society to navigate toward a transition to sustainability (Kates et al., 2001). With this goal in mind, this study has two broad goals: first, to identify and advance our understanding of the roles of various watershed and lake characteristics and their effect in rendering lakes vulnerable to eutrophication; second, to preserve water quality in lakes by considering the active management of activities within the watershed to sustain water quality. This thesis provides guidance as to which characteristics make lakes susceptible to eutrophication and how best to make choices that influence lake behavior in a positive manner.

1.1 External Loading

The primary source of phosphorus (P) from undisturbed watersheds is the chemical weathering of soils and bedrock that contain the mineral apatite ($\text{Ca}_5(\text{PO}_4)_3(\text{OH}, \text{F}, \text{Cl})$; Filippelli, 2008). P may be transported in water in particulate organic and inorganic phases, and dissolved organic or dissolved inorganic forms (Wetzel, 2001). P mobilization by dissolved organic carbon or soil acidification has been linked to the

mobilization of aluminum (Al) and iron (Fe) hydroxides ($\text{Al}(\text{OH})_3$ and $\text{Fe}(\text{OH})_3$), due to desorption from secondary Al- and Fe-hydroxide surfaces in soil (Reinhardt et al., 2003). Acidification does not always directly correlate with an increase in Fe dissolution, indicating other factors such as changing redox conditions and elevated concentration of dissolved organic carbon may cause enhanced Fe mobilization (Reinhardt et al., 2003).

Anthropogenic activities create external inputs of P to surface water through agriculture, deforestation, industrial activities, water treatment plants, and urbanization. Intensified agriculture directly contributes to increased P export from the watershed through application of fertilizers and increased soil erosion (Dillon and Kirchner, 1975). Deforestation functions via two mechanisms to solubilize and mobilize P. First, burning converts P from plant matter into soluble ash. Second, enhanced erosion in the cropped areas transports surface soil rich in organic matter as well as secondary Al- and Fe-hydroxides (Filippelli, 2008). Land development of riparian zones, wetlands, and shorelines destroy natural buffer zones where P can be sequestered, increasing the delivery of P to lakes (Fisher and Acreman, 2004).

1.2 Internal Phosphorus Loading to Lakes

Einsele (1936) and Mortimer (1941) pioneered the concept of lake internal P cycling, introducing the process as an important mechanism contributing to eutrophication. Their work provided the paradigm in which oxygenated sediment retains P through adsorption to $\text{Fe}(\text{OH})_3$. Following the reductive dissolution of $\text{Fe}(\text{OH})_3$ under anaerobic conditions, P is released as bioavailable PO_4 (Petticrew and Arocena, 2001; Amirbahman et al. 2003). P stored internally in the sediment accounts for the main

summer P load in boreal lakes (Nürnberg, 2009) making it a significant factor when considering lake vulnerability. Internal P cycling involves a combination of chemical, biological, and physical processes (Boström et al., 1988; Nürnberg, 2009). Major chemical mechanisms include interaction of P with organic, secondary “mineral” phases, and primary mineral surfaces (Boström et al., 1988; Petticrew and Arocena, 2001; Homyak et al., 2014). Biological mechanisms include hyper-accumulation and release of P by bacteria and some algae species (Gächter et al., 1988; Barbiero and Welch, 1992; Khoshmanesh et al., 2001; Carey et al., 2014). Physical mechanisms include variations in temperature, thermal stratification, and induced mixing by altered lake circulation (Christophoridis and Fytianos, 2006; Hupfer and Lewandowski, 2008).

1.2.1 Chemical Mechanisms

1.2.1.1 The Role of Iron

A reducing environment in the hypolimnion occurs when oxygen is depleted by aerobic respiration of organic matter, resulting in the reduction of insoluble Fe(III) (as Fe(OH)₃) in the upper sediment to soluble Fe(II), dissolution of the Fe(OH)₃, and release of adsorbed P into the overlying hypolimnion. Oxygen depletion is influenced by the decomposition rate of organic matter, which is temperature dependent, and the onset of stratification that inhibits lake mixing (Nürnberg, 1995). The phosphate that is associated with the surface of Fe(OH)₃ represents the upper estimate of potentially mobile P under reducing conditions (Rydin et al., 2000; Kopáček et al., 2005). In lakes in non-calcareous areas, P is largely associated with the surfaces of Fe(OH)₃ and Al(OH)₃, and organic matter.

Amirbahman et al. (2003) estimated sediment $\text{Fe}(\text{OH})_3$ reductive dissolution rate by following rates of changes in hypolimnetic $\text{Fe}(\text{II})$, SO_4^{2-} , and $\text{S}(-\text{II})$ concentrations over time, in a study of 11 Maine lakes. Using these rates, they predicted sediment P flux into the water column. The measured and predicted hypolimnetic P fluxes agreed well, in all but two lakes; two outlier lakes had Fe fluxes similar to the high P lakes, but showed significantly lower P fluxes. A subsequent study showed that excess sediment $\text{Al}(\text{OH})_3$ in the two outlier lakes had effectively sequestered P and inhibited its release following the onset of anoxia (Lake et al., 2007).

1.2.1.2 The Role of Aluminum

Thermodynamically, P as orthophosphate adsorbs more favorably onto $\text{Fe}(\text{OH})_3$ than $\text{Al}(\text{OH})_3$. However, the $\text{Al}(\text{OH})_3$ surface effectively competes with the $\text{Fe}(\text{OH})_3$ surface for P adsorption in lake sediment with a high $\text{Al}(\text{OH})_3$ concentration, limiting P release into the water column under anoxic conditions (Kopáček et al., 2005; Homyak et al., 2014). Al is not a redox sensitive element. Thus, $\text{Al}(\text{OH})_3$ remains insoluble under anaerobic conditions provided that the hypolimnion pH remains between 5.5 and 8.5. $\text{Al}(\text{OH})_3$ has a high sorption capacity for P (Kopáček et al., 2000; Rydin et al., 2000). Under anaerobic conditions, available sites on $\text{Al}(\text{OH})_3$ surface allow for P liberated from $\text{Fe}(\text{OH})_3$ to be adsorbed (Kopáček et al., 2005; Hupfer and Lewandowski, 2008). Lake remediation by Al treatment (alum) has proven effective at lowering internal P loading potential because the Al addition can bind excess P in the hypolimnetic sediment, resulting in irreversible sequestration (Rydin et al., 2000; Jensen et al., 2015). Longevity and effectiveness of treatment depend on the lake morphometry, Al dose, and extent to

which P export from the watershed has been reduced (Welch and Cooke, 1999; Huser et al., 2015).

Psenner et al. (1984) developed a 5-step sequential extraction method for sediment that estimates Fe-associated P and Al-associated P (steps 2 and 3). The extraction sequence has been broadly used in sediment-P research. The bicarbonate-dithionite (BD) extractable P (step 2; section 2.3) represents the fraction of potentially mobile P associated with reducible $\text{Fe}(\text{OH})_3$. Kopáček et al. (2005) titrated lake sediment with dissolved Al in the laboratory. They proposed operational thresholds to estimate potential sediment P release following the reductive dissolution of $\text{Fe}(\text{OH})_3$: (1) in step 2 and 3, if $(1 \text{ M NaOH extractable Al}) / (0.1 \text{ M bicarbonate-dithionite (BD) extractable Fe})$ ratio ($\text{Al}_{\text{NaOH}}:\text{Fe}_{\text{BD}}$) is > 3 , or (2) $(1 \text{ M NaOH extractable Al}) / (0.1 \text{ M bicarbonate-dithionite extractable P})$ ratio ($\text{Al}_{\text{NaOH}}:\text{P}_{\text{BD}}$) is > 25 , then P is effectively and irreversibly sequestered by sediment $\text{Al}(\text{OH})_3$ during anoxic events. The BD-extractable P represents the fraction of potentially mobile P associated with reducible $\text{Fe}(\text{OH})_3$. Measuring these ratios for lake sediment allows identification of lakes that are susceptible to internal P release following the onset of hypolimnetic anoxia (Lake et al., 2007; Homyak et al., 2014).

Lake et al. (2007) tested the model developed by Kopáček et al. (2005) on six dimictic (lake mixing pattern in which lakes mix twice per year) Maine lakes that developed summer hypolimnetic anoxia. Consistent with the model, they observed that lakes whose sediment equaled or exceeded the $\text{Al}_{\text{NaOH}}:\text{Fe}_{\text{BD}} > 3$ and $\text{Al}_{\text{NaOH}}:\text{P}_{\text{BD}} > 25$ ratios released negligible P. However, even though meeting one of these thresholds is sufficient for the inhibition of sediment P release, sediment conditions where $\text{Al}_{\text{NaOH}}:\text{Fe}_{\text{BD}}$

< 3 and $Al_{NaOH}:P_{BD} < 25$ ratios are not sufficient requirements for sediment P release (Lake et al., 2007). Significant sediment P release also requires the presence of an anoxic hypolimnion.

1.2.2 Biological Mechanisms

Bacteria can act as a catalyst to fuel anoxic conditions or can play a direct role in the storage and release of P (Boström et al., 1988; Khoshmanesh et al, 2001). Gächter et al. (1998) demonstrated that microorganisms can directly contribute significant amounts of P to a lake. Some cultures of microbes accumulate P as polyphosphate, and hydrolyze and release it following the onset of anoxia.

Alternatively, biological activity can assist, in addition to physical mixing, with the vertical mobility of P in the water column; for example, *Gloeotrichia echinulate* (*Gloeotrichia*) is a species of cyanobacteria present in oligotrophic lakes across the northeastern U.S. (Carey et al., 2014) and capable of P translocation in the water column by adjusting their buoyancy. *Gloeotrichia* hyper-accumulate P from the nutrient-rich bottom to the photic zone, and may contribute a significant portion of the internal loading of a lake (Barbiero and Welch, 1992).

1.2.3 Physical Mechanisms

Physical characteristics within the lake also affect internal P release. Lake shape, surface area, average depth, and surface area/volume ratio all affect lake hydraulics and the internal mixing regime that controls the rate at which the hypolimnetic P can reach the epilimnion. For some lakes, the morphometry substantially influences chemical and

biological conditions. For example, shallow lakes often experience increased hypolimnetic temperatures that cause increased biological activity. These lakes may have a high sediment oxygen demand that causes anoxia, potentially followed by sediment P release and rapid mixing of the shallow water column.

1.3 Internal Mixing

Temperate lakes are generally either dimictic or polymictic (Wetzel, 2001). Dimictic lakes have two mixing events per year and thermally stratify throughout the summer and winter. Polymictic lake dynamics involve frequent or continuous mixing throughout the year. A stable hypolimnion in a consistently stratified lake allows insignificant vertical mass transfer. As such, epilimnetic oxygen does not reach the bottom and the hypolimnion may develop anoxia. However, internally released P may not reach the photic zone with a concentration significant to affect eutrophication. However, in lakes with an unstable hypolimnion, significant vertical mass transfer may occur whereby oxygen is mixed into the hypolimnion and internally released P can reach the photic zone.

Two opposing forces govern lake mixing: those supplying energy to mix and those inhibiting mixing. Mixing is attributed to destabilizing forces such as wind, cooling or warming from above or below, the temperature of maximum density (4°C), inflow, outflow, and artificial destratification devices. The stabilizing force is primarily the buoyancy that is caused by density differences with depth due to temperature or salinity gradients (Robertson and Imberger, 1994; Gerten and Adrian, 2002). Minor destabilizing processes are unable to overturn a lake in a prolonged warm and calm period. Therefore,

the hypolimnetic and epilimnetic waters remain distinct with relatively little mass transfer between the two (Robertson and Imberger, 1994). Conversely, storm events with high winds and significant precipitation can induce mixing, introducing large amounts of reduced substances (e.g., Fe(II)) and nutrients (e.g., PO₄) into the epilimnetic water (Effler et al., 2004). As duration of stratification increases, the ability of a lake to replenish dissolved oxygen to the hypolimnion decreases, allowing anoxic conditions to cover a greater areal extent of sediment for a longer period of time (Huttula et al., 1993; North et al., 2014). This results in intensified internal loading and stimulation of phytoplankton growth during and after vertical mixing (Wilhelm and Adrian, 2008). In such cases, an intense storm can effectively mix the lake and cause a deterioration of water quality due to nutrient upwelling.

In the last century, average regional temperature in the northeastern U.S. has increased by 2° F (McAvaney et al., 2001). Researchers predict recent warming is linked with alteration of thermal structures within lakes. For example, Hondzo and Stefan (1993) ran model simulations for a variety of lakes. They found that an increase in annual air temperature caused warmer surface water temperature, in small deep Minnesota lakes. However, hypolimnetic temperature decreased by as much as 3.5 °C, likely due to stratification occurring earlier in the season at lower temperatures. A longer stratification period leads to more serious issues with greater oxygen depletion in the hypolimnion during late summer. In shallow lakes, rises in epilimnetic and hypolimnetic temperatures are similar in both magnitude and occurrence (Hondzo and Stefan, 1993). Therefore, hypolimnetic warming is dependent upon lake depth as well as weather variability or climate change (Jankowski et al., 2006).

In this study, we have investigated the controls on epilimnetic total P (henceforth epilimnetic P or total P) in 24 Maine lakes. We focused on determining the P, Al, and Fe concentrations in the sediments to evaluate potential for internal P release. We also quantified land use factors such as agricultural land across each watershed in order to identify vulnerable lakes. This study includes a variety of lakes; the water column data used in our analysis of vulnerability were from one specific point in time and place within each lake. Thus, parameters representing in-lake stability, hypolimnetic temperature, and epilimnetic P reflect instantaneous lake conditions, which can be used to identify cause and effect relationships between independent and dependent variables. We propose models that consider in-lake physiochemical, climate/weather, and watershed characteristics to predict epilimnetic lake P, which allow us to evaluate and compare lake's vulnerability to eutrophication. The following analyses are used to predict critical statistical thresholds relating to vulnerability for a population of lakes. Thresholds in this study represent increased probability of eutrophication upon approach or exceedance.

CHAPTER 2: METHODS AND MATERIALS

2.1 Field Sites

My study included field and laboratory components for 2015. The 2015 portion included sampling sediment and water from 24 lakes located primarily in central and southwestern Maine (Table 2.1; Appendix D; Appendix F). Land use of the 24 watersheds ranged from developed (a mix of agriculture, residences, roads, impervious surfaces, etc.) to forested. The direct watershed areas ranged from 781 to 25,213 ha, lake areas (174 to 3453 ha), and mean depth (4 to 23.5 m).

We classified trophic range of each lake based on Wetzel's (2001) classification in which oligotrophic lakes have total P < 10 ppb, mesotrophic lakes have 10 < total P < 30 ppb, and eutrophic lakes have 30 < total P < 100 ppb. The 2015 lakes spanned oligotrophic to mesotrophic conditions (Table 2.1). None of the lakes were classified as eutrophic.

Table 2.1 Selected Properties of the 2015 Lakes. Results are reported in order of increasing total epilimnetic P. Epilimnetic P, Chlorophyll a, and Secchi depth are for August 2015. Cultivated crop and hay/pasture lands are reported from 2004 (MELCD).

Lake	Midas	Epilimnetic P, ppb	CHL A	Secchi, m	Watershed Area, ha	Lake Area, ha	Maximum Depth, m	Mean Depth, m	Cultivated Crops, ha	Hay/Pasture, ha
Pleasant P	224	1.9	<1	15.98	1484	420	60.4	23.5	0	0
Tunk L	4434	2.6	1.4	10.9	2936	838	67.7	21.6	0	1
Clearwater P	5190	3.3	1.2	9.91	1598	322	39	18.3	0	15
Thompson L	3444	3.5	2.1	10.35	10802	1788	36.9	10.7	65	504
Embden P	78	4	1.6	9.81	4493	624	48.2	18.9	0	1
Square P	3916	4	2.4	7.5	1240	355	13.4	6.1	7	13
Pleasant L	3446	4.2	2.7	5.1	2009	539	18.9	8.8	13	53
Hopkins P	4538	4.4	1.6	5.95	781	174	19.8	7.9	1	0
Taylor P	3750	5.1	3.2	5.5	3772	264	13.4	5.2	32	371
Meddybemps L	177	5.2	3.3	6.25	9867	2719	17.7	4.3	131	27
Long P	5272	5.3	4.6	7.34	6080	1035	32.3	10.7	75	81
Mousam L	3838	5.5	2.4	7.8	5455	397	29.9	5.2	40	313
Auburn L	3748	6.1	2.3	8.67	3558	921	36	11	43	286
Great P	5274	6.8	4.3	7.05	11878	3453	21	6.4	192	237
Messalonskee L	5280	7.5	3.5	5.35	12428	1494	34.4	10.1	319	749
Damariscotta L	5400	7.5	5.4	6.25	11496	1896	34.7	9.1	186	800
McGrath P	5348	9.3	2.9	6.1	1136	189	8.2	4.9	23	7
Salmon L (Ellis P)	5352	10.7	5	5.1	1077	281	17.4	7	46	15
Unity P	5172	12.6	25.3	1.33	25213	1040	12.5	6.7	1310	2227
East P	5349	12.6	3.6	5.34	1917	695	8.2	5.5	13	11
China L	5448	13.9	17.1	1.8	8282	1594	25.9	8.5	213	657
North & Little P	5344	19	5.2	4.65	5543	1024	6.1	4	231	212
Sabattus P	3796	19.2	22.1	1.85	7403	798	5.8	4.3	195	961
Webber P	5408	21	6.4	2.25	2650	499	12.5	5.5	100	209

2.2 Aqueous Collection and Analysis

Lakes in Table 2.1 were sampled in June and August 2015 at the deepest point for water samples, and sampled only in June for sediment samples. Dissolved oxygen (DO) and temperature were measured (YSI-52 probe) in 1-2 m increments from the surface to 1 m from the sediment surface. Integrated epilimnion core samples were collected using a flexible rubber sampling tube from the water surface to 1 m into the thermocline. Water samples from the hypolimnion were collected with a Kemmerer from 1 m from the sediment-water interface. Secchi disk transparency was determined on descent and ascent to determine water clarity (Tables 2.1).

Sub-samples were taken for closed-cell pH, anions (SO_4^{2-} , NO_3^- , Cl^-), unfiltered total cations (Ca, Mg, Na, K, Al, and Fe), total P, dissolved organic carbon (DOC), and chlorophyll a. Cation samples were acidified in the field with 50% nitric acid to a $\text{pH} < 2$. Closed-cell pH was measured by using a TitraLab TIM860 Titration Manager. Ion chromatography (Dionex DX-500) was used to analyze the anions. Following ammonium peroxydisulfate digestion (250 °C, 0.5 h), total P was measured with a Varian Cary 50 spectrophotometer using a molybdate blue coloring reagent. A high resolution ICP-MS (Thermo Element 2) was used to measure cation concentrations. For quality control, blank, replicate, and analyte-spiked samples were run every ten field samples; the error was within 5% for all samples.

2.3 Sediment Collection and Analysis

Sediment samples were obtained from each lake at two locations with a Hongve gravity corer (Hongve, 1972). The sampling locations were at the deepest point of each

lake, and at a depth equal to one half of the deepest point. Sampling location of the half depth points were not recorded via GPS. Samples at 0-2 cm and 8-10 cm were composited from three cores collected within a 3 m radius, and were transferred into Whirl-pak™ bags, placed on dry ice in the dark, and transferred to the laboratory, where they were kept frozen until analysis.

The sediment 5-step sequential extraction procedure followed a modified version of Psenner et al. (1984). The first (ion-exchangeable fraction) was omitted because several studies on Maine lake sediments indicated that the typical extractable base cations (except Ca), Al, Fe, and P in the first extraction were <1% of the second and third extraction. We also eliminated the fifth (total residual extractable fraction). Two grams of wet sediment were sequentially extracted with 25 ml of solution as follows: (2) 0.11 M NaHCO₃ and 0.11 M sodium dithionite (NaS₂O₄) at 40 °C for half an hour to extract Fe (Fe_{BD}) and the associated P (P_{BD}) via the reductive dissolution of Fe(OH)₃. (3) 1.0 M NaOH at 25 °C for 16 hr to extract Al (Al_{NaOH}) due to the dissolution of Al(OH)₃, and P (P_{NaOH}) that is largely associated with organic matter and Al(OH)₃. This step also leads to dissolution of some, probably slightly crystallized, Fe(OH)₃ that was not dissolved in the previous step. (4) 0.5 M HCl at 25 °C for 16 hr to extract P associated with any calcite (CaCO₃) or apatite (Ca₅(PO₄)₃(OH, Cl, F) present (Kopáček et al., 2005), as well as Al(OH)₃ and Fe(OH)₃ that did not dissolve in the previous two extractions. Calcite has not been observed in the sediment of any of these lakes. The extractions were conducted in 35 mL centrifuge tubes (Thermo Scientific™ Nalgene Polycarbonate), which were rinsed in DI water, not the reagents. Following extraction, the tubes were centrifuged at 3,000 rpm for 15 min. Concentrations of P, Al, Fe, and Ca were determined using

inductively coupled plasma atomic emission spectrometry (ICP-AES; Thermo Element 2). For quality control, blank and replicate samples were run every ten field samples. A sub-sample of the homogenized sediment was dried at 100 °C to determine water weight percent, followed by combustion at 550 °C to determine the loss-on-ignition (LOI), equated to the organic matter content.

2.4 Pre-existing Data Compilation

The Maine Department of Environmental Protection (DEP) provided water and sediment chemistry (Appendix B) and morphometry for 106 lakes sampled from 2010 to 2012. Water samples included separate samples for total cations (Ca, Mg, Na, K, Al, Fe), anions (Cl^- , NO_3^- , SO_4^{2-}), DOC, acid neutralization capacity (ANC), total epilimnetic (core) and hypolimnetic (1 m from bottom) P, chlorophyll a, and closed-cell pH. Profiles of temperature and dissolved oxygen (DO), and Secchi disk transparency depth were determined for each lake. The samples were collected in August of 2010-2012. Sediment chemistry consisted of Al, Fe, and P concentrations in the 0-2 cm and 8-10 cm intervals, for extractions BD, NaOH, and HCl using the Psenner method. Sample collection, extraction, and analysis followed the same procedure mentioned in sections 2.2 and 2.3 and occurred in the same laboratory. Lake morphometry information consisted of lake elevation, flushing rate, maximum depth, average depth, watershed area, and layer area and volume at each meter by depth.

The Lakes Environmental Association (LEA) provided data for 23 lakes sampled in August 2013 (Appendix B). These data consisted of the same parameters as the DEP lakes with the exception of water column cations, anions, or ANC metrics. Sampling and processing procedures were the same as described in sections 2.2 and 2.3 and analysis was in the same laboratory.

Average, maximum, minimum, and cumulative precipitation at each lake were obtained from Weather Underground (<https://www.wunderground.com/>). Data spanned two time periods, one starting January 1st to the sampling date and the other from May 1st to the sampling date (Appendix E). Data collected from this web site originates from the National Weather Service. Precipitation data provided the basis to assess the effect of drought or intense storms on lake water quality.

Stream Stats (<https://water.usgs.gov/osw/streamstats/>) from the United States Geological Survey (USGS) was used to access watershed information pertaining to each lake. Information included the percentage of storage for the combined water bodies and wetlands (from the National Wetlands Inventory) and the mean basin slope, which was computed from 10 m digital elevation model (DEM) from Stream Stats. (<https://www.nrcs.usda.gov/wps/portal/nrcs/detail/soils/survey/>).

Maine Geographical Information Systems (MEGIS; <http://www.maine.gov/megis/>) were accessed to acquire the land cover spatial data in each watershed (Appendix D; F). This information was collected from MELCD (Maine Land Cover Dataset; <http://www.maine.gov/megis/catalog/metadata/melcd.html#ID0EUEA>), a land cover map derived from Landsat Thematic Mapper 5 and 7 from the years 1999-2000. Spatial data

were collected with a spatial resolution of 30 m. SPOT 5 panchromatic imagery from 2004 was used, to refine this map. The SPOT 5 imagery was collected with a spatial resolution of 5 m. The 1999-2000 maps were refined to reflect 2004 conditions.

2.5 Model Development

MELCD and ArcGIS version 10.4 were utilized to construct field maps (Appendix F) and create parameters to represent human impact. These data were used to explore the ratio of land cover area relative to the lake or watershed area. We were able to identify agricultural land area in the lake watershed and create parameters such as Agricultural area: Lake Area (Ag:LA) ratio based on the direct lake watershed and the surface area of the lake. Direct watershed or sub-watershed refers to the topographic features contiguous to one lake; it does not account for chain of lake effects or the entire watershed. Agriculture lands were identified in ArcGIS by the most current land cover map for the state of Maine (MELCD; Appendix D). Other parameters such as Adjacent Agriculture: Lake Area (AdjAg:LA) ratio were quantified by including only the land cover types contiguous to the lake, or the land in close proximity to the lake. This includes land that is separated from the lake by a narrow layer of a different land type. Land cover type is variable in shape; therefore, each lake was independently evaluated to determine adjacent land cover.

To evaluate the effect of development, the road:watershed ($m^2:m^2$) ratio was calculated (Appendix D), with the assumption that road density is proportional to development density and population, greater external P input. The DEP provided watershed and lake shapefiles consisting of surface area and length of roads. MEGIS

provided a road shapefile and type (private, secondary, forestry-related, gated, etc.). The surface areas of roads in each watershed were calculated. ArcGIS from Environmental Systems Research Institute (ESRI) was used to delineate direct watersheds and clip roads to the selected watershed. Google Earth was used to measure road widths, providing the basis for the calculation of total road area.

Spatial data were examined using regression tree analysis, multiple linear regression, and quantile regression using R statistical software with the August epilimnetic P as the dependent variable. The statistical analyses allowed for an exploration of approaches to advance the understanding of lake dynamics, for example: the regression tree examined the population of lakes based on epilimnetic P for significant variables and relatable thresholds, while multiple linear regression equations were used to predict epilimnetic P values, and quantile regression was used as a development tool to relate the management of Agricultural area within the watershed to epilimnetic P. This three-tiered approach to statistical exploration allowed for the development of models to inform management in terms of sustainability solutions. Significance of each parameter in the model was based on a p-value ≤ 0.05 . Before modeling using the multiple linear and quantile regression methods, all variables were examined for normal distribution. Many variables presented positive skew, providing rationale to use log transforms. Values for the regression tree were not log transformed.

2.5.1 Regression Tree Analysis

A decision or regression tree was developed to identify critical statistical thresholds for predicting epilimnetic P through the use of a partition model. A regression

tree explains the variation of a single response variable (epilimnetic P) by one or more explanatory variables (De'ath and Fabricius, 2000). The tree performs dichotomous splits according to the relationship between the response and predictor variables by identifying groupings of predictor values that minimize residual sum of squares (RSS) within group variance (Huser et al., 2015). The recursive partitioning is repeated within each of the groups for all predictors (Quinn and Keough, 2002); the predictor variables can be used repeatedly throughout the tree, which allows the variable to be reevaluated after the previous splits have been made.

Regression tree analysis was used to develop a model able to predict a target variable value based on multiple predictor variables. Regression trees begin with the "root" (complete unsplit data) at the top, and branches down with nodes for each division and end in leaves (terminal nodes) where branches terminate (Quinn and Keough, 2002). The value listed at each split node represents the mean value from the response variable (Quinn and Keough, 2002); this contrasts with traditional regression, which predicts an individual value for each observational value.

A larger sample size produces a better model. A small change to the training data can cause a very different series of splits, which limits predictive performance and introduces uncertainty (Hastie et al., 2001). To combat over-fitting it is possible to 'prune' the tree to produce a generalized model. The goal is to have a balance between simplicity, in connection with the fewest nodes and explained variance in the response variable (Quinn and Keough, 2002). Cross validation was used to test error on regression tree analysis; this method involves separating the data into a calibration and validation set

to calculate the percent of variation explained between the observed and the predicted values.

We utilized a calibration set of the 24 lakes from 2015, limiting the number of significant splits available to the partition model. We set the minsplit number, the minimum number of observations required for a split, to 5 and adjusted the complexity parameter (which determines the amount by which splitting improves the relative error) to 0.001. Any split that did not improve the model by 0.001 was not pursued, affecting the overall model fit. A complex tree is unable to form accurate generalization from the training data set, and therefore unable to accurately predict the fit of the test set. Regression tree analysis was performed in R (R Core Team, 2015) using the package rpart (2015), version 4.1-10 (Therneau et al., 2016).

2.5.2 Linear Regression Analysis

Typically a regression model is used to investigate the relationships between one dependent and various independent variables. Multiple linear regressions were used to form predictive models by quantifying the strength of the relationship between response (epilimnetic P) and predictor variables. Model validation was completed to determine whether the results of statistical evaluations were capable of describing the data with certainty. The calibration set (2015, Table 2.1 and 2.2) was used to evaluate the regression relationships. The validation set (DEP + LEA, Table 2.2) was used to understand the validity of the predictive relationship. The lowest AIC indicates the best fit (Quinn and Keough, 2002). The AIC is a measure of the relative quality of a model for a set of data, and provides a means for model selection. AIC seeks a model in which the

likelihood is maximized and number of parameters is minimized. The ΔAIC of a model determines the difference between AIC of that model and the model with the lowest AIC. A $\Delta\text{AIC} < 2$ indicates that the models are considered equally optimal, while $\Delta\text{AIC} > 10$ denotes that models are significantly different (Burnham and Anderson, 2002; Brett and Benjamin, 2008). Residual sum of squares (RSS) was calculated as a measure for the amount of error remaining between the observed and predicted August epilimnetic P concentrations. A minimized RSS value identifies the model that explains a greater amount of the data.

Table 2.2: Data from the Study (2015) and other organizations (DEP + LEA).

Origin	<i>n</i>	Epilimnetic <i>p</i>	<i>P</i>_{BD}	<i>Al</i>_{NaOH}:<i>P</i>_{BD}	<i>Z</i>_{avg}	<i>Sch</i>	Ag:WA	Ag:LA	AdjAg:WA	Rd:WA	<i>T</i>_{hyp}	DOC	pH
2015	24	✓	✓	✓	✓	✓	✓	✓	✓	✓	✓	✓	✓
DEP	96	✓	✓	✓	✓	✓	✓	✓	✓	✓	✓	✓	✓
LEA	23	✓	✓	✓	✓	✓	✓	✓	✓	✓	✓	X	✓
Total	143	143	143	143	143	143	143	143	143	143	143	120	137*

* Indicates data missing from the DEP.

2.5.3 Percentile Selection Quantile Regression Analysis

Quantile regression (QR) is a robust statistical method capable of estimating rates of change over the entire distribution of a response variable (Koenker and Bassett Jr., 1978). It is effective for datasets with unequal variation due to complex interactions among variables (Cade and Noon, 2003), specifically when not all the factors affecting the response variable can be taken into account (Xu et al., 2015). System complexity can also be illustrated by unequal variation in the dataset; meaning more than one slope is affecting the relationship between the response and predictor variables (Cade and Noon, 2003).

Using QR, we explored the response of Ag:WA ratio to epilimnetic P across a range of quantiles. Quantiles are the points in a distribution that relate to the rank order of values in that distribution. For example: for $\tau=0.80$, 80% of the values for the dependent variable are less than or equal to the specified function of the independent variable(s) (Cade and Noon, 2003). The basic equation for the quantile regression function is:

$$Y^{(\tau)} = b_0^{(\tau)} + b_1^{(\tau)}(X) + \varepsilon_i^{(\tau)}$$

where, $b_0^{(\tau)}$ and $b_1^{(\tau)}$ describe the intercept and slope relating the τ^{th} quantile of Y to X, and $\varepsilon_i^{(\tau)}$ denotes the residual term for the τ^{th} quantile with an unknown distribution. For this study, X and Y represent Ag:WA ratio and log epilimnetic P, respectively.

Adopting the method of percentile selection (Xu et al., 2015) provided the basis to create subsets within the data by ranking the lake average depth (Z_{avg}) and $Al_{NaOH}:P_{BD}$ ratio based on the 50th and 75th percentiles, and to sort the Ag:WA ratio and epilimnetic P accordingly. QR analysis was applied to these subsets, the distributions were fit by the 80th quantile model. The 80th quantile models predict epilimnetic P concentration threshold targets (target = 15 ppb) allowing us to predict how much Ag:WA ratio should be adjusted in order to maintain the threshold value of epilimnetic P in the system. Utilizing the 80th percentile, allows for a more conservative approach for predicting the threshold value. QR analysis was performed in R (R Core Team, 2015) using the package `quantreg` (2016), version 5.26 (Koenker et al., 2016).

CHAPTER 3: RESULTS

We hypothesized that in-lake physiochemical characteristics, climate/weather factors, and watershed characteristics control lake water quality.

3.1 Physiochemical Characteristics

Lake physiochemical characteristics include morphometry, sediment chemistry, and water chemistry.

3.1.1 Morphometric Characteristics

The relationship between lake depth and surface area were quantified using the Osgood Index (OI; Osgood, 1988):

$$OI = \frac{Z_{avg}}{A_s^{1/2}} = \frac{1}{A_s^{3/2}} \int_0^{z_{max}} A(z) dz \quad \text{Eq. 1}$$

where, Z_{avg} is the area-averaged depth, A_s is the lake surface area, $A(z)$ is the lake area at depth z , and z_{max} is the maximum depth. Osgood suggested that lakes with $OI > 6$ develop a stable thermal stratification, whereas lakes with $OI < 6$ are susceptible to summer mixing. Our results (Figure 3.1) suggest that lakes with a high OI have a low August epilimnetic P concentration, whereas lakes with a high epilimnetic P concentration have a low OI. In general, shallow lakes that have a low OI are more susceptible to mixing by wind. Therefore, internally released P from the sediment may reach the epilimnion at a faster rate. In deeper lakes with a high OI, internally released P from bottom sediment may not reach the epilimnion rapidly, or even until fall overturn.

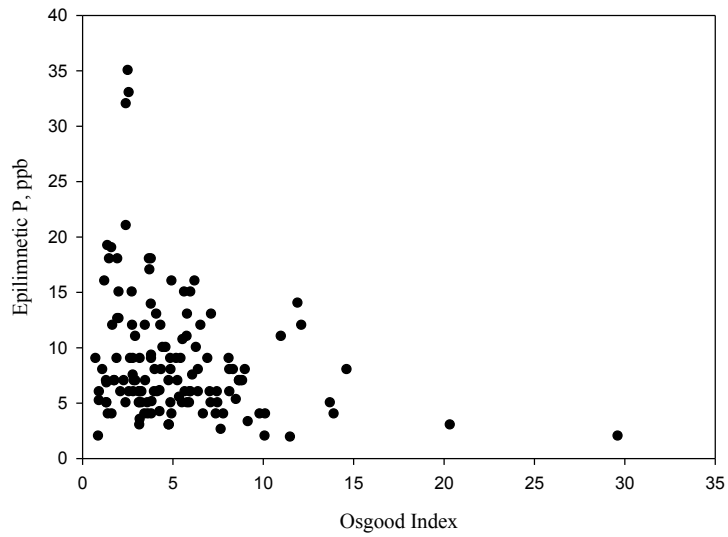


Figure 3.1: The Osgood Index (Eq. 1) versus the August epilimnetic P. Includes 143 (2015 + DEP + LEA) Maine lakes. Linear regression represents an $R^2 = 0.06$ and p-value < 0.05 .

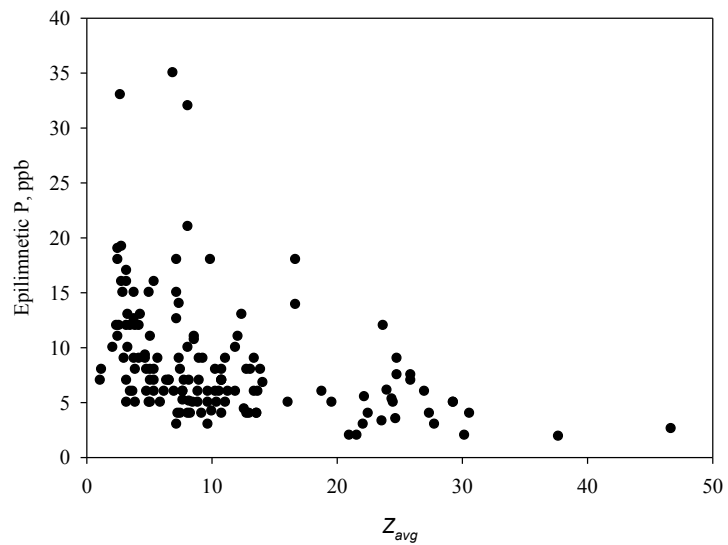


Figure 3.2: The area-averaged depth (Eq. 2) versus the August epilimnetic P. Including 143 (2015 + DEP + LEA) Maine lakes. Linear regression represents an $R^2 = 0.15$ and p-value < 0.05 .

The relationship between the average depth (Eq. 2) and the August epilimnetic P is:

$$z_{avg} = \frac{1}{A_S} \int_0^{z_{max}} A(z) dz \quad \text{Eq. 2}$$

(Figure 3.2). Similar to its relationship with OI, deeper lakes tend to have lower August epilimnetic P, and all high epilimnetic P lakes are relatively shallow and more susceptible to having high epilimnetic P concentrations due to vertical mixing.

We also considered watershed area:lake area (WA:LA) ratio as a surrogate for hydraulic residence time which is a measure of the average length of time that water remains in storage. A low WA:LA ratio, for example, indicates longer residence time and higher percentage of internally loaded P. Conversely, lakes with higher WA:LA ratios are likely more driven by external P sources (Fraterrigo and Downing, 2008; Huser et al., 2015). However WA:LA was not significantly correlated to epilimnetic P and did not significantly contribute to any of the analyses (Table C2, Appendix C).

3.1.2 Surficial Sediment Fractionation

Internal P loading is an important source of P to lakes undergoing summer anoxia. In these lakes the predominant mechanism involves the reductive dissolution of sediment $\text{Fe}(\text{OH})_3$ and the release of sediment-bound P from the $\text{Fe}(\text{OH})_3$ into the overlying water (Mortimer, 1941).

3.1.3 Sediment Phosphorus

The total extractable sediment P concentration ($TP_{\text{ext}} = P_{\text{BD}} + P_{\text{NaOH}} + P_{\text{HCl}}$) ranged from 25 to 218 $\mu\text{mol g}^{-1}$ for the 24 (2015) lakes (Table B1, Appendix B). For the low epilimnetic P lakes (defined as August epilimnetic TP < 10 ppb), the largest percentage of TP_{ext} was in the NaOH fraction, ranging from 43 to 94% of TP_{ext} . For these lakes, the reducible P_{BD} fraction ranged from 4 to 55% of TP_{ext} . For lakes with epilimnetic TP > 10 ppb, the sediment P_{NaOH} and P_{BD} fractions were 43 to 80% and 10 to 50% of TP_{ext} , respectively. The P_{HCl} fraction remained relatively low at 4 to 13% of TP_{ext} . The TP_{ext} for the set of 119 (DEP + LEA) lakes ranged from 14 to 190 $\mu\text{mol g}^{-1}$. The largest percentage of TP_{ext} for these lakes was in the P_{NaOH} fraction with an average of 81%.

3.1.4 Sediment Iron

The total extractable Fe concentration (TFe_{ext}) ranged from 98 to 1,376 $\mu\text{mol g}^{-1}$ for the 24 (2015) study lakes (Table B1, Appendix B). Regardless of lake productivity, most TFe_{ext} was in the BD- and HCl-extractable fractions, ranging from approximately 19 to 82% and 8 to 78%, respectively. On average 87% of TFe_{ext} consisted of BD- and HCl-extractable fractions. TFe_{ext} for the set of 119 (DEP + LEA) lakes ranged from 54 to 1,843 $\mu\text{mol g}^{-1}$; on average 75% consisted of Fe_{BD} and Fe_{HCl} fractions.

3.1.5 Sediment Aluminum

The total extractable Al concentration (TAl_{ext}) ranged from 232 to 713 $\mu\text{mol g}^{-1}$ for the 24 (2015) study lakes (Table B1, Appendix B). Regardless of lake productivity level, 98% of TAl_{ext} was in the Al_{NaOH} and Al_{HCl} fractions, which ranged from

approximately 23 to 72% and 14 to 77%, respectively. The surficial sediment in Mousam Lake contained a high Al_{BD} fraction at 27% of TAl_{ext} . The TAl_{ext} for the 119 (DEP + LEA) lake set ranged from 188 to 1026 $\mu\text{mol g}^{-1}$; on average Al_{NaOH} plus Al_{HCl} fractions comprised 99% of extractable Al.

3.1.6 The $Al_{NaOH}:Fe_{BD}$ and $Al_{NaOH}:P_{BD}$ Ratios

Previous work has shown that sediment molar $Al_{NaOH}:Fe_{BD}$ and $Al_{NaOH}:P_{BD}$ ratios predict the mobilization potential of sediment P (Kopáček et al., 2005; Lake et al., 2007). These ratios are plotted against the epilimnetic P (Figures 3.3 and 3.4), and hypolimnetic P (Figures 3.5 and 3.6). Those studies showed that lakes with $Al_{NaOH}:Fe_{BD}$ ratios > 3 or $Al_{NaOH}:P_{BD}$ ratios > 25 release low P concentrations during anoxia. For the 24 (2015) study lakes, the $Al_{NaOH}:Fe_{BD}$ and $Al_{NaOH}:P_{BD}$ ratios ranged from 0.2 to 5.2 and 2.4 to 214.8, respectively (Appendix C). All (2015 + DEP + LEA) lakes with $Al_{NaOH}:Fe_{BD}$ ratios > 3 had lower epilimnetic P concentrations (Figure 3.3) and low hypolimnetic P concentrations (Figure 3.5).

Among the 24 (2015) study lakes, only Pleasant (Caratunk) and Hopkins had $Al_{NaOH}:Fe_{BD}$ ratios > 3 , corresponding to lakes with a low epilimnetic P concentrations; the sediment in the remaining 22 lakes did not exceed this ratio (Appendix C). The majority of lakes with relatively high epilimnetic P concentrations (> 15 ppb) had relatively low $Al_{NaOH}:P_{BD}$ ratios, although some had $Al_{NaOH}:P_{BD}$ ratios > 25 (Figure 3.4), illustrating that individual ratios may not predict epilimnetic P perfectly. For example, among the 24 (2015) study lakes: Square, Mousam, Auburn, and Messalonskee had $Al_{NaOH}:P_{BD}$ ratios < 25 but low epilimnetic P concentrations. These lakes had unfavorable

sediment geochemistry indicating that the lakes were capable of significant P release; however, low epilimnetic P concentrations were observed. Therefore, other factors such as Z_{avg} , Sch , $WA:LA$ ratio, and $Ag:WA$ ratio, among others, play a role in keeping these lakes from releasing internally loaded P into the epilimnetic water. For example Lake Auburn had a Sch of 867 J/m^2 on the sampling day, indicating a stratified lake. Conversely, North Pond had a high epilimnetic P concentration with an $Al_{NaOH}:P_{BD}$ ratio > 25 ; North Pond does not act as anticipated because it is shallow and on the day of sampling had a Sch of 5 J/m^2 . North Pond is likely affected by external P inputs because 8.0% of the watershed is comprised of agricultural lands. All (2015 + DEP + LEA) lakes with a low hypolimnetic P had $Al_{NaOH}:P_{BD} > 25$ (Figure 3.6), consistent with the model proposed by Kopáček et al. (2005).

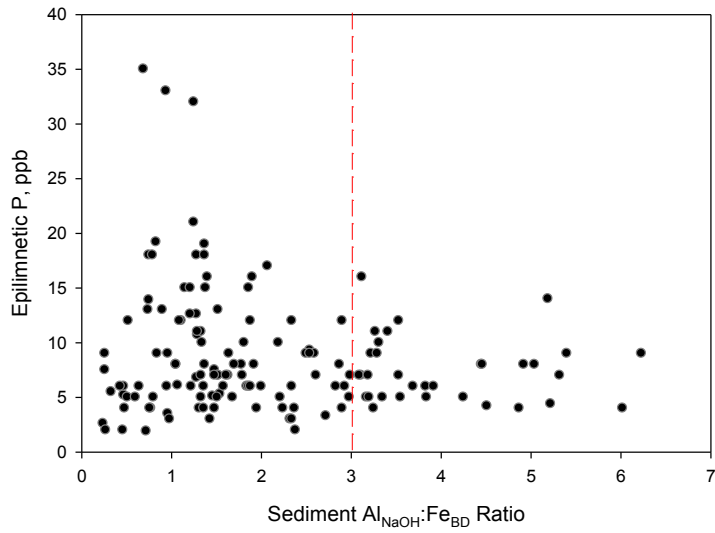


Figure 3.3: Sediment $Al_{NaOH}:Fe_{BD}$ versus Epilimnetic P. Including 143 (2015 + DEP + LEA) Maine lakes.

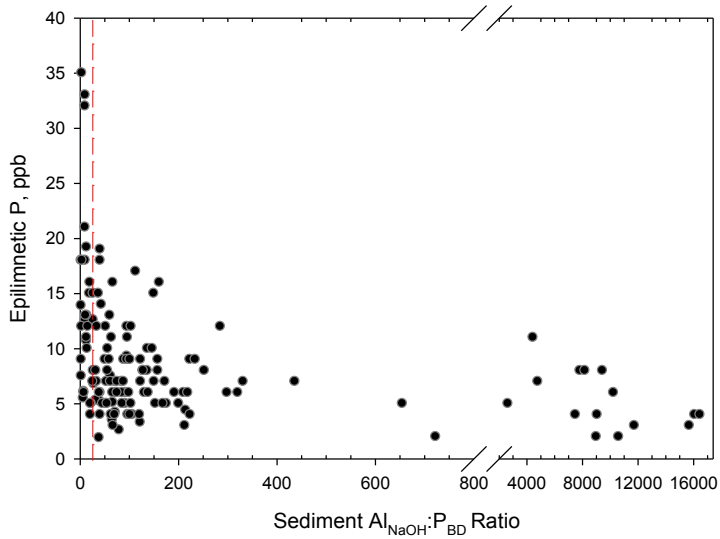


Figure 3.4: Sediment $Al_{NaOH}:P_{BD}$ ratio versus epilimnetic P. Including 143 (2015 + DEP + LEA) Maine lakes.

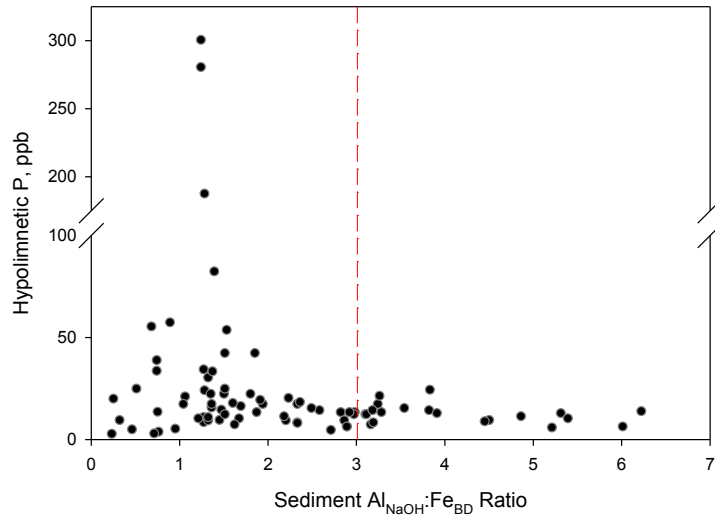


Figure 3.5: Sediment $Al_{NaOH}:Fe_{BD}$ ratio versus Hypolimnetic P. Including 84 (2015 + DEP + LEA) Maine lakes.

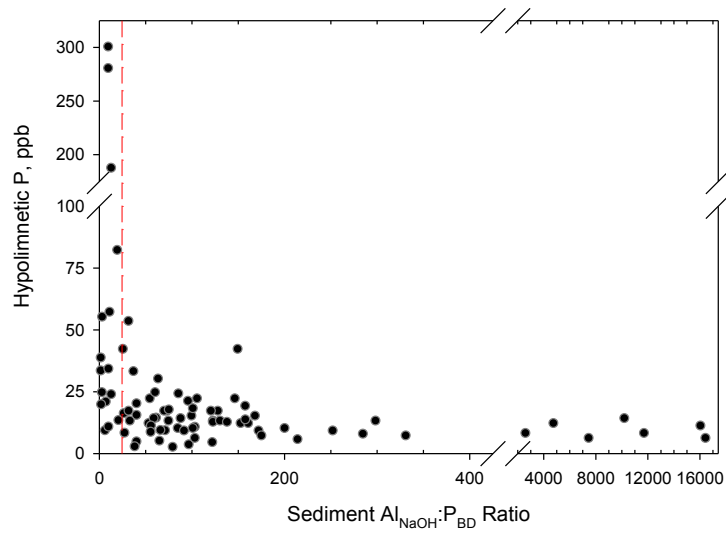


Figure 3.6: Sediment $Al_{NaOH}:P_{BD}$ ratio versus Hypolimnetic P. Including 84 (2015 + DEP + LEA) Maine lakes.

3.1.7 Water Chemistry

Statistical modeling suggests that among the aqueous species, lake DOC concentration and pH are the most important predictors for the August epilimnetic P concentrations (section 3.4). In recent decades, DOC concentrations have been increasing in surface waters of Europe and North America (Monteith et al., 2007). DOC is projected to continue increasing due to recovery from soil acidification and may be rebounding to levels typical of pre-industrial times (Monteith et al., 2007). DOC influence on the lake ecosystem is complex and not fully understood (Solomon et al., 2015). Increasing DOC attenuates light, decreasing the epilimnetic depth, and enhancing stratification (Solomon et al., 2015). Homyak et al. (2014) hypothesized that DOC may act as a transport mechanism for nutrients including P. DOC concentration in lakes is a result of watershed land cover type and water retention time in the lake (Gergel et al., 1999). Higher concentrations are generally due to the presence of wetlands.

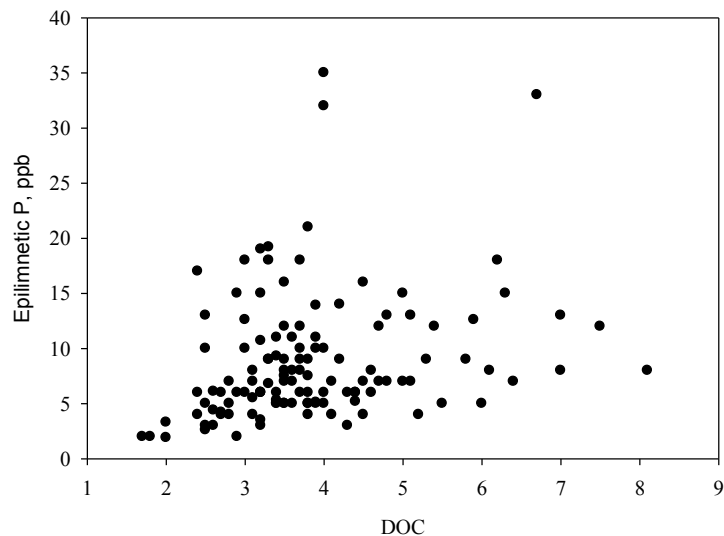


Figure 3.7: The DOC versus Epilimnetic P. Including 120 (2015 + DEP) Maine lakes. Linear fit provided an $R^2 = 0.086$ and p-value < 0.05 .

There is no relationship between lake DOC and epilimnetic P (Figure 3.7). For the 24 (2015) study lakes, DOC concentrations in the epilimnion ranged from 2.0 to 5.9 mg/L, similar to their concentrations in the hypolimnion that ranged from 1.9 to 5.8 mg/L. In the remaining lakes (DEP) epilimnetic DOC ranged from 1.7 to 8.1 mg/L (Appendix C).

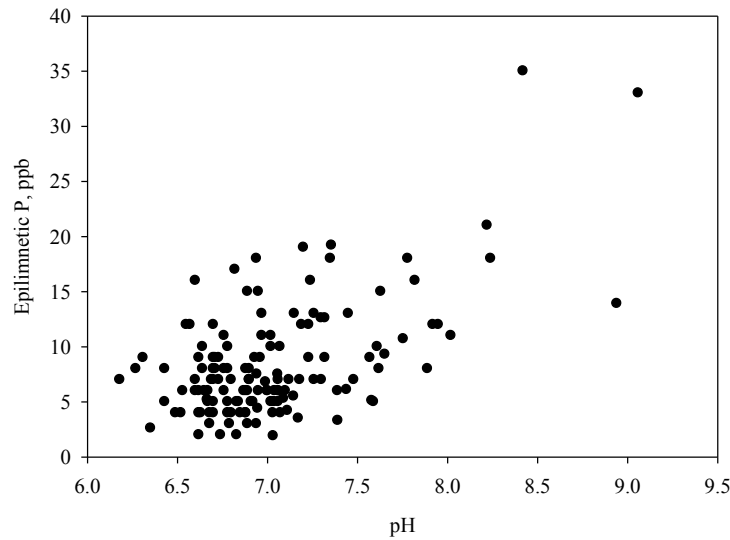


Figure 3.8: Epilimnetic pH versus Epilimnetic P. Including 137 (2015 + DEP + LEA) Maine lakes. Linear fit provided an $R^2 = 0.330$ and $p\text{-value} < 0.05$.

In this study, the relationship between epilimnetic pH and P is weak, but significant and positive (Figure 3.8). For the 24 (2015) lakes, pH ranged from 6.4 to 8.9 and hypolimnetic pH ranged from 5.8 to 7.1. The remaining lakes (DEP + LEA) had epilimnetic pH ranging from 6.2 to 9.1, epilimnetic P ranging from 2 to 35 ppb, and hypolimnetic P ranging from 6 to 300 ppb (Appendix C).

3.2 Climate Factors

Climate/weather factors include hypolimnetic water temperature, wind intensity, and precipitation, all of which potentially influence lake water quality. These factors in conjunction with the lake morphometric properties control lake thermal stratification.

Water temperature can affect the lake water quality in two ways:

(1) Warmer waters lead to higher levels of microbial activity that increase the sediment oxygen demand and may result in the onset of anoxia, especially in bottom waters. A warm hypolimnion can bring about a rapid depletion of dissolved oxygen if there is enough primary production to exceed the oxygen available, and subsequently release P and redox-sensitive species such as Fe(II) and Mn(II), from sediment. In lakes with warm bottom waters that are not thermally stable, upward mixing of P-rich waters is readily facilitated by wind. Our results show a weak but positive correlation between hypolimnetic temperature and August epilimnetic P (Figure 3.9).

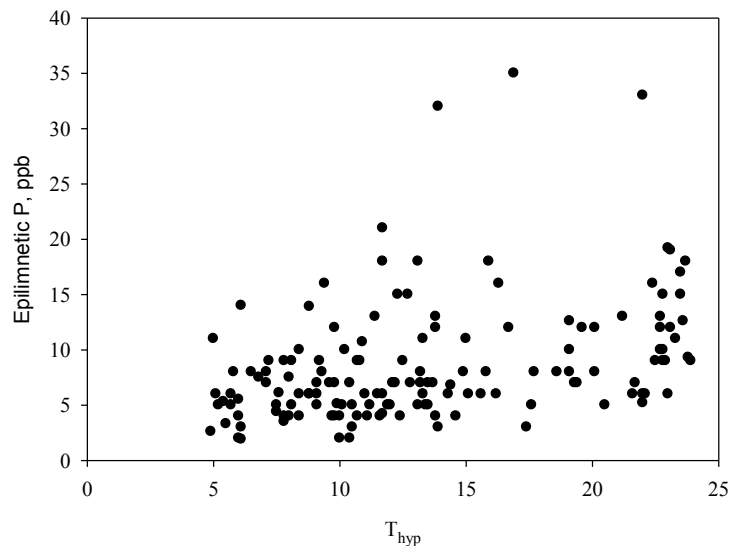


Figure 3.9: Hypolimnetic Temperature versus Epilimnetic P. Including 143 (2015 + DEP + LEA) Maine lakes. Linear fit provided an $R^2 = 0.15$ and p -value < 0.05 .

(2) The vertical temperature distribution of a lake affects its thermal stability.

Thermally stable lakes are characterized by cooler hypolimnia overlain by warmer epilimnia. In such lakes, the density difference between the two layers may cause sufficient buoyancy to counteract the destabilizing shear forces created by wind. Thermal stability is subject to change throughout the season depending on the climate and weather factors, such as storm intensity along with air and water temperature. The Schmidt stability (*Sch*) characterizes the thermal stability of a lake (Schmidt, 1928). *Sch* is the energy required to mix a unit lake surface area (e.g., J/m²), and is calculated by integrating the lake surface area at different depths and the vertical temperature distribution:

$$Sch = \frac{g}{A_s} \int_0^{z_{max}} (z - z_v) \rho(z) A(z) dz \quad \text{Eq. 3}$$

In Eq. 3, *g* is the acceleration of gravity, $\rho(z)$ is the density of the water at depth *z*, and *z_v* is the depth to the center of volume of the lake (Read and Muraoka, 2011),

$$z_v = \frac{\int_0^{z_{max}} z A(z) dz}{\int_0^{z_{max}} A(z) dz} \quad \text{Eq. 4}$$

Schmidt stability does not explicitly account for wind velocity, even though the destabilizing effect of wind is implicitly included in the homogenization of the density gradient (Robertson and Imberger, 1994). A strong thermal stability has a high *Sch* value. Therefore, lakes with a high *Sch* are less susceptible to physical mixing than lakes with a low *Sch*. In general, shallow lakes possess a low *Sch*. In theory, *Sch* in dimictic lakes approaches zero during the fall and spring turnovers, when the water column mixes

completely. Sch increases after the spring turnover and reach its maximum during the late summer. In fall, as the epilimnion gradually cools, Sch decreases to a minimum.

Our results show that lakes with $Sch > 600 \text{ J/m}^2$ in August have a low August epilimnetic P, suggesting that P-rich bottom waters migrate at a slower rate to the top in thermally stable lakes, and all high August epilimnetic P lakes have a lower Sch (Figure 3.10).

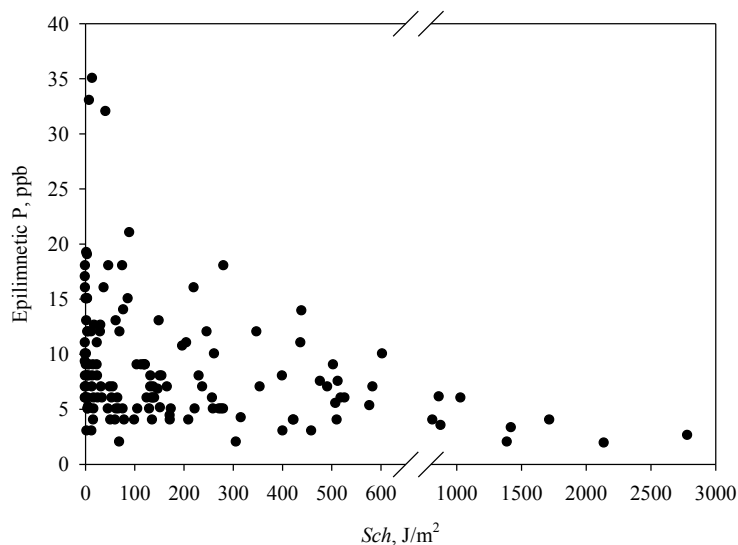


Figure 3.10: Schmidt Stability versus Epilimnetic P. Including 143 (2015 + DEP + LEA) Maine lakes.

(3) Increased precipitation may lead to increased P export from the watershed (Roy et al., 1999) and lake mixing may be enhanced if precipitation is substantial and associated with wind (Effler et al., 2004). To capture the effect of precipitation on lake water quality, we assessed the impact of cumulative rainfall data for a given year prior to the day (in August) of sampling in the MLR models. Precipitation parameters were not significantly correlated to epilimnetic P and did not significantly contribute to any of the models (Table C2, Appendix C).

3.3 Watershed Characteristics

Phosphorus exported from the watershed via surface runoff is an important external pollution source for the lake (Wetzel, 2001), making watershed hydrologic and land-use characteristics important parameters. Agriculture and other watershed land disturbances enhance dissolved and particulate P in surface runoff. Impermeable surfaces such as roads increase surface runoff. Conversely, wetlands and forests generally sequester P.

We hypothesized that agriculture is the most important watershed contributor to lake water quality. The effect of agriculture was assessed by calculating the hay/pasture and cultivated crop land area in watersheds and dividing by the watershed or lake area to obtain agricultural land:watershed area ratio (Ag:WA) and agricultural land:lake area ratio (Ag:LA). We also considered the contribution of the agricultural land adjacent to the lake to obtain the adjacent agricultural land:watershed area ratio (AdjAg:LA). Our results showed a weak but significant relationship between the Ag:WA ratio and August epilimnetic P concentrations (Figure 3.11). The effects of other landuse measures, such as urban development and road coverage, were considered, but did not contribute significantly to lake water quality (section 3.4).

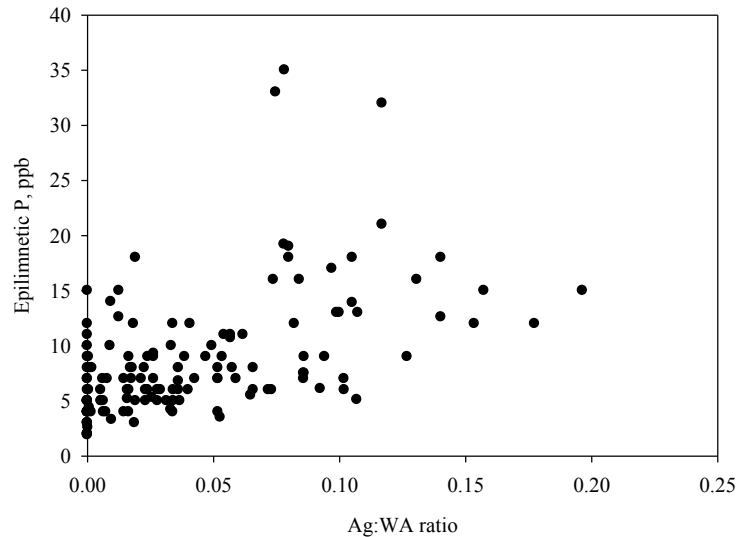


Figure 3.11: Ag:WA ratio versus Epilimnetic P. Including 143 (2015 + DEP + LEA) Maine lakes. Linear fit provided an $R^2 = 0.27$ and $p\text{-value} < 0.05$.

3.4 Statistical Modeling Results

3.4.1 Regression Tree

To determine the predictors of the August epilimnetic P concentrations, a decision tree was developed from the set of 24 (2015) study lakes (Figure 3.12). Independent variables for the epilimnetic P included physiochemical characteristics such as $Al_{NaOH}:P_{BD}$, P_{BD} , $Al_{NaOH}:Fe_{BD}$, OI, WA:LA, pH, and DOC; climate characteristics included hypolimnetic temperature (T_{hyp}), precipitation, and *Sch*; and watershed characteristics included Road:WA, Ag:WA, AdjAg:LA, and Ag:LA ratios. The data set for the 119 (DEP + LEA) lakes was used for model validation.

The average August epilimnetic P concentration for the 24 (2015) lakes was 8.1 ppb. The first threshold was *Sch* at 95 J/m^2 , below which lakes had an average P concentration of 14.0 ppb. These lakes were more susceptible to internal mixing of hypolimnetic P-rich water; 29% of the 24 (2015) study lakes and 54% of the validation

(DEP +LEA) lakes were in this category. For lakes with $Sch < 95 \text{ J/m}^2$, the first threshold was the AdjAg:LA ratio = 0.066; lakes above this ratio had the highest average P concentration of 20 ppb in this study.

Lakes with $Sch \geq 95 \text{ J/m}^2$ had lower average P concentration of 5.7 ppb; 71% of the 24 (2015) study lakes and 46% of the validation lakes were in this category. For this group of lakes, the next threshold was a $\text{pH} = 7.7$ with an average epilimnetic P concentration of 4.8 ppb. Lakes with $\text{pH} < 7.7$ were all oligotrophic with an average epilimnetic P concentration < 7.3 ppb; further splits for these low-epilimnetic P lakes were provided by Sch , Ag:WA ratio, Z_{avg} , and pH.

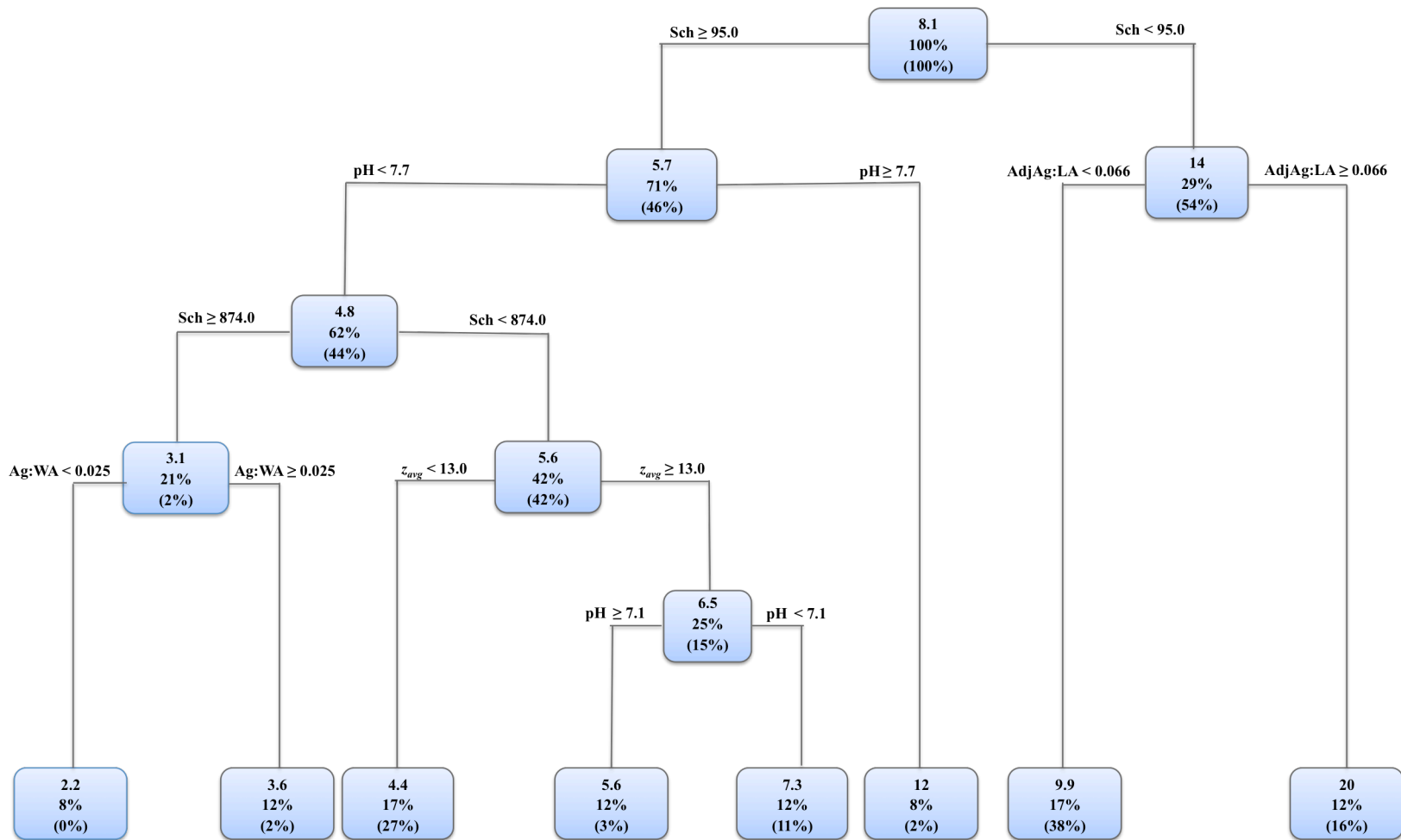


Figure 3.12: Regression Tree Analysis for Epilimnetic P. Regression threshold values for the mean August epilimnetic P concentration (top figure in each box, $\mu\text{g/L}$). Percentages are those of 24 (2015) lakes within each category; percentages in parentheses are those for the 119 (DEP + LEA) lakes. At each split, we continue to the left side of the branch determined by the '<' or '>' sign.

3.4.2. Multiple Linear Regression

Multiple linear regression (MLR) models were developed for the set of 24 (2015) study lakes. Out of the entire set of the predictor variables (Appendix C), lake August epilimnetic P concentrations were best predicted by different combinations of physiochemical parameters (i.e., $Al_{NaOH}:P_{BD}$, P_{BD} , DOC, pH, and Z_{avg}); climate factors (i.e., *Sch*, hypolimnetic temperature); and watershed characteristics (i.e., Rd:WA, Ag:WA, AdjAg:LA, and Ag:LA ratios).

Table 3.1 shows the MLR models with $R^2 > 0.70$. The performance of the three highest correlated models determined by the Akaike Information Criterion (ΔAIC) is shown in Figure 3.13. The top two models are distinguished by the change in the Akaike Information Criterion (ΔAIC) < 2 , suggesting that these models are equally optimal (Burnham and Anderson, 2002).

P_{BD} , AdjAg:LA ratio and lake Z_{avg} are common in the three highest correlated models, suggesting the importance of sediment chemistry, land use, and lake morphology in controlling the epilimnetic P concentrations. Models 1 and 3 also include DOC and the Al:P, respectively, as predictor variables. Combinations of these and other parameters in the three categories of physicochemical, watershed, and climate factors appear in all models.

We applied the MLR models to the set of 119 (DEP + LEA) lakes in order to validate the models (Table 3.1). DOC concentrations were not available for 23 lakes; thus, when DOC concentration was used as a predictor variable, data from only 96 lakes were used. The residual sum-of-squares (RSS), also known as the error sum-of-squares, was calculated as a measure for the deviation between the observed and predicted August

epilimnetic P concentrations. Models 1, 3, and 9 (Figure 3.14) had the lowest RSS values ranging between 3.84 and 3.90 (Table 3.1). These models use $\log P_{BD}$, $\log Al:P$, $\log Z_{avg}$, AdjAg:LA ratio, and DOC as the predictors.

Table 3.1 Multiple Linear Regression Equation Results from the 2015 Study Lakes. Variables include log P_{BD} , log Al:P, log *Sch*, log Average Depth (Z_{avg}), hypolimnetic temperature (T_{hyp}), Adjacent Ag:Lake Area (AdjAg:LA) ratio, Ag:Watershed Area (Ag:WA) ratio, Ag:Lake Area (Ag:LA) ratio, Road:Watershed Area ratio (Rd:WA), pH, and DOC.

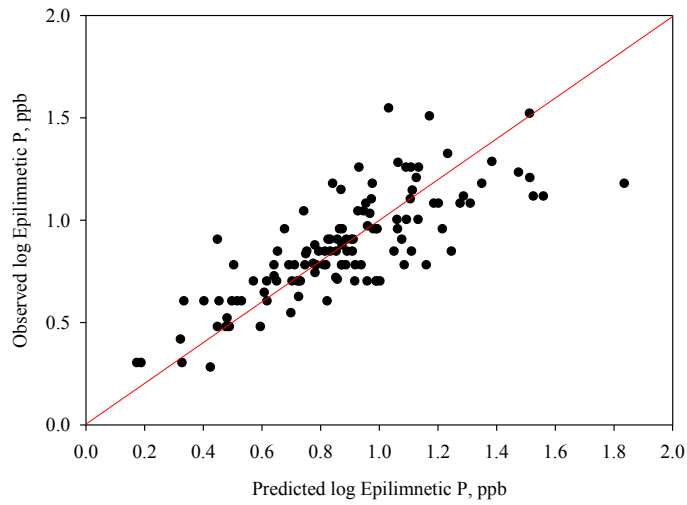
	Model	Calibration			Validation	
		R ²	AIC	ΔAIC	RSS ¹	n ²
1	$P_{BD} + Z_{avg} + \text{AdjAg:LA} + \text{DOC}$	0.844	-26.04	0.00	3.84	96
2	$P_{BD} + Z_{avg} + \text{AdjAg:LA}$	0.823	-25.08	0.96	4.92	119
3	$\text{Al:P} + Z_{avg} + \text{AdjAg:LA} + \text{DOC}$	0.826	-23.47	2.57	3.89	96
4	$P_{BD} + Z_{avg} + \text{AdjAg:LA} + \text{pH}$	0.825	-23.26	2.77	4.05	113
5	$\text{Al:P} + Z_{avg} + \text{AdjAg:LA}$	0.805	-22.69	3.34	4.87	119
6	$P_{BD} + Z_{avg} + \text{Ag:WA}$	0.804	-22.63	3.41	4.13	119
7	$P_{BD} + Z_{avg} + \text{Rd:WA}$	0.802	-22.41	3.63	9.19	119
8	$P_{BD} + \text{AdjAg:LA} + T_{hyp}$	0.788	-20.79	5.24	5.88	119
9	$\text{Al:P} + Z_{avg} + \text{Ag:WA}$	0.780	-19.89	6.15	3.90	119
10	$P_{BD} + Z_{avg} + \text{Ag:LA}$	0.755	-17.29	8.75	5.22	119
11	$\text{Al:P} + \text{AdjAg:LA} + T_{hyp}$	0.755	-17.25	8.79	6.19	119
12	$\text{Al:P} + \text{Sch} + \text{AdjAg:LA}$	0.741	-15.98	10.06	5.99	119
13	$P_{BD} + \text{Sch} + \text{AdjAg:LA}$	0.740	-15.78	10.26	5.48	119
14	$\text{Al:P} + Z_{avg} + \text{Ag:LA}$	0.718	-13.90	12.14	5.38	119

¹ RSS is the residual sum of squares.

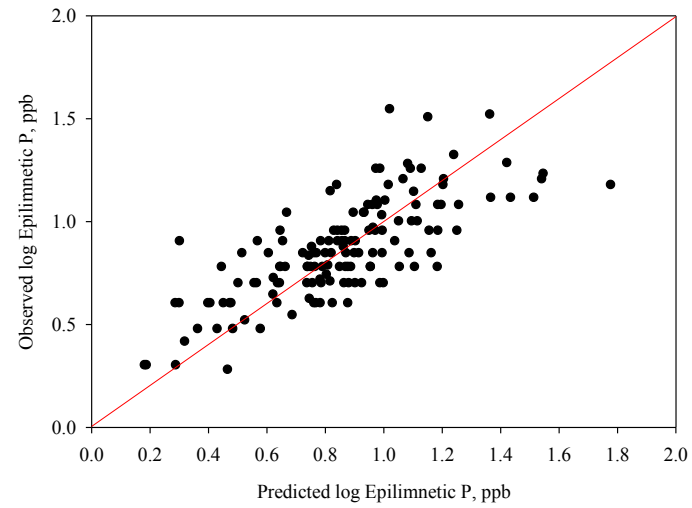
² n is the number of lakes used for model validation. $n = 96$ for the DEP lakes; the 23 LEA lakes do not have DOC concentration data and were not included in models 1 and 3. $n = 119$ for the DEP and the LEA lakes.

Table 3.2 Multiple Linear Regression Equation Coefficients. Results include the intercept, log P_{BD} , log Al:P, log Sch , log Average Depth (Z_{avg}), hypolimnetic temperature (T_{hyp}), Adjacent Ag: Lake Area (AdjAg:LA) ratio, Ag:Watershed Area (Ag:WA) ratio, Ag:Lake Area (Ag:LA) ratio, Road:Watershed Area (Rd:WA) ratio, DOC, and pH.

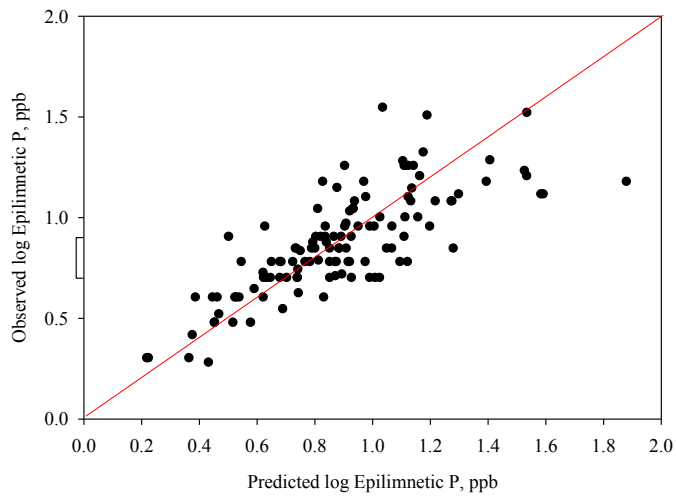
	Model	intercept	log P_{BD}	log Al:P	T_{hyp}	log Sch	log Z_{avg}	Adj Ag:LA	Ag: WA	Ag: LA	Rd: WA	DOC	pH
1	$P_{BD} + Z_{avg} + \text{AdjAg:LA} + \text{DOC}$	0.943	0.168				-0.481	0.933				0.056	
2	$P_{BD} + Z_{avg} + \text{AdjAg:LA}$	1.141	0.199				-0.523	0.957					
3	$\text{Al:P} + Z_{avg} + \text{AdjAg:LA} + \text{DOC}$	1.244		-0.128			-0.459	1.027				0.058	
4	$P_{BD} + Z_{avg} + \text{AdjAg:LA} + \text{pH}$	0.938	0.187				-0.515	0.904					0.029
5	$\text{Al:P} + Z_{avg} + \text{AdjAg:LA}$	1.522		-0.162			-0.499	1.047					
6	$P_{BD} + Z_{avg} + \text{Ag:WA}$	1.106	0.189				-0.509		2.024				
7	$P_{BD} + Z_{avg} + \text{Rd:WA}$	1.450	0.354				-0.656				-24.218		
8	$P_{BD} + \text{AdjAg:LA} + T_{hyp}$	0.227	0.215		0.027			1.072					
9	$\text{Al:P} + Z_{avg} + \text{Ag:WA}$	1.441		-0.141			-0.484		2.266				
10	$P_{BD} + Z_{avg} + \text{Ag:LA}$	1.160	0.282				-0.554			0.030			
11	$\text{Al:P} + \text{AdjAg:LA} + T_{hyp}$	0.665		-0.158	0.025			1.209					
12	$\text{Al:P} + Sch + \text{AdjAg:LA}$	1.323		-0.173		-0.157		1.135					
13	$P_{BD} + Sch + \text{AdjAg:LA}$	0.912	0.185			-0.160		1.126					
14	$\text{Al:P} + Z_{avg} + \text{Ag:LA}$	1.742		-0.244			-0.527			0.026			



(a)

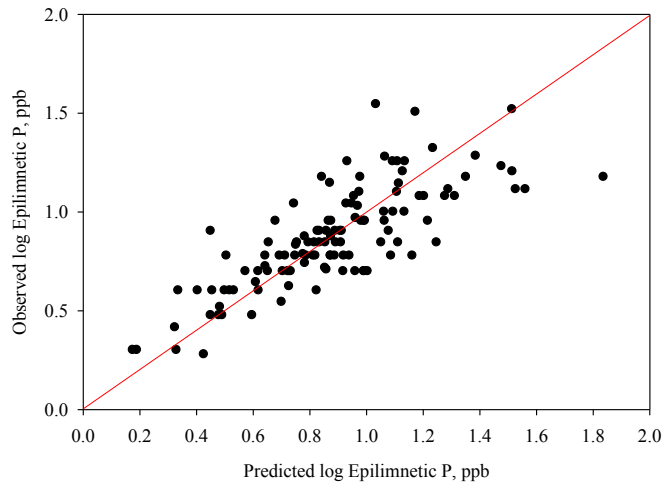


(b)

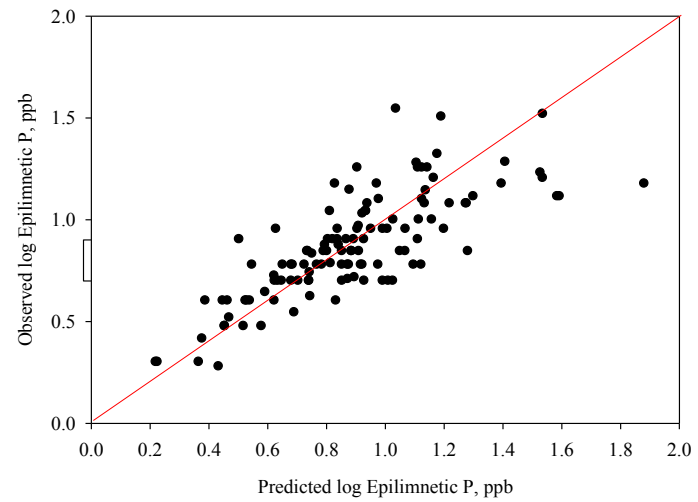


(c)

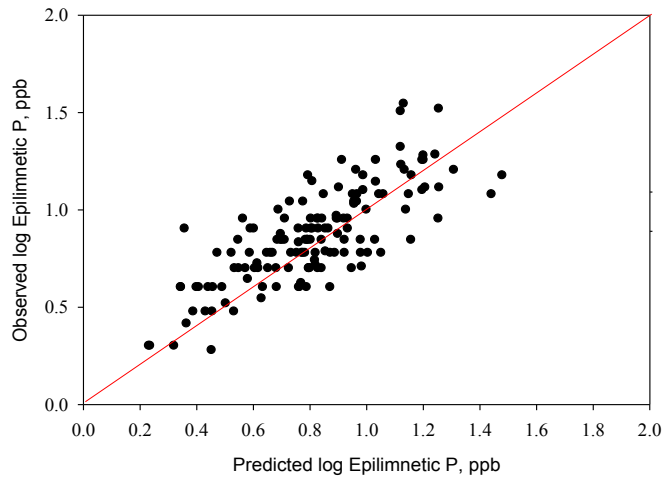
Figure 3.13: The Multiple Linear Regression Model Determined by AIC. The log predicted August epilimnetic P concentration versus the log measured P concentration of 120 (2015 + DEP) lakes (a, c) and 143 (2015 + DEP + LEA) lakes (b). Red line denotes the 1:1 line. The top three models according to AIC are shown. (a) Model 1, AIC = -26.04; (b) Model 2, AIC = -25.08; (c) Model 3, AIC = -23.47.



(a)



(b)



(c)

Figure 3.14: The Multiple Linear Regression Model Determined by RSS. The log predicted August epilimnetic P concentration versus the log measured P concentration of 120 (2015 + DEP) lakes (a, b) and 143 (2015 + DEP + LEA) lakes (c). Red line denotes the 1:1 line. The top three models according to RSS are shown. (a) Model 1, RSS = 3.84; (b) Model 3, RSS = 3.89; (c) Model 9, RSS = 3.90.

3.4.3 Quantile Regression

The quantile regression (QR) technique was utilized based on the results of MLR model 9 (Table 3.1) because the model provided the best fit when considering the full 119 (DEP + LEA) validation data points. Adopting a method of percentile selection (PS; Xu et al., 2015), we analyzed the response of Ag:WA ratio to epilimnetic P under ranked Al:P and Z_{avg} concentrations. We target lakes that may be more susceptible to the release of sediment reducible P, by using the lowest ranked sediment Al:P ratios. Ranked Al:P ratios range from 2.4 to 158.4 for the 75th percentile ($n = 108$), and 2.4 to 84.1 for the 50th percentile ($n = 73$). By ranking concentrations of Z_{avg} we target the lower Z_{avg} values i.e. shallower lakes that may be more susceptible to internal P release. Ranked Z_{avg} values range from 1.1 to 13.1 m for the 75th percentile ($n = 108$), and 1.1 to 8.3 m for the 50th percentile ($n = 73$). We did not report the 25th percentile because the number of data points is only 36. Consequently, the ranked data became more variable when considering upper boundary quantiles (90th quantile and above) for the model.

We used an arbitrary threshold of 15 ppb (log 1.18) for the August epilimnetic P and the 80th quantile model to assess lake vulnerability with respect to agricultural development in the watershed (Figure 3.15; 3.16; 3.17; 3.18). Below 15 ppb the lakes range from oligotrophic to lower mesotrophic, while above this threshold lakes are more at risk for eutrophication. The 80th quantile log P is the value where 80% of the lakes have concentrations less than or equal to 15 ppb. This analysis was performed for lakes with sediment Al:P ratios below the 75th and 50th percentiles (Figure 3.15; 3.16) and lakes with Z_{avg} values below the 75th and 50th percentiles (Figures 3.17; 3.18). The crossing of the 80th quantile model and the threshold P concentration marks the predicted Ag:WA

ratio that should not be exceeded in order to maintain an epilimnetic P concentration of 15 ppb. The threshold value for the Ag:WA ratio for lakes in the 75th percentile of sediment Al:P ratio is 0.11. When lakes in the 50th percentile of sediment Al:P ratio are considered, the threshold value for the Ag:WA ratio is reduced to 0.09 (Figure 3.15; 3.16). The Ag:WA ratio threshold for lakes in the 75th percentile of Z_{avg} is 0.078, which is further reduced to 0.068 for lakes in the 50th percentile of Z_{avg} (Figure 3.17; 3.18). Exceeding these threshold Ag:WA ratios predicts higher August epilimnetic P concentration than 15 ppb.

The PS-QR observations included the entire data set representing 143 lakes across Maine. Trophic state ranged primarily from oligotrophic to mesotrophic, with a few eutrophic lakes. The intercepts and slopes of the log epilimnetic P concentrations versus the Ag:WA ratio for various quantiles for lakes in the 75th percentile of Al:P ratios exhibit increases from 0.40 to 1.15, and a decrease from 3.50 to 3.10, respectively (Figure 3.15b; c). For lakes with the sediment Al:P ratios in the 50th percentile, the intercepts and slopes remain nearly unchanged, ranging from 0.40 to 1.20 and 3.50 to 3.10, respectively (Figure 3.16b; c). The intercepts and slopes for lakes in the 75th percentile of Z_{avg} exhibit increases from 0.56 to 1.15 and 2.00 to 3.20, respectively (Figure 3.17b; c). For lakes with Z_{avg} in the 50th percentile, the intercepts and slopes remain nearly unchanged ranging from 0.60 to 1.16 and 2.40 to 3.20, respectively (Figure 3.18b; c). The quantile slope estimates are not statistically different from the linear regression (LR) estimate (Figure 3.15c; 3.16c; 3.17c; 3.18c).

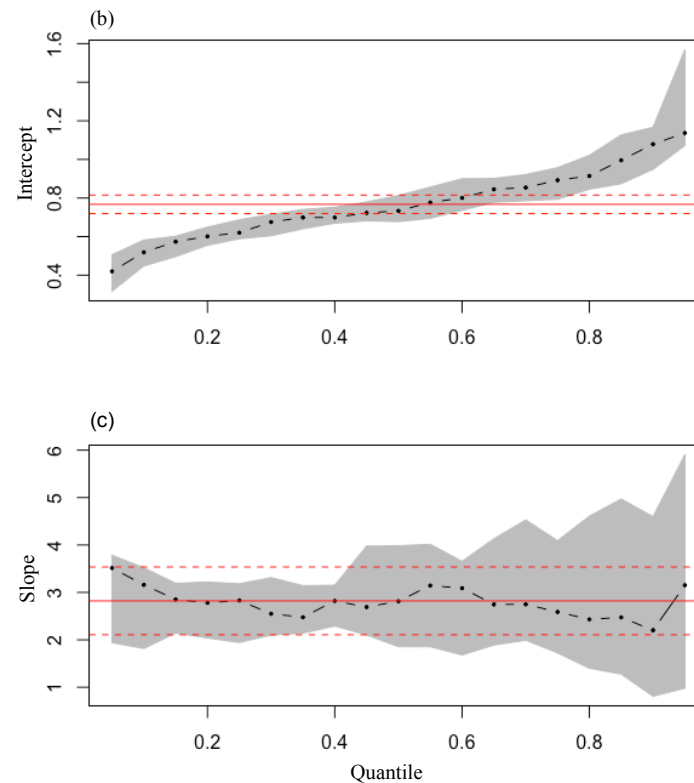
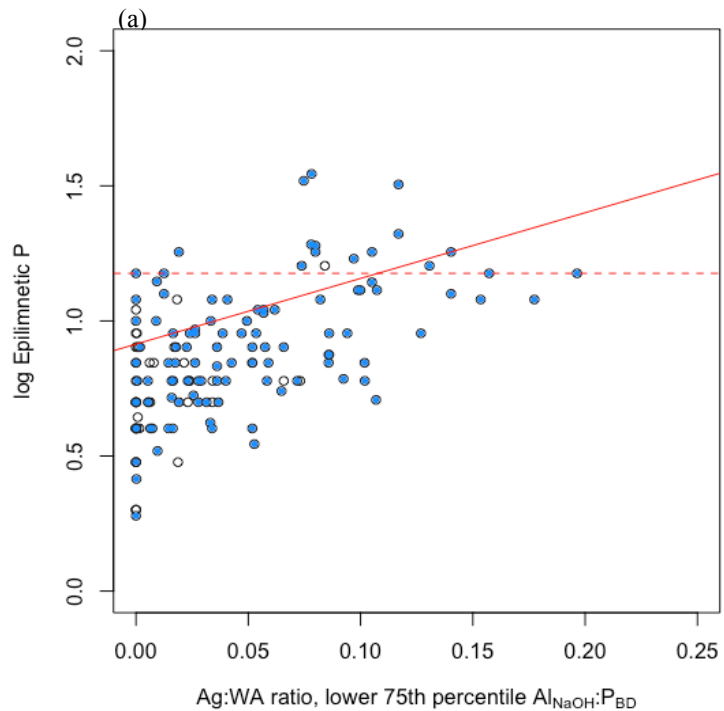


Figure 3.15: Ag:WA, lower 75th percentile Al:P versus log epilimnetic P: (a) The 80th quantile QR models (solid red line) for log epilimnetic P as a function of Ag:WA ratio (gray unfilled circles) for ranked Al:P values (75th; blue filled circles). The thresholds for the epilimnetic P concentrations for limiting a specific Ag:WA target (log epilimnetic P = 1.18 corresponds to 15 ppb, dashed red line). (b) intercepts (b_0 , black dotted lines: slope; gray bars: 95% confidence intervals; red dashed lines is the Linear Regression estimates) for the equation, $\log \text{ epilimnetic P} = b_0 + b_1 \log \text{ Ag:WA} + \varepsilon$ (b,c) with increasing quantiles of all observations. (c) The slopes are for the equation, $\log \text{ epilimnetic P} = b_0 + b_1 \log \text{ Ag:WA} + \varepsilon$ (b,c) (b_1 values are black dots, 95% confidence intervals are shaded gray: red solid line is the Linear Regression estimates).

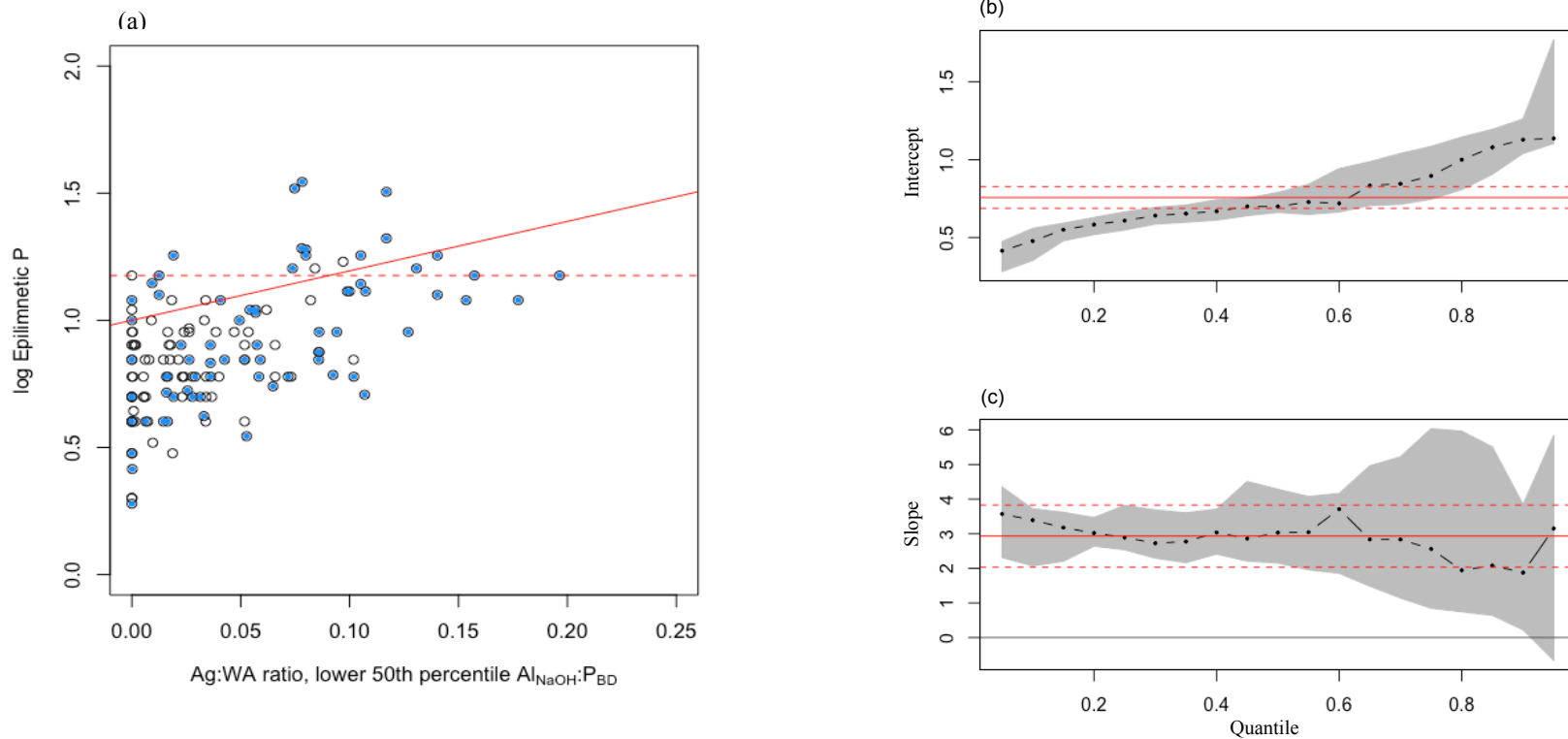


Figure 3.16: Ag:WA, lower 75th percentile Al:P versus log epilimnetic P: (a) The 80th quantile QR models (solid red line) for log epilimnetic P as a function of Ag:WA ratio (gray unfilled circles) for ranked Al:P values (50th; blue filled circles). The thresholds for the epilimnetic P concentrations for limiting a specific Ag:WA target (log epilimnetic P = 1.18 corresponds to 15 ppb, dashed red line). (b) intercepts (b_0 , black dotted lines: slope; gray bars: 95% confidence intervals; red dashed lines is the Linear Regression estimates) for the equation, $\log \text{ epilimnetic P} = b_0 + b_1 \log \text{ Ag:WA} + \varepsilon$ (b,c) with increasing quantiles of all observations. (c) The slopes are for the equation, $\log \text{ epilimnetic P} = b_0 + b_1 \log \text{ Ag:WA} + \varepsilon$ (b,c) (b_1 values are black dots, 95% confidence intervals are shaded gray: red solid line is the Linear Regression estimates).

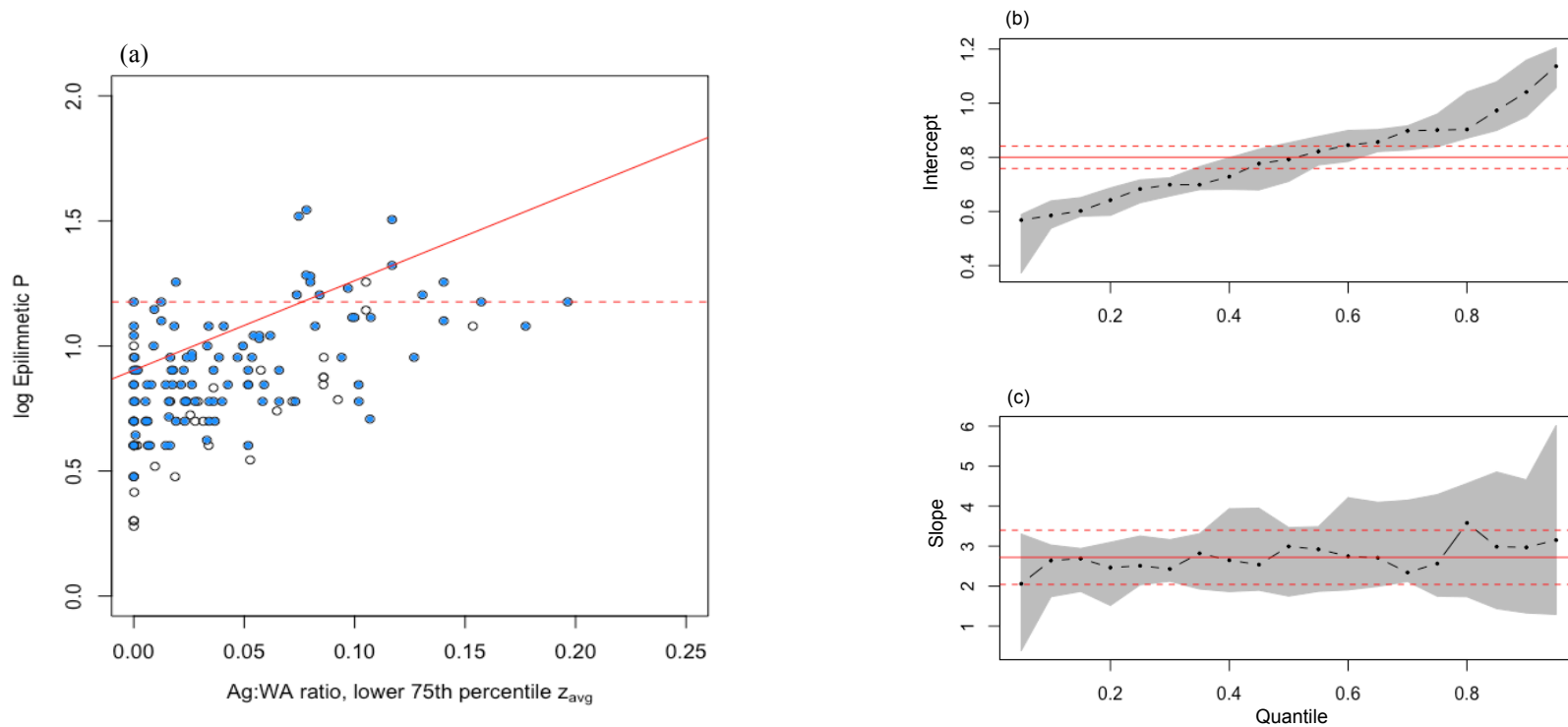


Figure 3.17: Ag:WA, lower 75th percentile Z_{avg} versus log epilimnetic P: (a) The 80th quantile QR models (solid red line) for log epilimnetic P as a function of Ag:WA ratio (gray unfilled circles) for ranked Z_{avg} values (75th; blue filled circles). The thresholds for the epilimnetic P concentrations for limiting a specific Ag:WA target (log epilimnetic P = 1.18 corresponds to 15 ppb, dashed red line). (b) intercepts (b_0 , black dotted lines: slope; gray bars: 95% confidence intervals; red dashed lines is the Linear Regression estimates) for the equation, $\log \text{ epilimnetic P} = b_0 + b_1 \log \text{ Ag:WA} + \varepsilon$ (b,c) with increasing quantiles of all observations. (c) The slopes are for the equation, $\log \text{ epilimnetic P} = b_0 + b_1 \log \text{ Ag:WA} + \varepsilon$ (b_1 values are black dots, 95% confidence intervals are shaded gray: red solid line is the Linear Regression estimates).

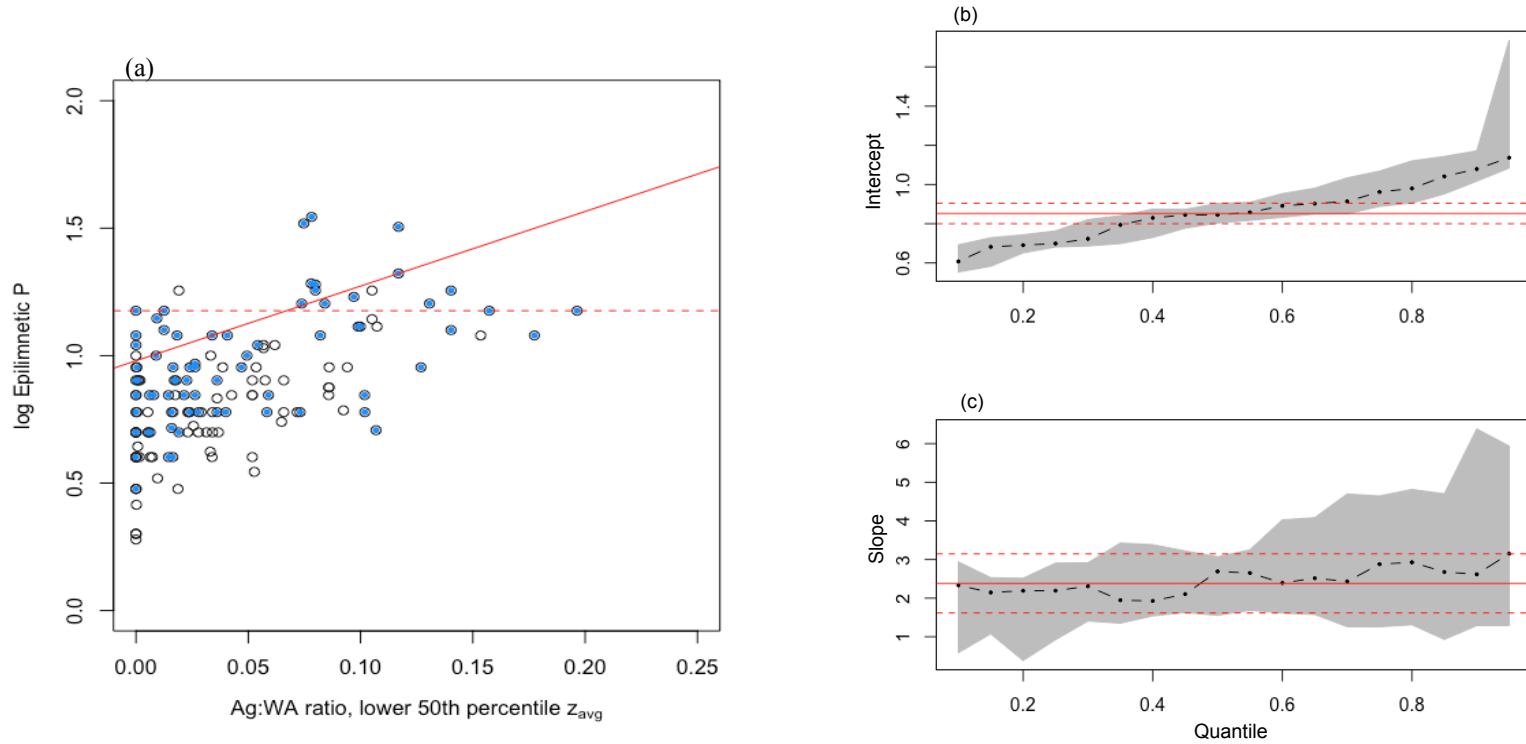


Figure 3.18: Ag:WA, lower 50th percentile Z_{avg} versus log epilimnetic P: (a) The 80th quantile QR models (solid red line) for log epilimnetic P as a function of Ag:WA ratio (gray unfilled circles) for ranked Z_{avg} values (50th; blue filled circles). The thresholds for the epilimnetic P concentrations for limiting a specific Ag:WA target (log epilimnetic P = 1.18 corresponds to 15 ppb, dashed red line). (b) intercepts (b_0 , black dotted lines: slope; gray bars: 95% confidence intervals; red dashed lines is the Linear Regression estimates) for the equation, $\log epilimnetic P = b_0 + b_1 \log Ag:WA + \epsilon$ (b,c) with increasing quantiles of all observations. (c) The slopes are for the equation, $\log epilimnetic P = b_0 + b_1 \log Ag:WA + \epsilon$ (b,c) (b_1 values are black dots, 95% confidence intervals are shaded gray: red solid line is the Linear Regression estimates).

CHAPTER 4: DISCUSSION

Phosphorus is the limiting nutrient in lake ecosystems, and thus controls lake productivity. Traditionally, models used to simulate and predict lake water quality have focused on external P inputs (Dillon and Kirchner, 1975; Vollenweider, 1976). However, these models fail to correctly model lakes in which internally loaded P contributes a significant amount of P (Søndergaard et al. 2013). This behavior occurs when lakes remain eutrophic after external P has been significantly reduced. In such lakes, internal loading is responsible for delaying the expected lake recovery (Jeppesen et al., 2005; Søndergaard et al., 2013). In our approach to predict the lake summer epilimnetic P concentration, we quantified the effects of physiochemical, climate, and watershed factors that relate to improved water quality to include both the internal and external P budgets. Our goal was to create simplified models that can be used for lake water quality management. We present three approaches for predicting water quality conditions based on quantified variables: the regression tree, multiple linear regression (MLR) models, and percentile selection quantile regression (PS-QR) model.

4.1 Regression Tree Model

Regression tree analysis is suitable for nonlinear relationships among the predictor and response variables (Figures 3.1-3.6; 3.9). In this approach, the response variable is based on several input variables. The model produces simple and interpretable results that can be validated. Regression trees explain the variation of a single response variable, in this case epilimnetic P, by splitting the data into homogenous groups (De'Ath and Fabricius, 2000). In the context of this study, however, the regression tree may be

best utilized as a first estimate to determine the dominant variables that predict lake water quality. The analysis predicts the statistical fit for a population of lakes to determine a statistical threshold value.

The regression tree determined *Sch*, AdjAg:LA, and pH to be the most important parameters in determining the response variable, epilimnetic P (Figure 3.12). Schmidt Stability (*Sch*) at 95 J/m^2 was the first threshold in the regression tree model. A low *Sch* indicates that a lake mixes more easily or has just partially mixed, and thus is potentially subject to upwelling of high P hypolimnetic waters, with a relatively small energy input normally provided by wind. A high *Sch* indicates a lake is less likely to mix. This split suggests the importance of water column thermal stability on epilimnetic P concentration.

The second threshold identified was AdjAg:LA, a watershed land-use characteristic. This parameter may be regarded as a proxy for external P inputs. The greater the AdjAg:LA ratio the greater the lake epilimnetic P concentration, as evidenced by the second split; lakes with AdjAg:LA ratio < 0.066 have epilimnetic P concentrations < 9.9 ppb, qualifying as oligotrophic. Together, lakes with a *Sch* $< 95 \text{ J/m}^2$ and a AdjAg:LA ratio > 0.066 have epilimnetic P concentrations > 20 ppb that places them in the mesotrophic-eutrophic category.

Lastly, pH proved to be an important lake chemical predictor variable in the regression tree. The model suggests that lakes with an epilimnetic pH ≥ 7.7 possess a higher mean epilimnetic P concentration (12 ppb), whereas lakes with a pH < 7.7 have a mean P concentration = 4.8 ppb. The identification of pH as a predictor variable in the regression tree may be due to its correlation with other significant predictor variables. pH correlates positively and significantly ($p < 0.05$) with sediment P_{BD} and the Ag:WA ratio

(data not shown), two parameters that are prominent predictors of the epilimnetic P in several of our top MLR models (Table 3.1). Ag:WA may link to pH through the use of soil amendments, such as CaCO_3 which produces alkalinity, and P-containing fertilizer which promotes higher pH through greater photosynthesis.

Surprisingly among the lake chemical predictor variables, sediment parameters such as P_{BD} and $\text{Al}_{\text{NaOH}}:P_{\text{BD}}$ were not identified as important to the regression tree. We expected predictors of internal release or internal storage (Carey and Rydin, 2011; Homyak et al., 2014) to be included in the regression tree, as thresholds for $\text{Al}_{\text{NaOH}}:P_{\text{BD}}$ have been previously established (Kopáček et al., 2005), and P_{BD} represents the potentially mobile P under anaerobic conditions (Rydin et al., 2000). Further, these two variables are predictors in our top MLR models (Table 3.1).

The regression tree model does not provide a parameter indicative of potential internal P load. However, this model does support our hypothesis that physiochemical, climate, and watershed characteristics are important in determining the epilimnetic P, as the first three splits encompass each of these factors. AdjAg:LA ratio is a predictor variable in our top MLR models (Table 3.1).

4.2 Multiple Linear Regression Models

We developed the MLR models to predict lake August epilimnetic P concentrations from a set of easily measurable predictor variables (Tables 4.1 and 4.2). The models were developed for a set of 24 (2015) lakes sampled within a two-week period in August 2015. To validate the models, we calculated the residual sum of the squares (RSS) for the August epilimnetic P concentrations on a set of 119 (DEP + LEA)

lakes (Table 3.1) that were sampled from 2010 to 2013 (Appendix C). The MLR models can be used as a predictive tool, allowing us to evaluate lake vulnerability to eutrophication and deterioration of water quality. Through epilimnetic P prediction, stakeholders, from homeowners to the Maine Department of Environmental Protection (DEP), can make decisions to best maintain or identify lakes for which remediation is a priority to improve water quality. The models and approach developed here can be used by regulatory agencies in other states to develop lake management strategies for similar lakes. This approach can be applied by the larger research community, as a blueprint to investigate the roles of these or other, as yet, untested predictor variables in lake water quality.

Models 1, 3, and 9 (Figure 3.14; Table 3.1) outperformed the other models in terms of providing the closest estimate for the measured epilimnetic P values. The MLR models with minimized residual error partially support our hypothesis that physiochemical, climate, and weather parameters influence epilimnetic P concentration. The most important predictors in the top MLR models are: $Al_{NaOH}:P_{BD}$, P_{BD} , Z_{avg} , DOC, Ag:WA, and AdjAg:LA (Table 3.1). These models each consist of one watershed parameter and two or more physiochemical parameters; these parameters act as proxies for internal and external P loading.

Ecologically it is reasonable that sediment $Al_{NaOH}:P_{BD}$ ratio and P_{BD} are included in the most effective models because they determine the extent to which internal P will be sequestered or released (Kopáček et al., 2005; Lake et al., 2007; Carey and Rydin, 2011; Homyak et al., 2014). It is also reasonable to include a proxy such as AdjAg:LA or Ag:WA for P export from the watershed, as evidenced by previous work focusing on the

external P budget of a lake (Dillon and Kirchner, 1974). The area-averaged depth, Z_{avg} , represents the relationship between lake depth and morphometry of the basin. Its value can be related to the lake bottom temperature, as well as the lake's propensity to mix vertically.

Parameters that reflect the effect of climate/weather, such as Sch , T_{hyp} and precipitation, did not appear in the top MLR models ($\Delta AIC < 2$; Table 3.1). As regional warming continues, it is likely to be accompanied by changes to water column temperature, precipitation, and increased storm frequency (Gerten and Adrian, 2002). Warming promotes a longer growing season in lakes. The Sch , as a weather-related parameter, does not definitively determine whether a lake mixes or remains stable (Robertson and Imberger, 1994), because it does not account for the effect of wind intensity. Further, Sch reflects the lake tendency to mix only immediately prior to the day of sampling, it is not reflective of the conditions over the entire season. However, Sch correlates strongly and significantly with Z_{avg} ($R^2 = 0.76$, $p < 0.001$). Statistically, including Z_{avg} in the MLR models results in stronger correlations compared to including Sch (Table 3.1). As such, Z_{avg} may be considered as a parameter that also reflects the tendency of a lake to mix.

Cumulative (from January-August and May-August) and maximum precipitation were tested in the regression tree model because increased precipitation leads to increased P export from the watershed; models including precipitation parameters failed to predict the August epilimnetic P significantly and were not included in Table 3.1 (Appendix C2.1).

A warmer hypolimnetic temperature enhances microbial metabolic rates, especially in the profundal sediment (Nürnberg, 1995). Therefore, a higher T_{hyp} should cause more extensive hypolimnetic anoxia and release of sediment P. However, T_{hyp} does not appear as a predictor variable in the top MLR models (Table 3.1).

The top MLR models gave nearly identical results in terms of R^2 (Table 3.1) likely due to sharing many similar variables. Given the limited number of lakes used for model calibration and validation ($n = 24$ and 119 , respectively) any of the models in Table 3.1 may be the most suitable for a given lake. For example, when applied to the validation data set of 119 lakes, model 9 nearly had the lowest error in predicting the epilimnetic P. As such, provided that the data are available, we propose that all of the models in Table 3.1 may be applied to predict the lake epilimnetic P. Individual lakes of significance, may be scrutinized for unusual conditions if their predicted P differs greatly from actual P (see section 4.4, below).

4.3 Percentile Selection-Quantile Regression

We employed the percentile selection quantile regression (PS-QR) method to detect the relative importance of the Ag:WA ratio in controlling the lake epilimnetic P for lakes at the lower end of the spectrum of sediment Al:P ratio and Z_{avg} . The law of limiting factors (Liebig's law of minimum) is a basic principle of ecology, which holds that when a process relies on several factors, the process will be constrained by the least available factor (Kaiser et al., 1994). In order to account for a limiting factor, a model must be able to consider the upper boundary of a distribution. Typical models, such as linear regression, measure goodness of fit over the entire distribution of data and include

effects of secondary factors (Cade et al., 1999); this approach models the distribution of data based on the conditional mean, which is ineffective when developing models based on limiting factors. QR is capable of measuring goodness of fit over a specific quantiles' distribution, and is therefore able to target limiting thresholds for populations by estimating changes within the upper boundary (Kaiser et al., 1994; Cade et al., 1999).

Since PS-QR is statistically robust and can be used as a tool for developmental planning and management of lakes based on limiting nutrients (such as epilimnetic P), we utilized it to predict the Ag:WA ratio thresholds required to control lake epilimnetic P concentrations. This approach is modeled after (Xu et al., 2015) in which threshold lake TP and TN concentrations were estimated for target Chl a concentrations in Lake Champlain, Vermont, USA.

In this study, the 80th quantile of the August epilimnetic P versus the Ag:WA ratio was selected based on the PS-QR models' slope (b_1), intercept (b_0), and number of lakes (n). In QR, the confidence interval endpoints may not be symmetric about the estimate (Koenker, 1994), which is consistent with the sampling distribution having a smaller n at the more extreme quantiles (Cade et al., 1999; Cade and Noon, 2003). Close to these extremes the sampling variation for quantiles is highly variable, and if the confidence intervals include the zero slope, the specific quantile is not considered significant. For example, the confidence interval for the 90th quantile of Figure 3.16c is narrow enough to exclude zero, but the confidence interval for the 95th quantile is wider and includes zero. The 95th quantile of the slope includes zero (Figure 3.16c). Therefore it is not significant nor a suitable quantile for the model. In this study, we used data from 108 lakes for the 75th percentile of the ranked Al:P ratios and Z_{avg} , and 73 lakes for the 50th percentile of

the ranked Al:P ratio and Z_{avg} from the original 143 lakes. At the 90th quantile, only 11 lakes for the 75th percentile and 7 lakes for the 50th percentile ranked Al:P ratios and Z_{avg} would have been included. Therefore, we chose to model the 80th quantile instead of the 90th or higher because it produces a greater range of upper regression quantiles with similar slope estimates, less sampling variation, and smaller confidence intervals (Figure 3.15; 3.16; 3.17; 3.18). However, quantiles greater than the 80th could be considered reasonable, with an addition of data from more lakes, as long as the slope and intercepts are statistically significant (Cade et al., 1999; Xu et al., 2015).

An advantage of PS-QR over the standard linear regression method is it can provide a more reliable prediction of the threshold Ag:WA ratio necessary to limit the lake summer epilimnetic P concentration to a specific target value. To constrain the epilimnetic P to a target concentration < 15 ppb in the 80th quantile, the predicted Ag:WA ratio thresholds for the lakes with the 75th and 50th percentile Al:P ratio are 0.11 and 0.09, respectively (Figure 3.15; 3.16). To constrain the epilimnetic P concentration to the same value, the predicted Ag:WA ratio thresholds for the lakes with the 75th and 50th percentile Z_{avg} are 0.078 and 0.068, respectively (Figure 3.17; 3.18). Therefore, threshold values for the Ag:WA ratios become more constrained when comparing lakes with 75th and 50th percentiles in the Al:P ratios and Z_{avg} values. This is reasonable considering that lakes in the lower percentiles of the Al:P ratios and Z_{avg} values are more vulnerable to eutrophication. Considering lakes in the 25th percentile of Al:P ratios and Z_{avg} values would decrease the threshold Ag:WA ratio in order to maintain the same predicted epilimnetic P concentration; however, we did not report the data because sample variance captured by the slope of the distribution increased significantly and the 80th quantile slope

is not significantly different from zero; therefore the 80th quantile would not be usable for this model.

The PS-QR method can be used as a management strategy to constrain predictor variable(s) to achieve a target water quality level; in this study, we used it to estimate the threshold Ag:WA ratio for lakes in a certain percentile Al:P ratios and Z_{avg} values for the target epilimnetic P concentration of 15 ppb. Thresholds were developed as a statistical fit for the population of lakes, not for an individual lake. Therefore thresholds represent an increased possibility of problems upon approaching or exceeding a threshold. The confidence in a prediction for an individual lake can be assessed by inspection of Figures 3.15-3.18. Smaller populations in any model increase the margin of error. The use of the Ag:WA ratio among other predictor variables is because its value can be managed by a regulatory agency through a combination of best management practices and zoning of land use.

4.4 Modeling Limitations

The models developed in this study utilized 24 lakes that were sampled in 2015. These lakes ranged from 1.9 to 21.0 ppb in the August epilimnetic P concentration, spanning oligotrophic to mesotrophic states. The data set that was used for model validation consisted of a total of 119 lakes that were sampled from 2010 to 2013 by the DEP and LEA; these lakes are mostly oligotrophic and mesotrophic, and cover a narrower range of productivity compared to the 2015 lakes. Developing predictive models for lakes with a full range of productivity (oligotrophic to eutrophic) typically improves model predictability for a wider range of lakes.

Assumptions made in the choice of modeling parameters may have added uncertainty to the results. Estimates of agricultural land were based on GIS landcover maps from 2004. These maps provide acreage of pasture/hay lands and cultivated croplands without consideration of the type of crops, frequency of cultivation, and specific agricultural practice with respect to the addition of fertilizers and pesticide.

Future research can focus on identification of lake-specific characteristics that relate to water quality problems. For example, by identifying unusual hydric soils or unusual lake hydraulics, researchers could begin to account for the remaining unexplained variation of epilimnetic P. We purposely chose boreal lakes without unusual hydraulic properties in order to decrease variability among the lakes as a whole. Future studies could include more dimensional lakes such as those with multiple deep basins (Sebago Lake, Maine), lakes with inflow/outflow locations in close proximity (Pushaw Lake, Maine), run of river dams in which there is limited water storage, and lakes affected by dam management practices concerning the spring refilling and fall draw down. There will always be exceptions to the models created because all the assumptions may not be valid for each individual lake.

Future refinement to this study could also focus on geological properties within the watershed to determine if certain areas are more susceptible to natural sources of external P. For example, the Presumpscot Formation is composed of marine clay, which has been glacially deposited along the coast of Maine (Davis et al., 1978) and contains P in the form of apatite. Generally, a lake with a watershed on marine clay has a trophic range from mesotrophic to eutrophic while a lake situated in till has a range from oligotrophic to mesotrophic (Lake et al., 2007); the Presumpscot Formation is significant

because clay-rich soils are easily eroded, which causes increased nutrient fluxes and higher sediment accumulation rates. The effects of natural P loading should be further studied by a comparison of watershed soils and yield of P, with and without Presumpscot Formation present.

CHAPTER 5: CONCLUSIONS

This study identified drivers of lake vulnerability to eutrophication. The lake vulnerability models developed here show that lake eutrophication is the result of the combined effects of physiochemical, climate, and watershed factors. Lakes with unfavorable sediment geochemistry (i.e., low $Al_{NaOH}:P_{BD}$ ratios or high P_{BD} concentrations) are more vulnerable to internal P release. Lakes that are susceptible to hypolimnetic P release are especially vulnerable if they do not stratify stably during the summer; lake thermal stability is driven by lake morphometry and temperature. Shallow lakes in general develop a weak thermal stratification and are at greater risk to internal mixing. These lakes can also develop a warmer hypolimnetic temperature with an increased sediment oxygen demand that facilitates internal P release. Land use patterns of lake watersheds identify potential additions of external P. Lakes with greater areas of adjacent agriculture enhance dissolved and particulate P in surface runoff. Together these stressors identify factors posing a risk to lake water quality.

Lake managers need good estimates for potentially mobile sediment P and additional external inputs of P to a lake. The models developed here can inform regulatory agencies and lake associations in their best management practices with respect to epilimnetic P. The regression tree can be used as an educational tool for landowners or stakeholders, as they can follow the paths and visually link the problems associated with eutrophication. This could be used as an outreach tool to educate landowners on practices they can adopt to keep water clean. The MLR models can be used to determine whether a lake is being adequately protected or if certain aspects have led to a higher vulnerability to water quality problems. Both the regression tree and MLR models can be used to

identify drivers controlling P, potentially identifying a lake's chief pollution problem, whether from within the sediment, various climate/weather effects, exports of P to the lake, or a combination of these factors. The QR tool will allow stakeholders to evaluate the tradeoffs of various actions to build consensus on the most effective approaches for sustainably managing the watershed. Furthermore, the QR approach would be of broad interest to lake water quality managers who are involved in watershed land use planning, especially with respect to nutrient loading. In order to best manage a lake we suggest the application of all of these models to further lake and watershed understanding and protect aquatic resources.

REFERENCES

- Amirbahman, A., Pearce, A. R., Bouchard, R. J., Norton, S. A., & Kahl, J. S. (2003). Relationship between hypolimnetic phosphorus and iron release from eleven lakes in Maine, USA. *Biogeochemistry*, 65(3), 369-386.
- Barbiero, R. P., & Welch, E. B. (1992). Contribution of benthic blue-green algal recruitment to lake populations and phosphorus translocation. *Freshwater Biology*, 27(2), 249-260.
- Boström, B., Andersen, J. M., Fleischer, S., & Jansson, M. (1988). Exchange of phosphorus across the sediment-water interface. *Hydrobiologia*, 170(1), 229-244.
- Brett, M. T., & Benjamin, M. M. (2008). A review and reassessment of lake phosphorus retention and the nutrient loading concept. *Freshwater Biology*, 53(1), 194-211.
- Burnham K.P. & Anderson D. R. (2002) *Model Selection and Multimodel Inference: A Practical Information-Theoretic Approach*, 2nd edn. Springer-Verlag, New York, NY.
- Cade, B. S., Terrell, J. W., & Schroeder, R. L. (1999). Estimating effects of limiting factors with regression quantiles. *Ecology*, 80(1), 311-323.
- Cade, B. S., & Noon, B. R. (2003). A gentle introduction to quantile regression for ecologists. *Frontiers in Ecology and the Environment*, 1(8), 412-420.
- Carey, C.C. and Rydin, E. (2011). Lake trophic status can be determined by the depth distribution of sediment phosphorus. *Limnology and Oceanography*, 56(6), pp.2051-2063.
- Carey, C. C., Weathers, K. C., Ewing, H. A., Greer, M. L., & Cottingham, K. L. (2014). Spatial and temporal variability in recruitment of the cyanobacterium *Gloeotrichia echinulata* in an oligotrophic lake. *Freshwater Science*, 33(2), 577-592.
- Christophoridis, C., & Fytianos, K. (2006). Conditions affecting the release of phosphorus from surface lake sediments. *Journal of Environmental Quality*, 35(4), 1181-1192.
- Davis, R. B., Bailey, J. H., Scott, M., & Norton, S. A. (1978). *TB88: Descriptive and Comparative Studies of Maine Lakes*.
- De'ath, G. and Fabricius, K.E. (2000). Classification and regression trees: a powerful yet simple technique for ecological data analysis. *Ecology*, 81(11), pp.3178-3192.

- Dillon, P.J., & Vollenweider, R.A. (1974). The application of the phosphorus loading concept to eutrophication research. Ottawa: National Research Council of Canada.
- Dillon, P. J., & Kirchner, W. B. (1975). The effects of geology and land use on the export of phosphorus from watersheds. *Water Research*, 9(2), 135-148.
- Effler, S. W., Wagner, B. A., O'donnell, S. M., Matthews, D. A., O'donnell, D. M., Gelda, R.K.,... & Cowen, E. A. (2004). An upwelling event at Onondaga Lake, NY: Characterization, impact and recurrence. *Hydrobiologia*, 511(1-3), 185-199.
- Einsele, W. 1936. Über die Beziehungen des Eisenkreislaufs zum Phosphatkreislauf im Eutrophen See. *Archiv für Hydrobiologie*, 29, 664–686.
- Filippelli, G. M. (2008). The Global Phosphorus Cycle: Past, Present, and Future. *Elements*, 4.2: 89-95.
- Fisher, J., & Acreman, M. C. (2004). Wetland nutrient removal: a review of the evidence. *Hydrology and Earth System Sciences*, 8(4), 673-685.
- Fraterrigo, J. M., & Downing, J. A. (2008). The influence of land use on lake nutrients varies with watershed transport capacity. *Ecosystems*, 11(7), 1021-1034.
- Gächter, R., Meyer, J. S., Mares, A. (1988). Contribution of bacteria to release and fixation of phosphorus in lake sediments. *Limnology and Oceanography*, 33 (6 part 2), 1542-1558.
- Gergel SE, Turner MG, Kratz TK. 1999. Dissolved organic carbon as an indicator of the scale of watershed influence on lakes and rivers. *Ecol Appl* 9:1377–90.
- Gerten, D., & Adrian, R. (2002). Effects of Climate Warming, North Atlantic Oscillation, and El Nino-Southern Oscillation on Thermal Conditions and Plankton Dynamics in Northern Hemispheric Lakes. *The Scientific World JOURNAL*, 2: 586-606.
- Hondzo, M., & Stefan, H. G. (1993). Regional water temperature characteristics of lakes subjected to climate change. *Climatic Change*, 24(3), 187-211.
- Homyak, P. M., Sickman, J. O., & Melack, J. M. (2014). Phosphorus in sediments of high-elevation lakes in the Sierra Nevada (California): implications for internal phosphorus loading. *Aquatic Sciences*, 76(4), 511-525.
- Hongve D. (1972) En bunnhenter som er lett å lage. *Fauna*, 25, 281-283).
- Hupfer, M. & Lewandowski, J. (2008). Oxygen Controls the Phosphorus Release from Lake Sediments—a Long-Lasting Paradigm in Limnology. *International Review of Hydrobiology*, 93(4-5), 415-432.

- Huser, B.J., Egemose, S., Harper, H., Hupfer, M., Jensen, H., Pilgrim, K.M., Reitzel, K., Rydin, E. and Futter, M. (2016). Longevity and effectiveness of aluminum addition to reduce sediment phosphorus release and restore lake water quality. *Water Research*, 97, pp.122-132.
- Huttula, T., Peltonen, A., Bilaletdin, A., & Saura, M. (1992). The effects of climatic change on lake ice and water temperature. *Aqua Fennica*, 22, 129-129.
- Jankowski, T., Livingstone, D. M., Bührer, H., Forster, R., & Niederhauser, P. (2006). Consequences of the 2003 European heat wave for lake temperature profiles, thermal stability, and hypolimnetic oxygen depletion: Implications for a warmer world. *Limnology and Oceanography*, 51(2), 815-819.
- Jensen, H. S., Reitzel, K., & Egemose, S. (2015). Evaluation of aluminum treatment efficiency on water quality and internal phosphorus cycling in six Danish lakes. *Hydrobiologia*, 751(1), 189-199.
- Jeppesen, E., Søndergaard, M., Jensen, J.P., Havens, K.E., Anneville, O., Carvalho, L., Coveney, M.F., Deneke, R., Dokulil, M.T., Foy, B.O.B. and Gerdeaux, D., 2005. Lake responses to reduced nutrient loading—an analysis of contemporary long-term data from 35 case studies. *Freshwater Biology*, 50(10), pp.1747-1771.
- Kaiser, M. S., Speckman, P. L., & Jones, J. R. (1994). Statistical models for limiting nutrient relations in inland waters. *Journal of the American Statistical Association*, 89(426), 410-423.
- Kates, R. W., Clark, W. C., Corell, R., Hall, J. M., Jaeger, C. C., Lowe, I., ... & Faucheux, S. (2001). Sustainability science. *Science*, 292(5517), 641-642.
- Khoshmanesh, A., Hart, B., Dancan, A., Beckett, R. (2002). Luxury Uptake of Phosphorus by Sediment Bacteria. *Water Research*, 36.3: 774-78.
- Koenker, R., & Bassett Jr, G. (1978). Regression quantiles. *Econometrica: Journal of the Econometric Society*, 33-50.
- Koenker, R. (1994). Confidence intervals for regression quantiles. *In Asymptotic Statistics*, (pp. 349-359). Physica, Heidelberg.
- Koenker, R., Portnoy, S., Ng, P. T., Zeileis, A., Grosjean, P., & Ripley, B. D. (2016). Package ‘quantreg’. Version 5.26. R Foundation for Statistical Computing: Vienna, Austria.
- Kopáček, J., Borovec, J., Hejzlar, J., Ulrich, K., Norton, S.A., Amirbahman, A. (2005) Aluminum control of phosphorus sorption by lake sediments. *Environmental Science & Technology*, 39(22), 8784-8789.

- Kopáček, J., Hejzlar, J., Borovec, J., Porcal, P., & Kotorova, I. (2000). Phosphorus inactivation by aluminum in the water column and sediments: Lowering of in-lake phosphorus availability in an watershedlake ecosystem. *Limnology and Oceanography*, 45(1), 212-225.
- Lake, B.A., Coolidge, K.M., Norton, S.A., Amirbahman, A. (2007). Factors contributing to the internal loading of phosphorus from anoxic sediments in six Maine, USA, lakes. *Science of the Total Environment*, 373(2–3), 534-541.
- McAvaney, B. J., Covey, C., Jousaume, S., Kattsov, V., Kitoh, A., Ogana, W., ... & AchutaRao, K. (2001). Model evaluation. In *Climate Change 2001: The scientific basis. Contribution of WG1 to the Third Assessment Report of the IPCC (TAR)* (pp. 471-523). Cambridge University Press.
- Monteith, D. T., Stoddard, J. L., Evans, C. D., De Wit, H. A., Forsius, M., Høgåsen, T., ... & Keller, B. (2007). Dissolved organic carbon trends resulting from changes in atmospheric deposition chemistry. *Nature*, 450(7169), 537.
- Mortimer, C.H. (1941). The exchange of dissolved substances between mud and water in lakes. *Journal of Ecology*, 29, 280–329.
- North, R. P., North, R. L., Livingstone, D. M., Köster, O., & Kipfer, R. (2014). Long-term changes in hypoxia and soluble reactive phosphorus in the hypolimnion of a large temperate lake: consequences of a climate regime shift. *Global change biology*, 20(3), 811-823.
- Nürnberg, G. K. (1995). The anoxic factor, a quantitative measure of anoxia and fish species richness in central Ontario lakes. *Transactions of the American Fisheries Society*, 124(5), 677-686.
- Nürnberg, G. K. (2009). Assessing internal phosphorus load—problems to be solved. *Lake and Reservoir Management*, 25(4), 419-432.
- Osgood, R. (1988). Lake mixis and internal phosphorus dynamics. *Arch. Hydrobiol.* 113: (4) 629-638.
- Petticrew, E. L., & Arocena, J. M. (2001). Evaluation of iron-phosphate as a source of internal lake phosphorus loadings. *Science of the total Environment*, 266(1), 87-93.
- Psenner, R., Pucsko, R., Sager, M. (1984). Die Fraktionierung organischer und Anorganischer Phosphorverbindungen von Sedimenten Versuch einer Definition ökologisch wichtiger Fraktionen. *Archive für Hydrobiologie Supplement*, 70, 111–55.

- Quinn, G. P., & Keough, M. J. (2002). *Experimental design and data analysis for biologists*. Cambridge University Press.
- R Core Team (2015). *R: A language and environment for statistical computing*. R Foundation for Statistical Computing, Vienna, Austria. URL <http://www.R-project.org/>.
- Read, J. S., & Muraoka, K. (2011). *Lake Analyzer Ver. 3.3 User Manual*. Global Lake Ecological Observatory Network.
- Reinhardt, R.L., Norton, S.A., Handley, M., Amirbahman, A. (2004). Dynamics of P, Al, and Fe during high discharge episodic acidification at the Bear Brook watershed in Maine, U.S.A. *Water, Air & Soil Pollution: Focus*, 4(2), 311-323.
- Robertson, D., Imberger, J. (1994) Lake number, a quantitative indicator of mixing used to estimate changes in dissolved oxygen. *International Review of Hydrobiology* 79(2) 159-176.
- Roy, S., Norton, S.A., Fernandez, I.J., Kahl, J.S. (1999). Linkages of P and Al export at high discharge at the Bear Brook watershed in Maine. *Environmental Monitoring and Assessment*, 55, 133-147.
- Rydin, E., Huser, B., & Welch, E. B. (2000). Amount of phosphorus inactivated by alum treatments in Washington lakes. *Limnology and Oceanography*, 45(1), 226-230.
- Schmidt, W. (1928) Ueber Temperatur and Stabilitaetsverhaeltnisse von Seen. *Geographiska Annaler*. 10, 145-177.
- Solomon, C. T., Jones, S. E., Weidel, B. C., Buffam, I., Fork, M. L., Karlsson, J., ... & Saros, J. E. (2015). Ecosystem consequences of changing inputs of terrestrial dissolved organic matter to lakes: current knowledge and future challenges. *Ecosystems*, 18(3), 376-389.
- Sondergaard, M., Jensen, P. J., & Jeppesen, E. (2001). Retention and internal loading of phosphorus in shallow, eutrophic lakes. *The Scientific World Journal*, 1, 427-442.
- Søndergaard, M., Bjerring, R., & Jeppesen, E. (2013). Persistent internal phosphorus loading during summer in shallow eutrophic lakes. *Hydrobiologia*, 710(1), 95-107.
- Spears, B. M., May, L. (2015). Long-term Homeostasis of Filterable Un-reactive Phosphorus in a Shallow Eutrophic Lake following a Significant Reduction in Catchment Load. *Science Direct: Geoderma*, 257-258, 78-85.
- Stumm, W., & Morgan, J. J. (1996). *Aquatic Chemistry: Chemical Equilibria and Rates in Natural Waters {Environmental Science and Technology}*. Wiley.

- Therneau, T., Atkinson, B., & Ripley, B. (2016). rpart: Recursive Partitioning and Regression Trees. 2015. R package version 4.1-10.
- Vollenweider, R. A. (1976). Advances in defining critical loading levels for phosphorus in lake eutrophication. *Memorie dell'Istituto Italiano di Idrobiologia*, Dott. Marco de Marchi Verbania Pallanza.
- Welch, E. B., & Cooke, G. D. (1999). Effectiveness and longevity of phosphorus inactivation with alum. *Lake and Reservoir management*, 15(1), 5-27.
- Wetzel, R.G. (2001). *Limnology: lake and river ecosystems*. 3rd ed. San Diego. Academic Press.
- Wilhelm, S., & Adrian, R. (2008). Impact of summer warming on the thermal characteristics of a polymictic lake and consequences for oxygen, nutrients and phytoplankton. *Freshwater Biology*, 53(2), 226-237.
- Xu, Y., Schroth, A. W., Isles, P. D., & Rizzo, D. M. (2015). Quantile regression improves models of lake eutrophication with implications for ecosystem-specific management. *Freshwater biology*, 60(9), 1841-1853.

APPENDIX A: MIDAS IDENTIFICATION

Table A1: Midas Identification. Organized by lakes from 2015, 2016, DEP, and LEA.

Lake	Midas	Lake	Midas
2015		2015	
	-		-
Auburn	3748	Parker	5186
China	5448	Pickerel	3826
Clearwater	5190	Pocasset	3824
Damariscotta	5400	Scammon	4446
East	5349	Upper Range	3688
Embden	78	Webb	4346
Great	5274	Whitter	5184
Hopkins	4538	DEP	
Long	5272		-
McGrath	5348	Alamoosook	4336
Meddybemps	177	Anasagunticook	3604
Messalonskee	5280	Baskahegan	1078
Mousam	3838	Bay of Naples	9685
North	5344	Biscay	5710
Pleasant	224	Brackett	1068
Pleasant	3446	Branch	4328
Sabattus	3796	Branch (Upper Middle)	4492
Salmon	5352	Bubble	4452
Square	3916	Cedar	2004
Taylor	3750	Center	760
Thompson	3444	Chickawaukie	4822
Tunk	4434	China	5448
Unity	5172	Cobbosseecontee	5236
Webber	5408	Cochnewagon	3814
2016		Cold Rain	3376
	-	Cold Stream	2146
Abrams	4444	Crystal	3452
David	5666	Crystal (Beals)	3626
Echo	5814	Damariscotta	5400
Flying	5182	Dexter	3830
Georges	4406	Dyer Long	5386
Kimball	5330	Eagle	4606
Lower Range	5664	East	5349
Lovejoy	3760	Echo	4624
Middle Range	3762	Echo (Crotched)	5814
Minnehonk	5812	Fish	4802
Molasses	4448	Flanders	4388
		Gassabias	4782

Table A1: Continued

Lake	Midas	Lake	Midas
Grand (East)	1070	Pleasant River	1210
Grand (West)	1150	Pushaw	80
Hadlock (Lower)	4610	Pushaw (Little)	2156
Hadlock (Upper)	4612	Raymond	3690
Halls	3780	Rocky	4330
Hermon	2286	Round	4620
Highland	3454	Round (Little)	4618
Hobbs	4806	Salmon	5352
Hodgdon	4628	Sandy (Freedom)	5174
Horseshoe	4788	Sawyer	386
Jacob Buck	4322	Seal Cove	4630
Jo-Mary (Upper)	243	Seboeis	954
Jordan	4608	Sennebec	5682
Kingsbury	262	Sheepscot	4896
Knight	3884	Somes	4614
Lake George	2608	Spednik	121
Lermond	4800	Threemile	5416
Lobster	2948	Toddy	5490
Long	447	Togus	9931
Long	4316	Unity	5172
Long	5780	Washington	4894
Long (Great)	4622	Webb (Weld)	3672
Mattakeunk	2242	Webber	4857
McGrath	5348	Webber	5408
Meddybemps	177	Wesserunett	70
Megunticook	4852	Wilson	3682
Messalonskee	5280	Wilson	3920
Millinocket	2020	Wilson (Lower)	342
Molunkus	3038	Wilson (Upper)	410
Moose	2590	Woodbury	5240
Musquash	1088	LEA	-
Nequasset	5222	Back Main Basin	3199
Nicatous	4766	Bear Pond Main Basin	3420
North	5344	Beaver Pond Main Basin	5582
North	5690	Brandy Pond Main Basin	9685
Ossipee (Little)	5024	Crystal Lake Main Basin	3452
Parker	3388	Granger Pond Main Basin	3126
Parks	4272	Hancock Pond	3132
Pattee	5458	Highland Main Basin	3454
Pease	5198		
Pennesseewassee	3434		

Table A1: Continued

Lake	Midas
Highland NE. Basin	3454
Island Pond Main Basin	3448
Keoka Main Basin	3416
Keyes Main Basin	3232
Little Moose Main Basin	3424
Long Basin 1	5780
Long Basin 1 (re-test)	5780
Long Basin 2	5780
Long Basin 3	5780
Long East Cove	5780
McWain Main Basin	3418
Moose Pond Main Basin	3134
Moose Pond N. Basin	3134
Moose Pond S. Basin	3134
Peabody Main Basin	3374
Sand Pond Main Basin	3130
Stearns Main	3234
Trickey Pond	3382
Woods Pond	3456

APPENDIX B: SEDIMENT AND WATER CHEMISTRY DATA

Table B1: Sediment Chemistry from the Surface (0-2 cm). Data from the surface short cores taken from the 2015, 2016, DEP, and the LEA.

Midas	Sample Date	%LOI	BD-Al, $\mu\text{mol/g}$	NaOH-Al, $\mu\text{mol/g}$	HCl-Al, $\mu\text{mol/g}$	BD-Fe, $\mu\text{mol/g}$	NaOH-Fe, $\mu\text{mol/g}$	HCl-Fe, $\mu\text{mol/g}$	BD-P, $\mu\text{mol/g}$	NaOH-P, $\mu\text{mol/g}$	NaOH-rP, $\mu\text{mol/g}$	NaOH-nrP, $\mu\text{mol/g}$	NaOH-rP:P	HCl-P, $\mu\text{mol/g}$
2015														
3748	6/26/15	12.6	3.2	120.5	326.3	92.8	23.2	263.1	15.4	18.5	NA	NA	NA	9.1
5448	6/24/15	23.1	1.9	86.6	289.1	210.4	41.0	871.5	53.1	136.2	NA	NA	NA	28.6
5190	7/8/15	22.3	5.0	370.5	236.8	74.6	63.5	81.8	3.0	44.0	NA	NA	NA	2.3
5400	7/13/15	17.9	2.5	382.3	328.0	132.4	147.1	149.8	5.0	44.5	NA	NA	NA	2.6
5349	6/25/15	16.7	3.8	151.6	133.6	83.2	28.8	86.0	6.2	17.5	NA	NA	NA	1.2
78	7/9/15	30.8	8.4	272.5	137.1	275.2	88.0	67.4	2.8	35.8	NA	NA	NA	1.8
5274	7/6/15	25.4	4.5	216.8	197.0	124.2	48.2	117.1	7.7	46.5	NA	NA	NA	4.2
4538	7/10/15	32.8	15.9	416.7	189.1	48.9	33.9	29.8	1.9	33.2	NA	NA	NA	1.6
5272	7/6/15	30.6	6.1	313.1	267.9	146.3	61.5	168.0	9.7	52.6	NA	NA	NA	3.6
5348	7/2/15	23.8	6.4	255.8	217.3	101.5	40.0	107.8	5.4	33.1	NA	NA	NA	5.0
177	6/30/15	18.1	2.1	112.2	118.1	153.9	58.7	564.7	3.0	41.5	NA	NA	NA	4.7
5280	7/2/15	32.7	22.3	325.8	160.2	903.4	147.7	216.5	82.5	64.6	NA	NA	NA	2.6
3838	6/29/15	42.6	136.7	288.3	69.6	1125.8	144.8	105.8	42.3	41.2	NA	NA	NA	1.3
5344	6/25/15	18.6	2.9	177.6	104.6	66.5	39.0	49.1	2.8	21.9	NA	NA	NA	2.6
224	7/8/15	16.9	9.0	224.9	254.2	268.5	54.5	153.1	5.8	42.7	NA	NA	NA	2.7
3446	7/7/15	24.8	9.1	202.8	127.9	31.9	15.2	51.1	2.8	25.4	NA	NA	NA	1.7
3796	6/26/15	14.3	11.1	159.9	272.2	179.7	25.3	223.8	11.8	20.7	NA	NA	NA	1.4
5352	7/2/15	18.8	2.8	140.8	161.1	137.8	20.8	158.3	25.2	23.2	NA	NA	NA	5.3
3916	6/29/15	47.4	12.7	159.0	111.3	196.6	29.8	61.5	7.4	27.5	NA	NA	NA	1.6
3750	7/9/15	19.6	4.2	207.0	256.6	134.5	37.0	175.3	7.4	29.3	NA	NA	NA	7.5

Table B1: Continued

Midas	Sample Date	%LOI	BD-Al, $\mu\text{mol/g}$	NaOH-Al, $\mu\text{mol/g}$	HCl-Al, $\mu\text{mol/g}$	BD-Fe, $\mu\text{mol/g}$	NaOH-Fe, $\mu\text{mol/g}$	HCl-Fe, $\mu\text{mol/g}$	BD-P, $\mu\text{mol/g}$	NaOH-P, $\mu\text{mol/g}$	NaOH-rP, $\mu\text{mol/g}$	NaOH-nrP, $\mu\text{mol/g}$	NaOH-rP:P	HCl-P, $\mu\text{mol/g}$
3444	7/7/15	27.6	20.0	374.8	129.5	356.0	53.8	134.4	5.7	49.6	NA	NA	NA	1.4
4434	6/30/15	11.2	2.9	147.2	432.4	510.6	127.3	545.6	1.8	39.4	NA	NA	NA	0.6
5172	7/1/15	15.3	2.5	152.6	150.2	95.6	23.0	141.8	13.1	29.3	NA	NA	NA	4.8
5408	6/24/15	15.0	3.9	152.4	252.2	248.2	9.7	268.4	46.7	41.4	NA	NA	NA	6.0
2016														
4444	6/24/16	11.9	1.7	361.9	161.4	109.7	69.8	95.9	10.6	24.2	NA	NA	NA	7.6
5666	6/28/16	33.4	3.7	308.1	141.8	97.0	39.0	65.3	5.5	41.8	NA	NA	NA	1.6
5814	6/23/16	26.1	3.7	426.6	180.8	149.6	96.4	91.7	7.8	52.6	NA	NA	NA	2.6
5182	6/23/16	21.7	9.4	520.0	227.3	281.1	158.7	217.6	11.5	46.7	NA	NA	NA	2.9
4406	6/27/16	14.9	2.7	348.8	143.0	124.2	67.5	101.7	13.7	18.6	NA	NA	NA	4.6
5330	6/29/16	24.3	5.0	436.2	151.9	64.1	71.8	65.1	4.5	31.7	NA	NA	NA	1.7
5664	6/30/16	22.2	1.7	280.3	235.1	134.7	53.4	118.6	4.9	32.6	NA	NA	NA	3.4
3760	6/22/16	29.7	2.6	374.0	172.1	103.4	54.6	94.9	4.9	41.4	NA	NA	NA	2.2
3762	6/22/16	25.1	2.7	433.6	196.9	107.9	61.0	88.7	6.2	52.2	NA	NA	NA	3.6
5812	6/29/16	29.3	16.9	502.3	185.8	450.5	233.3	273.0	31.9	53.0	NA	NA	NA	3.9
4448	6/24/16	6.7	1.7	273.1	76.6	22.1	51.2	38.9	1.4	17.4	NA	NA	NA	2.8
5186	6/29/16	23.4	1.6	306.8	174.7	61.3	44.1	80.3	2.8	35.9	NA	NA	NA	2.7
3826	6/30/16	33.7	3.9	163.5	80.9	103.2	20.8	41.8	5.2	21.5	NA	NA	NA	0.2
3824	6/30/16	12.4	1.2	184.2	213.1	122.8	43.9	116.9	4.3	23.3	NA	NA	NA	6.5
4446	6/27/16	58.9	6.1	192.6	36.6	109.2	20.3	24.1	7.2	25.0	NA	NA	NA	0.8
3688	6/23/16	30.4	5.0	252.9	131.1	67.6	27.8	46.5	7.7	36.3	NA	NA	NA	1.4
4346	6/24/16	14.9	2.7	355.8	110.8	79.0	67.5	62.3	2.8	29.4	NA	NA	NA	5.0
5184	6/28/16	51.2	4.6	207.6	71.8	30.4	15.4	27.2	9.4	35.4	NA	NA	NA	0.7
DEP														
70	8/9/11	24.4	3.2	312.0	149.0	228.0	145.8	141.0	6.1	44.0	20.0	23.6	0.5	2.8

Table B1: Continued

Midas	Sample Date	%LOI	BD-Al, $\mu\text{mol/g}$	NaOH-Al, $\mu\text{mol/g}$	HCl-Al, $\mu\text{mol/g}$	BD-Fe, $\mu\text{mol/g}$	NaOH-Fe, $\mu\text{mol/g}$	HCl-Fe, $\mu\text{mol/g}$	BD-P, $\mu\text{mol/g}$	NaOH-P, $\mu\text{mol/g}$	NaOH-rP, $\mu\text{mol/g}$	NaOH-nrP, $\mu\text{mol/g}$	NaOH-rP:P	HCl-P, $\mu\text{mol/g}$
80	8/24/11	17.4	1.6	222.0	141.0	123.3	70.9	90.4	4.1	35.7	18.6	17.1	0.5	3.8
121	8/24/11	26.5	3.1	308.0	144.0	61.5	59.6	71.9	2.0	43.3	20.1	23.2	0.5	2.8
177	9/23/10	20.6	2.5	269.0	200.0	399.0	180.6	227.6	6.6	81.3	51.2	30.0	0.6	3.3
243	9/1/11	24.8	5.3	454.0	110.0	170.0	140.4	54.0	0.0	43.0	12.0	31.2	0.3	1.5
262	8/30/10	18.6	7.3	676.0	239.0	73.0	140.0	91.2	3.0	51.5	20.5	31.0	0.4	2.7
342	9/1/11	20.3	3.5	345.0	243.0	141.0	103.3	113.0	5.1	34.0	16.0	18.3	0.5	2.5
386	8/23/11	17.2	3.7	327.0	109.0	111.6	65.9	63.0	2.2	20.9	7.4	13.6	0.4	0.5
410	9/1/11	15.7	2.9	208.0	344.0	279.4	133.1	554.0	3.8	29.0	15.0	14.0	0.5	2.4
447	9/23/12	26.5	2.1	123.0	95.0	32.0	15.9	44.5	1.7	11.1	2.5	8.6	0.2	1.0
760	8/30/10	35.7	5.2	118.0	90.7	68.0	24.1	53.0	8.0	10.3	4.1	6.2	0.4	2.8
954	8/23/10	30.9	6.0	361.0	59.1	141.0	140.0	25.2	1.6	27.0	12.5	14.5	0.5	1.4
1068	8/24/11	7.8	1.3	122.0	81.0	52.0	25.1	38.0	1.3	15.0	4.0	10.9	0.3	5.4
1070	8/24/11	21.3	8.5	383.0	115.0	358.8	101.7	63.6	8.2	49.0	21.6	27.4	0.4	2.8
1078	8/22/11	20.6	2.0	217.0	164.0	134.5	93.4	110.4	0.9	37.1	17.6	19.5	0.5	3.5
1088	8/22/11	27.6	3.8	392.0	109.0	96.0	126.3	43.0	0.0	38.0	15.0	23.1	0.4	1.5
1150	9/23/10	21.3	3.2	181.0	86.0	318.3	61.8	70.0	2.9	28.5	13.3	15.3	0.5	1.4
1210	8/25/10	30.1	16.5	557.0	69.6	321.0	150.0	42.1	6.5	40.2	19.7	20.5	0.5	1.4
2004	8/23/10	25.5	6.6	883.0	136.0	75.6	134.0	32.9	1.4	51.4	19.8	31.6	0.4	3.3
2020	8/15/11	20.7	3.6	170.0	185.0	260.1	79.3	215.1	3.2	31.0	19.9	11.2	0.6	3.4
2146	8/17/11	25.3	2.9	180.0	100.0	88.0	47.1	28.2	1.8	21.6	8.7	12.9	0.4	1.2
2156	8/24/11	30.0	1.3	114.0	137.0	66.0	34.4	95.0	5.8	18.0	8.0	10.1	0.4	5.3
2242	8/17/11	33.0	1.0	150.0	97.0	28.8	16.3	47.4	6.6	13.6	4.1	9.5	0.3	1.7
2286	9/2/10	55.4	7.7	148.0	151.0	152.0	13.6	130.0	13.8	19.7	8.5	11.2	0.4	9.7
2590	8/30/10	20.9	12.2	288.0	90.7	130.0	67.1	58.3	5.3	28.4	13.7	14.7	0.5	1.7
2608	8/30/10	23.1	8.2	659.0	202.8	165.0	120.0	86.0	8.9	51.9	25.7	26.3	0.5	4.2

Table B1: Continued

Midas	Sample Date	%LOI	BD-Al, $\mu\text{mol/g}$	NaOH-Al, $\mu\text{mol/g}$	HCl-Al, $\mu\text{mol/g}$	BD-Fe, $\mu\text{mol/g}$	NaOH-Fe, $\mu\text{mol/g}$	HCl-Fe, $\mu\text{mol/g}$	BD-P, $\mu\text{mol/g}$	NaOH-P, $\mu\text{mol/g}$	NaOH-rP, $\mu\text{mol/g}$	NaOH-nrP, $\mu\text{mol/g}$	NaOH-rP:P	HCl-P, $\mu\text{mol/g}$
2948	8/30/10	13.0	16.1	242.0	143.0	342.0	90.0	120.0	5.3	27.1	15.5	11.5	0.6	12.3
3038	8/24/11	8.1	1.1	160.0	74.0	41.8	48.5	46.3	0.4	20.5	11.8	8.7	0.6	3.6
3376	8/25/11	33.4	3.0	199.0	47.0	26.5	12.3	15.2	4.6	29.6	9.6	20.0	0.3	1.4
3388	9/7/10	19.3	5.5	227.0	118.0	88.5	37.7	54.0	3.4	29.8	10.4	19.4	0.4	6.6
3434	9/1/10	30.5	9.0	521.0	185.0	122.0	82.6	81.7	8.8	48.7	20.4	28.3	0.4	5.0
3452	8/31/10	20.7	9.6	562.0	224.0	202.0	105.0	87.3	2.9	51.8	28.7	23.2	0.6	7.4
3454	8/16/11	30.5	3.5	512.0	NA	70.4	64.3	NA	0.0	65.1	32.2	32.9	0.5	NA
3604	8/18/11	19.1	5.7	269.0	186.0	82.8	41.6	75.5	2.9	31.4	16.2	15.3	0.5	5.2
3626	9/1/10	26.1	19.7	355.0	172.0	117.0	104.0	156.0	13.1	21.0	10.3	10.6	0.5	9.0
3672	8/10/11	19.5	4.8	323.0	236.0	157.7	89.2	173.5	1.9	37.9	22.1	15.7	0.6	2.8
3682	8/10/11	23.0	7.2	425.0	210.0	321.4	134.7	219.6	1.3	40.2	23.0	17.2	0.6	1.4
3690	8/31/10	27.5	7.1	366.0	123.0	83.8	41.1	64.0	10.8	42.7	14.8	27.9	0.4	4.7
3696	8/31/11	20.2	2.8	243.0	124.0	47.2	29.7	59.9	3.1	35.4	16.8	18.6	0.5	6.6
3712	8/19/10	31.8	12.9	422.0	111.0	205.0	82.3	67.7	7.4	49.5	24.5	25.1	0.5	2.6
3714	8/31/10	19.3	4.1	232.0	221.0	108.0	49.0	117.0	7.4	27.4	12.9	14.5	0.5	7.7
3734	8/19/10	18.1	4.8	361.0	136.0	116.0	76.4	98.6	7.5	31.7	18.4	13.3	0.6	3.0
3780	8/9/11	40.1	7.5	344.0	143.0	43.0	36.4	63.0	2.7	30.0	9.0	21.0	0.3	2.4
3814	8/23/11	21.2	2.8	228.0	199.0	113.1	51.6	133.6	11.4	27.2	13.9	13.4	0.5	5.4
3830	9/8/10	36.4	13.9	376.0	170.0	189.0	67.2	103.0	14.3	37.3	15.4	21.8	0.4	2.3
3884	9/7/10	38.7	6.6	179.0	91.4	197.0	52.0	123.0	12.8	23.7	11.6	12.0	0.5	2.0
3920	8/18/10	28.4	4.9	244.0	81.3	50.7	52.0	26.9	4.6	29.9	9.9	20.0	0.3	1.9
3922	8/18/10	25.7	4.8	353.0	66.9	111.0	52.9	34.6	6.3	37.3	22.0	15.3	0.6	2.6
4272	8/8/11	30.1	5.7	458.0	313.0	165.1	111.6	54.1	2.3	45.1	19.7	25.3	0.4	3.1
4316	8/17/10	13.8	2.5	290.0	162.0	149.0	72.0	123.1	4.5	24.3	13.2	11.2	0.5	3.8
4322	8/17/10	22.7	4.4	542.0	286.0	96.3	87.4	71.7	3.5	55.1	23.5	31.7	0.4	2.5

Table B1: Continued

Midas	Sample Date	%LOI	BD-Al, $\mu\text{mol/g}$	NaOH-Al, $\mu\text{mol/g}$	HCl-Al, $\mu\text{mol/g}$	BD-Fe, $\mu\text{mol/g}$	NaOH-Fe, $\mu\text{mol/g}$	HCl-Fe, $\mu\text{mol/g}$	BD-P, $\mu\text{mol/g}$	NaOH-P, $\mu\text{mol/g}$	NaOH-rP, $\mu\text{mol/g}$	NaOH-nrP, $\mu\text{mol/g}$	NaOH-rP:P	HCl-P, $\mu\text{mol/g}$
4328	8/17/10	18.8	6.6	528.0	215.0	422.0	125.0	94.0	2.5	46.8	24.8	22.0	0.5	1.9
4330	8/17/10	22.9	2.4	399.0	199.0	82.4	38.7	38.4	2.9	34.8	10.9	23.8	0.3	2.0
4336	8/17/10	10.4	1.6	265.0	86.4	95.3	67.6	60.0	3.0	22.3	14.0	8.3	0.6	2.3
4388	8/15/11	17.5	2.6	240.0	NA	34.0	43.9	NA	0.0	16.0	7.0	8.5	0.5	NA
4452	9/20/12	29.4	4.0	786.0	108.6	129.0	212.0	49.5	0.0	38.5	11.2	27.3	0.3	0.7
4492	8/25/10	26.6	26.8	319.0	71.5	66.6	42.5	19.0	1.8	20.3	7.5	12.8	0.4	1.2
4606	9/19/12	24.4	6.2	531.0	91.0	166.0	59.9	68.2	0.0	30.5	8.9	21.7	0.3	0.8
4608	9/19/12	23.7	4.1	451.0	322.0	843.8	137.5	862.1	0.0	34.4	13.5	20.9	0.4	2.7
4610	9/20/12	34.0	7.6	805.0	96.0	78.0	88.0	44.0	0.0	36.7	15.0	21.7	0.4	0.7
4612	9/20/12	35.3	7.2	824.0	86.5	63.0	74.9	41.0	0.0	38.3	13.6	24.7	0.4	1.1
4614	9/17/12	42.6	5.5	248.0	45.0	49.4	16.8	24.6	2.9	28.0	6.9	21.2	0.3	1.4
4618	9/20/12	46.4	4.1	178.0	37.0	37.0	14.0	15.0	3.4	20.1	4.4	15.6	0.2	0.4
4620	9/17/12	50.4	5.7	239.0	36.6	53.5	15.7	14.8	2.8	22.3	5.6	16.6	0.3	0.7
4622	9/19/12	22.3	6.9	299.0	145.0	1064.2	76.7	541.8	0.4	37.3	14.7	22.6	0.4	0.7
4624	9/17/12	22.7	3.1	375.0	154.0	57.0	74.0	49.0	0.0	27.5	8.9	18.6	0.3	1.7
4628	9/17/12	27.6	5.5	473.0	122.0	57.0	40.0	50.8	0.0	30.5	10.6	19.9	0.4	1.5
4630	9/17/12	25.1	5.2	588.0	199.0	121.7	132.2	65.1	0.0	31.4	10.8	20.6	0.3	1.1
4766	8/25/10	23.9	5.8	434.0	182.0	174.0	244.0	54.0	3.2	51.6	20.0	31.7	0.4	2.2
4782	9/8/11	32.8	3.2	409.0	125.0	45.7	36.2	23.2	0.0	32.7	8.7	24.1	0.3	1.5
4788	8/25/10	20.8	2.1	170.0	48.8	29.2	17.5	11.3	0.8	14.2	4.7	9.5	0.3	0.8
4800	9/1/10	23.2	25.2	572.0	238.0	214.0	103.5	135.0	7.6	39.3	17.6	21.6	0.5	4.0
4802	8/10/11	27.3	2.7	223.0	84.0	28.7	37.5	41.2	0.0	23.5	6.2	17.3	0.3	0.7
4806	8/10/11	18.1	2.1	272.0	207.0	72.8	59.4	102.3	2.4	35.2	17.8	17.4	0.5	2.1
4822	8/11/11	15.2	1.4	192.0	209.0	157.7	57.3	218.6	16.3	25.3	18.9	6.3	0.8	4.4
4852	8/11/11	23.7	4.2	94.0	108.0	183.9	45.0	305.5	11.3	21.2	13.7	7.6	0.6	1.9

Table B1: Continued

Midas	Sample Date	%LOI	BD-Al, $\mu\text{mol/g}$	NaOH-Al, $\mu\text{mol/g}$	HCl-Al, $\mu\text{mol/g}$	BD-Fe, $\mu\text{mol/g}$	NaOH-Fe, $\mu\text{mol/g}$	HCl-Fe, $\mu\text{mol/g}$	BD-P, $\mu\text{mol/g}$	NaOH-P, $\mu\text{mol/g}$	NaOH-rP, $\mu\text{mol/g}$	NaOH-nrP, $\mu\text{mol/g}$	NaOH-rP:P	HCl-P, $\mu\text{mol/g}$
4857	8/24/10	27.9	16.2	290.0	76.0	74.2	48.3	38.2	2.9	18.0	8.0	10.0	0.4	NA
4894	8/17/11	22.8	1.9	345.0	146.0	66.9	106.8	71.6	1.6	30.8	11.5	19.3	0.4	0.9
4896	8/31/10	24.5	9.7	399.0	393.0	421.0	217.0	291.0	10.1	85.4	61.0	24.4	0.7	3.9
5024	8/31/11	29.3	5.7	241.0	85.0	111.8	51.9	58.2	4.4	22.7	8.7	14.1	0.4	1.5
5172	8/11/11	15.1	2.4	161.0	NA	86.9	40.6	NA	15.1	26.3	13.9	12.4	0.5	NA
5174	8/11/11	50.5	2.3	147.0	39.0	53.0	25.7	32.0	2.2	18.0	5.0	12.7	0.3	1.0
5198	8/18/10	15.7	7.2	390.0	400.0	180.0	178.0	310.0	11.4	56.6	32.5	24.1	0.6	7.6
5222	9/6/11	13.7	3.5	407.0	322.0	104.3	122.8	255.9	2.8	35.4	24.6	10.8	0.7	3.3
5236	8/19/10	24.7	4.0	224.0	157.0	341.0	95.3	582.0	62.6	115.0	99.6	15.2	0.9	12.2
5240	9/2/10	28.5	18.9	340.0	115.0	154.0	108.0	148.0	10.5	22.7	12.1	10.6	0.5	1.7
5280	8/9/11	30.9	19.0	212.0	228.0	788.7	109.9	500.6	77.1	70.7	51.0	19.7	0.7	5.8
5344	8/22/11	15.7	1.6	194.0	153.0	101.3	40.9	73.1	4.7	29.1	13.9	15.2	0.5	5.3
5348	8/22/11	20.5	1.5	168.0	142.0	38.0	28.9	77.0	1.8	20.3	9.7	10.7	0.5	5.3
5349	8/22/11	16.3	1.1	191.0	155.0	118.7	40.2	94.0	7.1	19.6	10.0	9.5	0.5	6.2
5352	8/19/10	18.0	4.3	166.0	92.1	90.7	41.6	91.3	12.2	13.0	3.7	9.3	0.3	4.2
5386	9/1/10	25.2	14.1	490.0	181.0	143.0	125.0	96.7	5.1	41.1	21.2	19.9	0.5	2.6
5400	8/31/10	16.8	10.4	341.0	236.0	133.0	104.0	156.0	5.5	36.2	23.7	12.6	0.7	2.3
5408	8/26/10	13.0	20.9	174.0	129.0	105.0	51.3	128.0	16.7	21.6	15.4	6.3	0.7	4.0
5416	8/26/10	16.6	3.4	119.0	223.0	159.0	19.1	202.0	31.4	24.4	11.7	12.8	0.5	8.5
5448	8/26/10	16.1	1.7	112.0	248.0	142.0	8.8	394.0	46.7	38.7	26.9	11.8	0.7	11.9
5458	9/2/10	27.5	19.4	212.0	176.0	164.0	48.7	132.0	13.2	19.8	5.0	14.7	0.3	6.6
5490	8/15/11	31.0	5.1	361.0	104.0	71.7	56.2	46.4	1.4	39.5	14.5	25.0	0.4	1.8
5682	9/1/10	14.5	12.5	327.0	188.0	137.0	85.5	164.0	5.4	34.5	21.0	13.5	0.6	4.2
5690	8/17/11	15.3	4.0	411.0	334.0	158.8	142.4	207.5	10.9	44.5	32.0	12.5	0.7	7.7
5710	8/17/11	22.5	2.9	337.0	582.0	45.0	65.0	476.6	2.2	28.2	14.3	13.9	0.5	9.5

Table B1: Continued

Midas	Sample Date	%LOI	BD-Al, $\mu\text{mol/g}$	NaOH-Al, $\mu\text{mol/g}$	HCl-Al, $\mu\text{mol/g}$	BD-Fe, $\mu\text{mol/g}$	NaOH-Fe, $\mu\text{mol/g}$	HCl-Fe, $\mu\text{mol/g}$	BD-P, $\mu\text{mol/g}$	NaOH-P, $\mu\text{mol/g}$	NaOH-rP, $\mu\text{mol/g}$	NaOH-nrP, $\mu\text{mol/g}$	NaOH-rP:P	HCl-P, $\mu\text{mol/g}$
5780	8/30/11	20.8	4.7	519.0	172.0	158.0	163.4	92.0	1.6	63.0	35.0	27.8	0.6	4.9
5814	8/18/11	28.1	7.0	328.0	234.0	325.4	91.7	149.9	15.2	55.7	33.8	21.9	0.6	2.2
9685	8/16/11	12.0	1.9	269.0	NA	45.6	38.9	NA	0.1	30.1	14.1	16.0	0.5	NA
9931	8/31/10	26.4	7.0	190.0	136.0	180.0	70.7	231.0	45.0	56.3	43.1	13.2	0.8	6.7
LEA														
5780	7/11/13	14.7	1.8	267.8	119.5	90.5	58.3	56.5	1.2	34.6	NA	NA	NA	4.7
3418	6/18/13	24.6	4.4	406.4	126.8	96.7	48.6	39.2	1.4	43.1	NA	NA	NA	4.1
5780	7/11/13	18.4	7.8	409.0	119.3	286.5	112.1	64.8	3.2	46.1	NA	NA	NA	5.6
3130	7/18/13	28.2	6.0	364.7	88.1	75.5	37.3	29.1	3.0	39.2	NA	NA	NA	3.6
3382	7/9/13	30.8	2.7	179.3	104.2	37.5	18.5	31.2	2.5	32.9	NA	NA	NA	1.0
3424	7/3/13	31.8	4.1	267.5	131.6	29.1	22.0	43.1	2.2	33.6	NA	NA	NA	4.4
3199	7/12/13	28.8	4.8	327.2	105.1	144.9	104.0	42.0	3.1	41.9	NA	NA	NA	0.7
3134	6/27/13	31.8	4.7	274.6	76.4	67.8	28.5	43.8	2.6	35.5	NA	NA	NA	5.0
3416	6/18/13	30.0	9.0	578.2	166.3	110.1	77.9	64.1	3.6	58.4	NA	NA	NA	3.4
9685	7/11/13	11.1	0.6	234.1	147.1	48.8	31.3	70.6	1.8	24.3	NA	NA	NA	7.1
3420	7/17/13	31.4	5.7	560.3	175.9	108.5	64.8	67.0	5.8	66.9	NA	NA	NA	3.7
3454	7/1/13	27.6	1.1	386.5	156.7	88.6	50.8	35.9	2.1	47.7	NA	NA	NA	1.7
5582	8/26/13	35.6	3.4	400.2	121.6	48.3	26.4	27.4	3.9	48.8	NA	NA	NA	1.6
3134	6/27/13	30.2	3.5	351.6	223.6	190.7	70.4	100.5	3.3	50.6	NA	NA	NA	2.9
5780	7/11/13	23.0	3.0	364.2	124.5	154.7	73.4	62.0	4.8	44.6	NA	NA	NA	3.0
5780	7/11/13	19.5	2.4	318.8	128.0	109.5	55.0	51.9	2.6	33.3	NA	NA	NA	3.3
3132	7/18/13	32.1	2.1	253.9	104.4	80.6	27.3	24.7	2.5	29.2	NA	NA	NA	1.3
3126	7/18/13	25.8	3.2	311.9	86.5	49.3	21.3	16.3	5.6	43.0	NA	NA	NA	0.2
3234	7/1/13	39.8	5.7	456.0	128.8	97.3	47.6	31.1	5.2	56.6	NA	NA	NA	0.4
3374	6/24/13	25.9	1.8	211.6	118.1	76.3	19.0	28.9	5.2	31.0	NA	NA	NA	2.3

Table B1: Continued

Midas	Sample Date	%LOI	BD-Al, $\mu\text{mol/g}$	NaOH-Al, $\mu\text{mol/g}$	HCl-Al, $\mu\text{mol/g}$	BD-Fe, $\mu\text{mol/g}$	NaOH-Fe, $\mu\text{mol/g}$	HCl-Fe, $\mu\text{mol/g}$	BD-P, $\mu\text{mol/g}$	NaOH-P, $\mu\text{mol/g}$	NaOH-rP, $\mu\text{mol/g}$	NaOH-nrP, $\mu\text{mol/g}$	NaOH-rP:P	HCl-P, $\mu\text{mol/g}$
3134	6/27/13	27.2	1.8	311.9	108.0	72.2	31.7	37.1	2.0	32.7	NA	NA	NA	1.9
3452	7/31/13	19.8	3.1	404.7	156.3	151.1	61.8	71.4	2.6	39.5	NA	NA	NA	5.2
3454	7/1/13	28.3	1.8	435.0	151.3	73.0	50.1	39.6	2.6	55.0	NA	NA	NA	2.2
3448	8/1/13	32.2	2.6	407.0	100.4	36.9	28.9	22.3	2.6	37.9	NA	NA	NA	0.9
3232	7/16/13	31.5	3.1	490.4	172.9	72.0	54.0	51.2	3.5	48.3	NA	NA	NA	2.4
3456	9/10/13	40.6	8.1	712.4	102.1	192.6	114.7	51.0	2.5	55.8	NA	NA	NA	0.5
5780	NA	22.3	4.7	372.2	182.1	159.0	103.3	79.7	3.9	54.4	NA	NA	NA	4.2

Table B2: Sediment Chemistry from the Bottom (8-10 cm). Data reports the 2015, 2016, and DEP studies. The DEP did not provide the calcium fraction analysis and the LEA did not provide fractionation results for the deeper sediment.

Midas	Sample Date	%LOI	BD-Al, $\mu\text{mol/g}$	NaOH-Al, $\mu\text{mol/g}$	HCl-Al, $\mu\text{mol/g}$	BD-Fe, $\mu\text{mol/g}$	NaOH-Fe, $\mu\text{mol/g}$	HCl-Fe, $\mu\text{mol/g}$	BD-P, $\mu\text{mol/g}$	NaOH-P, $\mu\text{mol/g}$	NaOH-rP, $\mu\text{mol/g}$	NaOH-nrP, $\mu\text{mol/g}$	NaOH-rP:P	HCl-P, $\mu\text{mol/g}$
2015														
3748	6/26/15	8.3	2.5	79.7	298.9	50.2	3.9	247.0	4.0	16.9	NA	NA	NA	9.1
5448	6/24/15	11.3	0.9	72.8	271.2	56.8	25.6	267.5	7.1	15.7	NA	NA	NA	8.2
5190	7/8/15	24.9	6.1	219.4	199.4	31.6	31.4	65.0	2.3	33.6	NA	NA	NA	1.5
5400	7/13/15	6.1	4.2	345.1	318.2	77.6	118.6	133.1	3.2	34.2	NA	NA	NA	3.1
5349	6/25/15	14.7	0.7	156.2	165.1	15.5	23.1	97.3	1.0	9.5	NA	NA	NA	6.0
78	7/9/15	25.2	2.9	234.8	276.3	164.2	61.1	189.1	2.4	42.5	NA	NA	NA	3.2
5274	7/6/15	16.5	4.7	191.0	211.3	47.4	37.1	119.1	3.0	32.8	NA	NA	NA	5.2
4538	7/10/15	32.1	3.0	645.1	155.6	34.9	32.0	37.1	0.8	50.3	NA	NA	NA	2.8
5272	7/6/15	27.6	9.2	272.9	201.3	65.1	43.6	79.1	4.3	43.3	NA	NA	NA	2.4
5348	7/2/15	17.6	1.4	164.8	225.2	29.5	22.8	114.6	2.0	24.1	NA	NA	NA	7.7
177	6/30/15	4.7	2.5	46.3	216.5	13.2	1.1	260.0	0.4	2.0	NA	NA	NA	8.1
5280	7/2/15	23.8	5.4	278.9	267.6	124.3	73.2	171.1	7.1	41.7	NA	NA	NA	3.3
3838	6/29/15	33.0	3.7	435.3	237.9	133.2	88.1	119.1	5.4	64.9	NA	NA	NA	1.7
5344	6/25/15	15.1	1.0	178.2	171.8	46.0	12.3	97.6	2.2	28.3	NA	NA	NA	4.9
224	7/8/15	20.3	1.7	282.5	225.3	106.1	26.5	213.2	3.2	44.4	NA	NA	NA	3.6
3446	7/7/15	26.0	1.3	197.4	172.2	20.8	13.4	59.8	1.5	31.5	NA	NA	NA	4.3
3796	6/26/15	11.0	3.0	145.7	243.5	55.0	4.6	215.7	3.2	10.2	NA	NA	NA	3.8
5352	7/2/15	16.0	2.5	142.7	222.8	51.8	28.4	142.4	3.7	17.2	NA	NA	NA	6.1
3916	6/29/15	40.3	2.1	157.9	49.9	34.1	8.3	30.6	2.1	24.8	NA	NA	NA	NA
3750	7/9/15	16.6	1.8	162.9	220.3	47.2	14.7	159.9	2.4	24.8	NA	NA	NA	9.2
3444	7/7/15	21.3	2.1	372.6	147.8	98.3	41.2	115.8	2.5	47.7	NA	NA	NA	2.5

Table B2: Continued

Midas	Sample Date	%LOI	BD-Al, $\mu\text{mol/g}$	NaOH-Al, $\mu\text{mol/g}$	HCl-Al, $\mu\text{mol/g}$	BD-Fe, $\mu\text{mol/g}$	NaOH-Fe, $\mu\text{mol/g}$	HCl-Fe, $\mu\text{mol/g}$	BD-P, $\mu\text{mol/g}$	NaOH-P, $\mu\text{mol/g}$	NaOH-rP, $\mu\text{mol/g}$	NaOH-nrP, $\mu\text{mol/g}$	NaOH-rP:P	HCl-P, $\mu\text{mol/g}$
4434	6/30/15	51.5	1.6	508.3	323.4	162.9	223.8	89.4	1.0	60.5	NA	NA	NA	0.8
5172	7/1/15	13.5	2.3	122.0	195.9	56.6	30.3	134.4	3.7	25.4	NA	NA	NA	5.0
5408	6/24/15	11.5	3.7	89.0	275.5	77.0	14.2	264.0	8.3	32.6	NA	NA	NA	6.6
2016														
4444	6/24/16	10.9	2.3	347.7	160.4	44.9	69.2	90.0	2.9	20.5	NA	NA	NA	7.4
5666	6/28/16	29.4	2.0	261.2	166.8	39.8	29.8	66.3	2.6	42.0	NA	NA	NA	2.4
5814	6/23/16	21.7	2.3	405.0	226.4	69.3	79.9	94.5	3.6	56.5	NA	NA	NA	2.5
5182	6/23/16	14.3	3.4	411.8	269.8	70.8	86.4	141.9	2.0	35.0	NA	NA	NA	3.2
4406	6/27/16	15.0	1.3	330.5	131.9	103.4	72.1	88.9	12.7	18.4	NA	NA	NA	4.3
5330	6/29/16	22.9	2.0	407.7	156.4	34.3	81.3	56.8	1.3	36.5	NA	NA	NA	1.6
5664	6/30/16	19.5	1.4	319.4	279.0	62.5	55.6	133.5	2.5	34.0	NA	NA	NA	5.5
3760	6/22/16	26.5	1.3	249.0	232.7	70.0	45.0	98.9	3.3	38.2	NA	NA	NA	3.2
3762	6/22/16	23.5	1.8	306.0	165.8	35.9	35.9	62.8	2.8	42.2	NA	NA	NA	3.7
5812	6/29/16	20.6	4.4	440.0	303.8	134.8	117.8	168.7	6.0	53.2	NA	NA	NA	3.4
4448	6/24/16	6.3	3.0	323.4	113.5	26.7	65.9	72.1	0.5	8.8	NA	NA	NA	6.5
5186	6/29/16	21.3	1.3	246.1	209.8	33.0	30.6	86.4	1.3	37.0	NA	NA	NA	3.8
3826	6/30/16	50.7	2.7	170.3	62.9	35.3	17.1	41.4	0.5	16.8	NA	NA	NA	0.6
3824	6/30/16	11.8	1.2	231.1	200.8	55.9	50.6	113.2	2.7	21.9	NA	NA	NA	10.9
4446	6/27/16	61.5	2.5	199.0	37.7	77.9	25.7	28.2	3.3	20.2	NA	NA	NA	0.4
3688	6/23/16	26.2	1.6	154.5	131.4	27.4	13.0	36.3	2.6	30.6	NA	NA	NA	2.1
4346	6/24/16	10.9	3.3	364.8	104.6	42.1	67.1	65.4	1.2	22.3	NA	NA	NA	5.4
5184	6/28/16	46.0	2.1	178.7	59.9	11.0	8.6	23.2	3.2	28.2	NA	NA	NA	1.7
DEP														
70	8/9/11	24.7	1.6	328.0	198.0	65.6	98.2	70.9	2.8	40.1	21.6	18.5	0.5	2.3
80	8/24/11	14.8	1.2	346.0	173.0	51.0	95.3	83.0	1.8	41.8	23.6	18.2	0.6	5.8

Table B2: Continued

Midas	Sample Date	%LOI	BD-Al, $\mu\text{mol/g}$	NaOH-Al, $\mu\text{mol/g}$	HCl-Al, $\mu\text{mol/g}$	BD-Fe, $\mu\text{mol/g}$	NaOH-Fe, $\mu\text{mol/g}$	HCl-Fe, $\mu\text{mol/g}$	BD-P, $\mu\text{mol/g}$	NaOH-P, $\mu\text{mol/g}$	NaOH-rP, $\mu\text{mol/g}$	NaOH-nrP, $\mu\text{mol/g}$	NaOH-rP:P	HCl-P, $\mu\text{mol/g}$
121	8/24/11	24.0	2.1	237.0	120.0	25.6	37.4	56.8	1.1	36.3	20.0	16.3	0.6	4.8
177	9/23/10	6.6	2.3	94.0	118.0	16.1	24.8	132.1	0.0	2.2	1.3	0.9	0.6	7.9
243	9/1/11	25.9	4.3	532.0	170.4	87.1	145.0	47.2	0.0	50.1	25.2	24.9	0.5	1.9
262	8/30/10	23.4	7.3	372.0	103.0	35.4	51.6	39.1	1.5	35.2	19.9	15.4	0.6	1.4
342	9/1/11	19.3	2.6	380.0	262.5	92.1	102.4	92.6	1.6	32.6	18.5	14.1	0.6	2.4
386	8/23/11	15.4	1.4	190.0	186.0	69.0	48.2	101.8	1.6	19.8	11.0	8.7	0.6	1.2
410	9/1/11	13.1	1.6	223.0	334.0	141.0	162.4	406.3	0.9	34.4	20.8	13.6	0.6	1.3
447	9/23/12	19.5	0.7	70.0	130.0	1.0	5.5	25.0	0.0	4.0	1.0	2.7	0.2	2.0
760	8/30/10	43.2	2.4	167.0	97.3	17.5	24.8	46.6	1.5	14.0	6.7	7.3	0.5	4.8
954	8/23/10	29.0	3.8	479.0	143.0	47.1	124.0	50.3	0.9	39.7	19.5	20.2	0.5	4.8
1068	8/24/11	4.9	0.9	90.0	56.4	8.4	17.2	22.6	0.5	10.5	4.0	6.5	0.4	5.3
1070	8/24/11	20.8	3.9	359.0	214.0	80.0	113.0	92.0	4.0	61.8	32.6	29.2	0.5	4.0
1078	8/22/11	18.4	1.0	142.0	170.0	67.0	75.4	282.4	0.2	23.6	16.2	7.4	0.7	5.3
1088	8/22/11	27.6	2.8	435.0	156.5	77.0	138.9	47.6	0.0	51.4	29.9	21.5	0.6	2.4
1150	9/23/10	18.7	2.1	205.0	194.0	113.5	82.5	97.5	1.6	36.9	19.5	17.4	0.5	2.5
1210	8/25/10	29.6	5.0	501.0	145.0	68.8	129.0	42.0	1.7	50.5	29.4	21.2	0.6	1.1
2004	8/23/10	26.6	2.5	873.0	183.0	16.1	99.0	29.4	0.4	57.3	27.9	29.4	0.5	3.5
2020	8/15/11	15.9	2.2	208.0	187.0	89.0	106.0	169.0	1.4	31.5	23.6	7.9	0.8	5.7
2146	8/17/11	24.4	2.6	386.0	209.0	41.0	68.0	39.0	2.1	57.2	34.7	22.6	0.6	2.7
2156	8/24/11	29.4	1.9	196.0	142.1	41.8	39.8	81.0	1.2	20.7	8.9	11.8	0.4	5.9
2242	8/17/11	39.9	1.1	167.0	116.0	11.0	22.1	48.8	1.8	15.5	6.5	9.0	0.4	1.6
2286	9/2/10	17.0	2.1	120.0	116.0	42.7	16.7	80.2	2.9	16.1	9.6	6.5	0.6	5.9
2590	8/30/10	20.4	7.3	446.0	183.0	35.4	78.7	74.8	1.7	49.2	27.0	22.2	0.6	4.1
2608	8/30/10	19.6	5.8	348.0	178.0	31.0	55.8	51.2	1.9	41.9	23.3	18.6	0.6	4.6
2948	8/30/10	10.2	9.5	113.0	114.0	62.9	48.8	122.0	2.0	14.1	9.1	5.0	0.7	8.9

Table B2: Continued

Midas	Sample Date	%LOI	BD-Al, $\mu\text{mol/g}$	NaOH-Al, $\mu\text{mol/g}$	HCl-Al, $\mu\text{mol/g}$	BD-Fe, $\mu\text{mol/g}$	NaOH-Fe, $\mu\text{mol/g}$	HCl-Fe, $\mu\text{mol/g}$	BD-P, $\mu\text{mol/g}$	NaOH-P, $\mu\text{mol/g}$	NaOH-rP, $\mu\text{mol/g}$	NaOH-nrP, $\mu\text{mol/g}$	NaOH-rP:P	HCl-P, $\mu\text{mol/g}$
3038	8/24/11	8.3	0.8	181.0	144.0	23.0	53.0	97.0	0.1	24.3	15.6	8.8	0.6	5.8
3376	8/25/11	34.2	2.3	177.0	74.0	22.3	9.4	13.7	3.0	33.6	14.0	19.6	0.4	1.0
3388	9/7/10	13.8	1.5	99.1	69.5	12.4	8.0	16.7	0.5	14.0	5.3	8.7	0.4	4.2
3434	9/1/10	28.6	6.0	422.0	164.0	24.5	48.2	56.3	2.0	37.2	23.1	14.1	0.6	5.0
3452	8/31/10	17.7	15.6	361.0	170.0	25.3	41.4	58.7	1.5	37.0	22.8	14.2	0.6	7.4
3454	8/16/11	28.8	2.3	353.0	NA	23.6	32.1	NA	0.0	42.2	21.9	20.4	0.5	NA
3604	8/18/11	17.7	3.9	290.0	161.0	27.9	32.2	62.0	1.5	34.9	21.9	13.0	0.6	5.2
3626	9/1/10	17.8	11.9	195.0	141.0	41.5	46.3	76.9	2.5	11.8	7.8	4.0	0.7	8.2
3672	8/10/11	17.2	2.4	299.0	286.0	65.0	91.1	173.5	0.1	40.7	30.1	10.6	0.7	4.2
3682	8/10/11	21.4	4.4	422.0	274.0	97.0	138.0	192.0	0.2	40.7	26.0	14.8	0.6	2.0
3690	8/31/10	21.9	4.5	140.0	98.2	25.7	14.3	32.8	2.8	23.3	11.1	12.3	0.5	3.7
3696	8/31/11	15.5	1.2	138.0	119.0	26.7	17.5	48.6	1.4	25.4	14.3	11.2	0.6	8.2
3712	8/19/10	29.5	4.8	384.0	129.0	61.3	42.3	43.9	3.4	44.0	22.8	21.2	0.5	2.6
3714	8/31/10	16.2	6.4	166.0	224.0	42.8	30.8	89.3	2.3	27.8	15.1	12.7	0.5	7.8
3734	8/19/10	13.0	3.1	441.0	217.0	47.1	92.6	110.5	2.4	32.6	21.4	11.3	0.7	5.3
3780	8/9/11	36.1	4.1	359.0	169.7	35.6	39.0	69.3	0.0	23.3	9.1	14.2	0.4	2.4
3814	8/23/11	15.9	0.9	155.0	200.0	32.5	31.9	118.0	1.2	17.1	9.1	8.1	0.5	7.3
3830	9/8/10	33.5	8.3	336.0	141.0	36.1	46.8	64.7	2.8	31.0	17.5	13.5	0.6	3.0
3884	9/7/10	37.1	4.0	229.0	137.0	83.2	49.8	99.1	3.2	29.2	16.3	13.0	0.6	2.8
3920	8/18/10	26.5	2.5	212.0	99.5	15.7	29.0	19.3	1.5	32.0	13.2	18.8	0.4	1.7
3922	8/18/10	26.4	2.4	265.0	143.0	38.7	42.1	36.1	2.2	49.5	31.7	17.8	0.6	3.0
4272	8/8/11	27.0	2.7	290.0	261.0	12.6	43.2	25.1	0.6	35.1	18.6	16.5	0.5	3.0
4316	8/17/10	NA	NA	NA	NA	NA	NA	NA	NA	NA	NA	NA	NA	NA
4322	8/17/10	25.1	2.8	296.0	261.3	21.5	62.7	34.4	0.9	35.9	17.9	18.0	0.5	1.3
4328	8/17/10	14.9	2.5	375.0	196.0	54.4	75.0	83.4	1.4	35.3	22.1	13.2	0.6	3.1

Table B2: Continued

Midas	Sample Date	%LOI	BD-Al, $\mu\text{mol/g}$	NaOH-Al, $\mu\text{mol/g}$	HCl-Al, $\mu\text{mol/g}$	BD-Fe, $\mu\text{mol/g}$	NaOH-Fe, $\mu\text{mol/g}$	HCl-Fe, $\mu\text{mol/g}$	BD-P, $\mu\text{mol/g}$	NaOH-P, $\mu\text{mol/g}$	NaOH-rP, $\mu\text{mol/g}$	NaOH-nrP, $\mu\text{mol/g}$	NaOH-rP:P	HCl-P, $\mu\text{mol/g}$
4330	8/17/10	30.4	2.2	201.0	38.4	7.5	12.2	10.9	0.6	12.9	5.3	7.6	0.4	0.6
4336	8/17/10	11.5	1.4	264.0	118.0	35.0	51.7	94.2	1.3	20.9	14.4	6.5	0.7	2.1
4388	8/15/11	18.2	2.1	347.0	NA	34.9	66.6	NA	0.0	25.1	12.3	12.8	0.5	NA
4452	9/20/12	27.6	2.1	724.0	95.0	38.3	136.9	24.5	0.0	53.2	27.1	26.0	0.5	0.7
4492	8/25/10	28.8	9.4	612.0	175.0	39.0	54.5	27.1	1.0	52.8	28.2	24.6	0.5	2.3
4606	9/19/12	26.7	4.6	754.0	187.0	102.3	116.0	67.8	0.0	49.3	26.3	22.9	0.5	0.8
4608	9/19/12	26.0	3.1	604.0	217.0	144.3	147.2	68.4	0.0	53.0	33.0	20.1	0.6	1.7
4610	9/20/12	36.4	3.8	677.0	69.0	25.1	39.5	20.8	0.0	39.4	19.2	20.2	0.5	0.6
4612	9/20/12	26.0	2.6	677.0	120.0	19.9	40.9	35.8	0.0	51.0	33.1	18.0	0.7	2.5
4614	9/17/12	42.3	2.2	169.0	44.0	11.0	11.2	16.0	0.6	17.0	6.0	10.1	0.4	0.6
4618	9/20/12	47.0	2.8	269.0	52.0	15.5	13.9	16.5	0.9	27.2	10.1	17.1	0.4	0.4
4620	9/17/12	50.9	2.3	186.0	41.0	8.6	7.3	12.6	0.0	14.8	4.4	10.4	0.3	0.7
4622	9/19/12	16.6	1.7	347.0	168.0	51.0	85.6	63.0	0.0	32.0	16.1	15.9	0.5	2.8
4624	9/17/12	19.2	1.4	328.0	171.0	35.0	73.0	47.1	0.0	28.1	13.5	14.6	0.5	1.7
4628	9/17/12	26.1	2.6	488.0	127.0	17.5	20.4	43.1	0.0	38.4	19.6	18.8	0.5	2.1
4630	9/17/12	20.3	2.7	452.0	164.0	36.2	100.7	52.0	0.0	24.5	12.8	11.7	0.5	0.8
4766	8/25/10	27.8	1.8	383.0	161.0	39.6	164.0	35.1	1.0	47.4	22.3	25.1	0.5	2.6
4782	9/8/11	33.2	1.9	295.0	141.0	12.3	18.4	18.4	0.0	23.2	7.2	16.0	0.3	1.9
4788	8/25/10	18.6	0.5	199.0	144.0	19.7	18.4	21.4	0.6	23.6	11.0	12.6	0.5	2.4
4800	9/1/10	25.2	9.2	254.0	109.0	25.4	37.9	42.1	1.4	24.1	10.8	13.2	0.5	1.3
4802	8/10/11	25.5	2.5	257.0	134.0	23.7	41.3	57.0	0.0	27.8	11.0	16.8	0.4	1.1
4806	8/10/11	16.2	0.9	239.0	202.0	38.1	46.4	81.1	0.4	27.7	13.4	14.3	0.5	2.4
4822	8/11/11	10.4	1.3	171.0	212.0	42.7	38.4	165.6	2.3	18.4	13.8	4.6	0.8	3.7
4852	8/11/11	14.5	3.9	238.0	161.0	89.2	86.7	177.2	3.0	29.7	20.4	9.3	0.7	2.3
4857	8/24/10	21.6	13.5	448.0	168.0	18.6	68.6	77.4	1.0	28.5	12.6	15.9	0.4	5.0

Table B2: Continued

Midas	Sample Date	%LOI	BD-Al, $\mu\text{mol/g}$	NaOH-Al, $\mu\text{mol/g}$	HCl-Al, $\mu\text{mol/g}$	BD-Fe, $\mu\text{mol/g}$	NaOH-Fe, $\mu\text{mol/g}$	HCl-Fe, $\mu\text{mol/g}$	BD-P, $\mu\text{mol/g}$	NaOH-P, $\mu\text{mol/g}$	NaOH-rP, $\mu\text{mol/g}$	NaOH-nrP, $\mu\text{mol/g}$	NaOH-rP:P	HCl-P, $\mu\text{mol/g}$
4894	8/17/11	27.1	0.9	406.0	162.0	11.0	52.0	54.0	0.7	35.1	13.6	21.5	0.4	1.8
4896	8/31/10	19.9	14.3	256.0	191.0	89.8	76.6	105.0	4.3	31.7	20.6	11.1	0.7	2.9
5024	8/31/11	20.7	3.5	197.0	227.0	58.0	26.0	48.0	4.0	36.8	25.0	11.9	0.7	1.4
5172	8/11/11	11.9	1.5	132.0	NA	41.0	28.0	-	2.7	23.5	14.7	8.8	0.6	NA
5174	8/11/11	57.2	1.2	167.0	43.3	27.8	25.0	36.7	0.1	15.3	4.9	10.4	0.3	1.2
5198	8/18/10	14.6	1.9	296.0	234.0	45.0	134.0	147.0	2.4	36.5	24.1	12.4	0.7	3.9
5222	9/6/11	10.3	5.8	204.0	302.0	50.0	55.0	236.0	1.5	21.0	16.5	4.5	0.8	3.5
5236	8/19/10	20.0	2.4	114.0	66.0	76.3	31.7	109.8	22.3	18.5	14.4	4.1	0.8	1.4
5240	9/2/10	20.7	9.6	280.0	242.0	58.4	57.6	114.0	3.0	29.2	17.4	11.7	0.6	4.5
5280	8/9/11	18.4	6.0	304.0	237.0	84.6	80.6	138.1	4.9	37.5	26.6	10.9	0.7	4.1
5344	8/22/11	15.1	0.7	171.0	168.0	31.8	32.5	72.9	1.0	22.0	11.5	10.5	0.5	6.9
5348	8/22/11	17.1	1.1	150.0	207.0	27.0	25.0	93.0	0.8	20.8	11.7	9.1	0.6	9.5
5349	8/22/11	14.5	0.7	125.0	170.0	35.5	22.7	93.1	1.2	12.5	6.3	6.2	0.5	7.1
5352	8/19/10	12.2	3.4	139.0	193.0	41.8	28.7	106.0	3.0	16.0	8.7	7.3	0.5	8.2
5386	9/1/10	24.6	4.3	369.0	172.0	52.1	72.8	82.7	1.9	45.8	27.6	18.2	0.6	4.9
5400	8/31/10	11.4	5.9	368.0	198.0	50.4	115.0	131.0	2.3	30.8	22.5	8.3	0.7	3.4
5408	8/26/10	10.8	5.7	182.0	204.0	48.4	56.5	202.0	5.1	27.6	22.5	5.2	0.8	6.1
5416	8/26/10	NA	NA	NA	NA	NA	NA	NA	NA	NA	NA	NA	NA	NA
5448	8/26/10	8.6	1.4	50.9	198.0	40.3	1.7	168.0	2.8	7.5	3.5	4.1	0.5	8.7
5458	9/2/10	22.9	13.7	125.0	160.0	44.0	25.5	86.0	2.9	12.9	5.7	7.2	0.4	6.7
5490	8/15/11	31.0	2.2	230.0	97.0	16.0	25.4	40.8	0.0	23.5	8.5	15.1	0.4	2.1
5682	9/1/10	12.6	4.6	271.0	170.0	50.5	90.0	137.0	2.1	30.7	21.0	9.7	0.7	3.9
5690	8/17/11	12.8	2.5	320.0	144.0	59.7	102.2	142.0	3.4	29.8	23.2	6.6	0.8	2.4
5710	8/17/11	19.3	3.1	392.0	99.0	28.0	74.4	43.0	1.5	37.1	21.3	15.8	0.6	1.2
5780	8/30/11	15.5	1.6	328.0	157.1	40.3	55.5	64.4	0.3	42.2	27.1	15.0	0.6	7.6

Table B2: Continued

Midas	Sample Date	%LOI	BD-Al, $\mu\text{mol/g}$	NaOH-Al, $\mu\text{mol/g}$	HCl-Al, $\mu\text{mol/g}$	BD-Fe, $\mu\text{mol/g}$	NaOH-Fe, $\mu\text{mol/g}$	HCl-Fe, $\mu\text{mol/g}$	BD-P, $\mu\text{mol/g}$	NaOH-P, $\mu\text{mol/g}$	NaOH-rP, $\mu\text{mol/g}$	NaOH-nrP, $\mu\text{mol/g}$	NaOH-rP:P	HCl-P, $\mu\text{mol/g}$
5814	8/18/11	24.0	2.4	258.0	242.0	81.0	74.6	117.2	3.5	43.8	29.1	14.7	0.7	3.0
9685	8/16/11	10.3	1.1	188.0	NA	18.1	23.9	NA	0.0	23.3	12.5	10.8	0.5	NA
9931	8/31/10	12.2	3.6	201.0	166.0	57.6	40.0	116.0	4.0	28.6	18.2	10.4	0.6	7.8

Table B3: Sediment Calcium Fractionation (0-2; 8-10 cm). Data reports the surface short cores (0-2 cm) and bottom short core (8-10 cm) taken from the 24 lakes (2015) and the 18 chain lakes (2016). The DEP and LEA did not provide the calcium fraction analysis.

Lake Study	Midas	Sample Date	BD-Ca,	NaOH-Ca,	HCl-Ca,	BD-Ca,	NaOH-Ca,	HCl-Ca,
			$\mu\text{mol/g}$	$\mu\text{mol/g}$	$\mu\text{mol/g}$	$\mu\text{mol/g}$	$\mu\text{mol/g}$	$\mu\text{mol/g}$
			0-2 cm	0-2 cm	0-2 cm	8-10 cm	8-10 cm	8-10 cm
2015	3748	6/26/15	39.3	1.8	23.0	26.2	NA	25.3
	5448	6/24/15	52.8	2.9	29.6	34.7	1.3	21.9
	5190	7/8/15	58.9	5.1	13.4	58.1	3.0	16.1
	5400	7/13/15	30.6	4.2	10.7	20.2	2.8	10.9
	5349	6/25/15	42.5	1.6	6.8	27.6	1.6	17.8
	78	7/9/15	40.9	4.9	8.3	52.1	3.6	17.4
	5274	7/6/15	49.8	3.3	16.5	34.5	2.2	16.9
	4538	7/10/15	46.3	7.6	10.7	48.5	6.2	20.4
	5272	7/6/15	84.0	5.8	19.9	47.8	3.4	16.0
	5348	7/2/15	122.8	5.9	22.8	64.7	3.9	32.3
	177	6/30/15	14.4	2.1	11.2	12.2	NA	20.5
	5280	7/2/15	65.9	7.8	11.1	46.4	4.4	20.6
	3838	6/29/15	81.7	9.5	5.2	52.4	6.6	17.1
	5344	6/25/15	24.9	2.5	8.2	32.6	0.3	19.5
	224	7/8/15	48.1	4.4	10.8	36.4	0.3	15.9
	3446	7/7/15	48.3	3.4	10.8	46.1	3.0	19.1
	3796	6/26/15	71.3	1.8	10.3	42.0	NA	21.4
	5352	7/2/15	56.1	NA	16.7	44.0	1.9	20.7
	3916	6/29/15	61.9	5.5	10.8	39.8	NA	11.0
	3750	7/9/15	73.8	3.4	27.4	54.7	1.4	34.5
	3444	7/7/15	60.7	0.8	10.6	40.6	1.3	15.4
	4434	6/30/15	26.3	2.8	10.0	34.3	6.2	9.5
	5172	7/1/15	41.2	1.4	24.1	38.4	2.5	22.2

Table B3: Continued

Lake Study	Midas	Sample Date	BD-Ca, $\mu\text{mol/g}$	NaOH-Ca, $\mu\text{mol/g}$	HCl-Ca, $\mu\text{mol/g}$	BD-Ca, $\mu\text{mol/g}$	NaOH-Ca, $\mu\text{mol/g}$	HCl-Ca, $\mu\text{mol/g}$
	5408	6/24/15	49.4	NA	16.5	31.1	0.8	16.3
2016	4444	6/24/16	28.4	3.8	15.1	24.1	2.9	15.5
	5666	6/28/16	101.6	8.6	19.0	74.7	9.6	20.9
	5814	6/23/16	70.0	7.8	14.6	62.5	7.4	21.5
	5182	6/23/16	62.0	8.1	17.3	43.3	6.8	21.8
	4406	6/27/16	32.7	4.0	11.2	29.3	2.8	10.0
	5330	6/29/16	43.6	7.4	12.8	42.3	7.5	13.2
	5664	6/30/16	77.0	5.9	21.4	76.0	8.4	30.3
	3760	6/22/16	99.2	8.2	18.6	76.7	6.7	25.4
	3762	6/22/16	108.7	8.3	22.4	70.1	5.5	21.6
	5812	6/29/16	67.4	10.9	17.3	52.2	9.1	24.2
	4448	6/24/16	12.4	3.0	6.7	15.2	2.7	12.8
	5186	6/29/16	74.6	6.5	17.9	60.2	6.2	22.8
	3826	6/30/16	105.1	8.1	12.6	94.3	8.1	11.9
	3824	6/30/16	54.0	3.5	21.7	41.5	4.0	29.8
	4446	6/27/16	119.3	13.0	13.4	111.4	11.5	18.5
	3688	6/23/16	122.7	8.6	19.0	81.5	4.8	21.7
	4346	6/24/16	31.2	3.9	12.9	23.2	3.7	13.8
	5184	6/28/16	247.4	13.2	25.1	158.8	11.2	27.5

Figure B1: Sequential Extraction (P, Fe, Al) of Sediment Cores. Reported date includes summer 2015 in $\mu\text{mol g}^{-1}$ dry weight (dw) at depth (0-2; 8-10 cm).

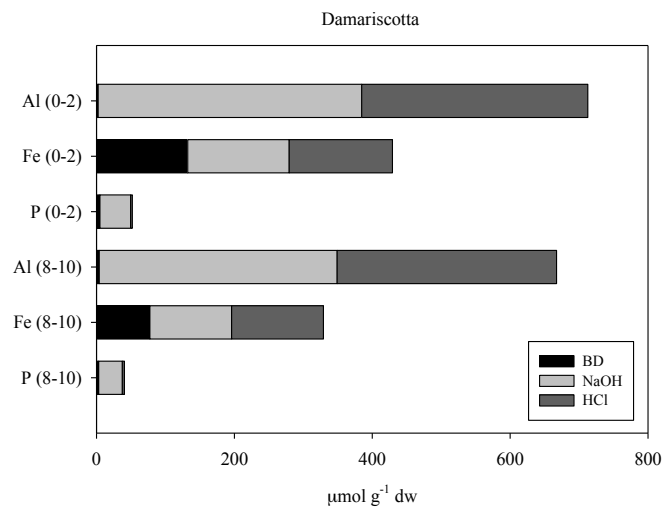
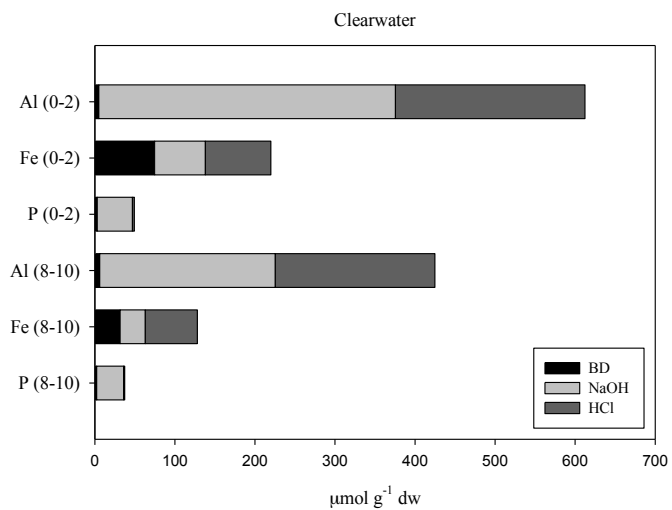
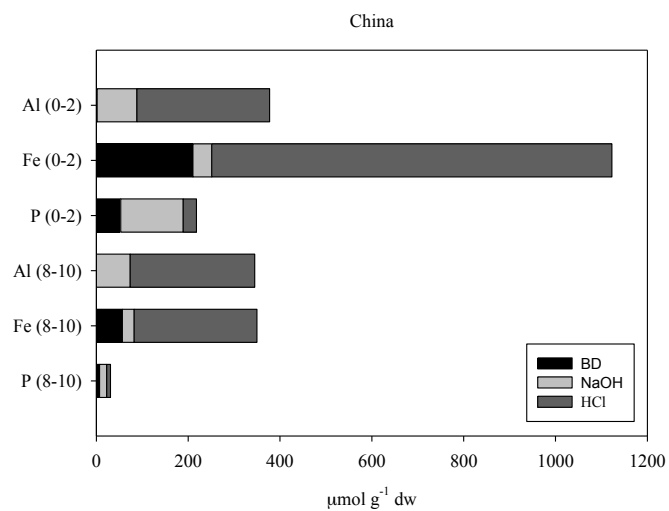
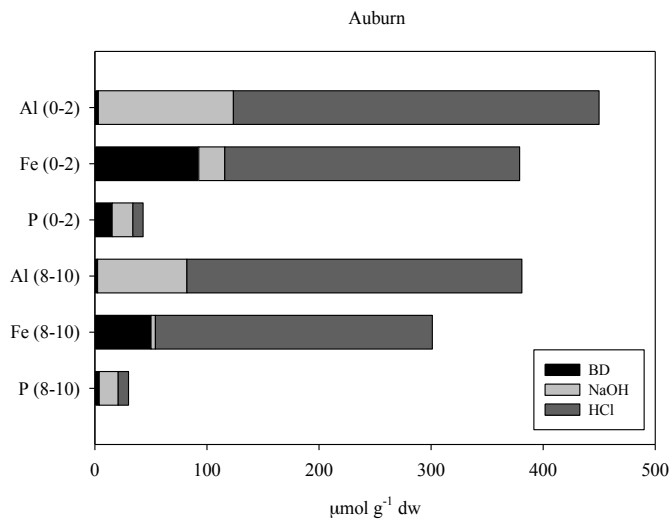


Figure B1: Continued

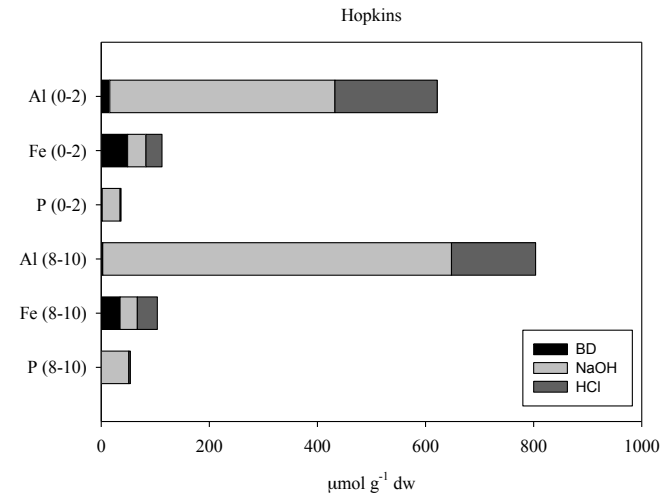
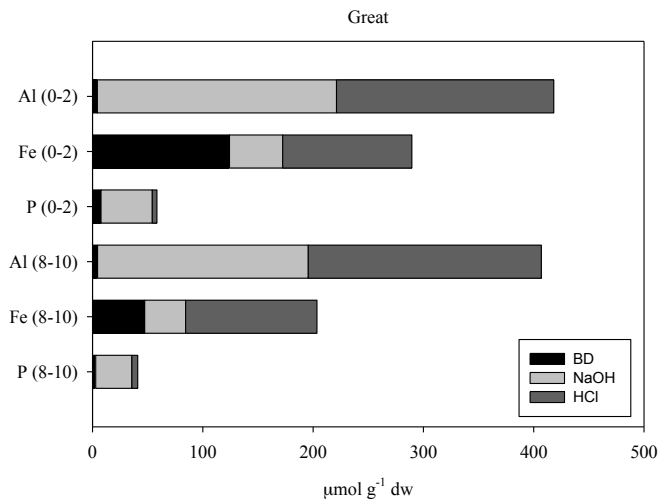
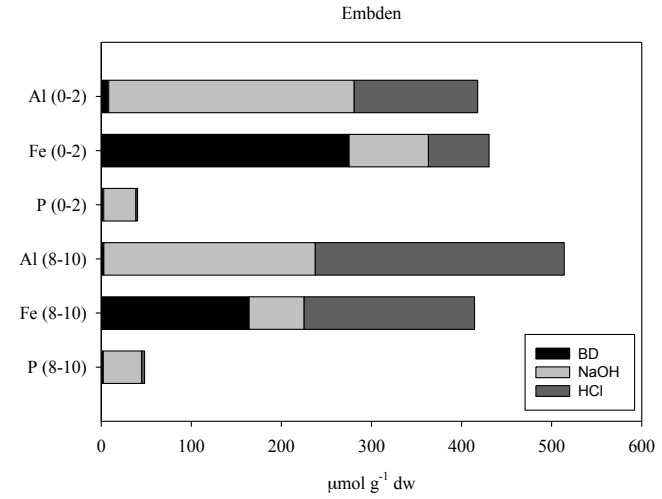
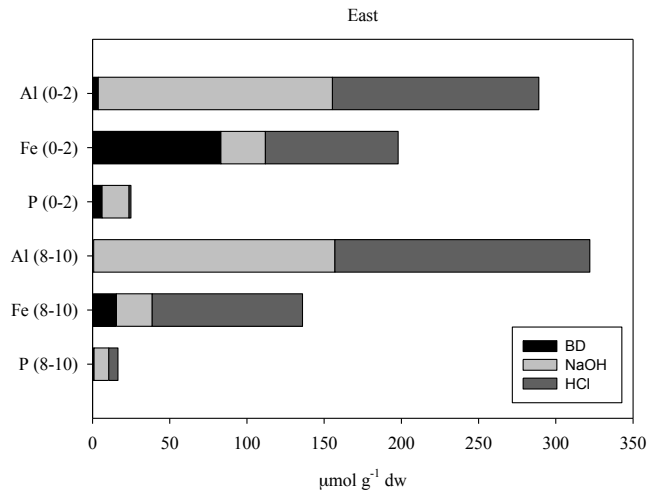


Figure B1: Continued

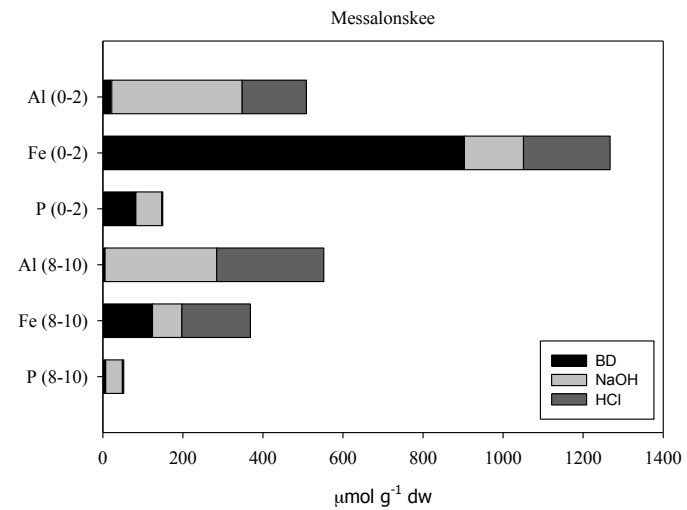
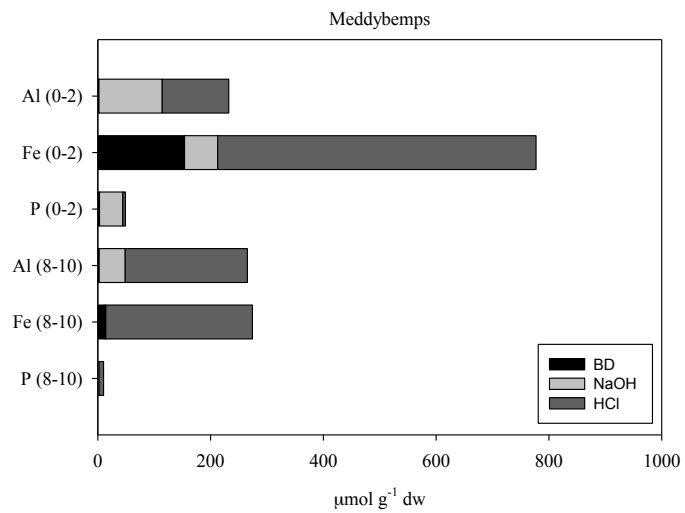
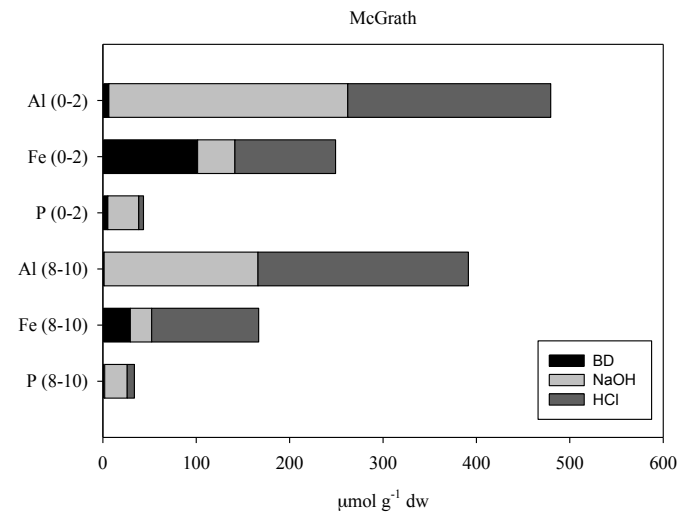
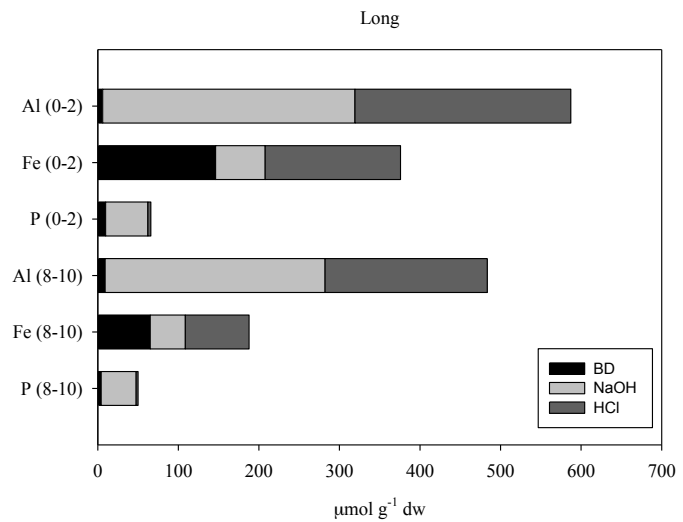


Figure B1: Continued

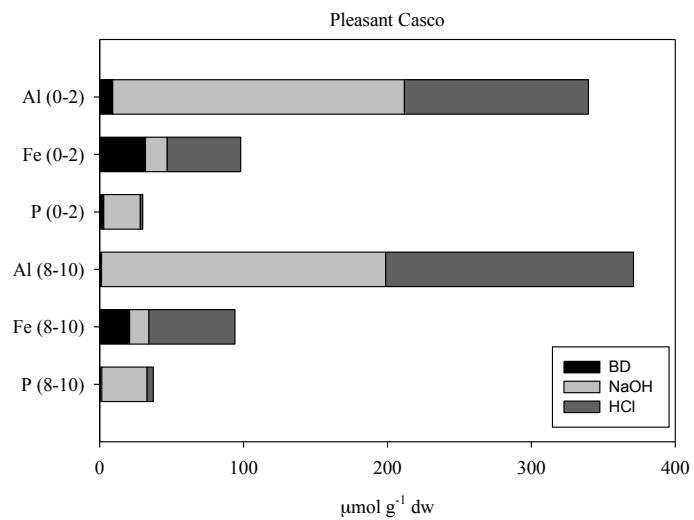
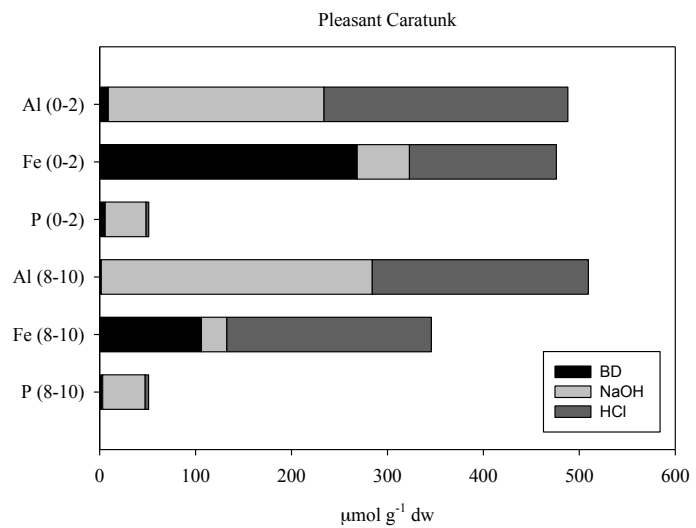
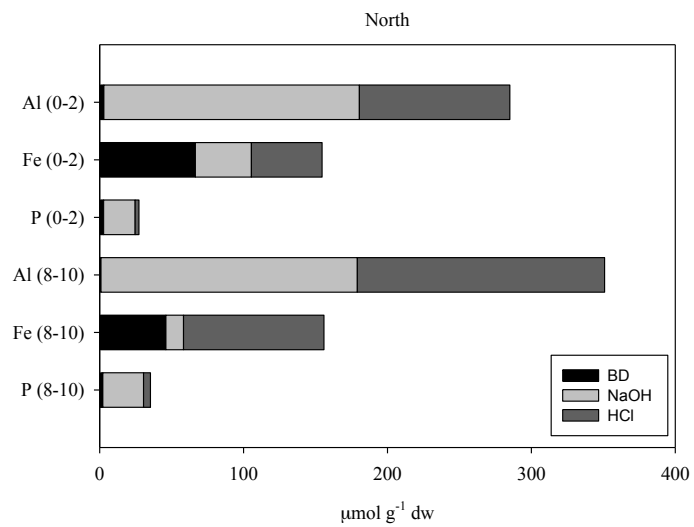
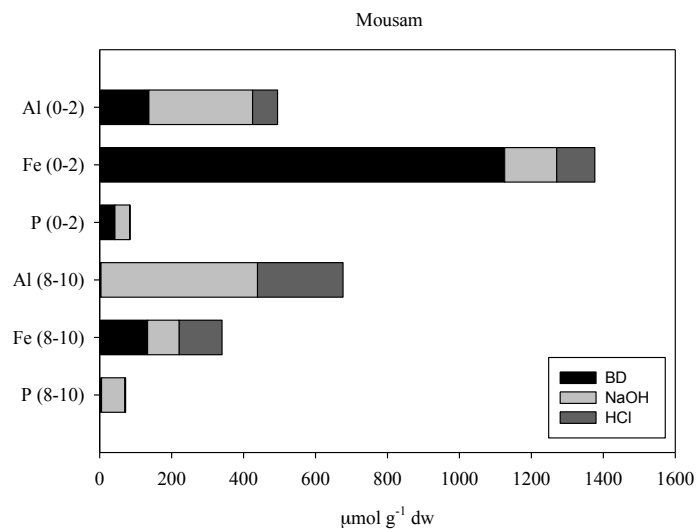


Figure B1: Continued

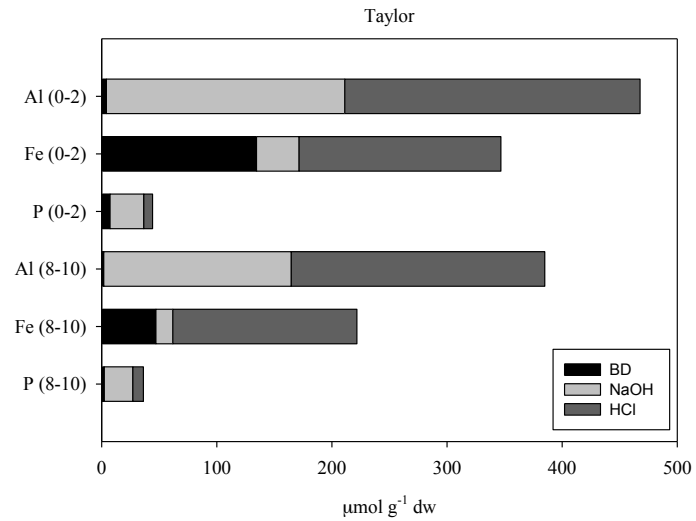
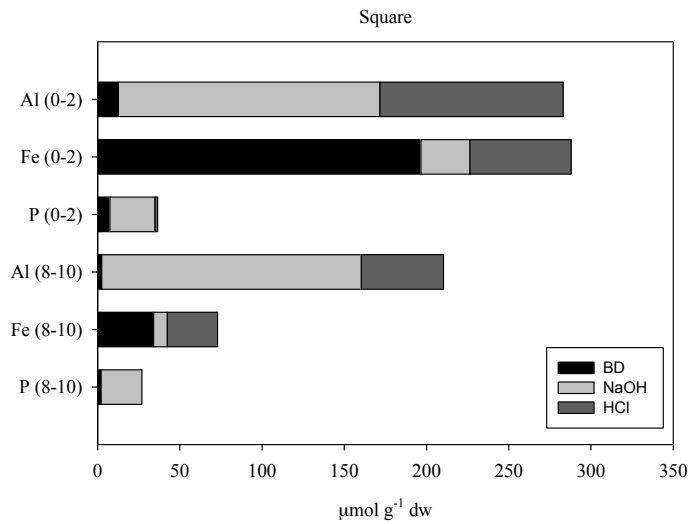
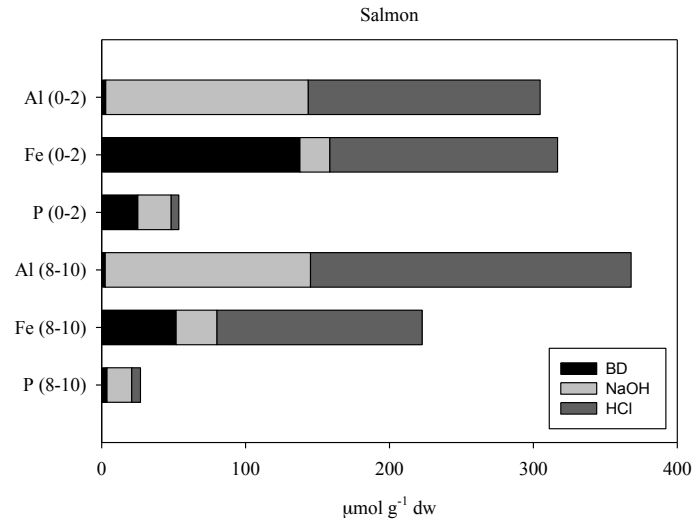
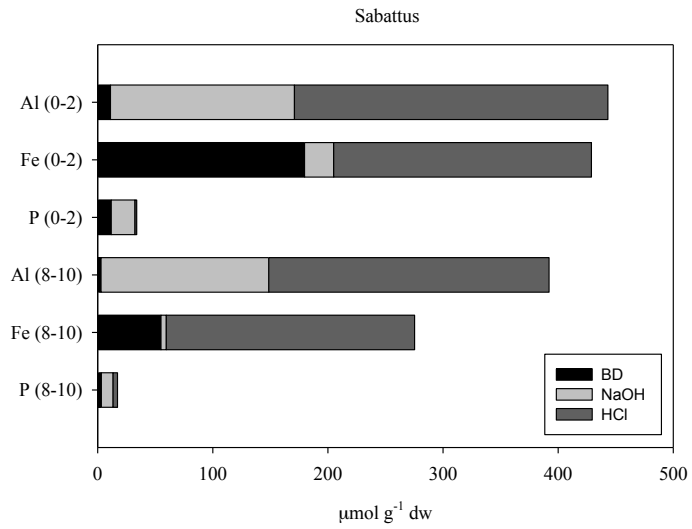


Figure B1: Continued

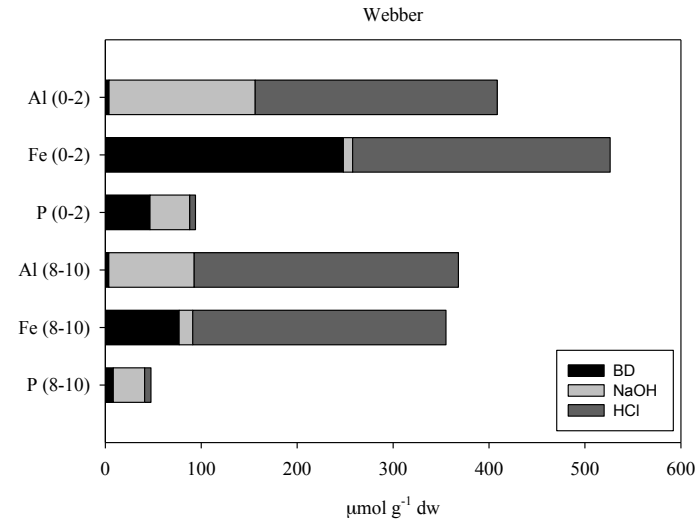
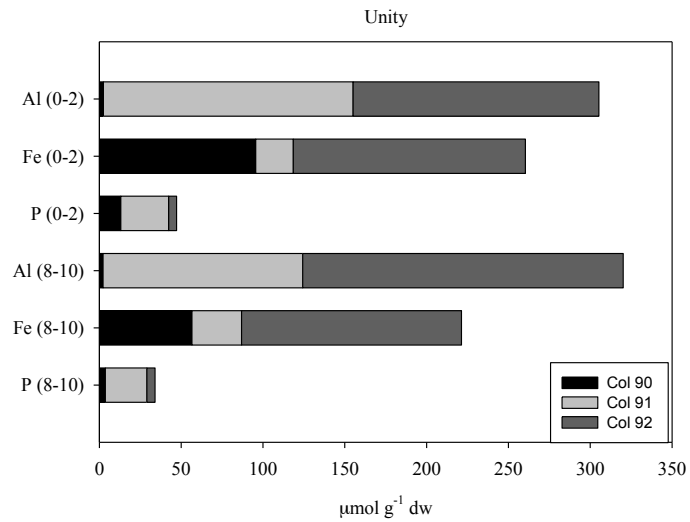
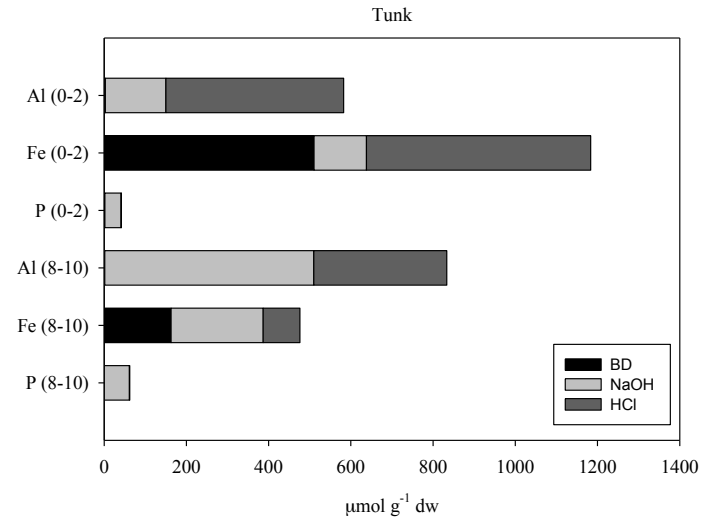
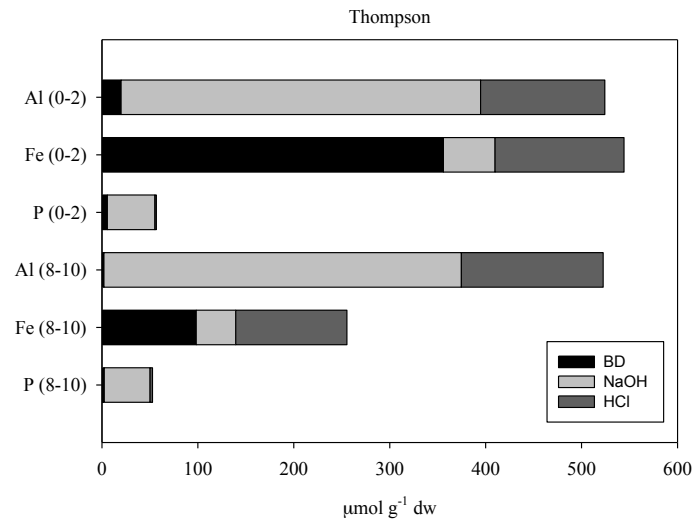


Table B4: Cations and Secchi Transparency. Results include epilimnetic Total Al, Fe, Mg, Ca, Na, K, and secchi for all samples in this study.

Midas	Date	Al, ug/L	Fe, ug/L	Mg, mg/L	Ca, mg/L	Na, mg/L	K, mg/L	Secchi, m
2015								
78	8/25/15	10.98	6.74	0.40	2.50	1.11	0.36	9.81
177	8/14/15	14.21	19.05	0.35	1.61	1.99	0.21	6.25
224	8/25/15	6.75	3.17	0.83	1.56	0.54	0.18	15.98
3444	8/12/15	8.83	7.10	0.50	2.80	3.45	0.37	10.35
3446	8/20/15	5.44	6.25	0.53	2.88	5.39	0.39	5.10
3748	8/27/15	5.23	16.76	0.78	4.83	5.64	0.63	8.67
3750	8/20/15	6.52	28.97	0.88	6.22	6.37	0.72	5.50
3796	8/12/15	22.01	261.56	1.49	8.14	6.09	1.09	1.85
3838	8/24/25	4.47	17.07	0.80	3.79	6.12	0.60	7.80
3916	8/24/25	2.72	34.45	0.99	3.85	6.76	0.50	7.50
4434	8/14/15	31.83	3.58	0.21	0.55	1.57	0.21	10.90
4538	8/26/15	14.19	3.57	0.28	1.28	1.11	0.23	5.95
5172	8/11/15	7.40	56.37	1.17	5.30	2.72	0.62	1.33
5190	8/18/15	7.67	9.17	0.66	3.00	1.53	0.37	9.91
5272	8/19/15	3.91	8.20	0.55	3.10	3.05	0.44	7.34
5274	8/19/15	4.25	9.15	0.61	3.17	3.09	0.46	7.05
5280	8/13/15	5.22	45.99	1.06	5.54	3.71	0.55	5.35
5344	8/13/15	47.15	80.44	0.67	3.21	3.77	0.43	4.65
5348	8/11/15	13.43	27.01	0.82	9.17	4.21	0.88	6.10
5349	8/18/15	6.15	24.69	0.56	3.09	2.89	0.37	5.34
5352	8/13/15	5.69	45.83	1.06	8.84	4.10	0.75	5.10
5400	8/28/15	5.23	19.33	0.67	2.41	3.85	1.01	6.25
5408	8/10/15	5.65	52.98	0.87	5.85	3.87	0.92	2.25

Table B4: Continued

Midas	Date	Al, ug/L	Fe, ug/L	Mg, mg/L	Ca, mg/L	Na, mg/L	K, mg/L	Secchi, m
5448	8/10/15	3.34	12.93	1.03	7.84	4.65	1.04	1.80
2016								
4444	8/12/16	16.59	61.75	0.57	1.47	2.68	0.43	5.03
5666	8/8/16	14.24	53.86	0.71	3.83	3.78	0.76	4.90
5814	8/8/16	14.12	21.12	0.71	4.76	3.81	0.90	8.60
5182	8/10/16	14.13	54.26	0.73	5.33	4.55	0.73	6.35
4406	9/2/16	6.29	206.29	0.75	2.38	3.40	0.71	2.70
5330	8/10/16	23.03	71.34	0.38	1.61	1.84	0.38	4.78
5664	8/26/16	8.03	44.61	1.07	5.86	6.42	0.77	5.85
3760	8/23/16	14.79	93.97	0.81	6.03	4.02	0.68	6.30
3762	8/26/16	9.46	22.10	1.04	5.87	6.35	0.70	6.60
5812	8/23/16	12.12	34.57	0.77	5.73	4.77	0.77	6.78
4448	9/1/16	24.17	30.05	0.49	1.61	2.81	0.72	7.59
5186	8/11/16	13.80	13.53	0.63	3.79	2.77	0.62	7.60
3826	8/26/16	7.29	129.66	0.81	6.27	4.30	0.99	2.20
3824	8/11/16	6.67	42.99	0.76	5.89	4.00	0.75	5.60
4446	9/1/16	26.16	295.05	0.70	1.85	3.13	0.22	2.50
3688	8/26/16	4.71	16.96	1.00	5.65	4.81	0.68	7.21
4346	9/1/16	80.21	184.47	0.62	1.32	3.37	0.56	4.20
5184	8/11/16	21.32	36.53	0.66	5.05	1.32	0.43	4.90
DEP								
70	8/9/11	5.00	11.00	1.36	5.68	3.81	0.72	5.05
80	8/24/11	19.00	47.00	1.25	6.07	4.63	0.48	4.25
121	8/24/11	5.00	12.00	0.53	3.68	1.21	0.26	6.16
177	9/23/10	5.00	17.00	0.56	2.26	3.45	0.27	6.40
243	9/1/11	29.00	11.00	0.37	1.78	0.78	0.25	6.66

Table B4: Continued

Midas	Date	Al, ug/L	Fe, ug/L	Mg, mg/L	Ca, mg/L	Na, mg/L	K, mg/L	Secchi, m
262	8/30/10	10.00	12.00	0.51	1.42	1.53	0.27	6.56
342	9/1/11	12.00	7.00	0.75	2.37	0.80	0.34	7.55
386	8/23/11	13.00	20.00	0.66	2.38	2.18	0.42	2.47
410	9/1/11	5.00	30.00	0.85	2.64	0.81	0.41	3.45
447	9/23/12	24.00	70.00	2.08	2.53	16.20	0.43	1.46
760	8/30/10	5.00	15.00	1.99	8.83	1.56	0.31	4.83
954	8/23/10	43.00	15.00	0.40	1.55	1.38	0.28	6.84
1068	8/24/11	5.00	2.50	0.59	3.80	2.59	0.36	6.56
1070	8/24/11	5.00	2.50	0.59	4.22	1.29	0.28	7.85
1078	8/22/11	43.00	40.00	0.42	1.56	1.61	0.19	4.67
1088	8/22/11	29.00	16.00	0.41	1.49	1.69	0.18	6.32
1150	9/23/10	5.00	2.50	0.41	1.98	1.35	0.33	9.14
1210	8/25/10	58.00	41.00	0.37	1.25	3.06	0.33	5.69
2004	8/23/10	11.00	2.50	0.35	1.93	1.07	0.28	6.55
2020	8/15/11	22.00	15.00	0.37	2.38	1.20	0.48	5.98
2146	8/17/11	14.00	9.00	0.47	2.27	1.84	0.35	7.61
2156	8/24/11	5.00	31.00	1.90	11.70	2.74	0.69	3.02
2242	8/17/11	5.00	6.00	0.51	11.00	2.72	0.54	8.33
2286	9/2/10	5.00	58.00	2.04	9.14	7.31	0.43	1.68
2590	8/30/10	5.00	27.00	1.08	4.67	1.77	0.46	5.50
2608	8/30/10	5.00	11.00	0.93	3.57	1.74	0.46	7.72
2948	8/30/10	15.00	34.00	0.82	4.06	1.00	0.29	5.85
3038	8/24/11	31.00	32.00	0.82	3.28	0.88	0.24	5.21
3376	8/25/11	33.00	19.00	0.49	2.26	2.67	0.35	4.34
3388	9/7/10	5.00	9.00	0.65	2.87	5.75	0.50	5.69
3434	9/1/10	5.00	5.00	0.74	5.58	5.50	0.84	5.56

Table B4: Continued

Midas	Date	Al, ug/L	Fe, ug/L	Mg, mg/L	Ca, mg/L	Na, mg/L	K, mg/L	Secchi, m
3452	8/31/10	25.00	14.00	0.61	2.87	5.60	0.54	5.40
3454	8/16/11	5.00	7.00	0.42	2.19	3.16	0.27	7.23
3604	8/18/11	11.00	12.00	0.47	3.00	1.88	0.46	6.28
3626	9/1/10	5.00	20.00	1.16	11.70	7.39	1.21	4.67
3672	8/10/11	5.00	11.00	0.48	2.81	1.62	0.47	4.65
3682	8/10/11	5.00	42.00	0.46	2.49	3.36	0.60	5.43
3690	8/31/10	5.00	10.00	0.86	4.11	5.07	0.53	5.20
3780	8/9/11	5.00	16.00	0.32	1.83	1.18	0.22	5.03
3814	8/23/11	5.00	15.00	1.17	6.71	7.99	0.99	2.25
3830	9/8/10	5.00	31.00	0.89	7.46	4.81	0.58	5.90
3884	9/7/10	5.00	187.00	1.14	3.84	8.21	0.85	4.13
3920	8/18/10	5.00	9.00	0.79	3.82	5.05	0.52	6.74
4272	8/8/11	15.00	16.00	0.50	2.03	2.76	0.33	5.97
4316	8/17/10	5.00	44.00	0.87	5.27	5.44	0.59	4.10
4322	8/17/10	5.00	7.00	0.51	1.99	2.46	0.35	7.14
4328	8/17/10	5.00	2.50	0.44	1.60	3.22	0.29	10.92
4330	8/17/10	5.00	10.00	0.39	1.30	1.70	0.24	4.10
4336	8/17/10	5.00	20.00	0.69	3.07	4.51	0.50	5.74
4388	8/15/11	31.00	36.00	0.48	1.36	2.82	0.38	4.56
4452	9/20/12	10.00	7.00	0.40	1.62	3.04	0.21	7.30
4492	8/25/10	82.00	9.00	0.45	1.88	1.72	0.37	7.39
4606	9/19/12	5.00	2.50	0.43	1.49	3.61	0.22	11.21
4608	9/19/12	15.00	2.50	0.46	1.65	3.20	0.22	12.60
4610	9/20/12	17.00	10.00	0.44	1.48	5.38	0.24	7.42
4612	9/20/12	21.00	19.00	0.38	1.52	4.44	0.22	6.89
4614	9/17/12	25.00	44.00	0.70	1.69	5.46	0.35	4.50

Table B4: Continued

Midas	Date	Al, ug/L	Fe, ug/L	Mg, mg/L	Ca, mg/L	Na, mg/L	K, mg/L	Secchi, m
4618	9/20/12	57.00	43.00	0.85	1.97	4.10	0.29	3.63
4620	9/17/12	18.00	42.00	0.52	1.09	5.14	0.27	4.78
4622	9/19/12	15.00	2.50	0.64	1.50	5.08	0.33	9.60
4624	9/17/12	5.00	2.50	0.70	2.32	7.96	0.45	7.91
4628	9/17/12	109.00	144.00	0.78	1.49	5.01	0.33	4.24
4630	9/17/12	5.00	19.00	0.73	1.69	5.00	0.32	6.30
4766	8/25/10	76.00	56.00	0.38	1.71	1.37	0.30	4.70
4782	9/8/11	62.00	44.00	0.36	1.61	1.20	0.19	2.45
4788	8/25/10	29.00	10.00	0.43	1.71	1.70	0.53	5.74
4800	9/1/10	5.00	15.00	0.72	2.19	3.98	0.59	6.70
4802	8/10/11	5.00	48.00	0.76	2.57	3.57	0.53	3.50
4806	8/10/11	5.00	20.00	0.78	2.52	3.59	0.61	5.70
4822	8/11/11	5.00	5.00	1.31	6.30	11.00	1.06	3.16
4852	8/11/11	5.00	13.00	0.83	3.06	4.86	0.59	7.30
4857	8/24/10	42.00	94.00	0.57	1.25	3.49	0.44	4.09
4894	8/17/11	5.00	9.00	0.60	1.88	3.48	0.55	7.48
4896	8/31/10	19.00	30.00	0.68	2.70	2.53	0.59	6.50
5024	8/31/11	5.00	8.00	0.91	4.82	8.70	0.93	8.45
5172	8/11/11	5.00	17.00	1.41	6.14	2.98	0.67	1.05
5174	8/11/11	5.00	43.00	0.86	5.08	3.29	0.79	3.85
5198	8/18/10	5.00	66.00	0.94	4.87	6.46	1.13	5.20
5222	9/6/11	18.00	57.00	0.81	1.82	3.82	0.52	5.85
5236	8/19/10	5.00	5.00	1.10	7.61	4.76	0.97	2.92
5240	9/2/10	5.00	14.00	0.87	7.08	7.55	1.01	7.21
5280	8/9/11	5.00	10.00	0.73	4.30	3.30	0.58	6.00
5344	8/22/11	5.00	19.00	0.69	2.52	3.41	0.53	3.90

Table B4: Continued

Midas	Date	Al, ug/L	Fe, ug/L	Mg, mg/L	Ca, mg/L	Na, mg/L	K, mg/L	Secchi, m
5348	8/22/11	10.00	19.00	0.97	10.10	4.70	0.98	5.90
5349	8/22/11	5.00	15.00	0.56	2.86	2.87	0.40	4.45
5352	8/19/10	5.00	11.00	0.92	8.17	4.22	0.92	3.82
5386	9/1/10	5.00	72.00	0.76	2.16	4.54	0.60	4.10
5400	8/31/10	5.00	9.00	0.81	2.50	4.29	0.82	7.20
5408	8/26/10	14.00	31.00	1.18	6.63	4.84	1.23	1.65
5416	8/26/10	5.00	29.00	0.97	5.38	5.07	0.96	1.30
5448	8/26/10	10.00	2.50	1.27	8.75	5.87	1.23	1.65
5458	9/2/10	5.00	14.00	1.82	8.39	4.24	0.62	5.10
5490	8/15/11	5.00	13.00	0.42	1.45	1.35	0.24	5.35
5682	9/1/10	12.00	122.00	0.93	3.20	4.30	0.76	4.46
5690	8/17/11	5.00	46.00	1.22	3.16	4.72	0.64	3.96
5710	8/17/11	12.00	19.00	0.71	2.18	3.81	0.65	4.44
5780	8/30/11	13.00	14.00	0.56	2.77	5.33	0.49	6.40
5814	8/18/11	5.00	7.00	0.59	4.15	3.04	0.53	7.02
9685	8/16/11	10.00	12.00	0.57	2.82	5.37	0.49	7.55
9931	8/31/10	5.00	2.50	0.80	4.24	6.28	0.89	1.93
LEA								
5780	7/11/13	NA	NA	NA	NA	NA	NA	NA
3418	6/18/13	NA	NA	NA	NA	NA	NA	6.28
5780	7/11/13	NA	NA	NA	NA	NA	NA	6.89
3130	7/18/13	NA	NA	NA	NA	NA	NA	6.29
3382	7/9/13	NA	NA	NA	NA	NA	NA	10.45
3424	7/3/13	NA	NA	NA	NA	NA	NA	7.19
3199	7/12/13	NA	NA	NA	NA	NA	NA	7.27
3134	6/27/13	NA	NA	NA	NA	NA	NA	5.96

Table B4: Continued

Midas	Date	Al, ug/L	Fe, ug/L	Mg, mg/L	Ca, mg/L	Na, mg/L	K, mg/L	Secchi, m
3416	6/18/13	NA	NA	NA	NA	NA	NA	6.06
9685	7/11/13	NA	NA	NA	NA	NA	NA	7.55
3420	7/17/13	NA	NA	NA	NA	NA	NA	5.70
3454	7/1/13	NA	NA	NA	NA	NA	NA	NA
5582	8/26/13	NA	NA	NA	NA	NA	NA	4.90
3134	6/27/13	NA	NA	NA	NA	NA	NA	7.96
5780	7/11/13	NA	NA	NA	NA	NA	NA	6.51
5780	7/11/13	NA	NA	NA	NA	NA	NA	7.05
3132	7/18/13	NA	NA	NA	NA	NA	NA	7.06
3126	7/18/13	NA	NA	NA	NA	NA	NA	6.30
3234	7/1/13	NA	NA	NA	NA	NA	NA	5.53
3374	6/24/13	NA	NA	NA	NA	NA	NA	8.05
3134	6/27/13	NA	NA	NA	NA	NA	NA	NA
3452	7/31/13	NA	NA	NA	NA	NA	NA	5.97
3454	7/1/13	NA	NA	NA	NA	NA	NA	7.20
3448	8/1/13	NA	NA	NA	NA	NA	NA	4.83
3232	7/16/13	NA	NA	NA	NA	NA	NA	6.87
3456	9/10/13	NA	NA	NA	NA	NA	NA	5.14
5780	7/11/13	NA	NA	NA	NA	NA	NA	NA

Table B5: Anions and pH. Results include epilimnetic Alkalinity (Alk), Conductivity (Cond), Cl⁻, NO₃⁻, SO₄³⁻, ANC, Si, and pH for all lakes in this study. Dates are the same as in Table B4.

Midas	Alk	Cond	Cl, µeq/L	NO ₃ , µeq/L	SO ₄ , µeq/L	ANC(µeq/L)	Si(mg/L)	pH
2015								
78	NA	NA	36.05	<1	43.73	NA	NA	7.07
177	NA	NA	97.55	<1	29.70	NA	NA	6.67
224	NA	NA	14.98	<1	54.23	NA	NA	7.11
3444	NA	NA	190.35	<1	52.80	NA	NA	7.17
3446	NA	NA	297.72	<1	48.53	NA	NA	7.03
3748	NA	NA	332.16	<1	62.30	NA	NA	7.44
3750	NA	NA	439.57	<1	52.89	NA	NA	7.58
3796	NA	NA	372.86	<1	87.50	NA	NA	7.36
3838	NA	NA	386.85	<1	52.08	NA	NA	7.15
3916	NA	NA	371.28	<1	43.18	NA	NA	7.03
4434	NA	NA	77.00	<1	44.80	NA	NA	6.35
4538	NA	NA	36.94	<1	39.97	NA	NA	6.95
5172	NA	NA	146.29	<1	52.89	NA	NA	7.32
5190	NA	NA	46.11	<1	59.30	NA	NA	7.39
5272	NA	NA	171.43	<1	38.67	NA	NA	7.09
5274	NA	NA	184.39	<1	39.01	NA	NA	6.99
5280	NA	NA	191.19	<1	45.40	NA	NA	7.06
5344	NA	NA	205.37	<1	35.70	NA	NA	7.20
5348	NA	NA	212.90	1.39	52.29	NA	NA	7.65
5349	NA	NA	156.48	1.00	39.50	NA	NA	7.30
5352	NA	NA	211.41	<1	52.60	NA	NA	7.76
5400	NA	NA	211.52	0.03	51.88	NA	NA	6.94
5408	NA	NA	230.87	1.35	56.34	NA	NA	8.22

Table B5: Continued

Midas	Alk	Cond	Cl, µeq/L	NO₃, µeq/L	SO₄, µeq/L	ANC(µeq/L)	Si(mg/L)	pH
5448	NA	NA	274.58	2.12	78.40	NA	NA	8.94
2016								
4444	NA	NA	110.67	0.05	13.43	NA	NA	6.85
5666	NA	NA	208.43	0.30	15.86	NA	NA	6.34
5814	NA	NA	193.97	0.25	17.69	NA	NA	7.35
5182	NA	NA	213.80	0.10	20.35	NA	NA	6.44
4406	NA	NA	126.99	0.08	8.92	NA	NA	NA
5330	NA	NA	79.45	0.03	13.85	NA	NA	6.44
5664	NA	NA	397.31	0.10	23.83	NA	NA	7.30
3760	NA	NA	134.37	0.08	12.03	NA	NA	7.20
3762	NA	NA	283.83	0.06	19.38	NA	NA	7.37
5812	NA	NA	157.19	0.08	15.87	NA	NA	7.36
4448	NA	NA	139.67	0.07	12.84	NA	NA	6.85
5186	NA	NA	170.62	0.23	16.54	NA	NA	7.15
3826	NA	NA	220.78	0.50	16.80	NA	NA	7.43
3824	NA	NA	201.10	0.20	16.99	NA	NA	7.43
4446	NA	NA	124.28	0.17	6.55	NA	NA	6.29
3688	NA	NA	231.79	0.04	17.86	NA	NA	7.30
4346	NA	NA	137.30	0.06	12.75	NA	NA	6.66
5184	NA	NA	81.49	0.13	13.17	NA	NA	7.14
DEP								
70	NA	NA	172.00	0.50	63.00	334	0.95	7.32
80	NA	NA	209.00	0.50	54.00	315	0.42	7.15
121	NA	NA	34.00	0.50	36.00	190	0.79	7.10
177	NA	NA	122.00	0.50	41.00	110	0.59	6.87
243	NA	NA	12.00	0.50	37.00	89.2	1.59	6.78

Table B5: Continued

Midas	Alk	Cond	Cl, µeq/L	NO₃, µeq/L	SO₄, µeq/L	ANC(µeq/L)	Si(mg/L)	pH
262	NA	NA	40.00	0.50	43.00	93.5	0.88	6.96
342	NA	NA	15.00	0.50	48.00	144	2.18	6.89
386	NA	NA	85.00	0.50	47.00	139	1.14	NA
410	NA	NA	11.00	0.50	46.00	172	2.4	7.02
447	NA	NA	738.00	0.50	117.00	151	1.12	6.73
760	NA	NA	33.00	0.50	69.00	503	0.74	7.61
954	NA	NA	36.00	0.50	34.00	77.3	0.79	6.62
1068	NA	NA	112.00	0.50	43.00	190	0.7	7.04
1070	NA	NA	42.00	0.50	40.00	216	0.94	6.92
1078	NA	NA	39.00	0.50	31.00	72.1	0.44	6.62
1088	NA	NA	53.00	0.50	33.00	73.3	1	6.88
1150	NA	NA	28.00	0.50	48.00	107	1.18	6.88
1210	NA	NA	119.00	0.50	40.00	64.9	1.78	6.53
2004	NA	NA	14.00	0.50	46.00	94.6	1.8	6.91
2020	NA	NA	10.00	0.50	35.00	145	2.44	7.04
2146	NA	NA	52.00	0.50	52.00	119	1.19	6.88
2156	NA	NA	106.00	0.50	83.00	655	1.06	7.63
2242	NA	NA	117.00	0.50	57.00	529	1.18	7.59
2286	NA	NA	258.00	0.50	39.00	589	1.23	9.06
2590	NA	NA	49.00	0.50	47.00	295	0.96	7.30
2608	NA	NA	32.00	0.50	54.00	218	0.91	7.39
2948	NA	NA	11.00	0.50	46.00	227	0.87	7.02
3038	NA	NA	16.00	0.50	34.00	187	0.93	7.06
3376	NA	NA	98.00	0.50	42.00	119	0.49	NA
3388	NA	NA	241.00	0.50	52.00	162	0.58	7.06
3434	NA	NA	191.00	0.50	53.00	313	1.38	7.57

Table B5: Continued

Midas	Alk	Cond	Cl, µeq/L	NO₃, µeq/L	SO₄, µeq/L	ANC(µeq/L)	Si(mg/L)	pH
3452	NA	NA	238.00	0.50	51.00	158	1.94	7.00
3454	NA	NA	134.00	0.50	40.00	109	0.85	6.62
3604	NA	NA	61.00	0.50	53.00	155	1.63	NA
3626	NA	NA	300.00	0.50	113.00	567	3.32	7.89
3672	NA	NA	44.00	0.50	52.00	152	1.31	7.12
3682	NA	NA	127.00	0.50	57.00	136	1.37	7.00
3690	NA	NA	163.00	0.50	51.00	257	2.06	7.26
3780	NA	NA	35.00	0.50	51.00	78	0.18	6.76
3814	NA	NA	359.00	0.50	65.00	368	0.91	7.82
3830	NA	NA	146.00	0.50	54.00	408	0.68	7.48
3884	NA	NA	304.00	0.50	55.00	254	1.22	6.97
3920	NA	NA	218.00	0.50	66.00	193	1.62	7.07
4272	NA	NA	98.00	0.50	38.00	113	1.68	6.78
4316	NA	NA	169.00	0.50	54.00	300	1.48	7.02
4322	NA	NA	65.00	0.50	52.00	110	0.81	6.84
4328	NA	NA	109.00	0.50	47.00	89.9	1.15	6.94
4330	NA	NA	46.00	0.50	45.00	76.7	0.73	6.78
4336	NA	NA	151.00	0.50	50.00	183	0.79	6.93
4388	NA	NA	110.00	0.50	40.00	72.7	1.68	6.70
4452	NA	NA	106.00	0.50	47.00	80.8	1.47	6.79
4492	NA	NA	32.00	0.50	50.00	105	2.22	6.67
4606	NA	NA	149.00	0.50	46.00	65.2	0.55	6.74
4608	NA	NA	121.00	0.50	52.00	74.3	1.32	6.83
4610	NA	NA	224.00	0.50	50.00	56.7	0.69	6.49
4612	NA	NA	160.00	0.50	46.00	70.9	0.7	6.52
4614	NA	NA	228.00	0.50	49.00	86.2	0.53	6.43

Table B5: Continued

Midas	Alk	Cond	Cl, µeq/L	NO ₃ , µeq/L	SO ₄ , µeq/L	ANC(ueq/L)	Si(mg/L)	pH
4618	NA	NA	149.00	0.50	45.00	119	0.75	6.57
4620	NA	NA	211.00	0.50	45.00	50.6	0.37	6.18
4622	NA	NA	210.00	0.50	57.00	68.2	0.49	6.62
4624	NA	NA	354.00	0.50	59.00	104	0.6	6.88
4628	NA	NA	207.00	0.50	40.00	71.8	1.41	6.27
4630	NA	NA	214.00	0.50	51.00	86.5	0.69	6.68
4766	NA	NA	27.00	0.50	32.00	87.6	1.54	6.71
4782	NA	NA	27.00	0.50	36.00	69.5	0.66	6.43
4788	NA	NA	29.00	0.50	46.00	104	1.45	NA
4800	NA	NA	142.00	0.50	50.00	122	0.57	6.95
4802	NA	NA	148.00	0.50	51.00	152	0.75	6.97
4806	NA	NA	151.00	0.50	54.00	154	0.31	6.82
4822	NA	NA	490.00	0.50	96.00	323	0.16	7.45
4852	NA	NA	226.00	0.50	53.00	168	0.81	6.89
4857	NA	NA	159.00	0.50	42.00	61	0.71	6.31
4894	NA	NA	177.00	0.50	39.00	89.5	0.41	6.76
4896	NA	NA	92.00	0.50	58.00	166	1.45	7.06
5024	NA	NA	430.00	0.50	54.00	218	0.76	7.06
5172	NA	NA	127.00	0.50	67.00	357	0.55	8.24
5174	NA	NA	126.00	0.50	53.00	295	1.42	7.24
5198	NA	NA	304.00	0.50	59.00	289	1.14	7.23
5222	NA	NA	149.00	0.50	50.00	118	1.16	6.64
5236	NA	NA	206.00	0.50	66.00	407	0.39	7.92
5240	NA	NA	270.00	0.50	68.00	377	1.1	7.62
5280	NA	NA	149.00	0.50	52.00	224	0.99	7.23
5344	NA	NA	152.00	0.50	43.00	139	0.09	6.94

Table B5: Continued

Midas	Alk	Cond	Cl, µeq/L	NO₃, µeq/L	SO₄, µeq/L	ANC(µeq/L)	Si(mg/L)	pH
5348	NA	NA	193.00	0.50	59.00	536	0.84	NA
5349	NA	NA	128.00	0.50	49.00	135	1.4	6.95
5352	NA	NA	193.00	0.50	59.00	462	0.58	8.02
5386	NA	NA	137.00	0.50	41.00	153	0.69	7.19
5400	NA	NA	182.00	0.50	54.00	153	1.19	7.18
5408	NA	NA	169.00	0.50	58.00	368	1.35	NA
5416	NA	NA	178.00	0.50	54.00	302	2.2	8.42
5448	NA	NA	216.00	0.50	95.00	436	1.09	7.78
5458	NA	NA	137.00	0.50	69.00	512	1.23	7.95
5490	NA	NA	40.00	0.50	35.00	86	0.55	6.78
5682	NA	NA	127.00	0.50	47.00	218	1.03	7.26
5690	NA	NA	205.00	0.50	56.00	205	0.73	6.89
5710	NA	NA	172.00	0.50	42.00	123	0.46	6.69
5780	NA	NA	216.00	0.50	49.00	140	1.1	6.90
5814	NA	NA	126.00	0.50	56.00	215	0.86	7.03
9685	NA	NA	219.00	0.50	51.00	141	0.99	NA
9931	NA	NA	237.00	0.50	53.00	219	0.74	7.35
LEA								
5780	NA	NA	NA	NA	NA	NA	NA	NA
3418	4.3	23.97	NA	NA	NA	NA	NA	6.67
5780	7.5	45.2	NA	NA	NA	NA	NA	6.70
3130	5	24.02	NA	NA	NA	NA	NA	6.71
3382	6.5	37.59	NA	NA	NA	NA	NA	6.63
3424	5	19.8	NA	NA	NA	NA	NA	6.90
3199	7.5	17.8	NA	NA	NA	NA	NA	6.83
3134	6.1	25.17	NA	NA	NA	NA	NA	6.70

Table B5: Continued

Midas	Alk	Cond	Cl, $\mu\text{eq/L}$	NO_3 , $\mu\text{eq/L}$	SO_4 , $\mu\text{eq/L}$	ANC($\mu\text{eq/L}$)	Si(mg/L)	pH
3416	6.9	32.46	NA	NA	NA	NA	NA	6.60
9685	7.9	37.5	NA	NA	NA	NA	NA	6.65
3420	6.1	28.68	NA	NA	NA	NA	NA	6.76
3454	NA	NA	NA	NA	NA	NA	NA	NA
5582	9.1	45.71	NA	NA	NA	NA	NA	6.73
3134	6.2	31.38	NA	NA	NA	NA	NA	6.70
5780	8.5	46.1	NA	NA	NA	NA	NA	6.80
5780	7.3	42	NA	NA	NA	NA	NA	6.80
3132	4.5	23.38	NA	NA	NA	NA	NA	6.68
3126	5.4	17.84	NA	NA	NA	NA	NA	6.64
3234	4.9	29.83	NA	NA	NA	NA	NA	6.60
3374	6	40.2	NA	NA	NA	NA	NA	6.85
3134	NA	NA	NA	NA	NA	NA	NA	NA
3452	8	42.9	NA	NA	NA	NA	NA	6.90
3454	6	30.2	NA	NA	NA	NA	NA	6.70
3448	6.5	35.3	NA	NA	NA	NA	NA	6.70
3232	5.7	40.95	NA	NA	NA	NA	NA	6.60
3456	4	24.01	NA	NA	NA	NA	NA	6.55
5780	NA	NA	NA	NA	NA	NA	NA	NA

APPENDIX C: MODEL PARAMETERS

Table C1.1: Significant parameters: Watershed and Chemistry. Parameters used for model regression consisting of epilimnetic and hypolimnetic P, chl a; agriculture and watershed characteristics: Ag:WA, AdjAg:LA, Ag:LA, WA:LA, Road:WA ratios; sediment chemistry parameters: $Al_{NaOH}:Fe_{BD}$, $Al_{NaOH}:P_{BD}$, and P_{BD} .

Midat	Date	Epi. P, ppb	Hypo. P, ppb	CHL a	Ag:WA ratio	AdjAg:LA ratio	Ag:LA ratio	WA:LA	Road:WA	$Al_{NaOH}:Fe_{BD}$	$Al_{NaOH}:P_{BD}$	P_{BD}
2015												
78	8/25/15	4.0	3.4	1.6	0.03	0.07	0.00	9.4	0.005	0.8	97.3	2.8
177	8/14/15	5.2	4.6	3.3	1.59	1.14	0.06	3.9	0.005	0.5	41.0	3.0
224	8/25/15	1.9	2.6	<1	0.00	0.00	0.00	4.7	0.009	0.7	39.0	5.8
3444	8/12/15	3.5	4.9	2.1	5.27	13.10	0.32	7.2	0.010	1.0	65.8	5.7
3446	8/20/15	4.2	9.1	2.7	3.31	4.17	0.12	3.6	0.011	4.5	71.9	2.8
3748	8/27/15	6.1	20.7	2.3	9.24	16.20	0.36	5.5	0.010	1.1	7.8	15.4
3750	8/20/15	5.1	9.2	3.2	10.69	5.60	1.53	14.6	0.011	1.5	66.8	3.2
3796	8/12/15	19.2	NA	22.1	7.80	31.34	1.45	10.3	0.010	0.8	13.5	11.8
3838	8/24/25	5.5	9.1	2.4	6.48	4.76	0.89	29.7	0.014	0.3	6.8	42.3
3916	8/24/25	4.0	13.2	2.4	1.64	1.76	0.06	5.2	0.014	0.8	21.4	7.4
4434	8/14/15	2.6	2.4	1.4	0.02	0.02	0.00	4.5	0.003	0.2	80.0	1.8
4538	8/26/15	4.4	5.5	1.6	0.08	0.00	0.00	4.5	0.008	5.2	214.8	1.9
5172	8/11/15	12.6	10.6	25.3	14.03	6.57	3.40	31.5	0.008	1.3	10.7	13.1
5190	8/18/15	3.3	4.3	1.2	0.96	0.86	0.05	5.1	0.008	2.7	122.7	3.0
5272	8/19/15	5.3	53.3	4.6	2.56	1.27	0.15	59.8	0.007	1.5	32.3	9.7
5274	8/19/15	6.8	8.1	4.3	3.61	3.07	0.12	6.5	0.006	1.3	28.1	7.7
5280	8/13/15	7.5	19.6	3.5	8.60	7.31	0.72	39.1	0.008	0.3	2.8	82.5
5344	8/13/15	19.0	15.3	5.2	7.99	6.63	0.43	8.4	0.009	1.4	40.9	2.8
5348	8/11/15	9.3	NA	2.9	2.63	3.24	0.16	6.0	0.012	2.5	95.6	5.4

Table C1.1: Continued

Midas		Epi. P, ppb	Hypo. P, ppb	CHL a	Ag:WA ratio	AdjAg:LA ratio	Ag:LA ratio	WA:LA	Road:WA	Al_{NaOH}:Fe_{BD}	Al_{NaOH}:P_{BD}	P_{BD}
5349	8/18/15	12.6	NA	3.6	1.25	0.97	0.03	2.8	0.012	1.2	27.0	6.2
5352	8/13/15	10.7	23.7	5.0	5.68	6.74	0.22	10.8	0.017	1.3	13.6	25.2
5400	8/28/15	7.5	14.2	5.4	8.58	22.36	0.52	18.7	0.010	1.5	62.1	5.0
5408	8/10/15	21.0	280.0	6.4	11.69	25.55	0.62	5.5	0.010	1.3	10.4	46.7
5448	8/10/15	13.9	33.3	17.1	10.51	27.13	0.55	12.0	0.008	0.8	2.4	53.1
2016												
3688	8/26/16	6.4	11.5	3.5	NA	NA	NA	NA	NA	3.3	34.2	10.6
3760	8/23/16	8.5	11.5	1.2	NA	NA	NA	NA	NA	3.2	55.8	5.5
3762	8/26/16	5.3	10.3	1.1	NA	NA	NA	NA	NA	2.9	54.9	7.8
3824	8/11/16	18.6	NA	0.9	NA	NA	NA	NA	NA	1.8	45.2	11.5
3826	8/26/16	8.0	NA	6.9	NA	NA	NA	NA	NA	2.8	25.4	13.7
4346	9/1/16	17.2	NA	1.9	NA	NA	NA	NA	NA	6.8	95.9	4.5
4406	9/2/16	20.0	310.0	5.8	NA	NA	NA	NA	NA	2.1	57.7	4.9
4444	8/12/16	12.0	NA	3.6	NA	NA	NA	NA	NA	3.6	76.3	4.9
4446	9/1/16	14.5	NA	1.9	NA	NA	NA	NA	NA	4.0	69.7	6.2
4448	9/1/16	4.8	NS	3.8	NA	NA	NA	NA	NA	1.1	15.7	31.9
5182	8/10/16	23.1	9.3	0.9	NA	NA	NA	NA	NA	12.4	188.8	1.4
5184	8/11/16	8.8	16.1	0.0	NA	NA	NA	NA	NA	5.0	108.8	2.8
5186	8/11/16	5.0	13.1	2.4	NA	NA	NA	NA	NA	1.6	31.3	5.2
5330	8/10/16	23.1	NA	0.9	NA	NA	NA	NA	NA	1.5	42.9	4.3
5664	8/26/16	9.3	NA	1.9	NA	NA	NA	NA	NA	1.8	26.9	7.2
5666	8/8/16	9.0	20.3	1.8	NA	NA	NA	NA	NA	3.7	33.0	7.7
5812	8/23/16	6.5	11.8	1.0	NA	NA	NA	NA	NA	4.5	126.3	2.8
5814	8/8/16	5.7	11.1	0.0	NA	NA	NA	NA	NA	6.8	22.1	9.4
DEP												

Table C1.1: Continued

Midas		Epi. P, ppb	Hypo. P, ppb	CHL a	Ag:WA ratio	AdjAg:LA ratio	Ag:LA ratio	WA:LA	Road:WA	Al _{NaOH} :Fe _{BD}	Al _{NaOH} :P _{BD}	P _{BD}
70	8/9/11	9.0	NA	6.2	12.69	14.74	1.08	8.2	0.010	0.8	51.0	6.1
80	8/24/11	13.0	NA	3.1	NA	NA	NA	NA	0.007	1.2	54.0	4.1
121	8/24/11	6.0	14.0	4.4	NA	NA	NA	101.5		2.6	151.1	2.0
177	9/23/10	6.0	NA	2.1	1.59	1.14	0.06	3.9	0.005	0.5	41.0	6.6
243	9/1/11	4.0	NA	2.1	0.00	0.00	0.00	8.6	0.002	1.5	9077.1	0.0
262	8/30/10	9.0	NA	2.4	0.00	0.00	0.00	20.9	0.008	3.2	223.5	3.0
342	9/1/11	3.0	NA	1.7	0.00	0.00	0.00	15.3	0.007	1.4	67.5	5.1
386	8/23/11	15.0	42.0	4.9	0.00	0.00	0.00	11.0	0.018	1.9	150.1	2.2
410	9/1/11	10.0	NA	4.6	0.00	0.00	0.00	NA	0.000	0.5	54.3	3.8
447	9/23/12	7.0	NA	1.7	0.00	0.00	0.00	443.6	0.000	2.6	70.9	1.7
760	8/30/10	10.0	NA	4.1	4.94	6.75	0.43	9.6	0.012	1.3	14.8	8.0
954	8/23/10	4.0	NA	1.9	0.15	0.00	0.01	9.3	0.003	1.3	224.0	1.6
1068	8/24/11	6.0	NA	1.9	4.00	2.12	0.18	8.8	0.012	1.6	92.5	1.3
1070	8/24/11	5.0	NA	2.4	NA	NA	NA	5.6	0.003	0.9	46.7	8.2
1078	8/22/11	9.0	NA	3.3	0.04	0.00	0.00	12.1	0.000	1.0	234.3	0.9
1088	8/22/11	8.0	NA	2.1	0.11	0.00	0.02	15.9	0.002	1.8	7835.9	0.0
1150	9/23/10	4.0	NA	1.9	0.00	0.00	0.00	10.1	0.001	0.5	63.3	2.9
1210	8/25/10	6.0	10.0	1.8	0.05	0.00	0.01	11.1	0.002	1.2	85.4	6.5
2004	8/23/10	5.0	NA	1.4	0.00	0.00	0.00	5.0	0.006	4.3	655.2	1.4
2020	8/15/11	5.0	NA	1.8	0.00	0.00	0.00	138.1	0.003	0.5	52.8	3.2
2146	8/17/11	6.0	NA	2.3	0.53	0.82	0.02	25.8	0.007	1.4	99.4	1.8
2156	8/24/11	15.0	NA	7.2	19.64	15.95	3.62	19.8	0.009	1.2	19.5	5.8
2242	8/17/11	5.0	NA	1.9	1.91	7.21	0.15	7.5	0.012	3.4	22.9	6.6
2286	9/2/10	33.0	NA	34.0	7.47	23.22	5.09	134.9	0.007	0.9	10.8	13.8
2590	8/30/10	7.0	12.0	3.0	4.26	5.96	0.77	36.4	0.007	1.5	53.9	5.3
2608	8/30/10	6.0	17.0	5.0	1.65	0.10	0.21	12.9	0.006	2.3	73.7	8.9

Table C1.1: Continued

Midas		Epi. P, ppb	Hypo. P, ppb	CHL a	Ag:WA ratio	AdjAg:LA ratio	Ag:LA ratio	WA:LA	Road:WA	Al _{NaOH} :Fe _{BD}	Al _{NaOH} :P _{BD}	P _{BD}
2948	8/30/10	5.0	NA	2.3	0.00	0.00	0.00	10.8	0.000	0.6	46.0	5.3
3038	8/24/11	7.0	NA	3.6	2.14	1.99	0.32	20.7	0.003	1.8	436.6	0.4
3376	8/25/11	14.0	NA	7.7	0.93	0.29	0.14	15.0	0.010	5.2	43.6	4.6
3388	9/7/10	6.0	NA	2.6	3.61	14.77	0.19	7.8	0.016	1.8	66.5	3.4
3434	9/1/10	9.0	14.0	2.5	9.41	18.29	1.00	15.0	0.015	2.6	59.5	8.8
3452	8/31/10	6.0	NA	2.2	6.58	17.48	0.90	14.1	0.010	1.9	192.4	2.9
3454	8/16/11	6.0	14.0	2.9	3.41	8.50	0.17	9.6	0.011	3.8	10248.3	0.0
3604	8/18/11	5.0	9.0	4.2	3.67	25.16	0.57	16.0	0.007	2.2	92.3	2.9
3626	9/1/10	8.0	16.0	2.1	2.26	0.00	0.16	10.4	0.026	1.7	27.2	13.1
3672	8/10/11	7.0	9.0	8.0	0.61	10.85	0.14	22.9	0.003	1.3	172.7	1.9
3682	8/10/11	6.0	NA	3.6	2.37	17.36	0.72	31.1	0.005	1.0	320.9	1.3
3690	8/31/10	7.0	13.0	3.4	2.63	0.48	0.25	9.7	0.010	3.0	33.8	10.8
3780	8/9/11	8.0	NA	4.5	1.78	4.89	0.08	4.5	0.012	4.5	127.9	2.7
3814	8/23/11	16.0	82.0	32.0	13.07	47.42	0.70	5.5	0.016	1.4	20.1	11.4
3830	9/8/10	7.0	42.0	3.7	5.90	9.29	1.28	54.1	0.008	1.5	26.2	14.3
3884	9/7/10	13.0	NA	4.4	9.99	44.05	0.45	5.0	0.015	0.7	13.9	12.8
3920	8/18/10	10.0	11.0	1.5	NA	NA	0.48	6.0	0.012	2.2	56.5	6.3
4272	8/8/11	5.0	10.0	2.1	0.63	2.71	0.03	16.7	0.007	1.7	200.7	2.3
4316	8/17/10	11.0	30.0	4.2	5.42	3.45	3.68	90.1	0.007	1.3	64.2	4.5
4322	8/17/10	5.0	12.0	3.4	0.55	2.16	0.05	9.3	0.009	3.0	153.3	3.5
4328	8/17/10	3.0	NA	1.5	1.87	2.21	0.12	6.6	0.007	1.0	213.0	2.5
4330	8/17/10	10.0	NA	2.9	0.90	3.80	0.08	9.0	0.007	3.3	137.3	2.9
4336	8/17/10	9.0	NA	3.2	2.40	6.45	0.29	64.7	0.008	1.6	88.8	3.0
4388	8/15/11	7.0	12.0	4.5	0.79	6.09	0.08	9.2	0.008	3.1	4798.8	0.0
4452	9/20/12	3.0	NA	2.3	0.00	0.00	0.00	15.3	0.016	2.3	15711.8	0.0
4492	8/25/10	5.0	7.0	2.0	0.00	0.00	NA	10.8	0.007	3.2	175.8	1.8

Table C1.1: Continued

Midas		Epi. P, ppb	Hypo. P, ppb	CHL a	Ag:WA ratio	AdjAg:LA ratio	Ag:LA ratio	WA:LA	Road:WA	Al _{NaOH} :Fe _{BD}	Al _{NaOH} :P _{BD}	P _{BD}
4606	9/19/12	2.0	NA	0.9	0.00	0.00	0.00	5.3	0.012	2.4	10613.6	0.0
4608	9/19/12	2.0	NA	0.9	0.00	0.00	0.00	6.7	0.004	0.5	9010.6	0.0
4610	9/20/12	4.0	11.0	2.4	0.00	0.00	0.00	33.0	0.028	4.9	16090.4	0.0
4612	9/20/12	4.0	6.0	2.3	0.00	0.00	0.00	21.8	0.008	6.0	16471.0	0.0
4614	9/17/12	5.0	24.0	2.0	0.00	0.00	NA	62.7	0.016	3.8	86.1	2.9
4618	9/20/12	12.0	NA	3.4	0.00	0.00	0.00	12.4	0.014	3.5	52.4	3.4
4620	9/17/12	7.0	NA	2.8	0.00	0.00	0.00	6.6	0.006	3.5	84.1	2.8
4622	9/19/12	2.0	NA	1.9	0.00	0.00	0.00	0.5	0.010	0.3	722.9	0.4
4624	9/17/12	4.0	6.0	2.0	0.00	0.00	0.00	6.5	0.019	2.9	7508.2	0.0
4628	9/17/12	8.0	NA	2.0	0.00	0.00	0.00	20.2	0.044	4.9	9455.8	0.0
4630	9/17/12	3.0	8.0	2.1	0.00	0.00	0.00	12.5	0.010	2.3	11759.2	0.0
4766	8/25/10	8.0	NA	2.8	0.18	0.00	0.01	9.4	0.003	1.1	136.8	3.2
4782	9/8/11	8.0	NA	3.9	0.08	0.00	0.00	6.9	0.004	5.0	8187.6	0.0
4788	8/25/10	6.0	NA	2.5	0.00	0.00	0.00	4.7	0.004	3.7	210.6	0.8
4800	9/1/10	6.0	13.0	2.3	10.19	26.29	0.59	35.7	0.025	1.9	75.5	7.6
4802	8/10/11	11.0	NA	4.7	0.00	0.00	NA	21.7	0.010	3.4	4457.6	0.0
4806	8/10/11	17.0	NA	6.8	9.70	62.43	0.79	7.9	0.014	2.1	113.4	2.4
4822	8/11/11	13.0	57.0	14.0	9.89	33.02	0.59	7.7	0.021	0.9	11.8	16.3
4852	8/11/11	6.0	NA	6.2	7.18	20.97	0.62	15.1	0.016	0.4	8.4	11.3
4857	8/24/10	9.0	15.0	4.2	1.65	11.90	0.15	8.2	0.009	2.5	100.3	2.9
4894	8/17/11	6.0	NA	2.3	2.39	5.80	0.09	5.1	0.019	2.0	219.1	1.6
4896	8/31/10	6.0	NA	2.0	2.90	5.66	0.44	24.4	0.010	0.6	39.5	10.1
5024	8/31/11	5.0	22.0	2.1	3.14	12.60	0.20	8.3	0.444	1.5	55.3	4.4
5172	8/11/11	18.0	34.0	61.0	14.03	6.57	3.40	31.5	0.008	1.3	10.7	15.1
5174	8/11/11	16.0	NA	5.5	7.38	9.58	0.71	12.3	0.013	1.9	67.1	2.2
5198	8/18/10	12.0	NA	3.5	17.74	4.75	2.75	14.0	0.015	1.1	34.3	11.4

Table C1.1: Continued

Midas		Epi. P, ppb	Hypo. P, ppb	CHL a	Ag:WA ratio	AdjAg:LA ratio	Ag:LA ratio	WA:LA	Road:WA	Al _{NaOH} :Fe _{BD}	Al _{NaOH} :P _{BD}	P _{BD}
5222	9/6/11	10.0	22.0	3.8	3.33	40.36	0.94	30.7	0.009	1.8	147.0	2.8
5236	8/19/10	12.0	24.5	11.0	15.35	19.12	0.71	15.8	0.010	0.5	3.6	62.6
5240	9/2/10	8.0	17.0	2.7	5.75	12.73	0.23	21.3	0.015	1.4	32.4	10.5
5280	8/9/11	9.0	NA	4.0	8.60	7.31	0.72	39.1	0.008	0.3	2.8	77.1
5344	8/22/11	18.0	NA	4.5	7.99	6.63	0.43	8.4	0.009	1.4	40.9	4.7
5348	8/22/11	9.0	NA	3.2	2.63	3.24	0.16	NA	0.012	2.5	95.4	1.8
5349	8/22/11	15.0	NA	11.0	1.25	0.97	0.03	2.8	0.012	1.2	27.0	7.1
5352	8/19/10	11.0	187.0	6.9	5.68	6.74	0.22	NA	0.017	1.3	13.6	12.2
5386	9/1/10	12.0	NA	3.4	8.21	19.77	1.57	31.9	0.009	1.9	95.5	5.1
5400	8/31/10	7.0	NA	4.5	8.58	22.36	0.52	18.7	0.010	1.5	62.2	5.5
5408	8/26/10	32.0	300.0	19.0	11.69	25.55	0.62	5.5	0.010	1.3	10.4	16.7
5416	8/26/10	35.0	55.0	53.0	7.82	2.16	0.49	14.9	0.011	0.7	3.8	31.4
5448	8/26/10	18.0	38.5	28.0	10.51	27.13	0.55	12.0	0.007	0.8	2.4	46.7
5458	9/2/10	12.0	NA	5.5	4.07	15.71	0.70	20.8	0.008	1.1	16.1	13.2
5490	8/15/11	8.0	9.0	3.7	1.71	0.00	0.11	6.8	0.006	2.9	252.9	1.4
5682	9/1/10	13.0	24.5	5.0	10.73	75.28	4.18	136.0	0.009	1.5	61.0	5.4
5690	8/17/11	15.0	33.0	7.6	15.73	91.70	1.60	37.9	0.012	1.4	37.6	10.9
5710	8/17/11	7.0	NA	5.3	1.75	6.31	0.15	50.0	0.012	3.1	150.9	2.2
5780	8/30/11	7.0	7.0	2.7	5.18	8.93	0.38	14.2	0.010	1.6	331.6	1.6
5814	8/18/11	5.0	NA	2.2	2.78	3.09	0.12	25.7	0.011	0.8	21.5	15.2
9685	8/16/11	5.0	8.0	2.6	2.31	6.08	0.10	105.2	0.014	3.2	2651.5	0.1
9931	8/31/10	18.0	NA	20.3	1.91	2.74	0.08	8.5	0.014	0.8	4.2	45.0
LEA												
5780	7/11/13	NA	NA	NA	5.18	8.93	0.38	14.2	0.010	1.8	218.2	1.2
3418	6/18/13	6.0	13.0	3.3	7.31	31.62	0.49	6.7	0.016	2.8	299.1	1.4
5780	7/11/13	8.0	17.0	2.4	5.18	8.93	0.38	14.2	0.010	1.1	128.8	3.2

Table C1.1: Continued

Midas		Epi. P, ppb	Hypo. P, ppb	CHL a	Ag:WA ratio	AdjAg:LA ratio	Ag:LA ratio	WA:LA	Road:WA	Al _{NaOH} :Fe _{BD}	Al _{NaOH} :P _{BD}	P _{BD}
3130	7/18/13	9.0	13.0	4.3	5.35	11.41	0.35	6.4	0.016	3.3	123.5	3.0
3382	7/9/13	4.0	17.0	1.5	1.45	0.00	0.04	3.1	0.015	3.3	70.8	2.5
3424	7/3/13	7.0	12.5	2.2	10.18	22.62	1.67	17.3	0.010	5.3	123.4	2.2
3199	7/12/13	5.0	10.5	1.8	0.54	4.63	0.06	35.9	0.009	1.3	103.9	3.1
3134	6/27/13	12.0	6.0	3.6	3.39	18.20	0.30	16.0	0.011	2.9	104.0	2.6
3416	6/18/13	16.0	12.0	2.8	8.41	35.51	0.69	8.4	0.018	3.1	161.5	3.6
9685	7/11/13	6.0	13.0	2.3	2.31	6.08	0.10	105.2	0.014	2.9	131.1	1.8
3420	7/17/13	11.0	21.0	3.5	6.18	17.87	0.46	7.4	0.012	3.3	96.6	5.8
3454	7/1/13	NA	NA	NA	3.41	8.50	0.17	9.6	0.011	2.8	184.4	2.1
5582	8/26/13	9.0	10.0	6.5	4.70	36.70	1.19	24.5	0.016	5.4	101.8	3.9
3134	6/27/13	4.0	22.0	1.6	3.39	18.20	0.30	16.0	0.011	1.4	106.3	3.3
5780	7/11/13	7.0	17.5	2.5	5.18	8.93	0.38	14.2	0.010	1.6	75.9	4.8
5780	7/11/13	4.0	17.0	2.0	5.18	8.93	0.38	14.2	0.010	2.0	121.3	2.6
3132	7/18/13	4.0	18.0	1.8	0.73	0.00	0.03	4.1	0.011	2.4	101.8	2.5
3126	7/18/13	8.0	8.5	6.3	3.61	12.53	0.28	8.2	0.016	4.5	56.1	5.6
3234	7/1/13	7.0	14.0	2.8	1.45	4.85	0.19	13.3	0.012	3.2	88.5	5.2
3374	6/24/13	4.0	20.0	2.5	0.64	0.61	0.03	4.6	0.006	2.2	40.9	5.2
3134	6/27/13	NA	NA	NA	3.39	18.20	0.30	16.0	0.011	3.0	154.1	2.0
3452	7/31/13	8.0	19.0	2.3	6.58	17.48	0.90	14.1	0.010	1.9	158.4	2.6
3454	7/1/13	5.0	15.0	2.6	3.41	8.50	0.17	9.6	0.011	3.6	168.8	2.6
3448	8/1/13	9.0	13.5	4.2	3.86	60.13	0.64	16.9	0.008	6.2	158.4	2.6
3232	7/16/13	6.0	12.5	3.3	2.78	17.75	0.38	13.9	0.012	3.9	138.7	3.5
3456	9/10/13	12.0	7.7	3.0	1.83	3.88	0.15	8.4	0.008	2.3	285.4	2.5
5780	7/11/13	NA	NA	NA	5.18	8.93	0.38	14.2	0.010	1.4	96.6	3.9

Table C1.2: Significant Parameters: Physiochemical and Climate. Parameters used for model regression consisting of epilimnetic and hypolimnetic P, chl a; morphometry and climate parameters: Z_{avg} , Sch , T_{hyp} , OI; and water chemistry parameters such as: DOC and pH.

Midas	Epi. P, ppb	Hypo. P, ppb	CHL a	Z_{avg}	Sch	Thyp	DOC	pH	OI
2015									
78	4.0	3.4	1.6	30.6	1719.5	6.0	2.7	7.1	7.4
177	5.2	4.6	3.3	7.7	6.5	22.0	4.4	6.7	0.9
224	1.9	2.6	<1	37.7	2141.0	6.1	2.0	7.0	11.5
3444	3.5	4.9	2.1	24.7	880.6	7.8	3.2	7.2	3.2
3446	4.2	9.1	2.7	10.0	316.7	11.7	2.7	7.1	4.3
3748	6.1	20.7	2.3	24.0	866.8	7.6	2.6	7.4	4.3
3750	5.1	9.2	3.2	8.2	152.6	9.9	3.9	7.6	3.9
3796	19.2	NA	22.1	2.8	3.0	23.0	3.3	7.4	1.4
3838	5.5	9.1	2.4	22.2	508.6	6.0	3.1	7.1	5.4
3916	4.0	13.2	2.4	7.3	100.1	11.1	2.4	7.0	3.8
4434	2.6	2.4	1.4	46.7	2785.3	4.9	2.5	6.4	7.7
4538	4.4	5.5	1.6	12.6	172.3	7.5	2.6	6.9	NA
5172	12.6	10.6	25.3	7.2	18.8	19.1	5.9	7.3	2.0
5190	3.3	4.3	1.2	23.6	1423.6	5.5	2.0	7.4	9.2
5272	5.3	53.3	4.6	24.4	577.7	5.4	3.4	7.1	8.5
5274	6.8	8.1	4.3	14.1	147.8	14.4	3.3	7.0	1.4
5280	7.5	19.6	3.5	24.8	477.5	6.8	3.8	7.1	2.8
5344	19.0	15.3	5.2	2.5	4.6	23.1	3.2	7.2	1.6
5348	9.3	NA	2.9	4.7	0.2	23.8	3.4	7.7	3.8
5349	12.6	NA	3.6	3.8	31.6	23.6	3.0	7.3	2.0
5352	10.7	23.7	5.0	8.6	197.6	10.9	3.2	7.8	5.6
5400	7.5	14.2	5.4	25.9	513.5	8.0	3.5	6.9	6.1
5408	21.0	280.0	6.4	8.1	90.2	11.7	3.8	8.2	2.4
5448	13.9	33.3	17.1	16.7	439.7	8.8	3.9	8.9	3.8
2016									
3688	6.4	11.5	3.5	NA	NA	10.6	NA	6.9	NA
3760	8.5	11.5	1.2	NA	NA	9.4	NA	6.3	NA
3762	5.3	10.3	1.1	NA	NA	7.3	NA	7.4	NA
3824	18.6	NA	0.9	NA	NA	24.7	NA	6.4	NA
3826	8.0	NA	6.9	NA	NA	25.3	NA	NA	NA
4346	17.2	NA	1.9	NA	NA	22.4	NA	6.4	NA
4406	20.0	310.0	5.8	NA	NA	11.5	NA	7.3	NA
4444	12.0	NA	3.6	NA	NA	20.1	NA	7.2	NA
4446	14.5	NA	1.9	NA	NA	22	NA	7.4	NA
4448	4.8	NS	3.8	NA	NA	14.8	NA	7.4	NA

Table C1.2: Conditions

Midas	Epi. P, ppb	Hypo. P, ppb	CHL a	Zavg	Sch	Thyp	DOC	pH	OI
5182	23.1	9.3	0.9	NA	NA	5.9	NA	6.9	NA
5184	8.8	16.1	0.0	NA	NA	18.3	NA	7.2	NA
5186	5.0	13.1	2.4	NA	NA	12.5	NA	7.4	NA
5330	23.1	NA	0.9	NA	NA	23.6	NA	7.4	NA
5664	9.3	NA	1.9	NA	NA	23.8	NA	6.3	NA
5666	9.0	20.3	1.8	NA	NA	16.1	NA	7.3	NA
5812	6.5	11.8	1.0	NA	NA	5.7	NA	6.7	NA
5814	5.7	11.1	0.0	NA	NA	6.5	NA	7.1	NA
DEP									
70	9.0	NA	6.2	3.0	8.1	23.9	4.2	7.3	1.9
80	13.0	NA	3.1	NA	NA	22.7	7.0	7.2	NA
121	6.0	14.0	4.4	10.6	17.9	14.3	4.4	7.1	2.1
177	6.0	NA	2.1	7.7	1.2	16.2	4.0	6.9	0.9
243	4.0	NA	2.1	12.8	210.3	10.7	3.8	6.8	3.7
262	9.0	NA	2.4	13.4	122.1	10.8	3.5	7.0	5.2
342	3.0	NA	1.7	22.1	401.4	6.1	3.2	6.9	4.8
386	15.0	42.0	4.9	5.0	4.3	12.7	3.2	NA	6.0
410	10.0	NA	4.6	NA	NA	19.1	3.7	7.0	NA
447	7.0	NA	1.7	1.1	0.2	19.4	5.1	6.7	NA
760	10.0	NA	4.1	3.3	0.0	22.7	4.0	7.6	NA
954	4.0	NA	1.9	22.5	61.3	14.6	5.2	6.6	1.4
1068	6.0	NA	1.9	3.7	2.3	21.6	2.9	7.0	3.2
1070	5.0	NA	2.4	29.3	280.9	10.5	3.8	6.9	1.4
1078	9.0	NA	3.3	3.8	2.3	22.5	5.8	6.6	0.8
1088	8.0	NA	2.1	12.8	231.1	9.3	4.6	6.9	4.0
1150	4.0	NA	1.9	27.4	136.6	12.4	3.1	6.9	1.7
1210	6.0	10.0	1.8	11.9	26.0	13.3	4.6	6.5	2.6
2004	5.0	NA	1.4	3.2	5.5	20.5	3.5	6.9	3.3
2020	5.0	NA	1.8	19.6	174.6	11.2	3.8	7.0	1.4
2146	6.0	NA	2.3	11.3	135.2	11.5	3.7	6.9	4.0
2156	15.0	NA	7.2	2.9	1.6	22.8	6.3	7.6	2.8
2242	5.0	NA	1.9	5.1	17.6	17.6	3.4	7.6	3.2
2286	33.0	NA	34.0	2.7	8.7	22.0	6.7	9.1	2.6
2590	7.0	12.0	3.0	10.8	50.5	13.2	4.8	7.3	1.3
2608	6.0	17.0	5.0	13.4	258.4	8.8	3.4	7.4	7.5
2948	5.0	NA	2.3	24.5	223.1	9.1	6.0	7.0	2.4
3038	7.0	NA	3.6	7.8	1.7	21.7	6.4	7.1	2.3
3376	14.0	NA	7.7	7.4	77.9	6.1	4.2	NA	11.9
3388	6.0	NA	2.6	3.5	0.7	23.0	3.2	7.1	4.2
3434	9.0	14.0	2.5	9.3	105.2	12.5	3.3	7.6	3.2

Table C1.2: Continued

Midas	Epi. P, ppb	Hypo. P, ppb	CHL a	Zavg	Sch	Thyp	DOC	pH	OI
3452	6.0	NA	2.2	10.3	519.4	8.4	4.4	7.0	8.2
3454	6.0	14.0	2.9	9.7	54.4	11.7	3.2	6.6	2.8
3604	5.0	9.0	4.2	8.5	260.2	10.1	3.5	NA	5.8
3626	8.0	16.0	2.1	7.5	152.2	5.8	3.7	7.9	14.6
3672	7.0	9.0	8.0	5.4	166.6	12.1	3.1	7.1	2.9
3682	6.0	NA	3.6	18.8	527.1	5.1	2.4	7.0	6.0
3690	7.0	13.0	3.4	8.2	56.6	10.4	2.8	7.3	4.8
3780	8.0	NA	4.5	5.4	8.3	14.9	3.6	6.8	8.4
3814	16.0	82.0	32.0	3.2	38.3	16.3	3.5	7.8	5.0
3830	7.0	42.0	3.7	5.1	14.3	13.5	4.1	7.5	5.3
3884	13.0	NA	4.4	3.3	2.9	21.2	4.8	7.0	7.2
3920	10.0	11.0	1.5	8.1	603.6	10.2	2.5	7.1	4.5
4272	5.0	10.0	2.1	3.9	63.3	11.9	3.9	6.8	7.1
4316	11.0	30.0	4.2	5.1	24.5	15.0	3.6	7.0	5.8
4322	5.0	12.0	3.4	10.4	130.6	8.1	2.8	6.8	7.5
4328	3.0	NA	1.5	27.8	459.7	10.5	2.6	6.9	3.2
4330	10.0	NA	2.9	2.1	2.4	22.8	3.0	6.8	4.6
4336	9.0	NA	3.2	4.2	7.3	22.8	3.8	6.9	2.7
4388	7.0	12.0	4.5	6.4	32.5	13.7	4.7	6.7	3.0
4452	3.0	NA	2.3	7.2	3.5	17.4	2.5	6.8	20.4
4492	5.0	7.0	2.0	11.1	77.0	13.4	4.0	6.7	4.9
4606	2.0	NA	0.9	21.0	306.6	10.4	1.8	6.7	10.1
4608	2.0	NA	0.9	21.6	1392.1	6.0	1.7	6.8	29.6
4610	4.0	11.0	2.4	8.1	51.8	7.8	4.1	6.5	13.9
4612	4.0	6.0	2.3	8.3	16.8	10.0	4.5	6.5	10.1
4614	5.0	24.0	2.0	5.0	5.7	12.0	5.5	6.4	5.9
4618	12.0	NA	3.4	3.2	5.1	13.8	7.5	6.6	12.1
4620	7.0	NA	2.8	3.2	2.1	19.3	5.0	6.2	8.7
4622	2.0	NA	1.9	30.2	69.8	10.0	2.9	6.6	0.9
4624	4.0	6.0	2.0	13.6	79.6	11.6	2.8	6.9	7.8
4628	8.0	NA	2.0	3.9	4.3	18.6	8.1	6.3	9.0
4630	3.0	8.0	2.1	9.7	13.5	13.9	4.3	6.7	4.8
4766	8.0	NA	2.8	13.1	4.1	19.1	6.1	6.7	1.1
4782	8.0	NA	3.9	1.2	0.4	20.1	7.0	6.4	NA
4788	6.0	NA	2.5	4.8	0.2	22.0	3.8	NA	NA
4800	6.0	13.0	2.3	5.4	34.6	15.1	3.2	7.0	6.0
4802	11.0	NA	4.7	2.5	0.1	23.3	3.9	7.0	3.0
4806	17.0	NA	6.8	3.2	0.0	23.5	2.4	6.8	3.7
4822	13.0	57.0	14.0	4.3	62.6	13.8	2.5	7.5	5.8
4852	6.0	NA	6.2	13.7	140.9	8.8	2.7	6.9	3.2

Table C1.2: Continued

Midas	Epi. P, ppb	Hypo. P, ppb	CHL a	Zavg	Sch	Thyp	DOC	pH	OI
4857	9.0	15.0	4.2	5.7	24.2	10.7	5.3	6.3	4.9
4894	6.0	NA	2.3	7.0	5.5	22.1	3.0	6.8	3.3
4896	6.0	NA	2.0	27.0	1033.9	5.7	4.3	7.1	6.4
5024	5.0	22.0	2.1	16.1	276.7	5.2	2.5	7.1	5.5
5172	18.0	34.0	61.0	7.2	47.8	15.9	6.2	8.2	2.0
5174	16.0	NA	5.5	2.8	0.3	22.4	4.5	7.2	1.2
5198	12.0	NA	3.5	2.4	7.1	23.1	3.7	7.2	6.6
5222	10.0	22.0	3.8	11.9	262.4	8.4	3.9	6.6	6.3
5236	12.0	24.5	11.0	23.7	247.3	9.8	3.5	7.9	1.7
5240	8.0	17.0	2.7	13.9	155.8	6.5	3.1	7.6	4.4
5280	9.0	NA	4.0	24.8	504.1	7.2	3.7	7.2	2.8
5344	18.0	NA	4.5	2.5	0.3	23.7	3.3	6.9	1.5
5348	9.0	NA	3.2	4.7	16.4	22.9	3.3	NA	3.8
5349	15.0	NA	11.0	3.8	4.7	23.5	2.9	7.0	2.0
5352	11.0	187.0	6.9	8.6	206.0	13.3	3.4	8.0	NA
5386	12.0	NA	3.4	2.6	12.9	22.7	4.7	7.2	2.8
5400	7.0	NA	4.5	25.9	492.2	9.6	3.6	7.2	3.5
5408	32.0	300.0	19.0	8.1	41.8	13.9	4.0	NA	2.4
5416	35.0	55.0	53.0	6.9	14.8	16.9	4.0	8.4	2.5
5448	18.0	38.5	28.0	16.7	281.4	11.7	3.7	7.8	3.8
5458	12.0	NA	5.5	4.2	30.8	20.1	5.4	8.0	3.5
5490	8.0	9.0	3.7	4.8	24.9	13.2	3.5	6.8	4.9
5682	13.0	24.5	5.0	12.4	150.2	11.4	5.1	7.3	4.1
5690	15.0	33.0	7.6	7.2	87.2	12.3	5.0	6.9	5.7
5710	7.0	NA	5.3	9.0	355.0	9.8	4.5	6.7	8.8
5780	7.0	7.0	2.7	10.8	133.0	12.2	3.5	6.9	1.8
5814	5.0	NA	2.2	29.3	272.5	5.7	3.4	7.0	3.6
9685	5.0	8.0	2.6	8.9	46.6	13.5	3.6	NA	3.2
9931	18.0	NA	20.3	9.9	75.9	13.1	3.0	7.4	3.7
LEA									
5780	NA	NA	NA	10.8	NA	NA	NA	NA	NA
3418	6.0	13.0	3.3	6.2	138.3	11.0	NA	6.7	5.7
5780	8.0	17.0	2.4	10.8	133.1	17.7	NA	6.7	NA
3130	9.0	13.0	4.3	9.0	120.8	9.2	NA	6.7	5.5
3382	4.0	17.0	1.5	7.5	422.6	9.7	NA	6.6	9.8
3424	7.0	12.5	2.2	6.6	138.8	9.1	NA	6.9	8.9
3199	5.0	10.5	1.8	5.9	106.6	7.5	NA	6.8	13.7
3134	12.0	6.0	3.6	3.5	348.5	19.6	NA	6.7	NA
3416	16.0	12.0	2.8	5.4	221.1	9.4	NA	6.6	6.2
9685	6.0	13.0	2.3	8.9	66.2	15.6	NA	6.7	3.2

Table C1.2: Continued

Midas	Epi. P, ppb	Hypo. P, ppb	CHL a	Zavg	Sch	Thyp	DOC	pH	OI
3420	11.0	21.0	3.5	12.1	437.8	5.0	NA	6.8	11.0
3454	NA	NA	NA	9.7	NA	NA	NA	NA	2.8
5582	9.0	10.0	6.5	7.4	119.9	7.8	NA	6.7	8.1
3134	4.0	22.0	1.6	13.6	817.5	9.8	NA	6.7	5.0
5780	7.0	17.5	2.5	10.8	584.2	12.8	NA	6.8	1.8
5780	4.0	17.0	2.0	10.8	511.5	13.8	NA	6.8	NA
3132	4.0	18.0	1.8	13.0	172.7	8.0	NA	6.7	3.5
3126	8.0	8.5	6.3	5.1	15.1	15.8	NA	6.6	6.4
3234	7.0	14.0	2.8	6.6	238.4	7.1	NA	6.6	8.7
3374	4.0	20.0	2.5	9.2	423.8	8.4	NA	6.9	6.7
3134	NA	NA	NA	3.5	NA	NA	NA	NA	2.7
3452	8.0	19.0	2.3	10.3	400.3	7.1	NA	6.9	8.2
3454	5.0	15.0	2.6	9.7	68.1	13.1	NA	6.7	NA
3448	9.0	13.5	4.2	11.1	114.3	8.1	NA	6.7	7.0
3232	6.0	12.5	3.3	7.7	125.6	9.1	NA	6.6	7.1
3456	12.0	7.7	3.0	3.9	70.6	16.7	NA	6.6	4.3
5780	NA	NA	NA	10.8	NA	NA	NA	NA	NA

Table C2: Model Parameters: Coefficient of determination, R^2 . For significant parameters used for model regression. Negative sign (-) indicates negative correlation for R value.

	log Epi P	log Hypo P	log Chl a	WA:LA	OI	log Al:P	Al:Fe	log P _{no}	log Zavg	log Sch	Thyp	Ag:WA	Adj Ag:LA	Ag:LA
log Epi P	1.00	0.57	0.69	0.01	(-) 0.45	(-) 0.25	(-) 0.01	0.23	(-) 0.5	(-) 0.38	0.39	0.42	0.37	0.17
log Hypo P		1.00	0.36	0.12	(-) 0.11	(-) 0.33	(-) 0.00	0.44	(-) 0.12	(-) 0.06	0.01	0.38	0.43	0.03
log Chl a			1.00	0.09	(-) 0.40	(-) 0.29	(-) 0.02	0.21	(-) 0.28	(-) 0.23	0.24	0.51	0.41	0.43
WA:LA				1.00	0.02	(-) 0.13	(-) 0.04	0.18	0.05	0.02	(-) 0.06	0.09	(-) 0.00	0.14
OI					1.00	0.12	0.00	(-) 0.05	0.49	0.42	(-) 0.49	(-) 0.23	(-) 0.11	(-) 0.12
log Al:P						1.00	0.31	(-) 0.85	0.00	(-) 0.00	(-) 0.00	(-) 0.39	(-) 0.25	(-) 0.13
Al:Fe							1.00	(-) 0.18	(-) 0.03	(-) 0.01	0.00	(-) 0.05	(-) 0.04	(-) 0.03
log P _{no}								1.00	0.00	0.00	(-) 0.01	0.35	0.26	0.09
log Zavg									1.00	0.76	(-) 0.79	(-) 0.06	(-) 0.03	(-) 0.08
log Sch										1.00	(-) 0.85	(-) 0.03	(-) 0.02	(-) 0.07
Thyp											1.00	0.02	0.01	0.06
Ag:WA												1.00	0.46	0.56
Adj Ag:LA													1.00	0.10
Ag:LA														1.00

Table C2 continued: Coefficient of Determination, R^2 . MPJ and SPJ represent the maximum and cumulative precipitation from January in inches, respectively; MPM and SPM represent the maximum and cumulative precipitation from May in inches, respectively.

	Rd:WA	Wtlnd: WA	DOC	pH	MPJ	SPJ	MPM	SPM
log Epi P	0.07	0.03	0.29	0.33	(-) 0.04	(-) 0.12	(-) 0.15	(-) 0.15
log Hypo P	0.11	0.00	0.11	0.41	(-) 0.10	(-) 0.11	(-) 0.23	(-) 0.15
log Chl a	0.01	0.12	0.56	0.23	(-) 0.03	(-) 0.27	(-) 0.11	(-) 0.3
WA:LA	(-) 0.00	0.02	0.16	(-) 0.00	(-) 0.04	(-) 0.00	(-) 0.05	(-) 0.00
OI	(-) 0.01	(-) 0.35	(-) 0.34	(-) 0.03	(-) 0.00	0.21	0.00	0.19
log Al:P	(-) 0.05	(-) 0.07	(-) 0.15	(-) 0.24	0.12	0.09	0.20	0.13
Al:Fe	0.01	(-) 0.10	(-) 0.05	(-) 0.00	0.03	0.00	0.04	0.01
log P_{hd}	0.12	0.01	0.11	0.33	(-) 0.16	(-) 0.07	(-) 0.28	(-) 0.11
log <i>Zavg</i>	(-) 0.15	(-) 0.08	(-) 0.11	(-) 0.06	0.01	0.03	0.02	0.04
log <i>Sch</i>	(-) 0.04	(-) 0.16	(-) 0.18	(-) 0.02	(-) 0.00	0.01	0.00	0.01
Thyp	0.02	0.18	0.17	0.01	0.00	(-) 0.00	(-) 0.00	(-) 0.00
Ag:WA	0.05	0.04	0.46	0.30	(-) 0.14	(-) 0.23	(-) 0.24	(-) 0.23
Adj Ag:LA	0.02	(-) 0.00	0.07	0.34	(-) 0.08	(-) 0.18	(-) 0.13	(-) 0.15
Ag:LA	0.00	0.04	0.58	0.04	(-) 0.05	(-) 0.20	(-) 0.09	(-) 0.20
Rd:WA	1.00	(-) 0.06	(-) 0.01	0.12	(-) 0.33	0.00	(-) 0.21	0.00
Wtlnd: WA		1.00	0.37	(-) 0.01	0.06	(-) 0.03	0.04	(-) 0.03
DOC			1.00	0.06	0.00	(-) 0.19	(-) 0.01	(-) 0.22
pH				1.00	(-) 0.15	(-) 0.19	(-) 0.34	(-) 0.25
MPJ					1.00	0.00	0.88	0.00
SPJ						1.00	0.03	0.96
MPM							1.00	0.05
SPM								1.00

APPENDIX D: LAND COVER DATA

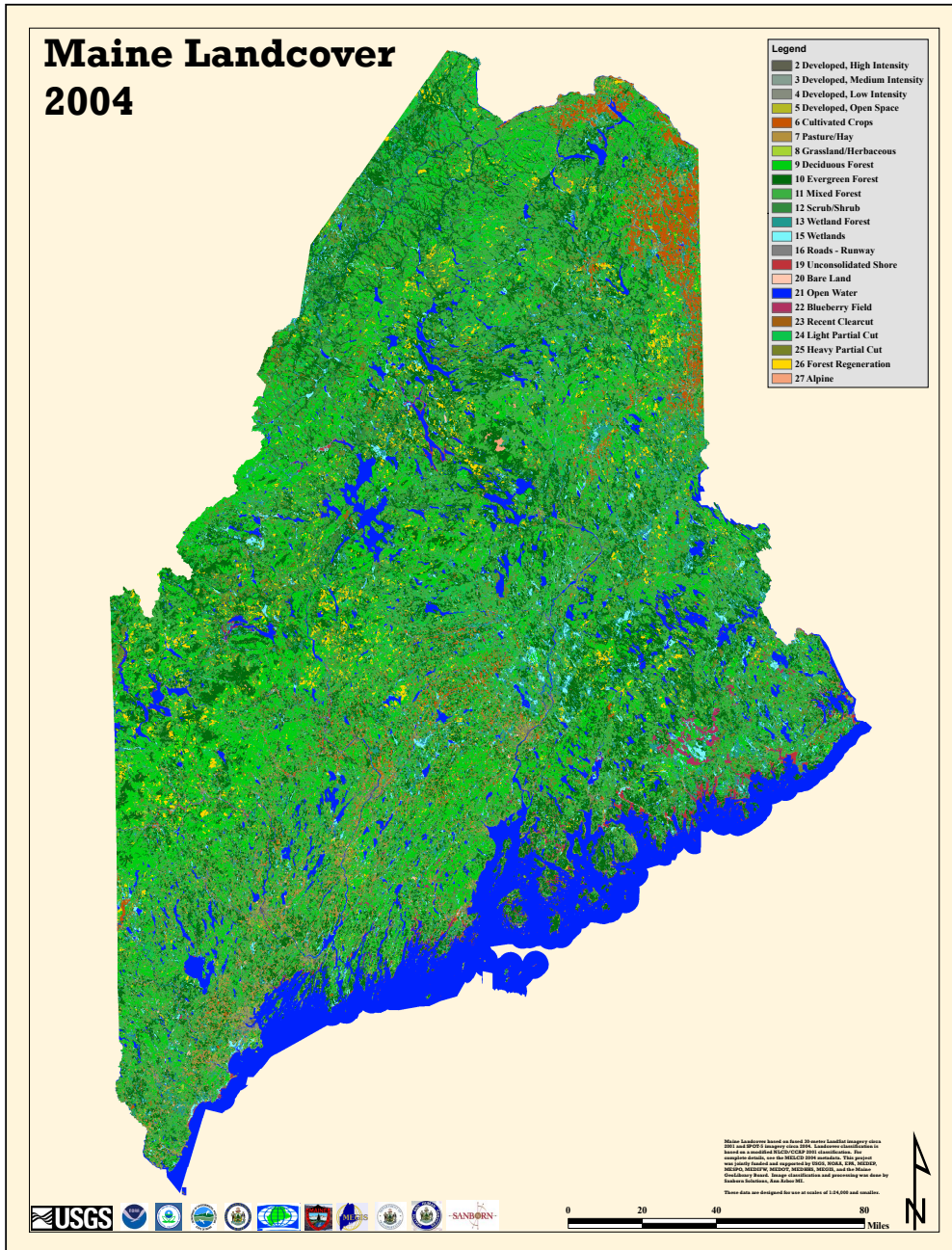


Figure D1: Land cover Map 2004 (MEGIS). The map is derived from the Landsat Thematic Mapper (5, 7) imagery, from 1999-2001. The map was refined to the state of Maine requirements using SPOT 5 panchromatic imagery from 2004.

Table D1: Land cover Identification Key.

Key	Land cover Type
2	Developed, High Intensity
3	Developed, Medium Intensity
4	Developed, Low Intensity
5	Developed, Open Space
6	Cultivated Crops
7	Pasture/ Hay
8	Grassland/ Herbaceous
9	Deciduous Forest
10	Evergreen Forest
11	Mixed Forest
12	Scrub/ Shrub
13	Wetland Forest
15	Wetlands
16	Roads/ Runway
19	Unconsolidated Shore
20	Bare Land
21	Open Water
22	Blueberry Field
23	Recent Clearcut
24	Light Partial Cut
25	Heavy Partial Cut
26	Forest Regeneration
27	Alpine

Table D2.1: Land cover Area (ha.) from type 2 to 12. Land cover area (hectare) data from 2004, with identification code in Table D1.

Midas	2	3	4	5	6	7	8	9	10	11	12
2015											
78	10.6	5.0	19.6	0.0	0.5	0.8	0.0	1357.1	167.5	670.5	11.4
177	9.8	12.4	14.5	3.5	130.5	26.6	0.0	796.1	649.5	2032.1	25.9
224	0.2	0.0	0.5	0.0	0.0	0.0	0.0	251.0	422.2	133.1	0.0
3444	8.8	17.2	56.5	4.6	65.5	504.2	11.2	1661.7	1501.4	3833.7	34.8
3446	0.7	5.7	14.7	0.0	13.0	53.5	11.1	108.7	275.6	740.9	13.6
3748	15.3	26.2	16.9	29.3	42.9	285.9	1.1	606.6	269.4	910.8	50.6
3750	3.3	12.2	53.8	4.8	32.3	371.1	10.2	519.1	396.3	1624.7	14.6
3796	16.0	42.7	96.4	82.7	194.7	960.7	4.9	734.9	738.3	2365.4	47.1
3838	17.0	19.5	68.6	5.2	40.0	313.3	1.4	416.7	895.6	2602.0	122.7
3916	1.0	0.4	0.8	0.0	7.1	13.3	0.0	190.6	117.6	291.3	6.1
4434	0.0	00.0	0.0	0.0	0.1	0.6	0.0	76.5	1254.6	615.6	30.8
4538	0.0	0.0	0.0	0.0	0.6	0.0	0.3	346.5	218.8	53.7	2.4
5172	45.6	83.5	164.5	29.9	1309.6	2227.4	9.8	4315.6	5242.8	7157.4	25.9
5190	0.2	0.4	7.7	0.0	0.0	15.4	0.0	897.9	81.2	181.2	8.5
5272	17.7	19.5	41.3	7.2	75.1	80.6	0.0	1313.7	724.1	2083.2	7.0
5274	31.6	37.4	103.7	57.4	191.8	237.1	6.2	1499.4	1015.4	3782.6	10.6
5280	70.0	85.6	216.1	11.0	319.3	749.4	5.3	1395.2	1222.9	4099.2	29.8
5344	6.3	11.2	25.1	0.0	231.1	212.0	0.0	1297.5	336.5	1492.2	2.5
5348	5.3	18.6	27.2	1.7	23.1	6.8	6.3	275.5	46.9	361.9	8.8
5349	4.5	5.6	8.8	0.0	13.0	11.0	0.0	217.7	224.5	612.8	2.3
5352	11.9	16.4	39.0	0.0	46.0	15.3	0.0	173.9	60.5	381.2	0.2
5400	16.2	30.7	63.1	8.2	186.2	800.3	4.4	2731.7	1307.2	3105.6	127.5
5408	7.5	6.4	52.4	45.5	100.5	209.4	6.0	887.3	63.7	613.4	18.3
5448	26.5	51.0	142.0	45.6	212.7	657.4	2.1	1353.0	652.5	2320.5	68.4
DEP											
70	11.4	13.2	41.6	40.5	272.4	325.3	2.7	417.4	823.5	1292.4	1.5
80	NA	NA	NA	NA	NA	NA	NA	NA	NA	NA	NA
121	NA	NA	NA	NA	NA	NA	NA	NA	NA	NA	NA
177	9.8	12.4	14.5	3.5	130.5	26.6	0.0	796.1	649.5	2032.1	25.9
243	0.0	0.0	0.0	0.0	0.0	0.0	0.0	1089.2	701.6	2179.9	221.2
262	0.2	0.4	1.2	0.0	0.0	0.0	0.0	219.2	140.0	292.5	36.0
342	0.0	0.0	0.0	26.8	0.0	0.0	0.0	457.3	325.5	568.0	29.6
386	0.2	0.8	0.0	0.3	0.0	0.0	0.0	98.5	0.0	123.5	8.0
410	0.0	0.0	0.0	0.0	0.0	0.0	0.0	1245.0	758.4	1205.4	258.3
447	2.9	0.3	5.7	0.0	0.0	0.0	1.4	0.0	217.4	32.2	13.8
760	0.0	0.7	1.2	0.0	55.1	8.9	0.0	165.9	94.4	521.3	0.2
954	0.4	2.4	0.0	0.0	0.0	22.8	7.4	1686.9	3449.8	3364.0	1503.1
1068	1.4	0.9	1.6	2.8	36.3	6.2	0.0	255.8	121.5	260.7	12.3

Table D2.1: Continued

Midas	2	3	4	5	6	7	8	9	10	11	12
1070	NA	NA	NA	NA	NA	NA	NA	NA	NA	NA	NA
1078	0.1	1.9	1.7	0.9	2.9	6.1	1.1	597.8	5934.1	3954.7	44.3
1088	0.0	1.1	0.6	0.0	4.5	0.7	0.0	641.9	1315.5	1600.3	5.2
1150	0.6	1.0	0.2	0.0	0.0	0.0	0.0	428.9	3204.3	3203.5	28.7
1210	1.2	2.2	0.0	0.0	0.0	1.9	0.4	398.2	1234.5	1005.7	62.0
2004	0.0	1.2	0.8	0.0	0.0	0.0	0.0	271.9	315.9	247.9	48.2
2020	0.8	6.7	1.8	0.0	0.0	0.0	5.9	1384.7	7593.9	4166.3	512.1
2146	5.2	2.6	10.1	2.6	15.0	15.0	0.5	804.9	658.2	1131.4	21.3
2156	1.5	5.7	15.5	7.9	515.9	123.6	26.7	376.5	275.8	1005.0	27.6
2242	0.6	2.0	1.3	0.0	7.0	24.0	0.0	264.6	138.1	629.8	18.9
2286	40.2	67.8	179.7	123.3	477.3	807.8	19.5	4162.6	2630.4	4645.4	55.3
2590	16.1	15.7	20.9	3.2	608.8	538.7	5.0	4512.4	3511.2	8237.0	123.5
2608	0.5	3.1	1.7	0.0	20.8	5.4	1.4	814.2	17.2	463.4	0.0
2948	0.0	0.0	0.0	0.0	0.0	0.0	0.0	2341.0	1710.5	2485.4	291.5
3038	0.0	1.1	0.0	0.0	100.8	48.7	24.2	1150.3	1045.5	2699.0	173.6
3376	0.0	0.2	7.3	0.0	0.0	2.0	0.0	14.0	51.9	111.7	0.0
3388	0.3	0.2	2.5	0.0	1.4	11.1	0.0	65.9	28.4	126.5	0.0
3434	6.7	9.8	17.9	0.0	30.9	351.3	0.2	472.4	449.7	1355.4	1.1
3452	5.4	8.3	28.2	3.4	45.9	109.2	0.9	170.1	365.6	719.7	33.9
3454	0.8	30.7	8.9	2.3	13.4	76.6	0.2	410.9	250.5	834.5	30.7
3604	0.0	1.6	0.3	0.3	44.7	96.6	0.2	821.3	912.3	1298.5	23.3
3626	0.3	0.2	0.1	0.1	0.0	3.2	0.0	13.4	3.8	91.2	1.9
3672	4.1	13.1	8.9	158.8	77.8	42.3	27.1	7418.9	4668.1	2228.3	118.7
3682	9.3	12.4	48.2	7.7	56.3	107.5	0.0	3818.2	596.1	914.7	21.5
3690	0.0	0.4	4.3	0.0	7.0	26.9	0.0	498.9	71.2	457.5	1.5
3780	0.0	0.0	0.0	0.0	1.4	0.0	0.0	50.2	2.5	3.4	0.1
3814	0.2	2.6	6.0	0.0	4.0	108.7	0.0	162.5	52.7	234.9	1.0
3830	1.7	1.7	3.1	0.0	67.3	68.7	2.6	290.6	339.2	1077.4	5.7
3884	1.5	0.0	1.3	5.9	0.0	8.5	0.0	0.0	0.3	36.5	0.1
3920	0.2	0.2	6.2	2.6	8.3	50.0	1.1	253.8	81.3	389.6	18.3
4272	0.0	1.7	0.0	0.0	1.6	0.0	0.0	67.9	56.7	26.1	2.6
4316	5.8	11.5	23.3	0.5	149.4	124.1	0.8	1676.5	879.5	1183.2	68.3
4322	1.9	0.3	4.4	0.0	3.7	0.0	0.0	242.5	64.0	85.3	12.7
4328	4.6	6.4	10.0	9.4	86.8	50.2	17.6	2515.6	1585.1	780.7	100.9
4330	0.0	1.3	0.0	0.0	5.0	0.2	0.0	306.1	30.0	58.7	0.0
4336	7.3	15.1	24.6	12.6	54.7	85.2	5.0	970.0	1470.3	1449.1	47.4
4388	1.8	2.0	2.0	0.0	12.8	3.0	5.0	128.8	757.1	580.9	45.2
4452	0.0	0.0	0.0	0.0	0.0	0.0	4.4	0.0	80.2	54.7	10.4
4492	NA	NA	NA	NA	NA	NA	NA	NA	NA	NA	NA
4606	0.3	2.4	0.4	0.0	0.0	0.0	4.7	0.2	149.7	285.4	15.1
4608	0.8	0.5	0.4	0.0	0.0	0.0	14.3	3.2	122.4	153.4	35.6

Table D2.1: Continued

Midas	2	3	4	5	6	7	8	9	10	11	12
4610	0.0	0.0	0.0	0.0	0.0	0.0	0.0	0.0	72.8	4.5	4.0
4612	0.9	0.4	0.0	0.0	0.0	0.0	6.6	0.0	136.9	93.9	24.2
4614	NA	NA	NA	NA	NA	NA	NA	NA	NA	NA	NA
4618	0.0	0.0	1.6	0.0	0.0	0.0	0.7	0.0	52.2	1.6	1.3
4620	0.0	0.0	0.0	0.0	0.0	0.0	0.0	0.0	77.8	6.8	0.0
4622	0.9	1.7	3.3	0.0	0.0	0.0	4.4	31.9	830.2	245.6	5.7
4624	0.1	1.8	1.8	0.0	0.0	0.0	4.2	0.8	258.2	147.6	13.2
4628	0.0	1.0	5.2	3.3	0.0	0.0	3.2	0.0	84.0	17.1	1.3
4630	5.7	5.0	7.3	0.0	0.0	0.0	7.3	0.0	364.8	265.7	1.9
4766	0.0	0.0	0.0	0.0	0.0	20.0	4.5	246.8	4326.2	2423.7	81.3
4782	0.0	0.0	0.0	0.0	1.9	0.0	0.0	172.2	875.9	808.7	0.0
4788	0.0	0.0	0.0	0.0	0.0	0.0	0.0	79.1	65.5	202.8	33.1
4800	1.3	0.9	5.1	0.0	2.7	29.9	0.0	169.0	1.8	10.0	2.6
4802	NA	NA	NA	NA	NA	NA	NA	NA	NA	NA	NA
4806	0.0	0.7	3.3	0.0	0.0	81.4	0.0	527.2	27.7	31.9	6.2
4822	11.6	13.3	46.4	14.7	28.3	53.1	0.0	387.7	3.1	60.5	1.0
4852	5.7	7.9	26.3	0.0	0.2	321.1	1.5	2189.7	420.6	621.5	42.2
4857	1.1	0.0	0.8	0.0	0.0	12.4	0.0	195.9	191.8	177.9	9.4
4894	0.1	4.4	5.0	4.1	8.3	13.5	0.0	63.4	146.4	364.9	0.0
4896	1.5	12.6	34.4	4.0	141.9	73.7	0.0	2273.7	811.5	2504.1	16.0
5024	4.4	4.6	37.0	0.0	8.2	37.0	0.0	242.0	121.8	548.1	59.2
5172	45.6	83.5	164.5	29.9	1309.6	2227.4	9.8	4315.6	5242.8	7157.4	25.9
5174	0.2	5.9	11.3	0.0	14.5	99.0	0.0	514.9	78.4	390.3	4.1
5198	0.7	0.5	7.9	0.0	12.9	96.4	0.4	120.6	103.0	182.8	1.6
5222	3.5	11.3	18.6	15.7	7.4	157.9	13.7	587.6	772.9	2210.9	36.6
5236	23.3	41.0	79.6	152.1	132.5	1451.2	3.5	1123.3	930.6	2621.8	54.3
5240	0.8	2.4	8.2	0.0	2.8	46.5	0.0	104.0	110.1	214.4	7.5
5280	70.0	85.6	216.1	11.0	319.3	749.4	5.3	1395.2	1222.9	4099.2	29.8
5344	6.3	11.2	25.1	0.0	231.1	212.0	0.0	1297.5	336.5	1492.2	2.5
5348	5.3	18.6	27.2	1.7	23.1	6.8	6.3	275.5	46.9	361.9	8.8
5349	4.5	5.6	8.8	0.0	13.0	11.0	0.0	217.7	224.5	612.8	2.3
5352	11.9	16.4	39.0	0.0	46.0	15.3	0.0	173.9	60.5	381.2	0.2
5386	1.9	8.2	10.7	0.0	107.4	129.5	18.2	738.8	250.5	1119.0	30.5
5400	16.2	30.7	63.1	8.2	186.2	800.3	4.4	2731.7	1307.2	3105.6	127.5
5408	7.5	6.4	52.4	45.5	100.5	209.4	6.0	887.3	63.7	613.4	18.3
5416	9.5	14.7	58.3	7.7	96.5	133.8	0.2	819.7	89.3	782.9	15.9
5448	26.5	51.0	142.0	45.6	212.7	657.4	2.1	1353.0	652.5	2320.5	68.4
5458	9.3	7.4	26.0	0.0	49.2	97.3	0.8	597.2	397.7	1611.5	6.8
5490	0.0	0.0	0.0	0.0	7.2	0.0	0.0	254.9	24.0	36.6	9.1
5682	17.9	37.8	63.0	0.0	25.6	1015.3	3.1	2819.7	1264.3	2287.5	106.3
5690	7.0	7.7	27.9	5.1	57.9	149.4	19.5	368.9	66.9	298.4	18.4

Table D2.1: Continued

Midas	2	3	4	5	6	7	8	9	10	11	12
5710	2.1	4.1	4.2	0.0	5.9	15.6	0.0	258.0	100.1	582.7	1.6
5780	98.5	74.1	227.4	86.2	116.2	693.8	4.5	1231.8	1688.8	4887.0	39.5
5814	7.6	7.6	18.0	0.0	18.5	34.9	0.0	293.1	300.7	567.4	0.2
9685	18.2	21.1	61.5	100.6	20.5	7.8	0.0	160.3	99.3	353.8	2.7
9931	4.4	1.9	16.6	4.0	9.4	13.0	0.2	370.7	3.3	100.7	2.1
LEA											
5780	98.5	74.1	227.4	86.2	116.2	693.8	4.5	1231.8	1688.8	4887.0	39.5
3418	2.0	1.6	0.9	0.0	3.7	83.6	0.0	69.7	278.3	268.4	1.1
5780	98.5	74.1	227.4	86.2	116.2	693.8	4.5	1231.8	1688.8	4887.0	39.5
3130	0.5	0.6	0.0	0.0	1.7	31.5	0.0	32.1	81.2	139.8	0.2
3382	0.0	1.0	8.6	3.2	0.0	5.6	0.0	40.4	16.6	146.3	0.0
3424	0.2	0.6	0.0	0.0	4.7	121.6	0.0	185.4	113.5	625.6	0.0
3199	0.0	0.0	0.0	0.0	4.2	0.0	0.0	316.0	17.9	125.7	0.0
3134	3.0	9.8	19.7	13.5	49.0	138.1	33.7	663.4	393.8	1640.6	22.0
3416	4.9	3.5	9.0	0.0	5.5	121.9	1.9	37.8	289.4	493.1	0.0
9685	18.2	21.1	61.5	100.6	20.5	7.8	0.0	160.3	99.3	353.8	2.7
3420	0.2	1.8	1.3	0.0	0.3	43.7	0.0	100.5	82.7	266.1	0.0
3454	0.8	30.7	8.9	2.3	13.4	76.6	0.2	410.9	250.5	834.5	30.7
5582	0.0	4.1	5.1	0.4	3.8	28.8	0.0	61.0	77.0	243.2	11.6
3134	3.0	9.8	19.7	13.5	49.0	138.1	33.7	663.4	393.8	1640.6	22.0
5780	98.5	74.1	227.4	86.2	116.2	693.8	4.5	1231.8	1688.8	4887.0	39.5
5780	98.5	74.1	227.4	86.2	116.2	693.8	4.5	1231.8	1688.8	4887.0	39.5
3132	0.0	0.0	1.3	0.0	3.7	5.5	0.0	169.1	46.5	283.0	0.0
3126	0.2	2.9	0.0	0.0	0.0	14.6	0.0	5.3	44.3	168.9	0.0
3234	0.0	0.8	0.0	0.0	0.4	19.0	0.0	307.5	133.6	602.6	1.2
3374	0.7	1.1	6.5	0.0	5.7	2.7	0.0	341.6	63.7	312.1	0.5
3134	3.0	9.8	19.7	13.5	49.0	138.1	33.7	663.4	393.8	1640.6	22.0
3452	5.4	8.3	28.2	3.4	45.9	109.2	0.9	170.1	365.6	719.7	33.9
3454	0.8	30.7	8.9	2.3	13.4	76.6	0.2	410.9	250.5	834.5	30.7
3448	0.0	2.3	0.6	0.0	4.0	23.7	0.4	20.2	202.3	213.9	15.1
3232	0.0	1.0	1.5	0.0	1.8	27.0	0.0	112.4	164.6	399.1	0.0
3456	0.3	2.7	2.3	2.4	6.9	21.2	0.7	47.6	222.8	332.0	3.8
5780	98.5	74.1	227.4	86.2	116.2	693.8	4.5	1231.8	1688.8	4887.0	39.5

Table D2.2: Land cover Area (ha.) from type 13 to 27. Land cover area (hectare) data from 2004, with identification code in Table D1.

Midas	13	15	16	19	20	21	22	23	24	25	26	27
2015												
78	34.2	23.2	111.9	6.5	3.3	644.4	0.0	20.7	534.3	231.9	639.7	0.0
177	1036.0	928.4	107.7	10.0	14.5	2755.9	264.7	149.2	441.7	285.8	172.6	0.0
224	0.1	1.7	20.6	0.1	0.0	420.5	0.0	0.0	113.3	43.1	77.2	0.0
3444	299.1	141.7	267.8	0.5	15.3	1761.2	0.0	0.0	401.5	125.5	90.4	0.0
3446	56.0	22.3	58.7	0.1	3.1	534.4	0.0	0.0	69.2	10.7	17.1	0.0
3748	22.5	36.8	101.1	0.7	66.3	952.3	0.0	0.0	79.3	37.9	6.2	0.0
3750	150.2	100.1	108.0	0.2	1.5	259.4	0.0	0.0	81.8	27.7	1.2	0.0
3796	441.5	135.9	246.8	0.7	109.3	799.4	228.9	34.2	122.9	0.0	7403.3	0.0
3838	61.3	118.8	109.1	0.2	0.7	371.0	0.0	0.0	266.2	25.9	0.0	0.0
3916	40.3	47.9	26.3	0.5	0.0	349.7	0.0	0.0	118.2	28.8	0.0	0.0
4434	14.8	38.9	8.1	26.9	0.0	792.0	0.0	0.0	6.7	28.1	42.9	0.0
4538	0.0	0.0	0.0	6.5	0.0	169.2	0.0	0.0	0.0	16.7	0.0	0.0
5172	1451.3	475.7	573.0	47.3	8.1	1068.5	0.0	14.3	309.7	280.5	372.4	0.0
5190	0.0	9.0	16.4	2.0	0.0	313.2	0.0	1.3	30.2	13.4	20.2	0.0
5272	195.0	34.5	53.6	13.6	0.0	1033.3	0.0	0.0	299.3	29.6	52.0	0.0
5274	696.9	151.4	116.0	45.0	19.5	3434.3	0.0	0.0	272.0	102.7	67.3	0.0
5280	888.4	382.5	217.1	24.4	62.0	1636.7	0.0	4.2	803.5	92.3	112.9	0.0
5344	237.9	176.9	91.0	13.3	28.1	1019.2	0.0	0.0	189.3	37.0	136.0	0.0
5348	31.5	8.5	23.8	2.9	0.4	180.0	0.0	0.0	42.9	48.0	16.1	0.0
5349	13.0	38.6	27.9	13.2	0.3	689.2	0.0	0.0	33.2	0.0	0.6	0.0
5352	8.9	3.0	18.5	3.5	0.2	287.0	0.0	0.0	7.9	4.1	0.0	0.0
5400	310.9	175.1	350.7	62.5	62.1	1841.2	95.2	0.0	103.7	49.4	64.5	0.0
5408	18.6	37.4	54.8	19.2	0.9	484.2	0.0	0.0	24.5	0.0	0.2	0.0
5448	424.0	257.5	268.9	44.5	9.7	1578.2	0.0	0.0	65.1	52.7	49.6	0.0
DEP												
70	182.7	17.2	113.4	12.0	0.0	555.4	0.0	0.0	496.4	88.5	4.3	0.0
80	NA	NA	NA	NA	NA	NA	NA	NA	NA	NA	NA	NA
121	NA	NA	NA	NA	NA	NA	NA	NA	NA	NA	NA	NA
177	1036.0	928.4	107.7	10.0	14.5	2755.9	264.7	149.2	441.7	285.8	172.6	0.0
243	42.3	92.3	71.2	0.2	0.2	766.7	0.0	0.0	79.6	17.3	189.2	0.0
262	0.0	2.8	31.3	0.1	1.4	174.2	0.0	15.4	298.0	106.6	129.9	0.0
342	4.4	3.8	7.1	0.2	0.0	556.4	0.0	0.6	28.3	0.0	17.8	0.0
386	0.0	0.0	3.2	0.0	0.3	32.6	0.0	3.6	0.0	0.0	0.0	0.0
410	138.0	109.1	3.6	1.2	0.6	389.4	0.0	101.6	81.1	61.4	128.5	0.0
447	2.7	9.3	28.0	1.5	0.0	7.4	0.0	0.0	5.2	4.5	0.0	0.0
760	24.5	6.3	36.6	0.0	0.0	150.4	0.0	0.0	167.6	46.6	15.8	0.0
954	548.1	578.8	287.4	0.2	1.4	2268.8	0.0	0.0	963.7	820.3	96.2	0.0
1068	13.3	3.0	38.0	0.0	0.0	237.5	0.0	0.0	18.3	31.5	21.2	0.0

Table D2.2: Continued

Midas	13	15	16	19	20	21	22	23	24	25	26	27
1070	NA	NA	NA	NA	NA	NA	NA	NA	NA	NA	NA	NA
1078	2998.9	909.1	181.0	0.0	0.6	2797.3	0.0	1.2	2543.5	1950.6	203.2	0.0
1088	264.6	57.1	45.5	4.7	0.0	325.6	0.0	0.2	342.5	79.8	0.0	0.0
1150	84.0	278.9	31.2	369.5	0.0	5456.0	0.0	0.0	182.2	104.6	57.9	0.0
1210	128.6	37.1	33.7	9.5	0.0	361.2	0.0	0.0	108.5	154.1	4.0	0.0
2004	0.0	0.0	10.6	0.3	0.7	273.3	0.0	0.0	90.6	6.1	42.2	0.0
2020	742.9	609.8	313.4	12.5	33.5	3694.2	0.0	68.4	633.7	464.2	393.2	121.1
2146	66.0	35.7	78.2	0.8	1.2	1469.8	0.0	889.3	405.7	7.7	0.0	0.0
2156	247.0	57.3	72.9	0.0	0.1	176.8	0.0	5.1	156.3	158.0	0.0	0.0
2242	10.6	27.1	30.2	27.1	0.0	202.0	0.0	0.0	226.7	4.8	4.0	0.0
2286	1503.0	439.3	421.2	20.1	4.3	252.6	0.0	0.0	481.7	675.6	200.6	0.0
2590	360.2	564.1	894.0	0.7	1.0	1484.0	0.0	33.4	2974.7	709.3	2353.5	0.0
2608	9.4	28.0	7.4	1.4	0.0	126.4	0.0	0.0	67.9	16.9	6.5	0.0
2948	170.4	227.9	7.8	0.5	2.0	1348.3	0.0	42.9	525.5	378.0	104.1	0.0
3038	431.4	207.8	106.3	0.0	0.0	465.3	0.0	0.0	289.3	235.0	0.0	0.0
3376	2.1	0.0	6.4	0.0	1.0	14.5	0.0	0.0	7.9	0.0	0.0	0.0
3388	8.8	3.1	18.4	0.0	3.8	66.5	0.0	0.0	8.0	1.5	0.0	0.0
3434	46.9	66.0	142.1	2.0	0.0	381.9	0.0	0.0	455.8	185.2	88.2	0.0
3452	23.6	21.5	81.2	0.4	0.0	172.2	0.0	13.2	349.6	155.3	52.2	0.0
3454	1.8	44.8	86.2	0.0	0.0	532.7	0.0	0.0	177.2	89.7	44.5	0.0
3604	74.2	50.4	26.9	2.5	0.0	247.0	0.0	18.7	156.9	4.6	72.2	0.0
3626	0.0	0.0	4.4	0.0	0.0	19.8	0.0	0.0	2.3	0.0	0.0	0.0
3672	128.4	250.9	172.9	39.9	18.2	844.0	0.0	2.6	2166.7	292.6	892.5	0.0
3682	71.2	66.7	24.9	0.9	26.3	228.3	0.0	33.2	387.6	358.2	124.4	0.0
3690	5.3	9.4	37.1	4.2	0.5	137.7	0.0	0.0	22.6	7.2	0.8	0.0
3780	0.0	2.0	0.7	0.0	0.4	18.3	0.0	0.0	0.0	0.0	0.0	0.0
3814	8.6	21.8	30.9	0.1	0.0	160.3	0.0	0.0	57.2	1.8	9.3	0.0
3830	46.8	44.5	52.1	0.1	0.0	106.0	0.0	0.0	178.2	2.7	17.1	0.0
3884	10.8	0.0	1.5	0.0	0.0	18.7	0.0	0.0	0.0	0.0	0.0	0.0
3920	0.0	3.0	17.1	0.1	0.0	120.9	0.0	0.0	36.9	9.9	0.0	0.0
4272	0.0	0.0	6.5	2.8	0.3	60.3	0.0	0.0	8.0	27.5	0.0	0.0
4316	72.4	104.4	123.3	3.7	2.1	74.3	0.0	7.6	126.3	292.5	118.9	0.0
4322	0.0	3.4	12.6	2.2	0.4	74.2	0.0	0.0	33.3	136.1	0.0	0.0
4328	118.9	100.9	190.7	59.3	0.2	1159.5	0.0	32.8	203.6	272.3	0.0	0.0
4330	2.5	0.0	15.1	0.7	0.0	64.1	0.0	0.0	13.4	75.2	0.0	0.0
4336	117.4	117.6	169.7	18.3	4.4	482.1	171.7	3.6	220.7	376.1	2.3	0.0
4388	48.1	40.9	12.6	8.3	3.7	209.3	0.0	0.0	17.6	78.6	27.2	0.0
4452	0.0	0.4	9.2	0.6	0.4	14.2	0.0	0.0	0.0	21.0	0.0	0.0
4492	NA	NA	NA	NA	NA	NA	NA	NA	NA	NA	NA	NA
4606	0.9	1.8	51.7	5.4	2.8	185.6	0.0	0.0	15.6	29.8	1.0	0.0
4608	0.0	1.7	28.5	7.5	5.0	68.3	0.0	0.0	7.6	32.3	0.0	0.0

Table D2.2: Continued

Midas	13	15	16	19	20	21	22	23	24	25	26	27
4610	0.0	0.0	9.5	0.2	0.0	14.6	0.0	0.0	0.0	3.0	0.0	0.0
4612	0.0	0.0	33.3	0.2	2.2	15.0	0.0	0.0	6.9	16.4	0.0	0.0
4614	NA	NA	NA	NA	NA	NA	NA	NA	NA	NA	NA	NA
4618	5.3	0.0	4.3	0.3	0.0	5.1	0.0	0.0	0.0	0.2	0.0	0.0
4620	0.0	0.0	4.8	0.5	0.0	15.0	0.0	0.0	4.7	0.0	0.0	0.0
4622	24.0	0.4	62.3	10.8	0.0	377.0	0.0	0.0	25.9	59.1	0.0	0.0
4624	0.2	1.4	51.8	8.6	0.0	87.9	0.0	0.0	3.7	17.2	0.0	0.0
4628	2.1	0.0	13.0	2.6	0.0	18.6	0.0	0.0	7.2	8.5	0.0	0.0
4630	13.2	0.0	27.9	7.0	0.0	104.8	0.0	0.0	3.4	43.1	0.0	0.0
4766	497.8	431.6	36.6	123.0	0.0	2000.3	0.0	0.0	426.4	346.1	199.8	0.0
4782	87.1	7.2	1.8	5.9	0.0	376.8	0.0	0.0	9.0	0.0	101.5	0.0
4788	0.0	0.0	0.8	6.3	0.0	85.7	0.0	0.0	12.0	8.3	15.5	0.0
4800	0.0	11.6	14.6	11.7	0.0	55.6	0.0	0.0	3.2	0.0	0.0	0.0
4802	NA	NA	NA	NA	NA	NA	NA	NA	NA	NA	NA	NA
4806	0.0	5.3	20.2	4.2	0.0	103.1	19.9	0.0	3.8	4.2	0.0	0.0
4822	0.0	3.2	34.8	6.3	0.0	138.3	15.5	0.0	1.9	3.9	0.0	0.0
4852	50.0	55.1	126.6	33.1	0.5	514.6	7.6	0.0	35.4	6.7	8.1	0.0
4857	24.9	12.9	11.2	4.7	0.0	85.7	0.0	0.0	4.1	16.4	6.8	0.0
4894	14.2	10.8	30.6	4.2	0.0	230.2	0.0	0.0	12.7	0.0	0.8	0.0
4896	493.3	127.1	134.4	13.8	0.0	484.7	84.8	1.6	105.9	47.8	64.6	0.0
5024	7.7	27.1	33.9	0.6	2.8	223.6	0.0	0.0	75.0	7.0	0.0	0.0
5172	1451.3	475.7	573.0	47.3	8.1	1068.5	0.0	14.3	309.7	280.5	372.4	0.0
5174	116.0	35.4	46.1	12.4	0.0	158.9	0.0	0.0	10.5	8.8	30.2	0.0
5198	24.3	3.2	10.1	0.0	0.0	39.8	0.0	1.0	11.2	0.0	0.0	0.0
5222	116.3	100.4	99.4	0.2	1.6	176.5	0.0	0.0	391.5	60.1	177.7	0.0
5236	205.2	315.0	252.5	1.1	35.7	2215.4	0.0	0.0	535.8	56.5	89.7	0.0
5240	20.8	6.6	30.0	0.0	0.0	214.1	0.0	0.0	74.7	13.2	1.3	0.0
5280	888.4	382.5	217.1	24.4	62.0	1636.7	0.0	4.2	803.5	92.3	112.9	0.0
5344	237.9	176.9	91.0	13.3	28.1	1019.2	0.0	0.0	189.3	37.0	136.0	0.0
5348	31.5	8.5	23.8	2.9	0.4	180.0	0.0	0.0	42.9	48.0	16.1	0.0
5349	13.0	38.6	27.9	13.2	0.3	689.2	0.0	0.0	33.2	0.0	0.6	0.0
5352	8.9	3.0	18.5	3.5	0.2	287.0	0.0	0.0	7.9	4.1	0.0	0.0
5386	60.1	133.4	58.2	23.6	11.5	150.4	0.0	0.0	27.8	5.3	0.8	0.0
5400	310.9	175.1	350.7	62.5	62.1	1841.2	95.2	0.0	103.7	49.4	64.5	0.0
5408	18.6	37.4	54.8	19.2	0.9	484.2	0.0	0.0	24.5	0.0	0.2	0.0
5416	150.1	102.3	76.6	15.6	1.7	466.5	0.0	0.0	47.2	20.3	36.9	0.0
5448	424.0	257.5	268.9	44.5	9.7	1578.2	0.0	0.0	65.1	52.7	49.6	0.0
5458	260.9	100.6	87.0	2.7	0.0	208.5	0.0	0.0	72.8	13.1	52.4	0.0
5490	14.4	2.6	1.8	2.4	0.0	63.8	0.0	0.0	0.0	4.9	0.0	0.0
5682	719.5	184.5	212.7	30.1	30.4	248.9	410.4	0.0	58.5	24.7	136.6	0.0
5690	57.2	36.9	40.1	22.4	0.0	129.9	0.0	0.0	4.0	0.2	0.0	0.0

Table D2.2: Continued

Midas	13	15	16	19	20	21	22	23	24	25	26	27
5710	25.4	10.9	37.7	11.9	0.0	144.4	0.0	0.0	21.3	5.4	0.0	0.0
5780	189.6	360.9	485.7	1.2	2.0	2120.9	16.7	13.6	1714.9	1311.5	285.1	0.0
5814	40.7	7.3	26.3	5.4	0.0	447.7	0.0	0.0	114.2	0.8	27.1	0.0
9685	16.1	25.7	8.6	0.8	0.4	291.6	0.0	0.0	34.5	4.0	0.0	0.0
9931	3.3	23.0	30.1	0.0	0.0	268.1	0.0	0.0	170.6	17.0	131.3	0.0
LEA												
5780	189.6	360.9	485.7	1.2	2.0	2120.9	16.7	13.6	1714.9	1311.5	285.1	0.0
3418	25.1	12.8	36.5	0.0	0.0	176.7	0.0	0.0	187.6	34.9	10.9	0.0
5780	189.6	360.9	485.7	1.2	2.0	2120.9	16.7	13.6	1714.9	1311.5	285.1	0.0
3130	1.0	6.1	10.2	0.0	0.0	94.2	0.0	0.0	129.1	78.1	14.6	0.0
3382	1.4	6.6	0.0	0.2	0.0	126.4	0.0	0.0	8.3	1.6	17.4	0.0
3424	1.2	7.7	21.8	0.0	0.0	75.5	0.0	0.0	61.2	12.7	9.8	0.0
3199	5.5	17.6	10.1	0.0	0.0	69.9	0.0	0.0	122.2	1.5	86.1	0.0
3134	42.3	117.9	119.1	0.1	0.0	630.5	0.0	0.0	974.0	589.7	56.1	0.0
3416	0.2	0.8	54.2	0.1	0.0	183.8	0.0	0.0	270.7	14.9	23.4	0.0
9685	16.1	25.7	8.6	0.8	0.4	291.6	0.0	0.0	34.5	4.0	0.0	0.0
3420	9.5	9.5	20.9	0.1	0.0	94.7	0.0	0.0	39.5	36.0	5.5	0.0
3454	1.8	44.8	86.2	0.0	0.0	532.7	0.0	0.0	177.2	89.7	44.5	0.0
5582	2.0	9.3	24.6	0.0	0.0	27.4	0.0	0.0	109.4	53.2	33.8	0.0
3134	42.3	117.9	119.1	0.1	0.0	630.5	0.0	0.0	974.0	589.7	56.1	0.0
5780	189.6	360.9	485.7	1.2	2.0	2120.9	16.7	13.6	1714.9	1311.5	285.1	0.0
5780	189.6	360.9	485.7	1.2	2.0	2120.9	16.7	13.6	1714.9	1311.5	285.1	0.0
3132	26.1	29.2	15.9	0.0	0.0	311.9	0.0	0.0	192.7	125.6	46.4	0.0
3126	0.0	8.3	10.7	0.0	0.0	51.8	0.0	0.0	57.4	39.4	1.2	0.0
3234	27.1	37.1	19.2	0.0	0.0	99.4	0.0	0.0	68.5	11.1	3.9	0.0
3374	25.0	21.6	19.8	0.0	0.0	296.5	0.0	0.2	167.2	14.3	38.5	0.0
3134	42.3	117.9	119.1	0.1	0.0	630.5	0.0	0.0	974.0	589.7	56.1	0.0
3452	23.6	21.5	81.2	0.4	0.0	172.2	0.0	13.2	349.6	155.3	52.2	0.0
3454	1.8	44.8	86.2	0.0	0.0	532.7	0.0	0.0	177.2	89.7	44.5	0.0
3448	5.5	7.3	13.3	0.0	0.0	43.1	0.0	0.0	128.8	26.6	10.0	0.0
3232	1.1	2.5	16.6	0.0	0.0	76.6	0.0	0.0	155.0	29.9	46.9	0.0
3456	26.3	36.4	40.2	0.3	0.7	185.7	0.0	0.5	217.0	378.6	5.5	0.0
5780	189.6	360.9	485.7	1.2	2.0	2120.9	16.7	13.6	1714.9	1311.5	285.1	0.0

Table D3.1: Adjacent Land cover Area (ha.) from type 2-12. Adjacent land cover area data from 2004, with identification code in Table D1, with types 2-12.

Midas	2	3	4	5	6	7	8	9	10	11	12
2015											
78	10.6	4.5	19.6	0.0	0.5	0.0	0.0	292.4	66.0	199.4	0.8
177	0.9	4.1	0.0	0.0	28.5	2.5	0.0	153.3	313.5	709.0	3.1
224	0.2	0.0	0.5	0.0	0.0	0.0	0.0	9.5	125.6	93.2	0.0
3444	4.6	8.4	25.7	4.6	21.2	213.1	7.5	931.3	521.3	1468.4	7.5
3446	0.4	5.0	13.2	0.0	4.1	18.4	0.9	88.7	137.8	454.4	10.5
3748	11.9	11.8	9.1	27.8	5.3	144.0	0.8	151.1	181.7	181.8	11.6
3750	1.1	3.9	29.1	4.7	1.1	13.7	0.0	100.0	59.9	134.2	2.2
3796	1.5	7.8	16.5	0.7	22.0	228.3	0.2	136.0	33.6	168.2	11.7
3838	4.2	2.1	6.3	2.4	7.7	11.2	0.0	13.4	406.7	206.2	12.7
3916	1.0	0.4	0.3	0.0	6.0	0.2	0.0	48.7	89.4	188.3	3.2
4434	0.0	0.0	0.0	0.0	0.1	0.0	0.0	21.2	790.9	282.4	13.9
4538	0.0	0.0	0.0	0.0	0.0	0.0	0.3	143.5	181.1	23.1	0.0
5172	3.3	6.1	18.0	6.5	19.0	49.3	0.0	131.7	128.2	307.2	0.2
5190	0.1	0.0	7.1	0.0	0.0	2.8	0.0	351.9	62.3	135.7	0.0
5272	11.2	8.4	23.7	0.0	1.7	11.4	0.0	306.5	468.8	626.2	1.1
5274	15.4	9.2	36.2	4.2	35.2	70.7	0.4	502.8	487.1	1349.9	1.2
5280	19.8	16.7	83.7	0.0	58.6	50.6	0.0	242.4	130.8	563.4	4.6
5344	4.9	4.3	21.7	0.0	22.3	45.7	0.0	243.8	80.5	483.2	0.6
5348	1.5	6.9	15.5	1.7	6.1	0.0	0.0	113.7	16.4	137.7	1.3
5349	3.6	2.9	6.8	0.0	3.4	3.4	0.0	49.7	155.6	298.8	1.9
5352	7.0	9.2	14.2	0.0	18.9	0.0	0.0	82.5	35.9	228.0	0.2
5400	7.0	9.8	18.7	1.0	26.5	397.4	1.0	641.5	581.2	773.5	8.9
5408	1.3	2.6	18.2	3.0	28.1	99.4	0.0	341.2	18.8	251.1	7.2
5448	10.1	24.6	69.4	15.8	53.8	378.7	0.6	487.4	292.2	448.4	4.7
DEP											
70	3.0	4.0	20.0	0.1	40.2	41.6	1.6	94.8	166.7	203.9	0.0
80	NA	NA	NA	NA	NA	NA	NA	NA	NA	NA	NA
121	NA	NA	NA	NA	NA	NA	NA	NA	NA	NA	NA
177	0.9	4.1	0.0	0.0	28.5	2.5	0.0	153.3	313.5	709.0	3.1
243	0.0	0.0	0.0	0.0	0.0	0.0	0.0	27.1	257.3	591.5	137.6
262	0.0	0.4	1.2	0.0	0.0	0.0	0.0	109.7	32.7	115.7	0.1
342	0.0	0.0	0.0	1.1	0.0	0.0	0.0	41.0	225.0	431.8	8.4
386	0.0	0.0	0.0	0.0	0.0	0.0	0.0	19.5	0.0	77.5	6.9
410	0.0	0.0	0.0	0.0	0.0	0.0	0.0	155.0	125.9	335.4	22.1
447	0.0	0.0	0.6	0.0	0.0	0.0	1.2	0.0	9.6	11.3	5.6
760	0.0	0.0	0.1	0.0	10.1	0.1	0.0	86.0	32.0	157.9	0.0
954	0.0	0.0	0.0	0.0	0.0	0.0	0.0	494.4	1621.2	1146.3	179.4
1068	0.7	0.0	0.0	0.0	2.1	2.9	0.0	94.6	111.0	140.9	1.1

Table D3.1: Continued

Midas	2	3	4	5	6	7	8	9	10	11	12
1070	NA	NA	NA	NA	NA	NA	NA	NA	NA	NA	NA
1078	0.0	0.0	0.0	0.0	0.0	0.0	0.0	25.7	2401.2	920.5	2.9
1088	0.0	0.7	0.6	0.0	0.0	0.0	0.0	235.4	211.8	437.4	0.0
1150	0.0	0.0	0.0	0.0	0.0	0.0	0.0	0.0	0.0	0.0	0.0
1210	0.0	0.5	0.0	0.0	0.0	0.0	0.0	54.7	523.1	348.7	5.3
2004	0.0	1.2	0.8	0.0	0.0	0.0	0.0	200.3	189.9	97.3	20.9
2020	0.0	0.5	0.0	0.0	0.0	0.0	1.7	543.9	2226.0	603.5	151.4
2146	4.6	2.5	10.5	2.2	4.3	7.8	0.0	567.3	388.0	705.1	6.2
2156	0.0	0.9	3.9	6.5	28.2	0.0	0.0	8.8	25.3	47.4	0.1
2242	0.0	0.0	0.0	0.0	0.0	14.6	0.0	58.5	40.1	250.8	5.7
2286	0.1	0.6	1.3	0.1	0.8	42.8	0.0	29.0	0.9	17.8	2.0
2590	0.2	0.4	0.0	0.0	70.9	17.1	0.0	677.1	171.4	811.0	4.4
2608	0.0	0.4	0.0	0.0	0.1	0.0	0.0	333.3	3.2	151.6	0.0
2948	0.0	0.0	0.0	0.0	0.0	0.0	0.0	380.3	941.7	951.1	18.5
3038	0.0	0.0	0.0	0.0	7.0	2.1	0.0	182.0	134.0	439.9	4.4
3376	0.0	0.0	0.0	0.0	0.0	0.0	0.0	0.3	37.7	43.7	0.0
3388	0.3	0.2	0.7	0.0	0.0	9.8	0.0	18.1	15.1	40.6	0.0
3434	2.0	3.8	6.3	0.0	4.2	65.6	0.0	20.7	194.0	450.0	0.2
3452	0.4	3.6	18.4	3.4	9.5	20.6	0.0	7.4	61.5	152.5	4.8
3454	0.7	28.9	4.7	0.5	2.7	42.3	0.0	142.3	125.8	353.4	11.3
3604	0.0	1.5	0.3	0.2	14.1	45.8	0.2	65.1	143.1	215.2	11.2
3626	0.2	0.1	0.0	0.1	0.0	0.0	0.0	0.7	3.8	23.1	0.8
3672	2.4	4.2	4.8	85.0	72.0	19.6	14.2	284.0	932.0	560.2	3.1
3682	4.5	4.5	30.2	7.6	12.1	27.4	0.0	111.4	24.2	145.9	2.2
3690	0.0	0.0	4.3	0.0	0.1	0.5	0.0	61.4	65.6	238.9	0.9
3780	0.0	0.0	0.0	0.0	0.9	0.0	0.0	28.9	2.5	2.8	0.0
3814	0.2	2.3	3.7	0.0	4.0	72.1	0.0	99.1	43.1	139.0	0.0
3830	0.8	0.4	0.2	0.0	1.7	8.1	0.0	49.2	76.4	215.7	1.2
3884	0.3	0.0	0.1	0.5	0.0	8.3	0.0	0.0	0.3	36.8	0.1
3920	0.0	0.0	0.0	0.1	1.9	8.6	0.0	4.8	33.1	77.8	0.0
4272	0.0	1.1	0.0	0.0	1.6	0.0	0.0	53.2	29.3	14.6	0.0
4316	3.3	0.0	1.6	0.0	0.0	2.3	0.0	103.9	92.3	151.2	6.2
4322	0.9	0.3	3.3	0.0	1.6	0.0	0.0	84.1	12.4	19.9	0.0
4328	1.3	1.3	6.4	0.2	18.3	7.3	0.0	801.8	1032.8	302.3	3.2
4330	0.0	0.8	0.0	0.0	2.4	0.0	0.0	152.4	13.9	23.3	0.0
4336	1.0	4.9	8.4	3.1	5.5	24.3	0.8	163.8	176.1	353.3	9.2
4388	0.0	0.9	0.0	0.0	12.8	0.0	0.0	23.1	132.8	261.7	13.8
4452	0.0	0.0	0.0	0.0	0.0	0.0	0.0	0.0	50.3	50.5	0.0
4492	NA	NA	NA	NA	NA	NA	NA	NA	NA	NA	NA
4606	0.0	0.6	0.4	0.0	0.0	0.0	0.5	0.0	81.7	124.4	3.0
4608	0.8	0.5	0.4	0.0	0.0	0.0	0.0	0.0	52.9	81.1	0.1

Table D3.1: Continued

Midas	2	3	4	5	6	7	8	9	10	11	12
4610	0.0	0.0	0.0	0.0	0.0	0.0	0.0	0.0	31.3	0.0	0.3
4612	0.4	0.2	0.0	0.0	0.0	0.0	0.0	0.0	19.9	4.5	2.3
4614	NA	NA	NA	NA	NA	NA	NA	NA	NA	NA	NA
4618	0.0	0.0	0.1	0.0	0.0	0.0	0.5	0.0	14.1	0.1	0.0
4620	NA	NA	NA	NA	NA	NA	NA	NA	NA	NA	NA
4622	0.3	1.2	3.3	0.0	0.0	0.0	3.4	31.8	576.7	202.1	0.3
4624	0.0	1.8	1.8	0.0	0.0	0.0	0.3	0.0	107.9	116.8	7.7
4628	0.0	1.0	4.5	3.4	0.0	0.0	3.2	0.0	57.2	17.1	1.3
4630	5.1	3.0	4.2	0.0	0.0	0.0	4.7	0.0	172.3	148.9	0.0
4766	0.0	0.0	0.0	0.0	0.0	0.0	4.5	39.3	1922.5	914.8	8.7
4782	0.0	0.0	0.0	0.0	0.0	0.0	0.0	41.7	510.3	486.9	0.0
4788	0.0	0.0	0.0	0.0	0.0	0.0	0.0	0.5	53.5	28.7	0.1
4800	0.9	0.2	4.1	0.0	0.0	14.6	0.0	100.2	1.8	3.2	0.0
4802	NA	NA	NA	NA	NA	NA	NA	NA	NA	NA	NA
4806	0.0	0.7	3.1	0.0	0.0	64.4	0.0	338.7	27.7	28.0	5.0
4822	9.4	9.6	36.0	6.8	2.7	43.0	0.0	168.2	1.1	50.1	1.0
4852	0.3	2.7	7.6	0.0	0.0	105.8	0.4	840.1	222.4	242.4	16.8
4857	0.5	0.0	0.0	0.0	0.0	10.2	0.0	87.2	8.1	37.8	0.4
4894	0.0	3.3	3.1	4.1	7.4	6.0	0.0	50.3	47.5	228.7	0.0
4896	0.2	2.0	9.5	2.5	2.8	24.4	0.0	218.0	124.3	335.9	0.0
5024	3.7	1.6	26.3	0.0	2.3	25.9	0.0	28.3	79.8	291.8	42.5
5172	3.3	6.1	18.0	6.5	19.0	49.3	0.0	131.7	128.2	307.2	0.2
5174	0.0	1.0	3.5	0.0	0.9	14.3	0.0	194.3	15.1	169.1	0.8
5198	0.0	0.0	0.1	0.0	0.0	1.9	0.0	65.1	20.1	20.4	0.0
5222	0.3	1.7	1.9	2.5	0.0	71.2	0.0	75.6	35.0	224.1	1.8
5236	5.7	22.5	44.2	126.1	52.2	370.9	0.0	462.8	526.5	1083.4	10.7
5240	0.0	0.8	7.0	0.0	0.9	26.3	0.0	48.6	96.7	88.8	7.6
5280	19.8	16.7	83.7	0.0	58.6	50.6	0.0	242.4	130.8	563.4	4.6
5344	4.9	4.3	21.7	0.0	22.3	45.7	0.0	243.8	80.5	483.2	0.6
5348	1.5	6.9	15.5	1.7	6.1	0.0	0.0	113.7	16.4	137.7	1.3
5349	3.6	2.9	6.8	0.0	3.4	3.4	0.0	49.7	155.6	298.8	1.9
5352	7.0	9.2	14.2	0.0	18.9	0.0	0.0	82.5	35.9	228.0	0.2
5386	0.2	1.9	3.2	0.0	7.3	22.0	0.0	185.6	29.7	321.3	0.0
5400	7.0	9.8	18.7	1.0	26.5	397.4	1.0	641.5	581.2	773.5	8.9
5408	1.3	2.6	18.2	3.0	28.1	99.4	0.0	341.2	18.8	251.1	7.2
5416	2.8	2.7	19.4	5.9	3.2	6.8	0.0	262.1	32.2	389.2	1.1
5448	10.1	24.6	69.4	15.8	53.8	378.7	0.6	487.4	292.2	448.4	4.7
5458	1.2	2.7	9.5	0.0	7.1	25.7	1.0	147.0	63.1	206.5	1.5
5490	NA	NA	NA	NA	NA	NA	NA	NA	NA	NA	NA
5682	0.7	1.1	8.3	0.0	0.0	161.4	0.0	69.1	8.1	57.0	4.8
5690	1.6	1.5	9.1	0.1	41.2	77.9	0.2	26.2	40.7	35.0	4.1

Table D3.1: Continued

Midas	2	3	4	5	6	7	8	9	10	11	12
5710	0.6	0.9	2.3	0.0	4.2	4.9	0.0	110.4	16.5	128.2	0.0
5780	26.2	37.7	108.6	21.0	46.4	143.0	0.7	734.4	455.2	1758.7	7.7
5814	4.5	6.7	9.0	0.0	5.1	8.7	0.0	257.9	197.6	388.1	0.2
9685	15.4	17.1	52.5	77.9	13.7	4.1	0.0	60.9	71.3	142.8	0.0
9931	3.0	0.6	9.1	3.5	7.3	0.0	0.2	156.2	3.3	87.7	0.9
LEA											
5780	26.2	37.7	108.6	21.0	46.4	143.0	0.7	734.4	455.2	1758.7	7.7
3418	0.6	1.0	0.0	0.0	0.7	55.1	0.0	13.7	111.6	86.3	1.1
5780	26.2	37.7	108.6	21.0	46.4	143.0	0.7	734.4	455.2	1758.7	7.7
3130	0.5	0.3	0.0	0.0	0.9	9.8	0.0	25.5	81.4	66.4	0.0
3382	NA	NA	NA	NA	NA	NA	NA	NA	NA	NA	NA
3424	0.2	0.0	0.0	0.0	0.7	16.3	0.0	70.4	35.4	293.0	0.0
3199	0.0	0.0	0.0	0.0	3.2	0.0	0.0	158.0	10.6	89.9	0.0
3134	0.9	5.8	7.4	4.5	30.3	84.4	33.5	572.3	267.5	1089.4	10.3
3416	3.7	2.3	7.1	0.0	1.9	63.4	0.0	27.2	141.9	266.4	0.0
9685	15.4	17.1	52.5	77.9	13.7	4.1	0.0	60.9	71.3	142.8	0.0
3420	0.0	0.4	0.4	0.0	0.3	16.6	0.0	34.5	19.8	53.5	0.0
3454	0.7	28.9	4.7	0.5	2.7	42.3	0.0	142.3	125.8	353.4	11.3
5582	0.0	2.4	2.8	0.3	0.5	9.5	0.0	0.0	9.9	35.0	10.4
3134	0.9	5.8	7.4	4.5	30.3	84.4	33.5	572.3	267.5	1089.4	10.3
5780	26.2	37.7	108.6	21.0	46.4	143.0	0.7	734.4	455.2	1758.7	7.7
5780	26.2	37.7	108.6	21.0	46.4	143.0	0.7	734.4	455.2	1758.7	7.7
3132	0.0	0.0	0.3	0.0	0.0	0.0	0.0	70.4	37.5	191.0	0.0
3126	0.0	0.8	0.0	0.0	0.0	6.5	0.0	0.3	32.0	124.4	0.0
3234	0.0	0.0	0.0	0.0	0.0	4.8	0.0	100.6	16.1	131.9	0.0
3374	0.7	0.9	4.8	0.0	1.8	0.0	0.0	285.1	34.4	233.3	0.5
3134	0.9	5.8	7.4	4.5	30.3	84.4	33.5	572.3	267.5	1089.4	10.3
3452	0.4	3.6	18.4	3.4	9.5	20.6	0.0	7.4	61.5	152.5	4.8
3454	0.7	28.9	4.7	0.5	2.7	42.3	0.0	142.3	125.8	353.4	11.3
3448	0.0	0.2	0.6	0.0	4.2	21.7	0.0	6.9	105.9	110.0	12.2
3232	0.0	0.5	1.5	0.0	1.8	11.8	0.0	35.3	29.3	70.2	0.0
3456	0.0	0.5	0.8	0.0	0.0	7.2	0.3	9.9	38.6	137.7	1.3
5780	26.2	37.7	108.6	21.0	46.4	143.0	0.7	734.4	455.2	1758.7	7.7

Table D3.2: Adjacent Land cover Area (ha.) from type 13 to 26. Adjacent land cover area data from 2004, with identification code in Table D1.

Midas	13	15	16	19	20	21	22	23	24	25	26
2015											
78	11.5	6.3	29.9	5.6	0.0	634.1	0.0	9.9	120.0	97.8	3.6
177	478.3	559.9	37.8	6.4	0.0	2746.2	0.5	37.3	172.5	55.2	55.8
224	0.0	1.7	13.8	0.1	0.0	420.5	0.0	0.0	40.7	32.5	62.2
3444	24.1	72.3	136.9	0.3	13.3	1750.6	0.0	0.0	77.5	10.4	8.0
3446	8.9	42.7	0.1	2.1	534.5	539.0	0.0	0.0	21.7	8.1	17.2
3748	18.2	28.1	55.0	0.7	52.9	952.4	0.0	0.0	20.8	2.1	0.9
3750	81.1	37.7	16.7	0.1	0.0	257.5	0.0	0.0	8.6	11.9	0.0
3796	71.5	26.7	62.4	0.4	32.4	799.0	0.0	0.0	20.9	5.8	10.8
3838	0.0	27.2	20.6	0.2	0.0	370.7	0.0	0.0	88.3	5.2	0.0
3916	0.0	45.9	19.8	0.5	0.0	348.1	0.0	0.0	43.5	0.6	0.0
4434	13.7	23.9	6.1	26.8	0.0	791.9	0.0	0.0	2.1	0.1	0.0
4538	0.0	0.0	0.0	6.5	0.0	169.3	0.0	0.0	0.0	1.6	0.0
5172	110.3	60.2	64.8	27.8	0.6	1016.4	0.0	0.0	25.6	20.2	17.8
5190	0.0	0.6	10.4	2.0	0.0	312.0	0.0	0.0	0.0	0.0	7.0
5272	68.1	7.7	7.5	13.6	0.0	1031.3	0.0	0.0	142.9	0.0	0.8
5274	566.8	132.0	17.5	37.3	5.0	3423.0	0.0	0.0	59.1	2.7	15.9
5280	28.8	247.5	19.1	17.2	0.0	1515.4	0.0	0.0	28.2	19.6	0.0
5344	100.8	7.1	28.9	9.3	21.5	1017.6	0.0	0.0	51.3	16.5	101.5
5348	6.2	8.5	3.0	2.8	0.0	180.0	0.0	0.0	21.4	0.7	2.0
5349	11.5	35.6	4.6	13.2	0.0	689.3	0.0	0.0	15.4	0.0	0.6
5352	0.0	3.0	1.3	3.5	0.0	286.9	0.0	0.0	7.7	3.1	0.0
5400	72.2	123.0	158.9	59.1	0.0	1839.4	43.4	0.0	24.4	13.9	14.1
5408	1.9	14.7	19.7	19.2	0.7	484.2	0.0	0.0	14.3	0.0	0.2
5448	21.1	94.5	135.9	41.6	0.0	1575.8	0.0	0.0	22.7	10.3	18.3
DEP											
70	126.5	13.3	28.4	10.7	0.0	555.4	0.0	0.0	152.7	34.2	0.0
80	NA	NA	NA	NA	NA	NA	NA	NA	NA	NA	NA
121	NA	NA	NA	NA	NA	NA	NA	NA	NA	NA	NA
177	478.3	559.9	37.8	6.4	0.0	2746.2	0.5	37.3	172.5	55.2	55.8
243	5.3	42.7	28.3	0.2	0.1	759.9	0.0	0.0	13.6	8.2	49.6
262	0.0	2.8	26.4	0.1	0.0	174.2	0.0	0.0	81.2	3.5	0.7
342	4.4	1.0	6.5	0.2	0.0	556.3	0.0	0.0	20.1	0.0	10.8
386	0.0	0.0	1.7	0.0	0.2	32.6	0.0	3.7	0.0	0.0	0.0
410	66.1	83.1	0.9	0.0	0.0	389.4	0.0	0.0	22.6	5.0	0.0
447	2.7	9.2	3.7	1.3	0.0	7.4	0.0	0.0	0.1	0.0	0.0
760	5.2	2.3	2.2	0.0	0.0	150.4	0.0	0.0	47.2	26.2	0.1

Table D3.2: Continued

Midas	13	15	16	19	20	21	22	23	24	25	26
954	224.2	309.2	99.7	0.2	0.2	2228.3	0.0	0.0	276.9	234.2	8.1
1068	12.7	1.1	22.6	0.0	0.0	237.5	0.0	0.0	8.9	18.0	0.0
1070	NA	NA	NA	NA	NA	NA	NA	NA	NA	NA	NA
1078	1161.7	430.8	47.9	0.0	0.6	2775.0	0.0	0.7	232.3	195.0	26.9
1088	15.0	31.7	17.4	4.7	0.0	325.6	0.0	0.2	31.2	17.3	0.0
1150	0.0	0.0	31.2	0.0	0.0	5456.0	0.0	0.0	0.0	0.0	0.0
1210	9.8	8.6	10.7	5.9	0.0	361.2	0.0	0.0	6.4	25.9	0.0
2004	0.0	0.0	6.9	0.3	0.7	273.3	0.0	0.0	37.8	0.0	0.0
2020	218.4	297.2	87.4	12.4	0.5	3665.0	0.0	0.0	94.2	198.5	22.5
2146	13.3	18.8	59.7	0.8	0.8	1469.7	0.0	0.0	249.8	70.5	0.0
2156	173.8	15.1	9.9	0.0	0.0	176.8	0.0	0.0	2.7	2.4	0.0
2242	0.5	23.3	5.3	26.4	0.0	202.0	0.0	0.0	20.5	3.6	0.0
2286	121.2	9.0	12.7	6.0	0.0	187.9	0.0	0.0	32.7	2.5	0.0
2590	67.3	175.0	107.3	0.1	0.0	1475.5	0.0	5.2	450.1	61.1	1284.0
2608	0.0	15.0	2.4	1.1	0.0	126.4	0.0	0.0	2.7	0.0	3.4
2948	94.0	190.8	0.5	0.5	0.3	1345.1	0.0	4.6	68.0	95.2	0.8
3038	56.7	64.6	27.6	0.0	0.0	458.5	0.0	0.0	138.0	44.9	0.0
3376	2.1	0.0	0.9	0.0	1.0	14.5	0.0	0.0	0.0	0.0	0.0
3388	8.2	3.1	15.5	0.0	3.8	66.5	0.0	0.0	0.6	0.0	0.0
3434	21.7	46.8	52.3	1.8	0.0	381.9	0.0	0.0	134.6	95.5	1.0
3452	2.8	14.8	37.4	0.1	0.0	172.2	0.0	12.0	85.1	40.7	8.3
3454	0.0	33.0	66.0	0.0	0.0	528.9	0.0	0.0	69.9	38.0	5.6
3604	23.6	16.2	11.0	2.2	0.0	238.3	0.0	2.6	60.5	4.6	6.7
3626	0.0	0.0	1.9	0.0	0.0	19.9	0.0	0.0	0.0	0.0	0.0
3672	110.2	77.5	69.5	37.5	7.9	844.0	0.0	0.0	198.8	13.3	11.2
3682	33.4	51.6	5.2	0.2	22.4	227.5	0.0	1.6	0.0	0.0	2.8
3690	4.5	0.0	22.2	3.7	0.0	137.4	0.0	0.0	8.8	2.4	0.0
3780	0.0	2.0	0.7	0.0	0.4	18.3	0.0	0.0	0.0	0.0	0.0
3814	0.7	21.8	18.9	0.1	0.0	160.6	0.0	0.0	39.9	1.8	6.2
3830	40.0	17.6	16.1	0.0	0.0	106.0	0.0	0.0	59.6	2.1	0.4
3884	10.8	0.0	1.5	0.0	0.0	18.7	0.0	0.0	0.0	0.0	0.0
3920	0.0	3.0	5.8	0.1	0.0	120.9	0.0	0.0	7.3	5.4	0.0
4272	0.0	0.0	5.1	2.8	0.3	60.3	0.0	0.0	8.0	0.9	0.0
4316	5.9	1.0	12.6	1.3	0.3	65.5	0.0	0.0	8.2	11.4	0.3
4322	0.0	0.0	8.1	2.2	0.3	74.3	0.0	0.0	9.9	12.2	0.0
4328	53.2	46.6	89.8	59.3	0.0	1159.4	0.0	0.0	29.8	33.3	0.0
4330	2.5	0.0	9.3	0.7	0.0	64.1	0.0	0.0	3.4	0.0	0.0
4336	47.4	10.8	70.5	18.0	0.2	463.2	44.1	0.0	53.0	82.1	0.0
4388	3.6	34.2	4.4	6.4	1.1	209.4	0.0	0.0	0.4	10.5	0.0
4452	0.0	0.4	5.3	0.6	0.0	14.2	0.0	0.0	0.0	0.0	0.0
4492	NA	NA	NA	NA	NA	NA	NA	NA	NA	NA	NA

Table D3.2: Continued

Midas	13	15	16	19	20	21	22	23	24	25	26
4606	0.9	0.0	34.0	5.0	0.0	185.6	0.0	0.0	7.9	4.5	0.0
4608	0.0	1.7	13.6	7.4	0.0	68.3	0.0	0.0	0.3	5.4	0.0
4610	0.0	0.0	4.6	0.2	0.0	14.6	0.0	0.0	0.0	0.0	0.0
4612	0.0	0.0	6.0	0.2	0.0	15.0	0.0	0.0	0.0	0.0	0.0
4614	NA	NA	NA	NA	NA	NA	NA	NA	NA	NA	NA
4618	5.0	0.0	0.2	0.3	0.0	5.1	0.0	0.0	0.0	0.0	0.0
4620	NA	NA	NA	NA	NA	NA	NA	NA	NA	NA	NA
4622	15.2	0.4	38.8	10.8	0.0	377.0	0.0	0.0	20.1	38.9	0.0
4624	0.2	1.3	40.1	8.3	0.0	87.9	0.0	0.0	3.7	3.6	0.0
4628	0.2	0.0	8.3	2.6	0.0	18.6	0.0	0.0	7.2	3.7	0.0
4630	0.0	0.0	17.2	5.2	0.0	104.8	0.0	0.0	0.2	33.2	0.0
4766	130.6	236.7	21.7	118.6	0.0	1997.5	0.0	0.0	145.3	119.0	0.0
4782	48.9	7.3	1.7	5.9	0.0	376.8	0.0	0.0	8.1	0.0	29.1
4788	0.0	0.0	0.3	6.3	0.0	85.7	0.0	0.0	0.2	0.0	0.0
4800	0.0	9.8	11.3	11.6	0.0	55.6	0.0	0.0	3.2	0.0	0.0
4802	NA	NA	NA	NA	NA	NA	NA	NA	NA	NA	NA
4806	0.0	5.3	16.1	4.1	0.0	103.1	20.2	0.0	1.9	2.2	0.0
4822	0.0	3.2	18.8	6.2	0.0	138.3	0.0	0.0	1.9	0.1	0.0
4852	46.7	30.9	70.4	30.8	0.3	504.5	0.0	0.0	17.5	0.0	8.1
4857	1.1	3.2	7.1	4.7	0.0	85.8	0.0	0.0	2.3	0.0	0.0
4894	8.1	10.2	26.7	4.2	0.0	230.2	0.0	0.0	10.1	0.0	0.8
4896	176.9	29.5	22.7	10.5	0.0	480.9	0.0	0.0	0.0	13.8	0.2
5024	0.0	11.9	27.8	0.6	0.0	223.6	0.0	0.0	7.5	6.5	0.0
5172	110.3	60.2	64.8	27.8	0.6	1016.4	0.0	0.0	25.6	20.2	17.8
5174	56.6	25.7	22.2	11.6	0.0	158.9	0.0	0.0	5.8	2.9	1.1
5198	12.0	0.0	0.3	0.0	0.0	39.8	0.0	0.0	0.0	0.0	0.0
5222	10.8	27.7	21.4	0.0	0.0	176.5	0.0	0.0	14.1	4.0	19.8
5236	70.2	164.0	146.8	1.1	0.0	2212.6	0.0	0.0	399.1	47.5	50.9
5240	3.2	6.6	25.1	0.0	0.0	213.7	0.0	0.0	55.6	5.2	0.9
5280	28.8	247.5	19.1	17.2	0.0	1515.4	0.0	0.0	28.2	19.6	0.0
5344	100.8	7.1	28.9	9.3	21.5	1017.6	0.0	0.0	51.3	16.5	101.5
5348	6.2	8.5	3.0	2.8	0.0	180.0	0.0	0.0	21.4	0.7	2.0
5349	11.5	35.6	4.6	13.2	0.0	689.3	0.0	0.0	15.4	0.0	0.6
5352	0.0	3.0	1.3	3.5	0.0	286.9	0.0	0.0	7.7	3.1	0.0
5386	10.2	55.8	22.8	19.9	0.2	148.5	0.0	0.0	2.5	0.0	0.0
5400	72.2	123.0	158.9	59.1	0.0	1839.4	43.4	0.0	24.4	13.9	14.1
5408	1.9	14.7	19.7	19.2	0.7	484.2	0.0	0.0	14.3	0.0	0.2
5416	21.9	57.1	33.3	14.5	1.7	466.5	0.0	0.0	6.3	0.0	0.2
5448	21.1	94.5	135.9	41.6	0.0	1575.8	0.0	0.0	22.7	10.3	18.3
5458	9.0	42.0	15.0	2.0	0.0	208.5	0.0	0.0	35.8	0.0	0.0
5490	NA	NA	NA	NA	NA	NA	NA	NA	NA	NA	NA

Table 3.2: Continued

Midas	13	15	16	19	20	21	22	23	24	25	26
5682	46.4	23.7	19.2	11.8	0.0	214.4	27.9	0.0	1.9	0.9	0.0
5690	8.1	11.2	15.9	14.5	0.0	129.9	0.0	0.0	0.3	0.0	0.0
5710	6.0	9.9	25.1	10.6	0.0	144.3	0.0	0.0	10.3	5.4	0.0
5780	39.1	122.7	247.5	1.1	1.1	2120.9	1.0	0.0	452.8	336.9	50.8
5814	21.3	6.9	20.4	5.4	0.0	447.7	0.0	0.0	60.4	0.6	13.6
9685	13.5	20.5	4.1	0.8	0.0	291.6	0.0	0.0	17.7	3.7	0.0
9931	3.3	10.9	21.9	0.0	0.0	268.1	0.0	0.0	68.4	13.0	77.5
LEA											
5780	39.1	122.7	247.5	1.1	1.1	2120.9	1.0	0.0	452.8	336.9	50.8
3418	1.5	6.3	17.8	0.0	0.0	176.7	0.0	0.0	88.3	18.0	1.1
5780	39.1	122.7	247.5	1.1	1.1	2120.9	1.0	0.0	452.8	336.9	50.8
3130	1.0	6.1	6.3	0.0	0.0	94.1	0.0	0.0	94.6	36.4	1.6
3382	NA	NA	NA	NA	NA	NA	NA	NA	NA	NA	NA
3424	1.2	5.5	7.4	0.0	0.0	75.5	0.0	0.0	23.0	4.8	9.6
3199	5.7	17.6	10.0	0.0	0.0	69.9	0.0	0.0	53.6	0.0	39.4
3134	23.6	116.5	87.4	0.1	0.0	630.5	0.0	0.0	601.2	518.8	43.2
3416	0.2	0.7	36.8	0.1	0.0	183.8	0.0	0.0	133.5	4.1	3.5
9685	13.5	20.5	4.1	0.8	0.0	291.6	0.0	0.0	17.7	3.7	0.0
3420	9.5	9.5	14.0	0.1	0.0	94.7	0.0	0.0	20.3	16.0	1.4
3454	0.0	33.0	66.0	0.0	0.0	528.9	0.0	0.0	69.9	38.0	5.6
5582	2.0	1.4	9.8	0.0	0.0	27.4	0.0	0.0	32.1	35.2	0.1
3134	23.6	116.5	87.4	0.1	0.0	630.5	0.0	0.0	601.2	518.8	43.2
5780	39.1	122.7	247.5	1.1	1.1	2120.9	1.0	0.0	452.8	336.9	50.8
5780	39.1	122.7	247.5	1.1	1.1	2120.9	1.0	0.0	452.8	336.9	50.8
3132	9.7	19.4	8.4	0.0	0.0	311.8	0.0	0.0	111.6	99.7	0.1
3126	0.0	7.2	7.6	0.0	0.0	51.8	0.0	0.0	38.4	33.7	1.2
3234	0.0	7.2	5.8	0.0	0.0	99.4	0.0	0.0	34.9	5.8	0.1
3374	14.4	15.0	12.3	0.0	0.1	296.6	0.0	0.2	84.0	14.3	2.4
3134	23.6	116.5	87.4	0.1	0.0	630.5	0.0	0.0	601.2	518.8	43.2
3452	2.8	14.8	37.4	0.1	0.0	172.2	0.0	12.0	85.1	40.7	8.3
3454	0.0	33.0	66.0	0.0	0.0	528.9	0.0	0.0	69.9	38.0	5.6
3448	5.5	6.6	7.9	0.0	0.0	43.1	0.0	0.0	56.3	5.3	0.0
3232	1.1	2.5	8.7	0.0	0.0	76.6	0.0	0.0	18.6	3.2	6.4
3456	0.0	3.9	23.6	0.3	0.3	185.7	0.0	0.0	130.2	140.0	0.0
5780	39.1	122.7	247.5	1.1	1.1	2120.9	1.0	0.0	452.8	336.9	50.8

Table D4: Road, Direct Watershed, and Lake Areas (ha.). Table of road coverage area, direct watershed area, and lake area in hectares for 2015, DEP, and LEA.

Midas	Road Area, ha	Lake Area, ha	Watershed Area, ha	Midas	Road Area, ha	Lake Area, ha	Watershed Area, ha
2015				954	45.3	2268.8	15601.7
78	23.7	644.4	4493.2	1068	12.8	237.5	1062.3
177	49.7	2755.9	9867.6	1070	56.9	6441.4	17120.5
224	13.3	420.5	1483.4	1078	0.2	2797.3	22131.0
3444	109.9	1761.2	10802.4	1088	9.1	325.6	4689.9
3446	21.5	534.4	2009.2	1150	9.7	5456.0	13431.5
3748	34.7	952.3	3558.2	1210	25.4	361.2	3542.6
3750	42.8	259.4	3772.5	2004	7.8	273.3	1309.8
3796	75.7	799.4	14806.7	2020	63.7	3694.2	20759.1
3838	76.3	371.0	5455.2	2146	38.5	1469.8	5621.1
3916	17.7	349.7	1239.9	2156	27.9	176.8	3255.5
4434	8.5	792.0	2936.5	2242	19.2	202.0	1618.8
4538	6.3	169.2	814.8	2286	114.8	252.6	17207.7
5172	190.4	1068.5	25212.9	2590	176.1	1484.0	26967.5
5190	12.2	313.2	1598.1	2608	9.9	126.4	1591.6
5272	42.8	1033.3	6080.3	2948	NA	1348.3	9635.9
5274	77.1	3434.3	11878.4	3038	22.5	465.3	6978.4
5280	104.7	1636.7	12428.0	3376	2.1	14.5	219.1
5344	47.2	1019.2	5543.1	3388	5.4	66.5	346.2
5348	13.7	180.0	1136.3	3434	60.7	381.9	4063.6
5349	22.3	689.2	1916.4	3452	24.3	172.2	2359.8
5352	18.3	287.0	1077.4	3454	29.9	532.7	2636.4
5400	112.4	1841.2	11496.3	3604	28.1	247.0	3852.2
5408	26.3	484.2	2650.3	3626	3.7	19.8	140.7
5448	69.8	1578.2	8281.9	3672	53.7	844.0	19574.9
DEP				3682	35.3	228.3	6913.7
70	46.9	555.4	4711.7	3690	12.7	137.7	1292.6
80	170.1	1893.8	23731.6	3780	0.9	18.3	78.9
121	145.4	6968.3	69004.6	3814	13.6	160.3	862.7
177	49.7	2755.9	9867.6	3830	18.5	106.0	2305.5
243	11.1	766.7	5450.8	3884	1.3	18.7	85.0
262	11.4	174.2	1449.2	3920	11.9	120.9	999.6
342	15.2	556.4	2025.8	4272	2.0	60.3	262.1
386	4.9	32.6	270.9	4316	35.2	74.3	5048.5
410	1.3	389.4	4481.5	4322	6.3	74.2	677.0
447	0.1	7.4	332.2	4328	53.4	1159.5	7305.3
760	15.7	150.4	1295.5	4330	3.9	64.1	572.3
				4336	46.5	482.1	5825.1

Table D4: Continued

Midas	Road Area, ha	Lake Area, ha	Watershed Area, ha
4388	15.1	209.3	1984.9
4452	3.1	14.2	195.4
4492	12.8	NA	NA
4606	9.0	185.6	752.9
4608	2.0	68.3	481.5
4610	3.0	14.6	108.7
4612	2.7	15.0	336.9
4614	7.2	41.5	448.1
4618	1.0	5.1	72.5
4620	0.7	15.0	109.6
4622	17.6	377.0	1683.1
4624	11.3	87.9	598.6
4628	7.3	18.6	167.1
4630	8.5	104.8	857.0
4766	31.4	2000.3	11164.1
4782	10.4	376.8	2447.9
4788	2.1	85.7	509.2
4800	8.0	55.6	320.3
4802	3.1	58.1	294.3
4806	11.9	103.1	839.1
4822	17.4	138.3	823.6
4852	73.1	514.6	4474.2
4857	6.8	85.7	756.2
4894	17.1	230.2	913.8
4896	70.8	484.7	7431.2
5024	133.8	223.6	1440.1
5172	190.4	1068.5	25212.9
5174	20.6	158.9	1537.0
5198	9.4	39.8	616.5
5222	44.5	176.5	4959.8
5236	107.6	2215.4	10319.9
5240	12.8	214.1	857.3
5280	104.7	1636.7	12428.0
5344	47.2	1019.2	5543.1
5348	13.7	180.0	1136.3
5349	22.3	689.2	1916.4
5352	18.3	287.0	1077.4
5386	25.6	150.4	2885.7
5400	112.4	1841.2	11496.3
5408	26.3	484.2	2650.3

Midas	Road Area, ha	Lake Area, ha	Watershed Area, ha
5416	31.8	466.5	2945.7
5448	69.8	1578.2	8281.9
5458	24.2	208.5	3601.2
5490	2.6	63.8	421.8
5682	87.9	248.9	9696.8
5690	15.7	129.9	1317.7
5710	15.4	144.4	1231.5
5780	161.1	2120.9	15649.9
5814	22.0	447.7	1917.4
9685	17.0	291.6	1227.4
9931	16.6	268.1	1169.6
LEA			
5780	161.1	2120.9	15649.9
3418	19.6	176.7	1193.8
5780	161.1	2120.9	15649.9
3130	9.8	94.2	620.8
3382	5.6	126.4	383.6
3424	11.9	75.5	1241.6
3199	7.1	69.9	776.6
3134	59.2	630.5	5516.3
3416	27.3	183.8	1515.1
9685	17.0	291.6	1227.4
3420	8.4	94.7	712.2
3454	29.9	532.7	2636.4
5582	11.0	27.4	694.8
3134	59.2	630.5	5516.3
5780	161.1	2120.9	15649.9
5780	161.1	2120.9	15649.9
3132	14.0	311.9	1257.0
3126	6.8	51.8	405.1
3234	15.3	99.4	1331.4
3374	8.3	296.5	1318.1
3134	59.2	630.5	5516.3
3452	24.3	172.2	2359.8
3454	29.9	532.7	2636.4
3448	5.7	43.1	717.1
3232	12.4	76.6	1036.0
3456	12.0	185.7	1533.8
5780	161.1	2120.9	15649.9

APPENDIX E: PRECIPITATION DATA

Table E1: Precipitation (precip) data. Reported beginning from both January to the sampling date and May to the sampling date, including the maximum, average, and sum values (inches) over this timeframe.

Midas	Maximum Precip January	Average Precip January	Sum Precip January	Maximum Precip May	Average Precip May	Sum Precip May
2015						
78	1.77	0.06	12.80	1.13	0.08	8.21
177	3.92	0.08	17.41	3.92	0.10	11.02
224	1.37	0.12	29.33	1.35	0.15	17.76
3444	1.30	0.07	14.14	1.30	0.11	9.47
3446	1.30	0.07	14.37	1.30	0.10	9.70
3748	1.30	0.07	16.57	1.30	0.11	11.90
3750	1.30	0.07	14.37	1.30	0.10	9.70
3796	1.30	0.07	14.14	1.30	0.11	9.47
3838	1.19	0.06	14.82	1.19	0.08	8.88
3916	1.19	0.06	14.82	1.19	0.08	8.88
4434	3.92	0.08	17.41	3.92	0.10	11.02
4538	3.92	0.08	17.93	3.92	0.10	11.54
5172	1.77	0.05	10.65	0.94	0.07	6.06
5190	1.65	0.10	20.24	1.30	0.12	12.46
5272	1.65	0.10	20.24	1.30	0.12	12.46
5274	1.65	0.10	20.24	1.30	0.12	12.46
5280	1.65	0.11	20.24	1.30	0.13	12.46
5344	1.65	0.11	20.24	1.30	0.13	12.46
5348	1.65	0.11	20.17	1.30	0.13	12.39
5349	1.65	0.10	20.24	1.30	0.12	12.46
5352	1.65	0.11	20.24	1.30	0.13	12.46
5400	1.65	0.11	22.42	1.49	0.13	14.66
5408	1.77	0.05	9.71	0.74	0.06	5.12
5448	1.77	0.05	9.71	0.74	0.06	5.12
DEP						
70	1.50	0.08	18.18	0.77	0.07	7.25
80	2.12	0.14	27.91	1.71	0.14	14.60
121	1.38	0.15	29.77	1.26	0.18	19.17
177	1.48	0.06	15.23	1.48	0.08	11.19
243	2.99	0.14	29.49	2.99	0.15	18.08
262	1.67	0.10	24.34	1.67	0.10	12.12
342	2.70	0.14	34.61	2.70	0.16	19.89
386	1.54	0.13	31.64	1.54	0.15	16.92
410	2.70	0.14	34.61	2.70	0.16	19.89
447	2.64	0.12	31.46	2.64	0.15	22.50
760	1.67	0.10	24.34	1.67	0.10	12.12

Table E1: Continued

Midas	Maximum Precip January	Average Precip January	Sum Precip January	Maximum Precip May	Average Precip May	Sum Precip May
954	1.79	0.12	23.04	1.79	0.13	12.96
1068	1.38	0.15	29.77	1.26	0.18	19.17
1070	1.38	0.15	29.77	1.26	0.18	19.17
1078	1.38	0.16	29.77	1.26	0.18	19.17
1088	1.38	0.16	29.77	1.26	0.18	19.17
1150	2.40	0.13	27.27	2.40	0.13	17.19
1210	1.48	0.05	12.39	1.48	0.07	8.35
2004	1.79	0.12	23.04	1.79	0.13	12.96
2020	1.46	0.13	24.82	1.08	0.13	13.41
2146	1.46	0.13	24.98	1.08	0.13	13.57
2156	2.12	0.14	27.91	1.71	0.14	14.60
2242	1.46	0.13	24.98	1.08	0.13	13.57
2286	2.04	0.11	22.78	0.96	0.09	10.20
2590	1.54	0.07	17.24	1.21	0.07	8.33
2608	1.54	0.07	17.24	1.21	0.07	8.33
2948	1.67	0.10	24.34	1.67	0.10	12.12
3038	1.46	0.13	26.35	1.08	0.13	14.94
3376	1.89	0.13	30.26	1.61	0.12	13.71
3388	2.92	0.09	22.21	1.27	0.08	10.03
3434	2.92	0.09	21.09	1.27	0.07	8.91
3452	3.15	0.13	30.48	3.15	0.10	12.67
3454	1.89	0.13	29.19	1.61	0.12	12.64
3604	1.91	0.09	20.63	1.91	0.10	11.35
3626	2.92	0.09	21.09	1.27	0.07	8.91
3672	1.50	0.08	18.32	0.77	0.07	7.39
3682	1.50	0.08	18.32	0.77	0.07	7.39
3690	2.92	0.09	21.09	1.27	0.07	8.91
3780	2.10	0.09	20.08	0.99	0.08	8.58
3814	1.91	0.09	21.04	1.91	0.10	11.76
3830	2.46	0.10	24.20	1.23	0.08	9.88
3884	2.87	0.13	31.31	2.30	0.09	11.40
3916	3.66	0.12	27.53	2.12	0.07	8.11
3920	3.66	0.12	27.53	2.12	0.07	8.11
4272	2.12	0.13	24.15	1.39	0.12	10.84
4316	2.04	0.12	21.64	0.73	0.10	9.06
4322	2.04	0.11	21.69	0.73	0.09	9.11
4328	1.48	0.05	11.98	1.48	0.07	7.94
4330	1.48	0.05	11.98	1.48	0.07	7.94
4336	1.48	0.05	11.98	1.48	0.07	7.94

Table E1: Continued

Midas	Maximum Precip January	Average Precip January	Sum Precip January	Maximum Precip May	Average Precip May	Sum Precip May
4388	1.02	0.05	11.20	1.02	0.06	6.19
4452	2.64	0.12	31.31	2.64	0.16	22.35
4492	2.04	0.11	22.67	0.96	0.10	10.09
4606	2.64	0.12	31.31	2.64	0.16	22.35
4608	2.64	0.12	31.31	2.64	0.16	22.35
4610	2.64	0.12	31.31	2.64	0.16	22.35
4612	2.64	0.12	31.31	2.64	0.16	22.35
4614	2.64	0.12	30.87	2.64	0.16	21.91
4618	2.64	0.12	31.31	2.64	0.16	22.35
4620	2.64	0.12	30.87	2.64	0.16	21.91
4622	2.64	0.12	31.31	2.64	0.16	22.35
4624	2.64	0.12	30.87	2.64	0.16	21.91
4628	2.64	0.12	30.87	2.64	0.16	21.91
4630	2.64	0.12	30.87	2.64	0.16	21.91
4766	2.04	0.11	22.67	0.96	0.10	10.09
4782	2.12	0.15	31.03	1.97	0.15	17.72
4788	2.04	0.11	22.67	0.96	0.10	10.09
4800	2.26	0.08	20.12	2.26	0.08	9.49
4802	0.91	0.07	15.11	0.89	0.06	6.28
4806	0.91	0.07	15.11	0.89	0.06	6.28
4822	0.91	0.07	15.11	0.89	0.06	6.28
4852	0.91	0.07	15.11	0.89	0.06	6.28
4857	2.20	0.07	17.69	1.85	0.06	7.06
4894	0.91	0.07	15.91	0.89	0.07	7.08
4896	1.54	0.07	17.24	1.21	0.07	8.33
5024	9.90	0.14	32.89	1.49	0.09	11.55
5172	1.50	0.08	18.32	0.77	0.07	7.39
5174	1.50	0.08	18.32	0.77	0.07	7.39
5198	1.54	0.07	16.40	1.21	0.07	7.49
5222	3.13	0.13	33.46	1.24	0.12	15.88
5236	2.46	0.09	21.51	0.95	0.06	7.19
5240	2.46	0.09	22.42	0.95	0.06	8.10
5280	1.91	0.09	19.13	1.91	0.10	9.85
5344	1.91	0.09	21.04	1.91	0.10	11.76
5348	1.91	0.09	21.04	1.91	0.10	11.76
5349	1.91	0.09	21.04	1.91	0.10	11.76
5352	2.46	0.10	21.31	0.95	0.07	6.99
5386	2.46	0.09	22.42	0.95	0.07	8.10
5400	3.34	0.12	29.51	2.51	0.13	15.86
5408	1.54	0.07	17.24	1.21	0.07	8.33

Table E1: Continued

Midas	Maximum Precip January	Average Precip January	Sum Precip January	Maximum Precip May	Average Precip May	Sum Precip May
5416	1.54	0.07	17.24	1.21	0.07	8.33
5448	1.54	0.07	17.24	1.21	0.07	8.33
5458	1.54	0.07	17.24	1.21	0.07	8.33
5490	2.12	0.14	25.19	1.39	0.13	11.88
5682	2.26	0.08	20.12	2.26	0.08	9.49
5690	0.91	0.07	15.91	0.89	0.07	7.08
5710	3.13	0.13	30.27	1.24	0.12	12.69
5780	4.63	0.14	34.91	4.63	0.15	18.36
5814	1.91	0.09	20.63	1.91	0.10	11.35
9685	1.89	0.13	29.19	1.61	0.12	12.64
9931	2.46	0.09	22.42	0.95	0.07	8.10
LEA						
5780	1.05	0.10	19.01	1.05	0.17	11.99
3418	1.05	0.08	14.22	1.05	0.15	7.20
5780	1.05	0.10	19.01	1.05	0.17	11.99
3130	1.05	0.10	19.25	1.05	0.15	12.23
3382	1.05	0.09	18.04	1.05	0.16	11.02
3424	1.05	0.09	17.38	1.05	0.16	10.36
3199	1.05	0.10	19.02	1.05	0.16	12.00
3134	1.05	0.09	15.39	1.05	0.14	8.37
3416	1.05	0.08	14.22	1.05	0.15	7.20
9685	1.05	0.10	19.01	1.05	0.17	11.99
3420	1.05	0.10	19.18	1.05	0.16	12.16
3454	1.05	0.09	16.90	1.05	0.16	9.88
5582	2.15	0.11	25.65	2.15	0.16	18.63
3134	1.05	0.09	15.39	1.05	0.14	8.37
5780	1.05	0.10	19.01	1.05	0.17	11.99
5780	1.05	0.10	19.01	1.05	0.17	11.99
3132	1.05	0.10	19.25	1.05	0.15	12.23
3126	1.05	0.10	19.25	1.05	0.15	12.23
3234	1.05	0.09	16.90	1.05	0.16	9.88
3374	1.89	0.14	24.90	1.61	0.15	8.35
3134	1.05	0.09	15.39	1.05	0.14	8.37
3452	2.04	0.10	21.68	2.04	0.16	14.66
3454	1.05	0.09	16.90	1.05	0.16	9.88
3448	2.04	0.10	21.71	2.04	0.16	14.69
3232	1.05	0.10	19.02	1.05	0.16	12.00
3456	2.15	0.11	28.25	2.15	0.16	21.23
5780	1.05	0.10	19.01	1.05	0.17	11.99

APPENDIX F: FIELD MAPS AND LOCATION

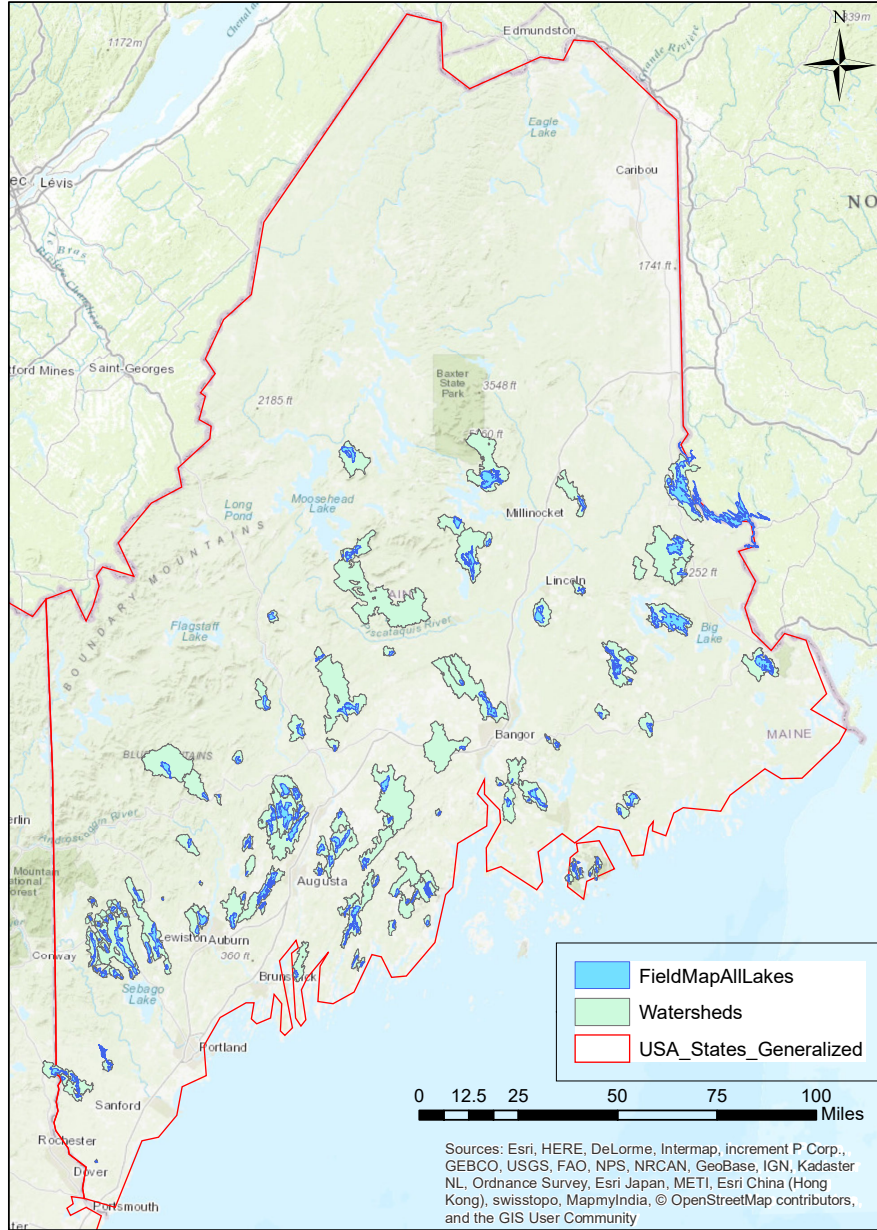


Figure F1: Map of All Study Sites (2015 + DEP + LEA).

Table F1: Latitude and Longitude of Sample Sites.

Midas	Latitude	Longitude	Midas	Latitude	Longitude
2015			5664	NA	NA
78	44.93002	-69.94942	5666	NA	NA
177	45.07812	-67.39989	5812	NA	NA
224	45.00000	-70.00000	5814	NA	NA
3444	44.08828	-70.49226	DEP		
3446	44.02313	-70.51890	70	44.82877	-69.76435
3748	44.15484	-70.24572	80	44.93207	-68.79489
3750	44.10937	-70.27902	121	45.66648	-67.70291
3796	44.15569	-70.10254	177	45.07812	-67.39989
3838	43.51829	-70.86478	243	45.59662	-68.95802
3916	43.56730	-70.88877	262	45.10805	-69.65791
4434	44.59309	-68.06811	342	45.47348	-69.52521
4538	44.78949	-68.45292	386	45.47587	-69.55603
5172	44.63267	-69.33733	410	45.49611	-69.49409
5190	44.72568	-70.08022	447	44.29894	-68.25668
5272	44.53087	-69.86854	760	45.12637	-69.29940
5274	44.54562	-69.85496	954	45.46331	-68.88313
5280	44.48882	-69.78232	1068	45.74734	-67.85553
5344	44.62965	-69.83641	1070	45.67799	-67.80356
5348	44.56619	-69.76167	1078	45.50793	-67.83540
5349	44.61267	-69.77957	1088	45.40693	-67.79702
5352	44.52060	-69.78636	1150	45.23427	-67.79879
5400	44.17599	-69.47588	1210	44.85740	-67.98280
5408	44.40474	-69.65847	2004	45.52415	-68.80660
5448	44.43288	-69.56964	2020	45.77675	-68.81272
2016			2146	45.28556	-68.52398
3688	NA	NA	2156	45.01694	-68.93648
3760	NA	NA	2242	45.34826	-68.31377
3762	NA	NA	2286	44.78071	-68.93905
3824	NA	NA	2590	44.91318	-69.54601
3826	NA	NA	2608	44.77748	-69.58460
4346	NA	NA	2948	45.86571	-69.54524
4406	NA	NA	3038	45.65983	-68.30424
4444	NA	NA	3376	43.93071	-70.65781
4446	NA	NA	3388	43.99273	-70.51502
4448	NA	NA	3434	44.21469	-70.57212
5182	NA	NA	3452	44.12538	-70.67132
5184	NA	NA	3454	44.07050	-70.73411
5186	NA	NA	3604	44.42017	-70.32136
5330	NA	NA	3626	44.28232	-70.26900

Table F1: Continued

Midas	Latitude	Longitude
3672	44.69500	-70.45172
3682	44.59583	-70.24938
3690	43.96946	-70.42401
3780	44.21894	-70.45704
3814	44.23103	-70.04435
3830	44.32020	-70.02988
3884	43.25595	-70.76232
3920	43.55762	-70.93620
4272	44.81475	-68.49757
4316	44.65675	-68.68365
4322	44.64470	-68.74536
4328	44.61419	-68.57198
4330	44.58874	-68.59670
4336	44.57581	-68.69672
4388	44.55192	-68.13376
4452	44.34430	-68.23855
4492	44.89641	-68.22517
4606	44.35513	-68.25176
4608	44.33324	-68.25525
4610	44.30990	-68.28992
4612	44.32108	-68.28691
4614	44.35924	-68.34562
4618	44.36727	-68.36428
4620	44.35327	-68.37781
4622	44.31439	-68.35458
4624	44.32178	-68.33580
4628	44.32342	-68.39736
4630	44.30321	-68.39634
4766	45.05844	-68.13756
4782	45.10444	-68.07240
4788	45.02014	-68.06924
4800	44.21615	-69.21109
4802	44.22625	-69.18520
4806	44.24334	-69.17352
4822	44.14192	-69.11361
4852	44.24426	-69.11061
4857	43.98933	-69.44760
4894	44.29221	-69.36783
4896	44.35873	-69.43467
5024	43.59641	-70.70685
5172	44.63267	-69.33733

Midas	Latitude	Longitude
5174	44.51508	-69.30497
5198	44.59711	-70.17640
5222	43.95073	-69.77071
5236	44.25087	-69.94375
5240	44.19493	-69.95101
5280	44.48883	-69.78232
5344	44.62965	-69.83641
5348	44.56619	-69.76167
5349	44.61267	-69.77957
5352	44.52060	-69.78636
5386	44.18584	-69.52181
5400	44.17599	-69.47588
5408	44.40474	-69.65847
5416	44.36676	-69.60731
5448	44.43288	-69.56964
5458	44.53130	-69.56234
5490	44.54176	-69.05426
5682	44.25629	-69.26632
5690	44.13116	-69.28700
5710	44.01432	-69.46965
5780	44.08275	-70.68175
5814	44.43398	-70.03114
9685	43.95480	-70.59010
9931	44.32389	-69.65798
LEA		
5780	44.06975	-70.66750
3418	44.18403	-70.67667
5780	44.02114	-70.64778
3130	43.95325	-70.76694
3382	43.93469	-70.60722
3424	44.13481	-70.73528
3199	44.21000	-70.81417
3134	44.06583	-70.81028
3416	44.17519	-70.71083
9685	43.95642	-70.59083
3420	44.15308	-70.71778
3454	44.09300	-70.74472
5582	44.06584	-70.77170
3134	44.05014	-70.79889
5780	44.08636	-70.68500
5780	43.98719	-70.61750

Table F1: Continued

Midas	Latitude	Longitude
3132	43.94147	-70.74667
3126	43.95422	-70.78556
3234	44.11925	70.77667
3374	43.94061	-70.69417
3134	44.00056	-70.79556

Midas	Latitude	Longitude
3452	44.12367	-70.67361
3454	44.06886	70.73333
3448	44.15933	-70.64250
3232	44.14508	-70.82111
3456	44.03353	-70.73500
5780	44.08636	-70.68500

Figure F2: The Land cover Type for the 2015 Study Sites.

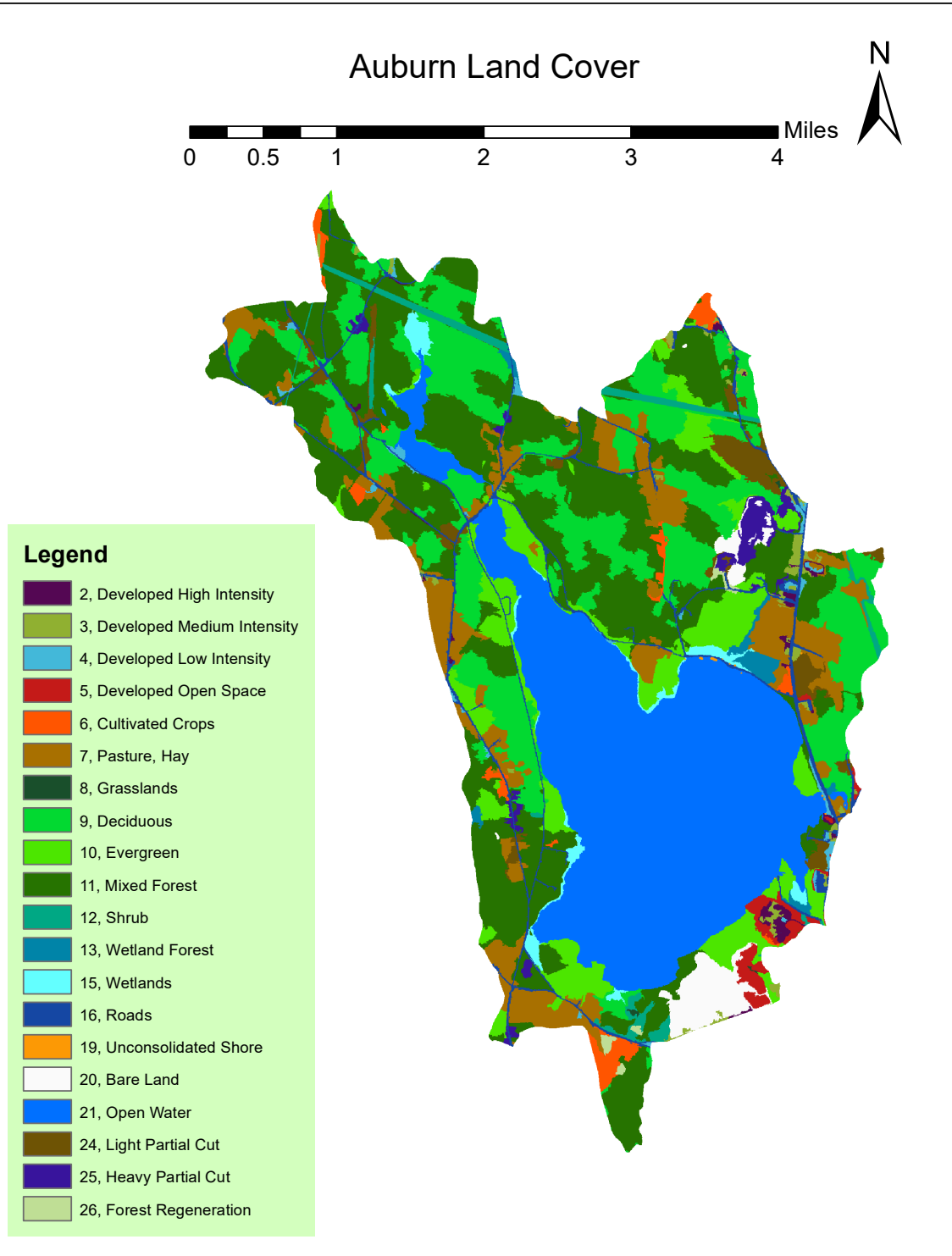


Figure F2: Continued

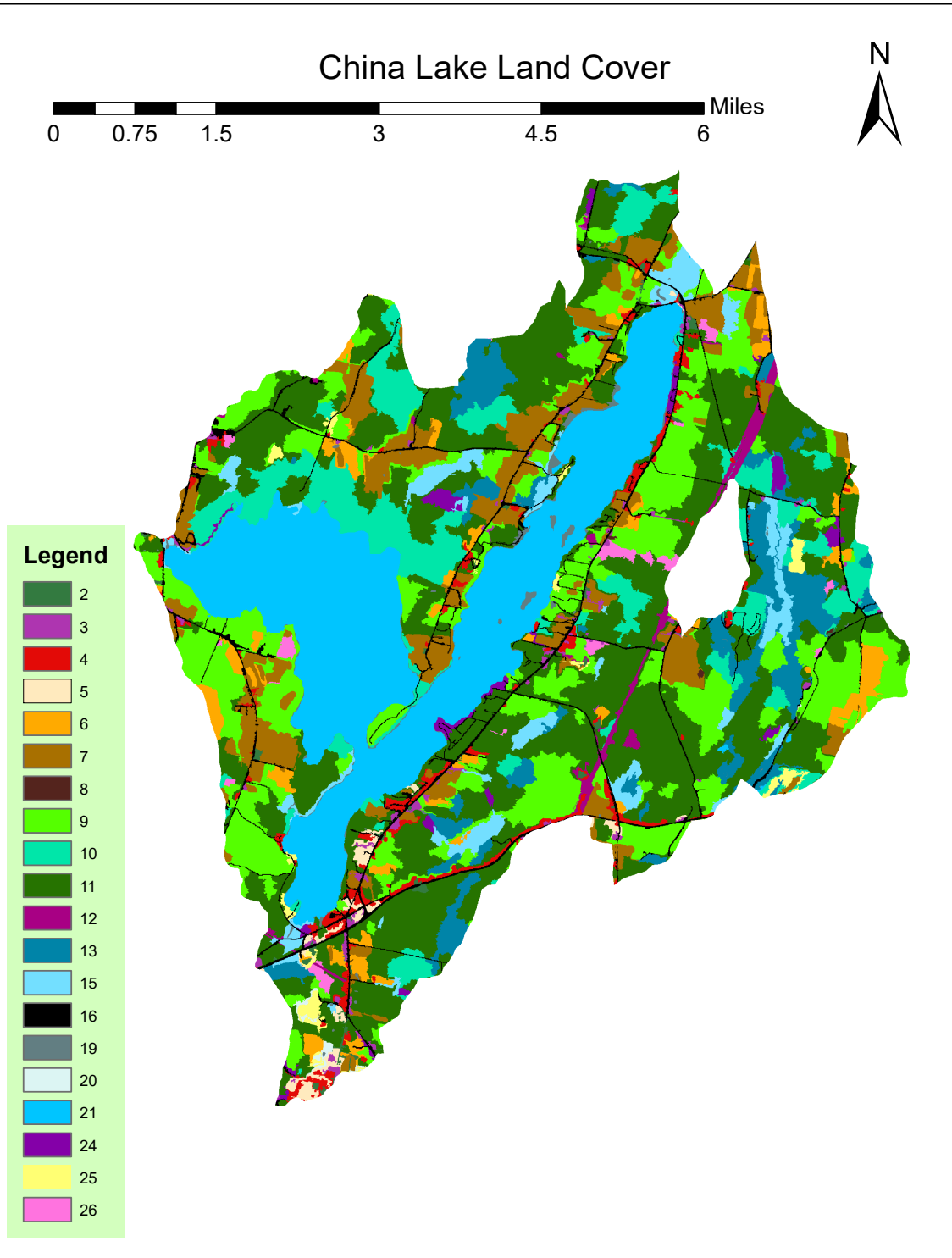


Figure F2: Continued

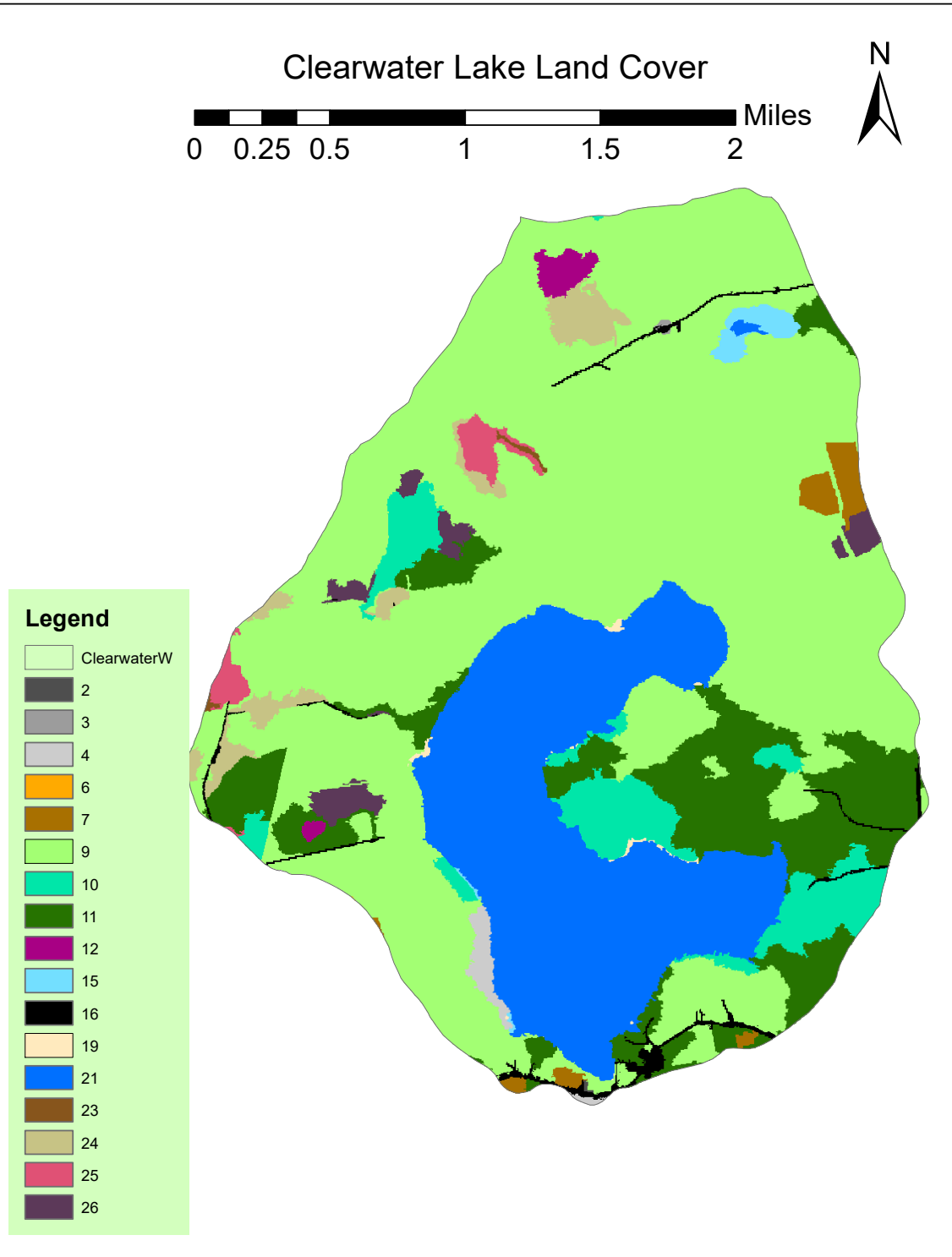


Figure F2: Continued

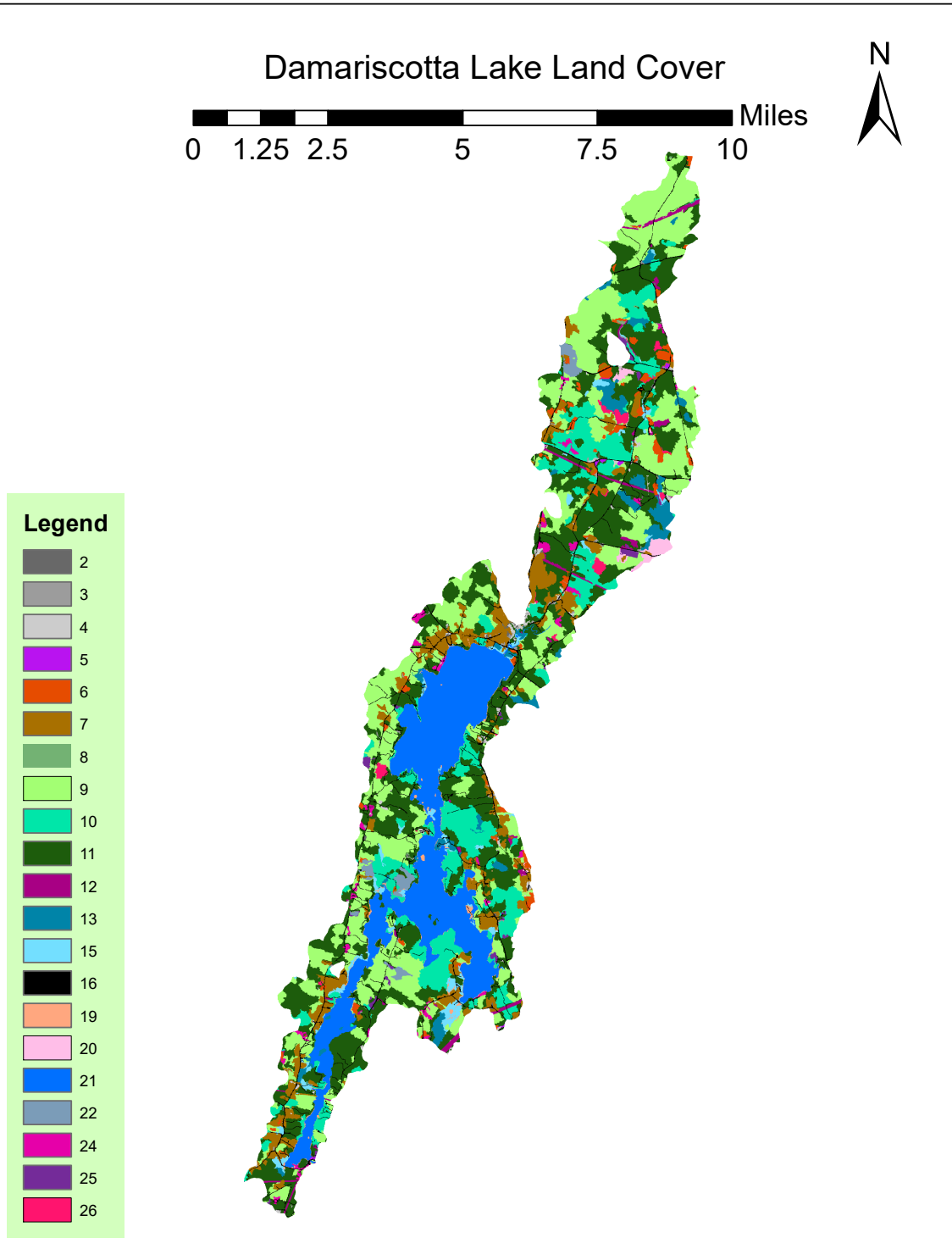


Figure F2: Continued

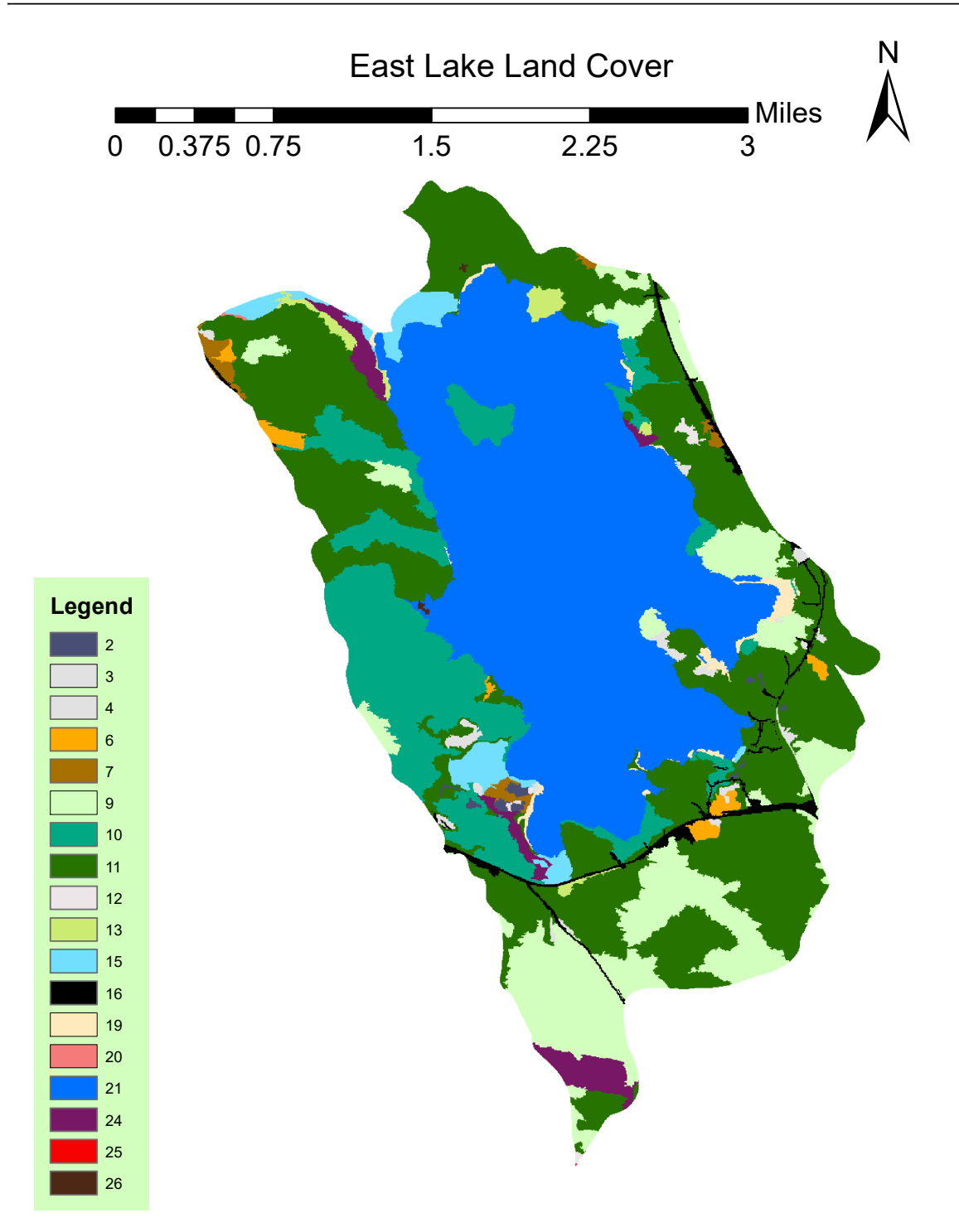


Figure F2: Continued

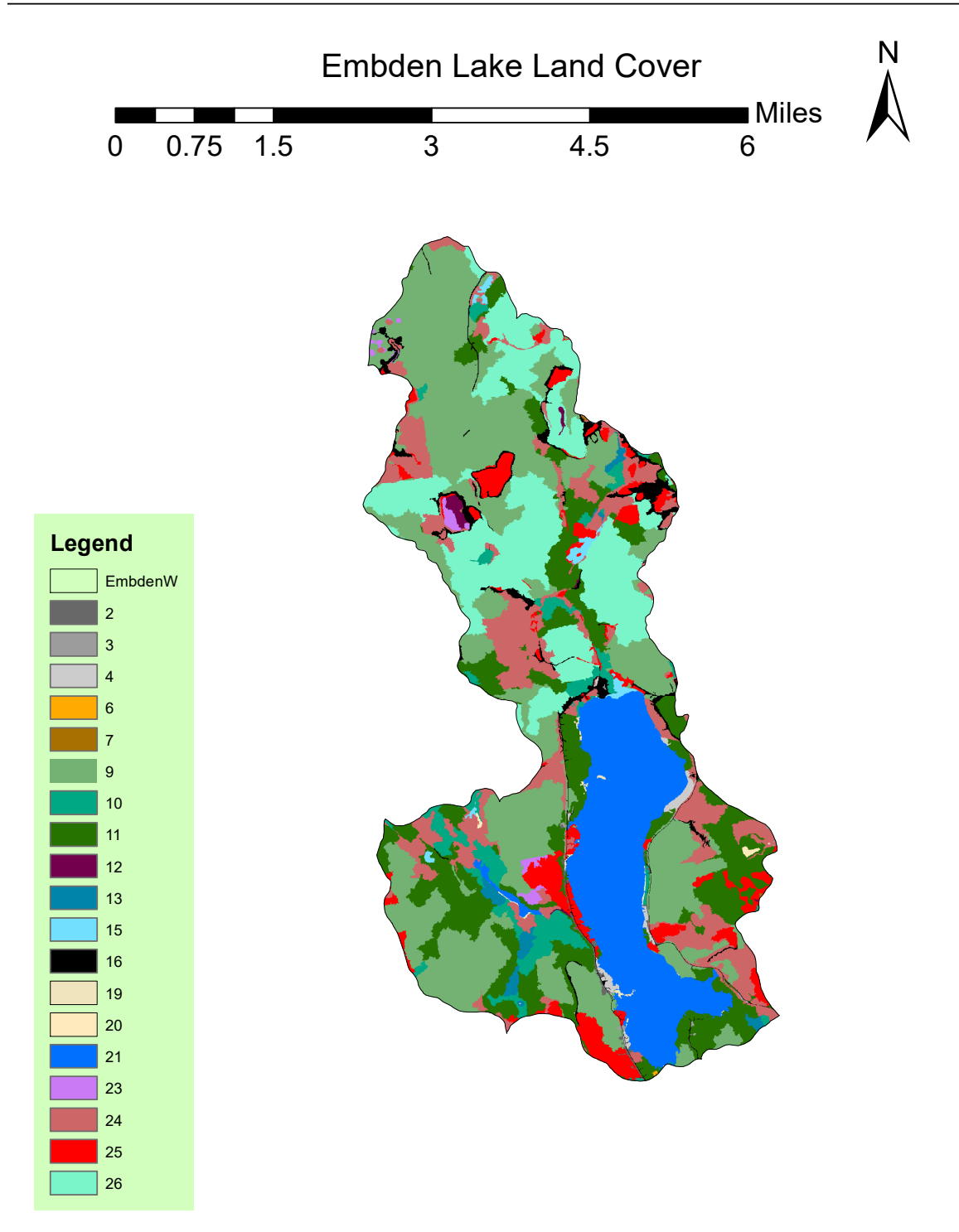


Figure F2: Continued

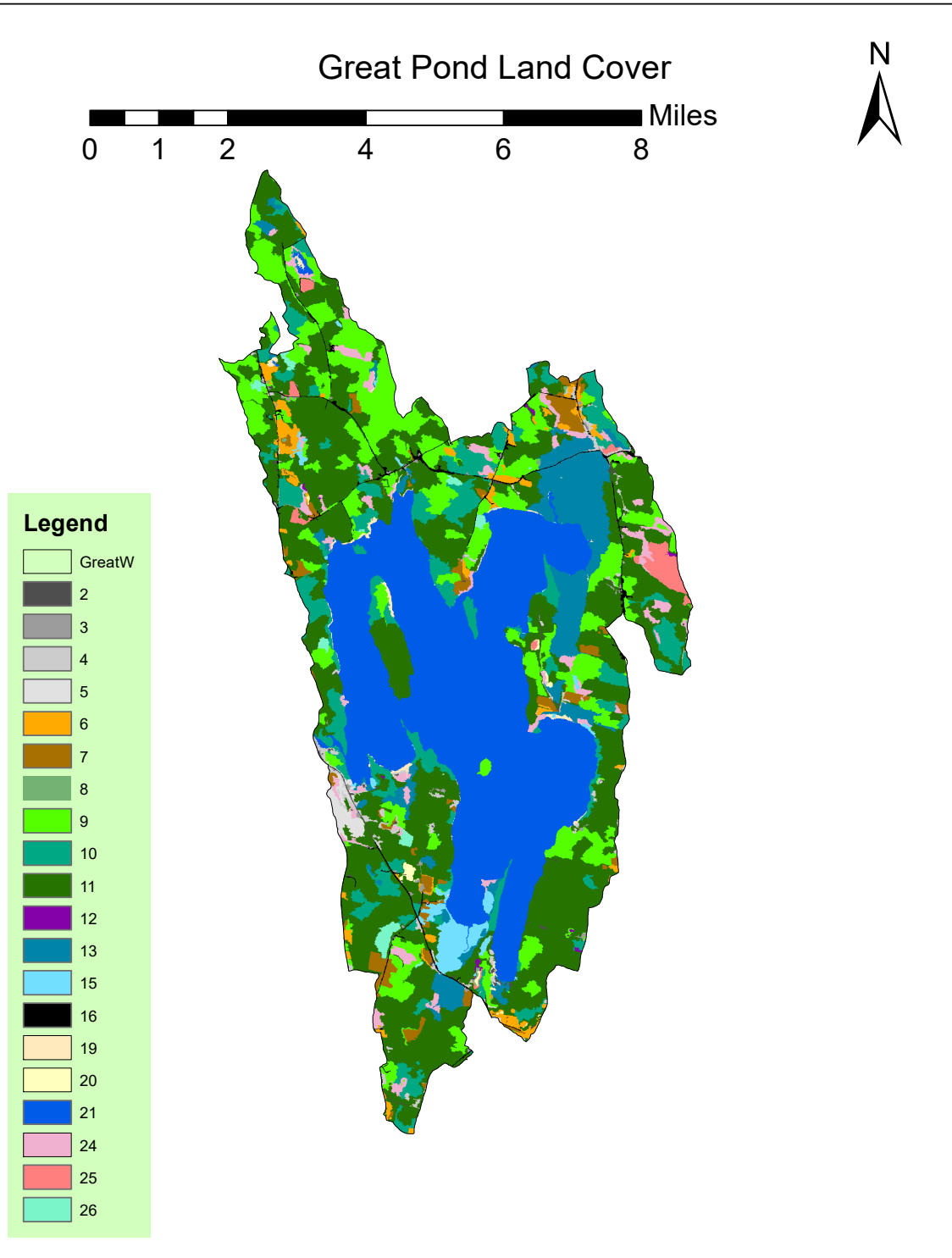


Figure F2: Continued

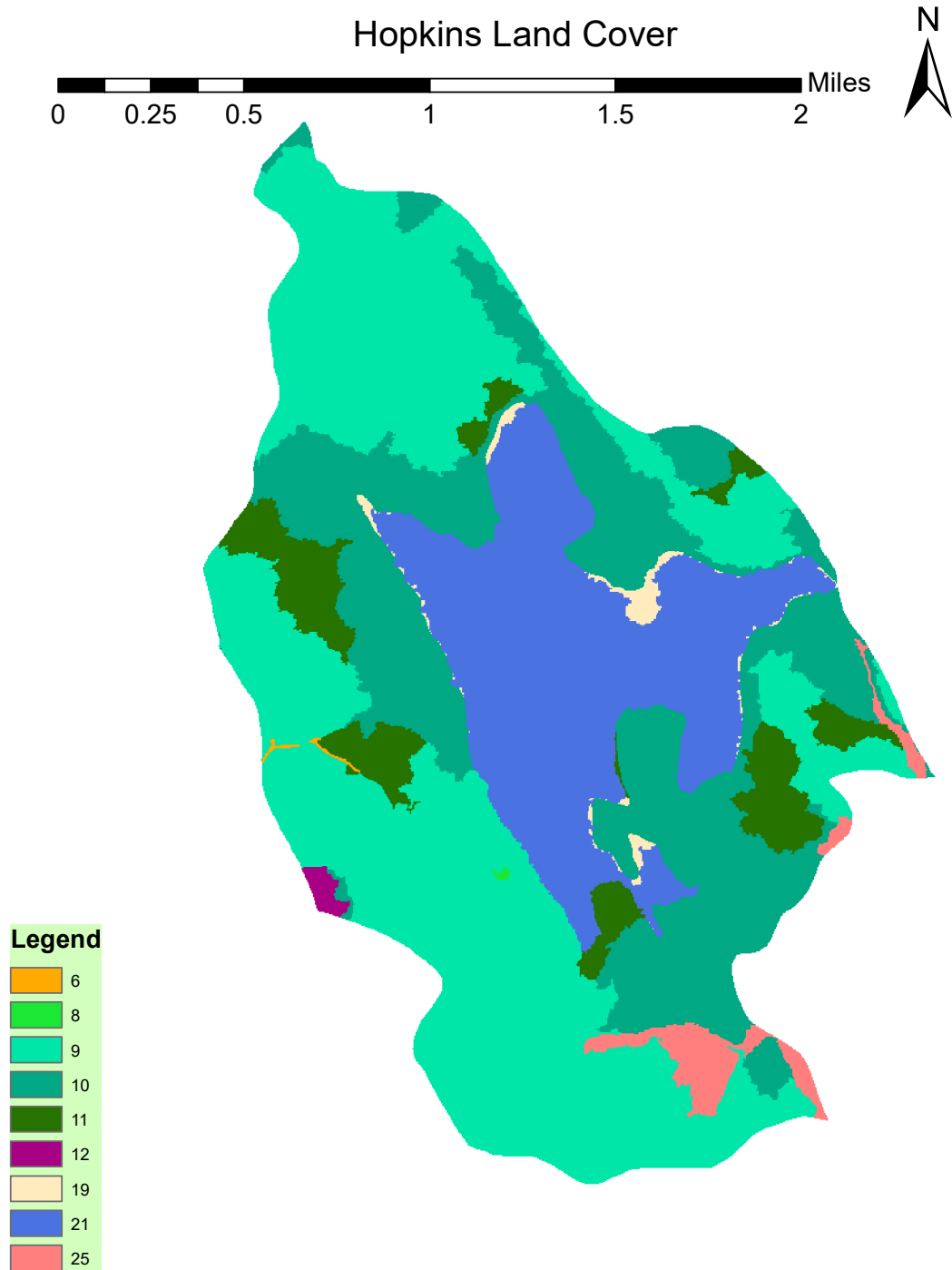


Figure F2: Continued

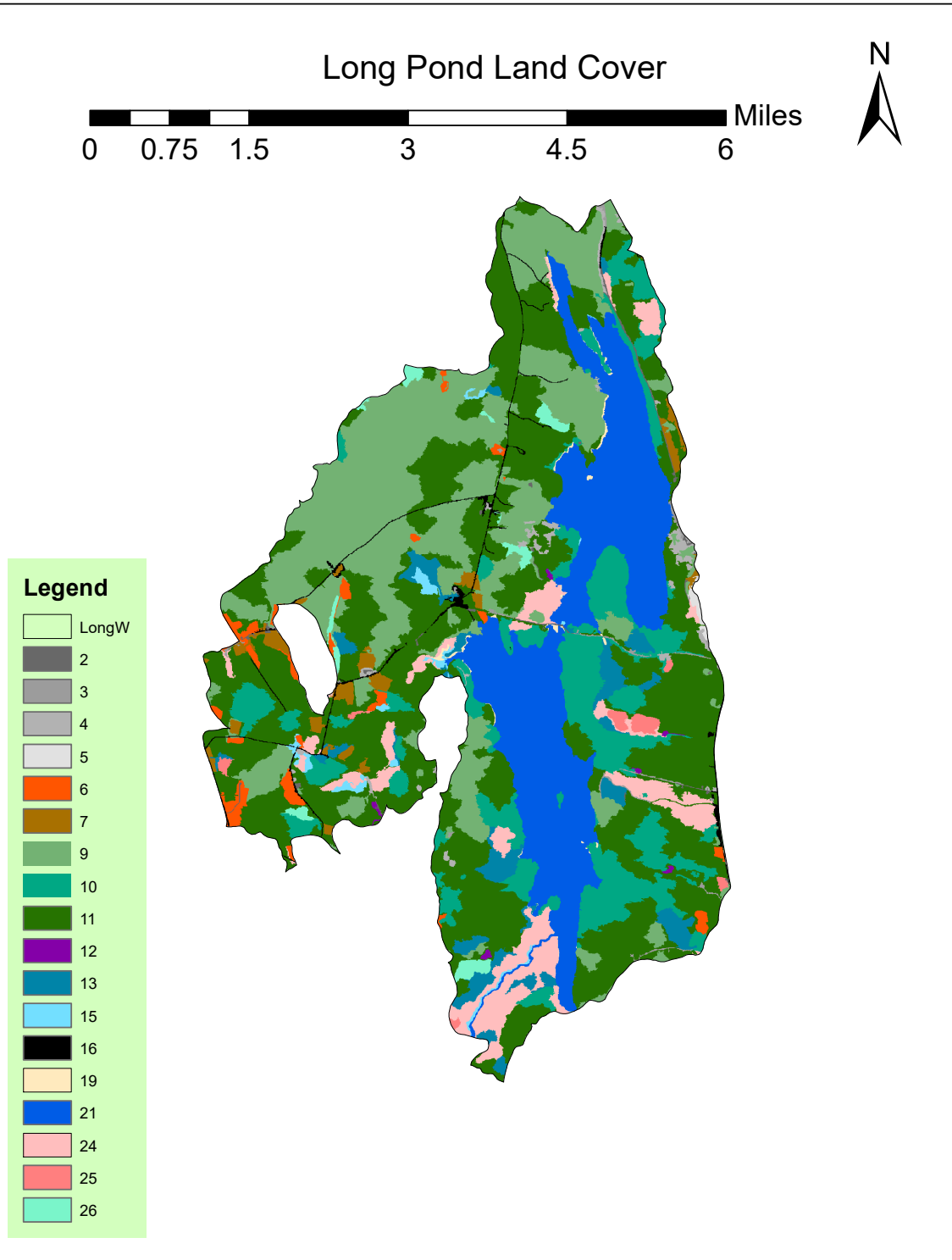


Figure F2: Continued

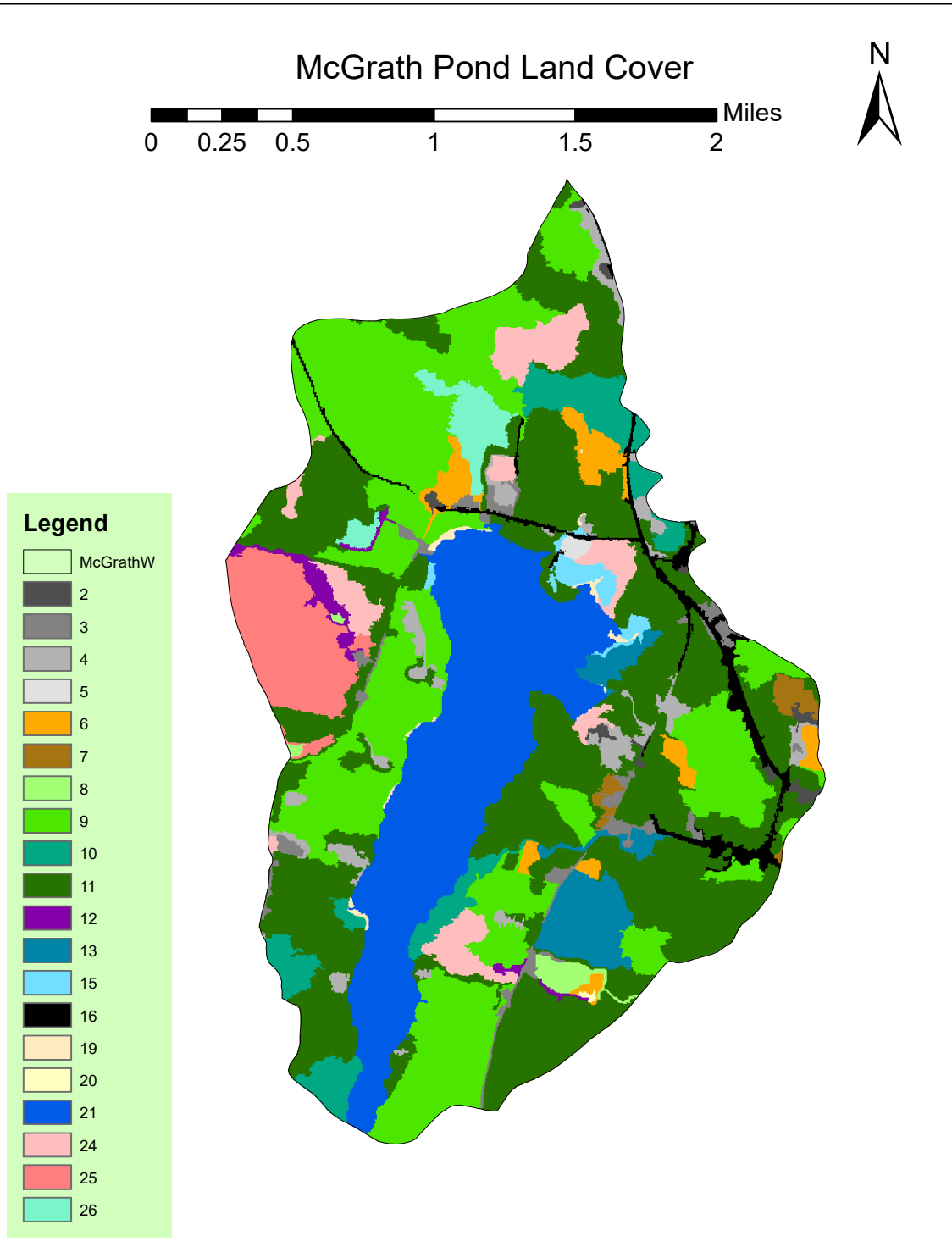


Figure F2: Continued

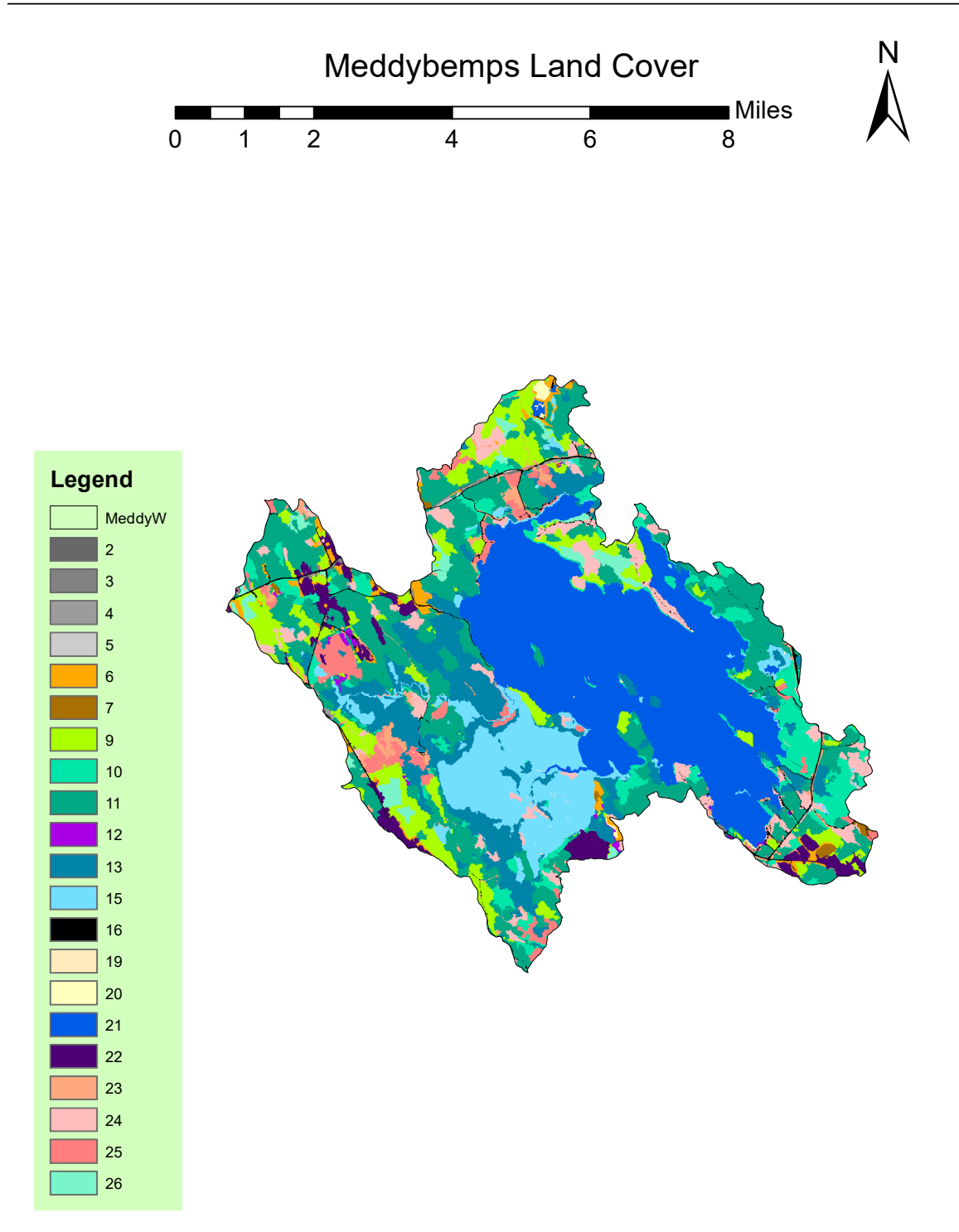


Figure F2: Continued

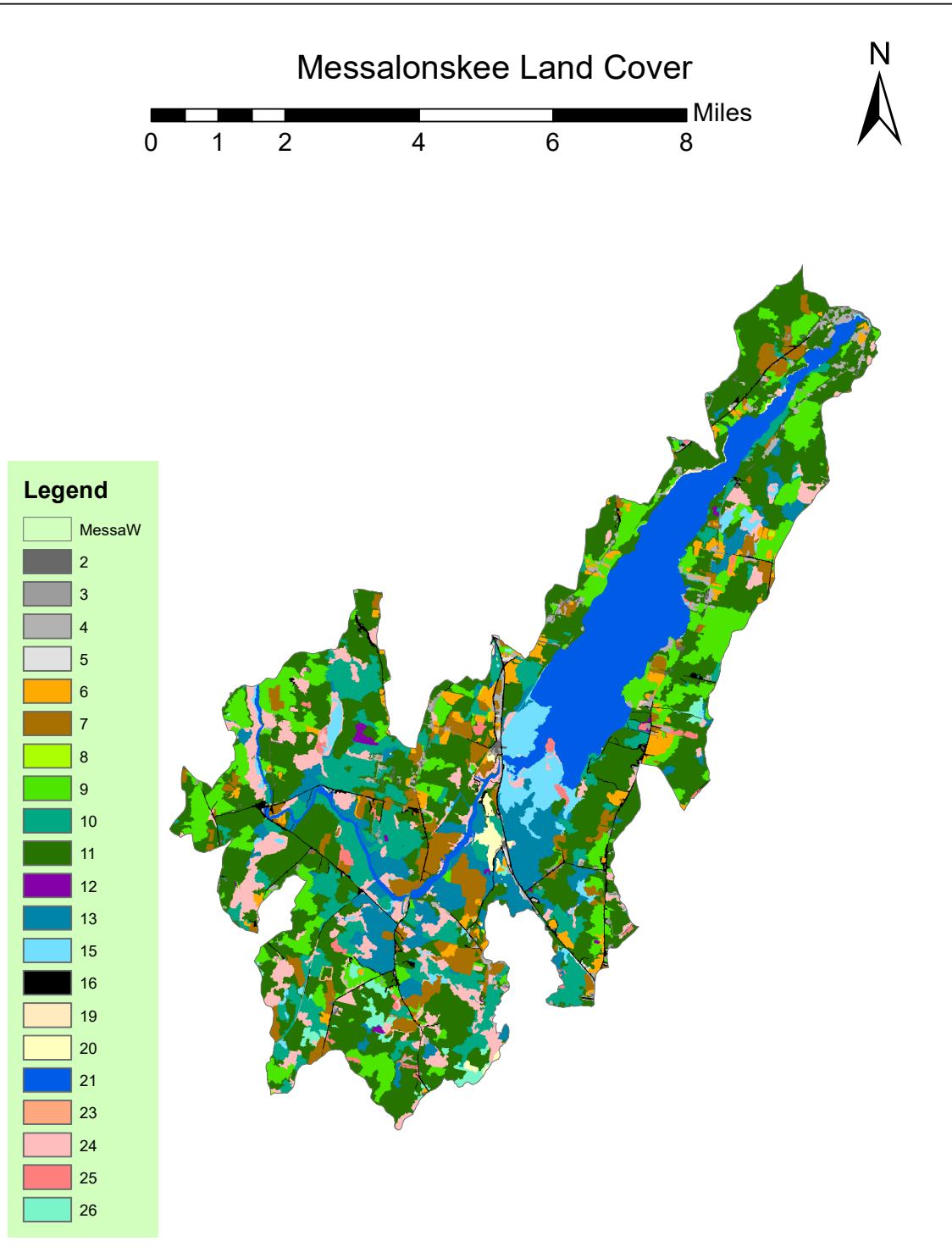


Figure F2: Continued

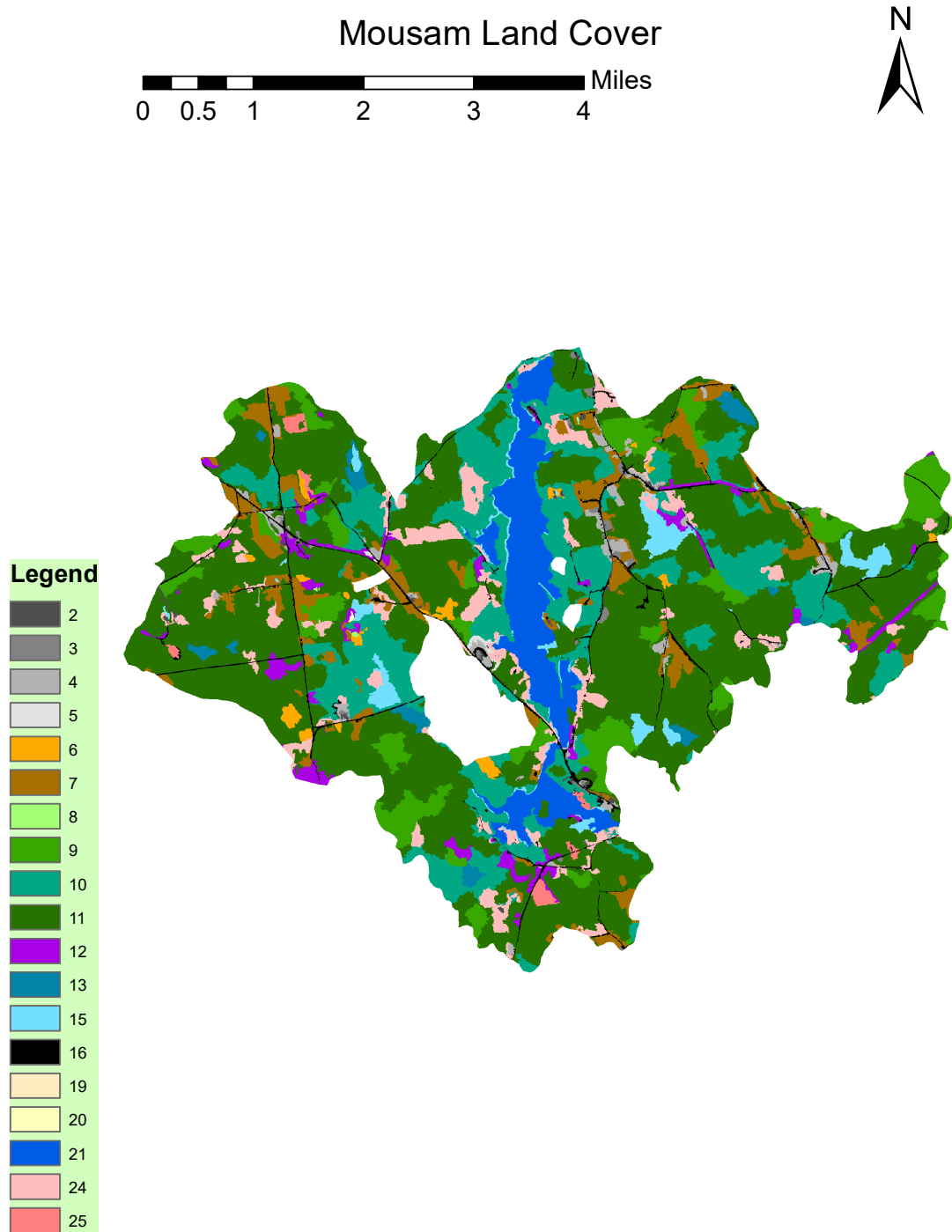


Figure F2: Continued

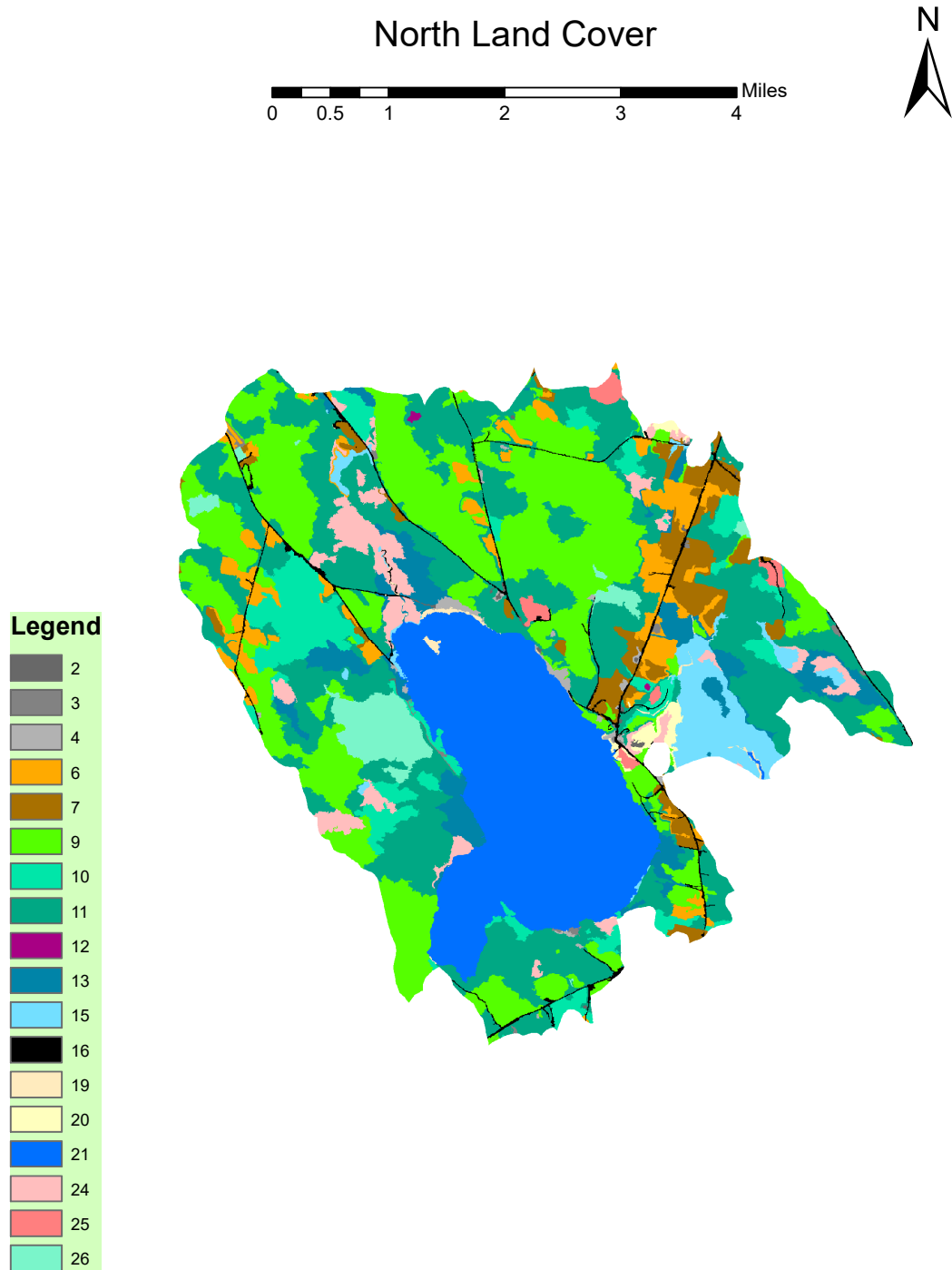


Figure F2: Continued

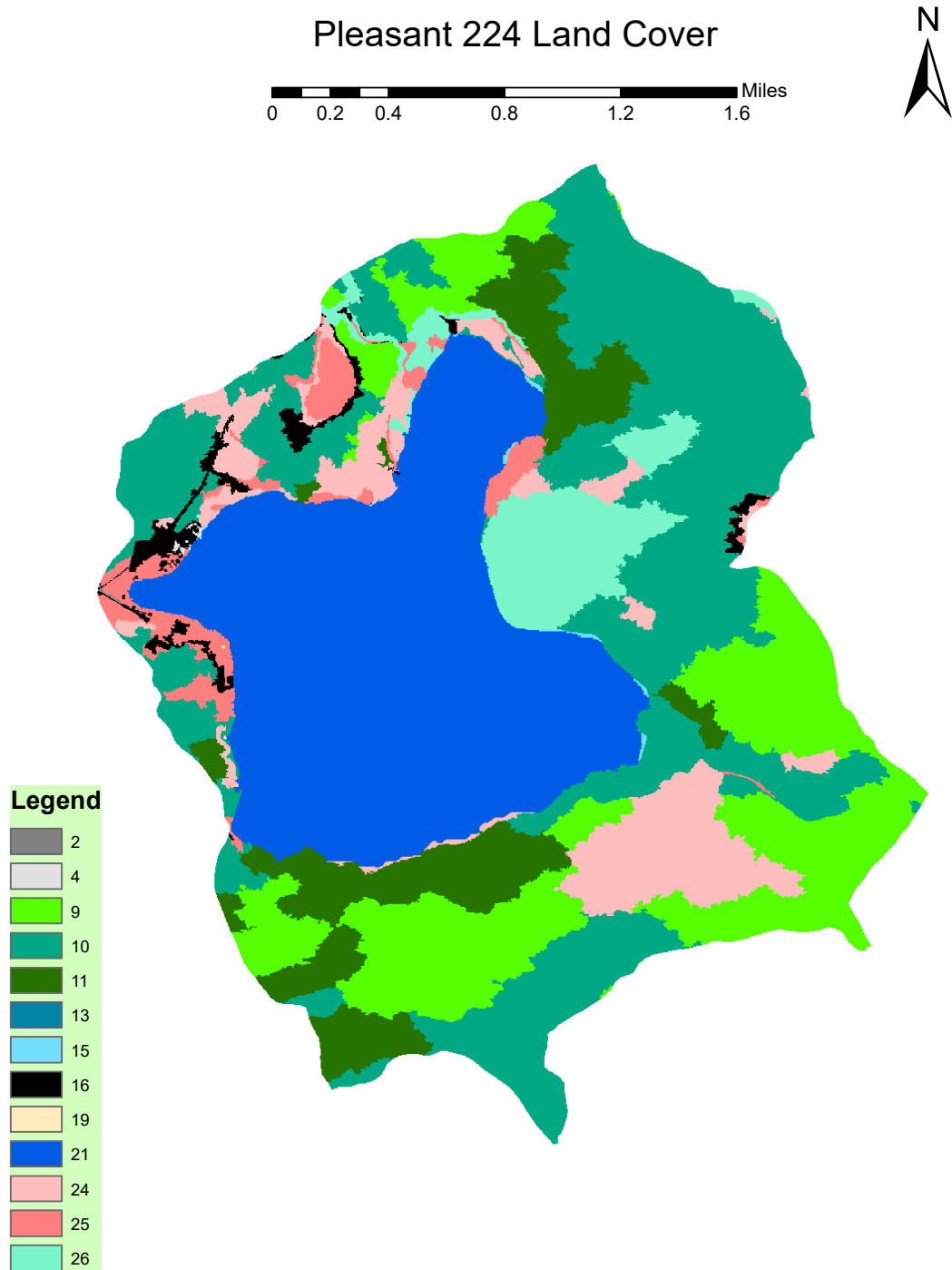


Figure F2: Continued

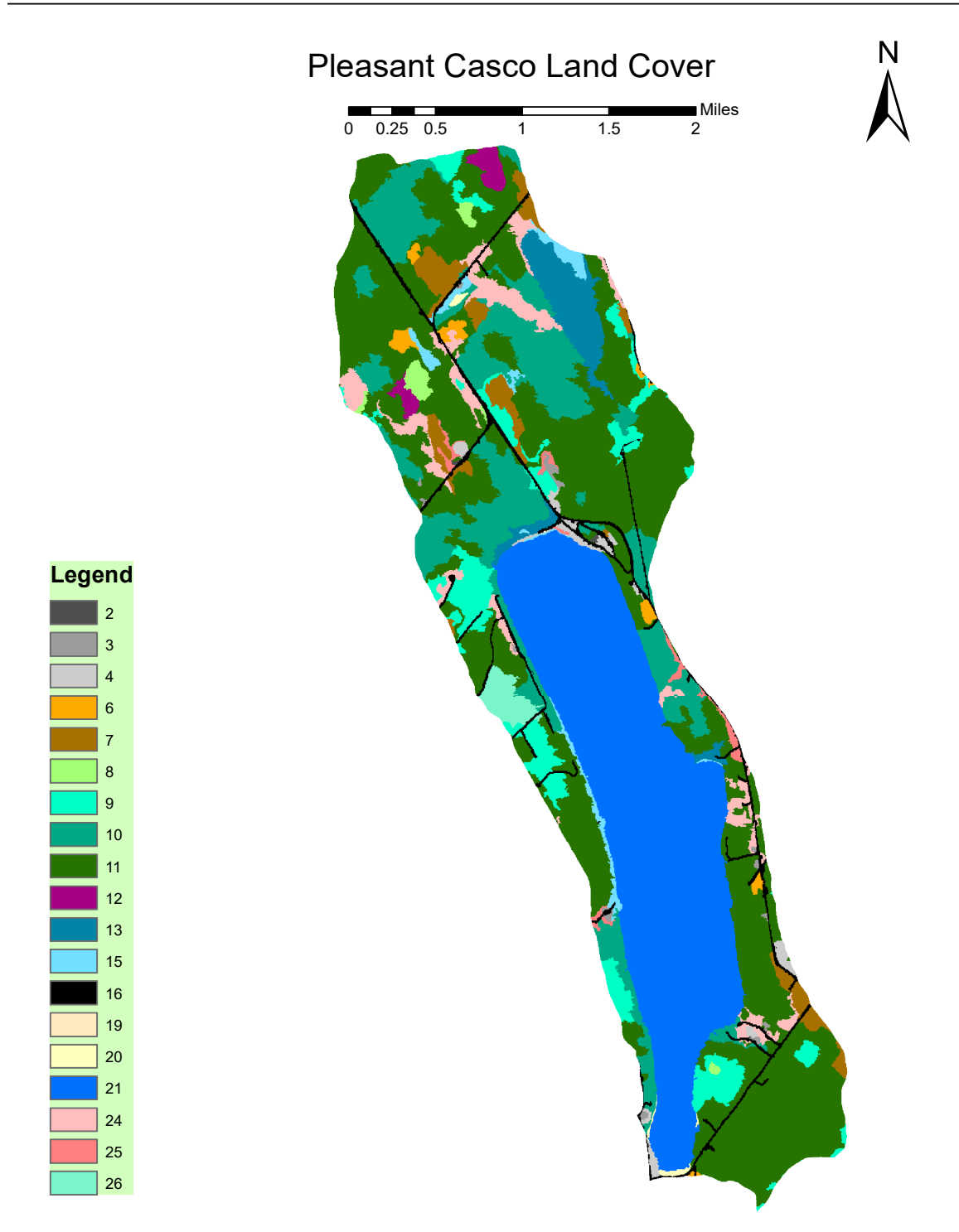


Figure F2: Continued

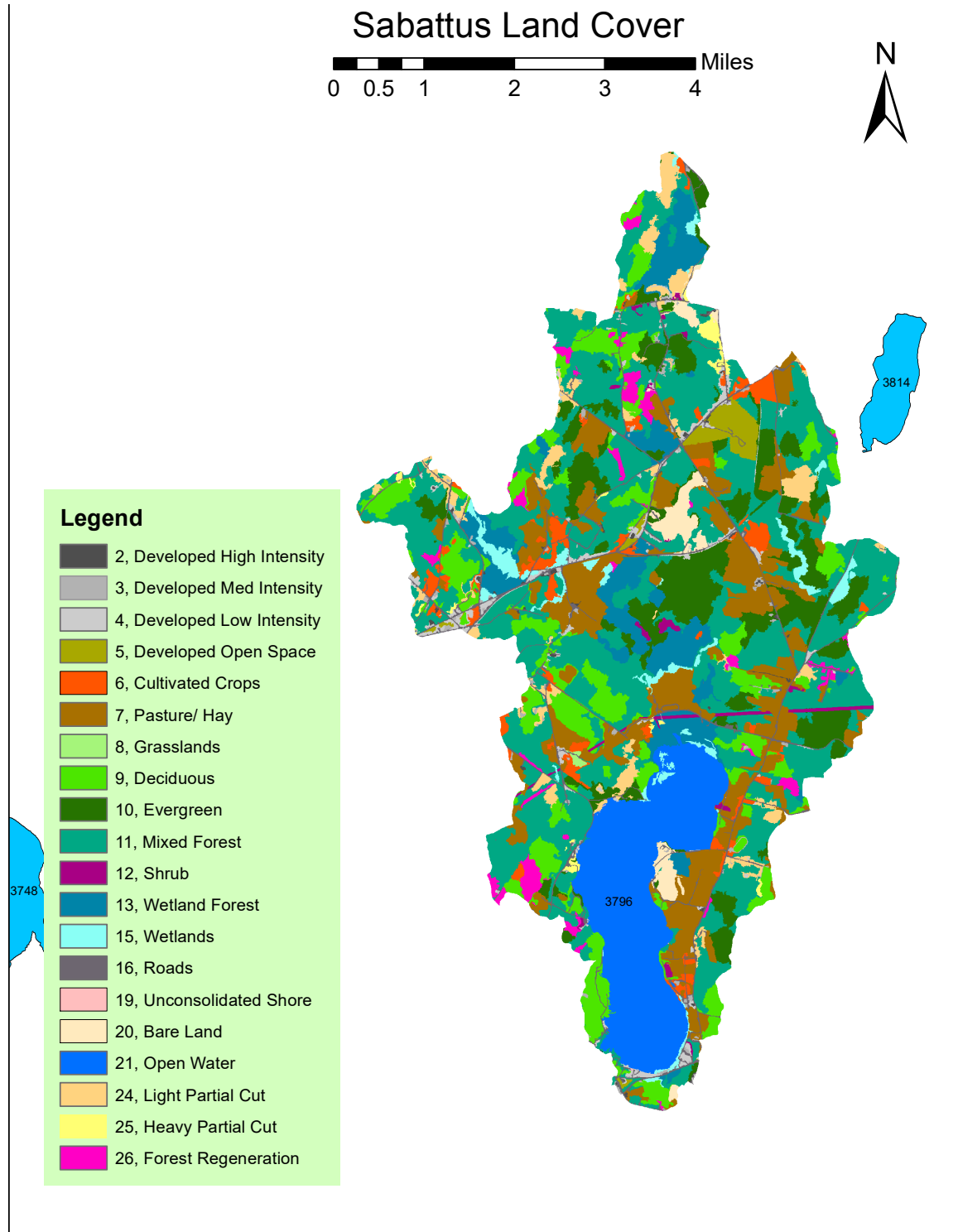


Figure F2: Continued

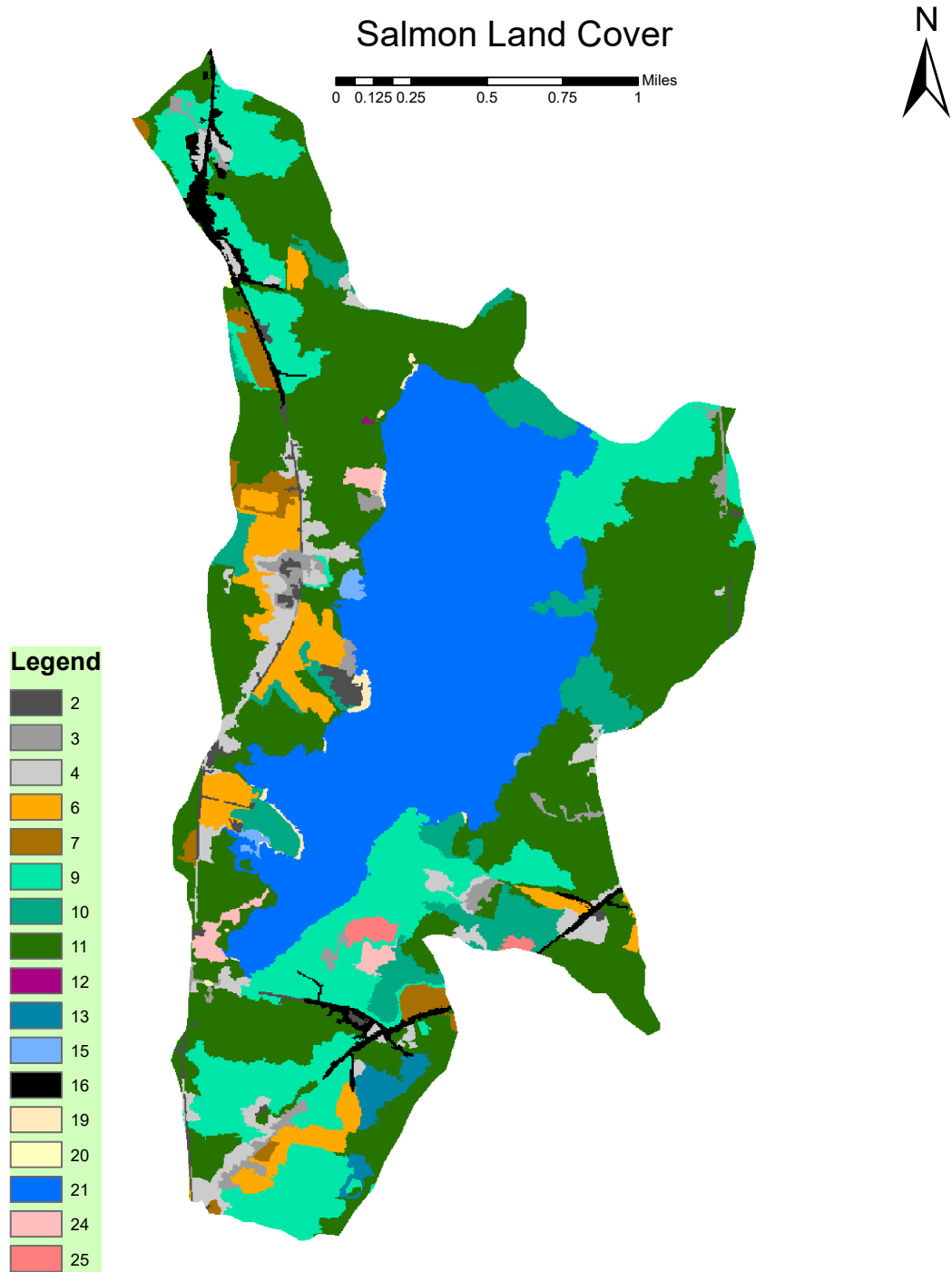


Figure F2: Continued

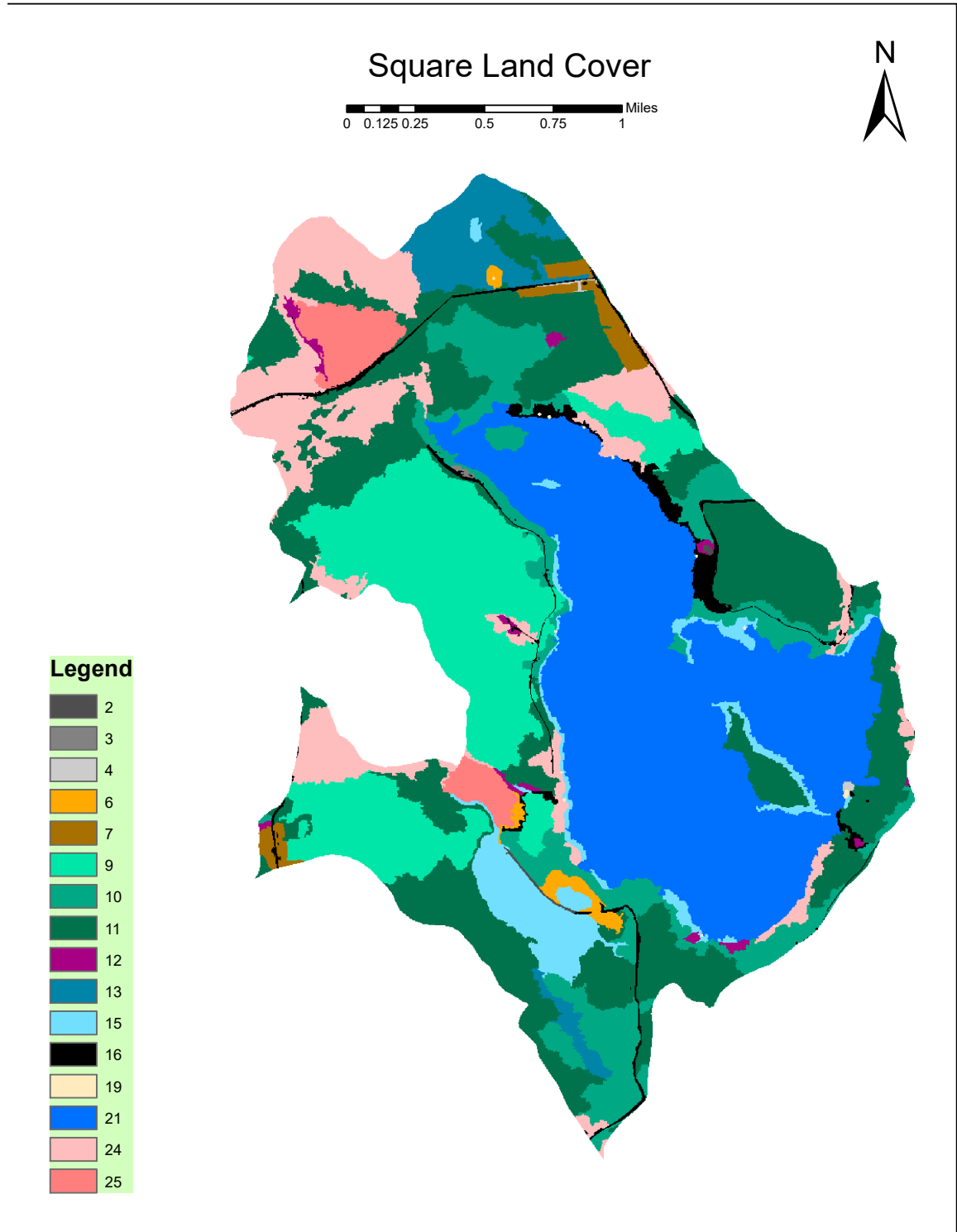


Figure F2: Continued

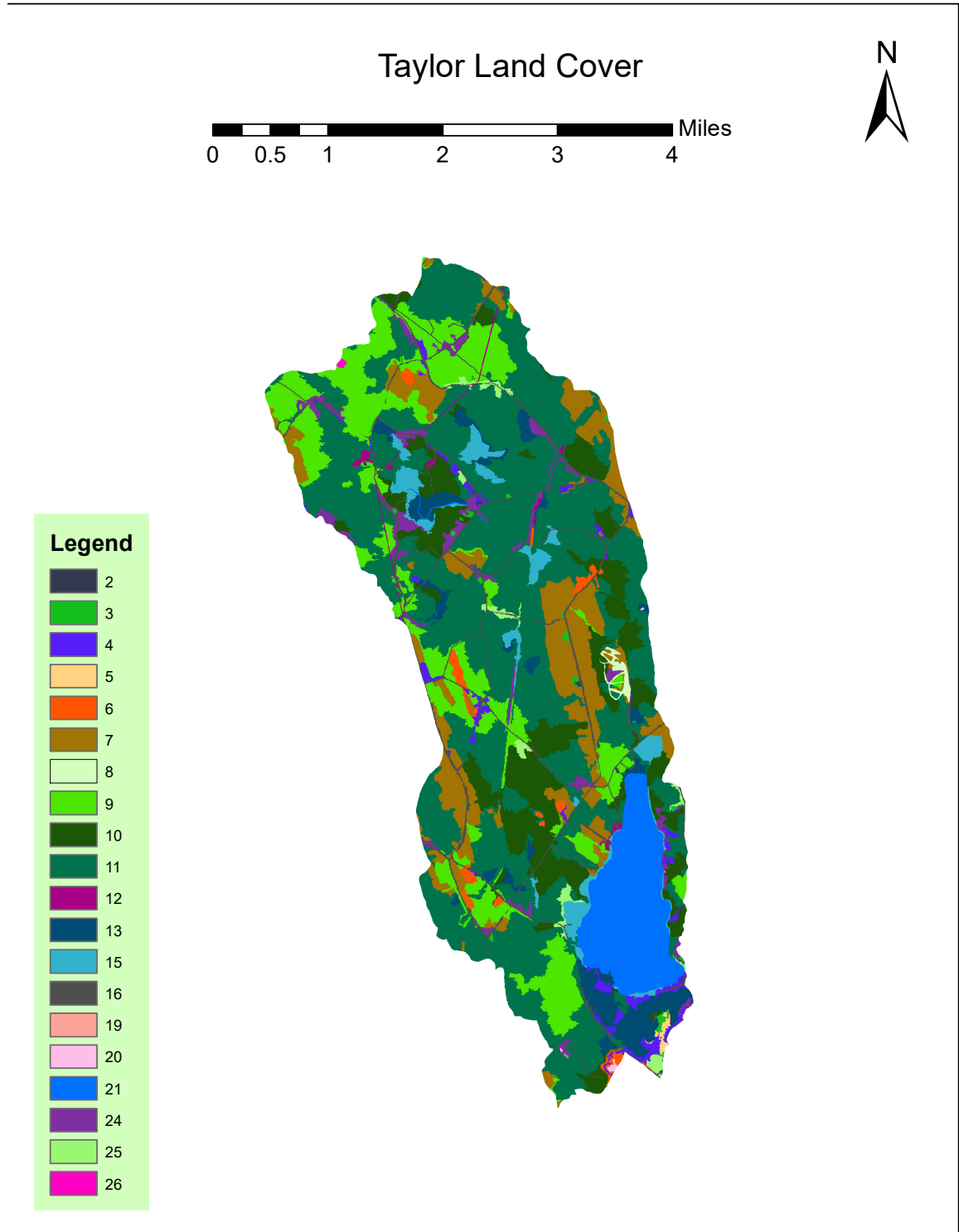


Figure F2: Continued

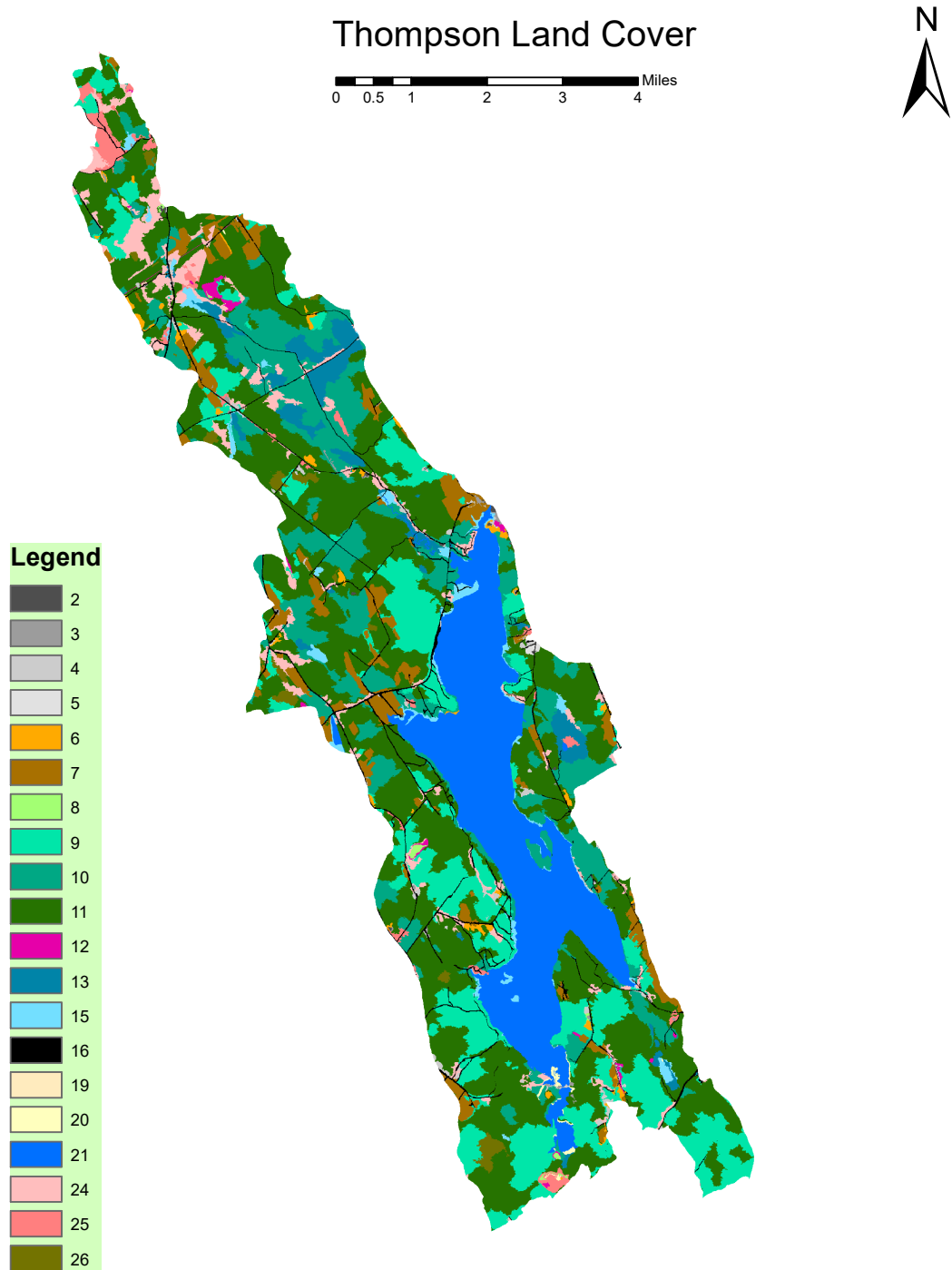


Figure F2: Continued

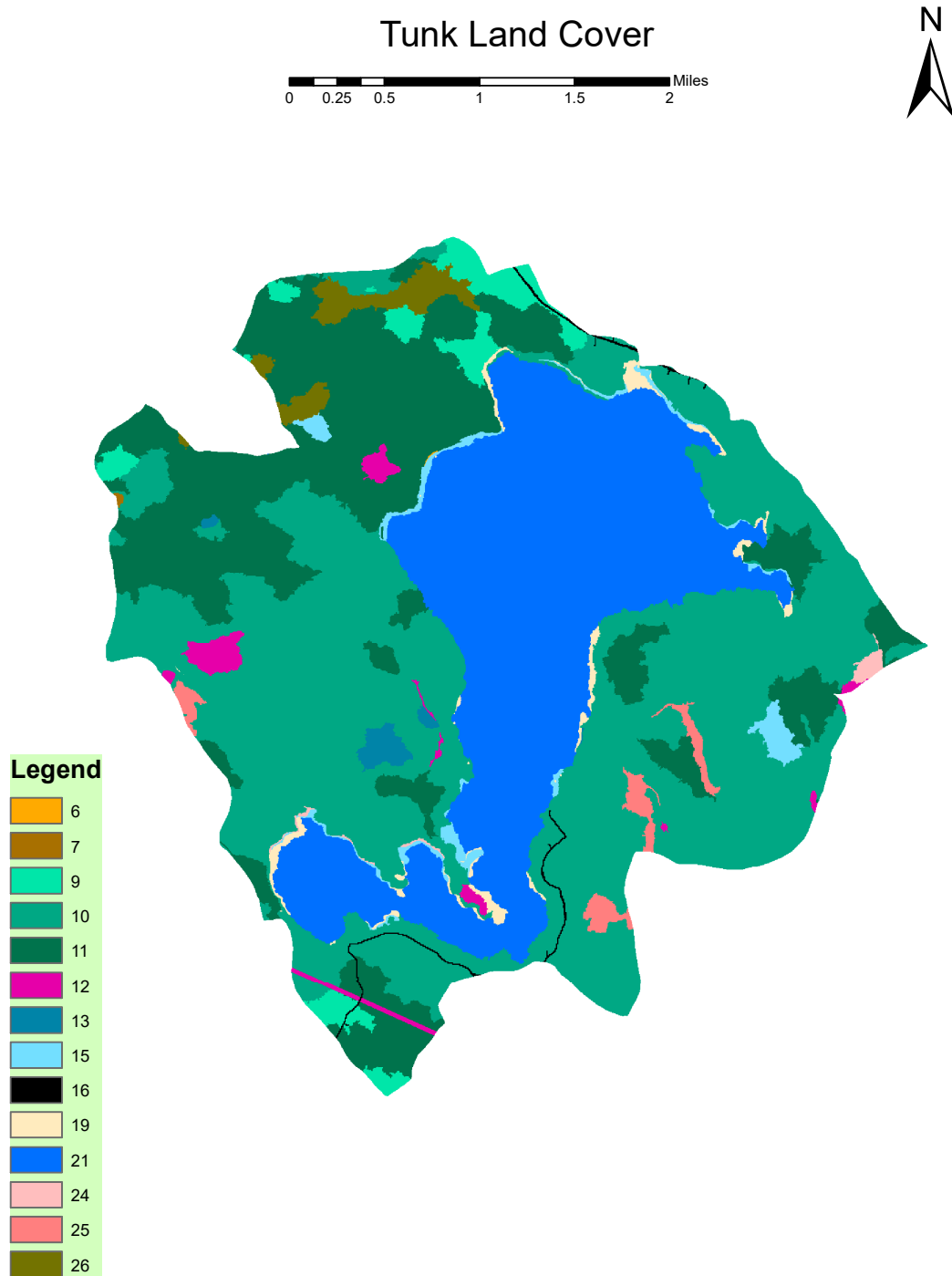


Figure F2: Continued

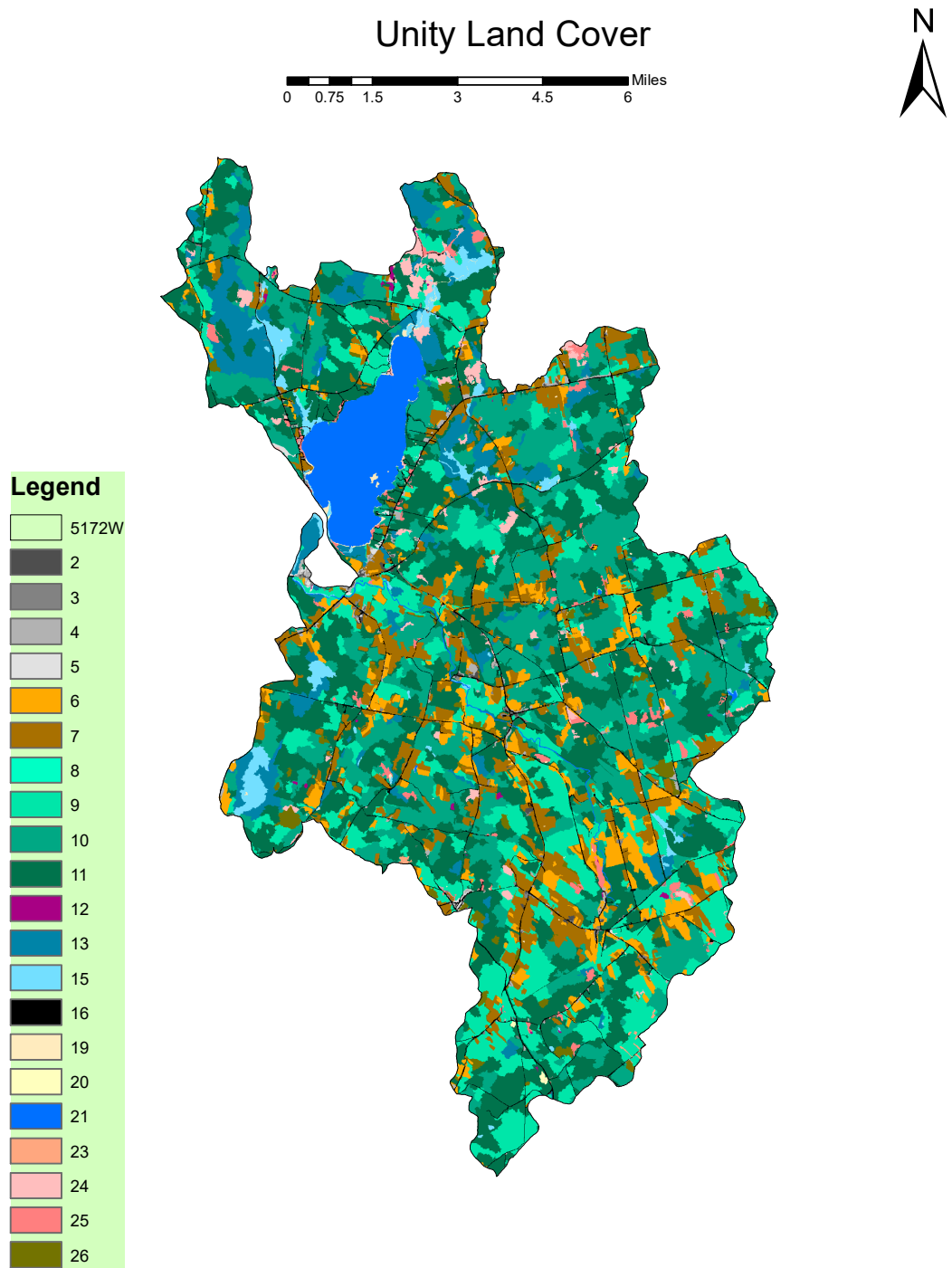
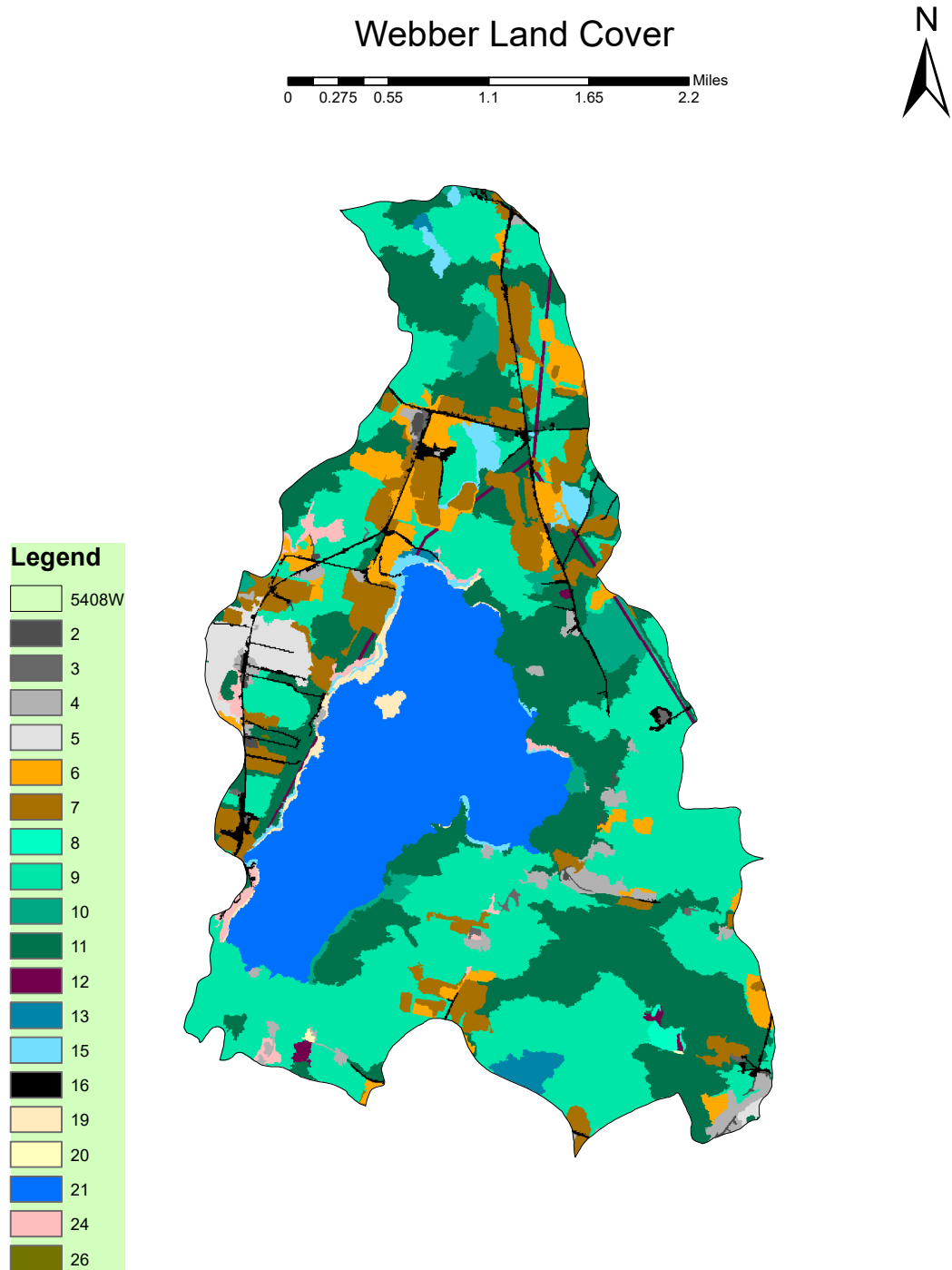


Figure F2: Continued



BIOGRAPHY OF THE AUTHOR

Kaci Fitzgibbon was born and raised in Marion, Ohio on July 5, 1993. She graduated from Pleasant High School in 2011 and graduated from Kent State University in 2015 with a Bachelor's of Science in Geology. She is a candidate for the Master of Science degree in Earth and Climate Sciences from the University of Maine in December 2017.